

REMOVAL OF BASIC DYES USING SUGARCANE  
BAGASSE

KHOO ENG CHEONG

MASTER OF SCIENCE

FACULTY OF ENGINEERING AND SCIENCE  
UNIVERSITI TUNKU ABDUL RAHMAN  
NOVEMBER 2012

**REMOVAL OF BASIC DYES USING SUGARCANE BAGASSE**

By

**KHOO ENG CHEONG**

A thesis submitted to the Department of Science, Faculty of Engineering and  
Science,  
Universiti Tunku Abdul Rahman,  
in partial fulfillment of the requirements for the degree of  
Master of Science  
November 2012

## ABSTRACT

The effectiveness using sugarcane bagasses as a sorbent for the removal of Basic Blue 3 (BB3), Methylene Blue (MB) and Basic Yellow 11 (BY11) from single and binary dye solutions was investigated. The removal of the studied dyes was pH dependent and the kinetics of dye sorption fitted well in pseudo-second order rate expression. All studied dye solutions fitted well in Langmuir isotherm with maximum sorption capacities of 23.64 mg/g, 28.25 mg/g and 67.11 mg/g for BB3, MB and BY11, respectively in single dye solutions. However, a decrease in maximum sorption capacities was observed in the binary solutions and this might be resulted from the competition of the same binding sites. Plackett-Burman design has been used to identify the most significant factors for the removal of dyes using natural sugarcane bagasse and the factors affecting the uptake of studied dyes were identified. The interaction between factors and their optimum levels for maximum percentage uptake of BB3 and MB in both single and binary dye solutions were determined using Response Surface Methodology (RSM). All the models were highly significant with correlation coefficients ( $R^2$ ) near to unity. The experimental values agreed well with the predicted values with percentage error of 2.45, 1.48, 2.20 and 1.54 for single BB3, single MB, binary BB3 and binary MB, respectively. In column studies, results revealed that breakthrough was influent concentration, flow rate and bed height dependent. The breakthrough curves exhibited the typical S shape of packed system. The experimental data were in good agreement with the predicted values in BDST modeling. All models used were found to be suitable for describing the sorption process of the dynamic

behaviour of the sugarcane bagasse column. The column regeneration studies were carried out and the sorbent was found to be reusable with minimal decrease in its sorption capacities.

## **ACKNOWLEDGEMENTS**

I would like to express my gratitude and sincere appreciation to my supervisor, Asst. Prof. Dr. Ong Siew Teng and co-supervisor, Associate Prof. Dr Hii Siew Ling for their sincere help, guidance, and suggestions during this MSc. project.

I would also like to take this opportunity to thanks all the lab staff of Chemistry Department Ms Adeline Kuek, Ms Rashidah and Mr Lee for providing assistance and helpful suggestion towards the success of this study

Last but not least, I wish to express my deepest gratitude to my family and friends for their encouragement and unconditional supports. This project would not been carried out smoothly without the help, guidance and support from all of them.

## APPROVAL SHEET

I certify that this project report entitled “**REMOVAL OF BASIC DYES USING SUGARCANE BAGASSE**” was prepared by **KHOO ENG CHEONG** and submitted as partial fulfillment of the requirements for the degree of Master of Science at Universiti Tunku Abdul Rahman.

Approved by

---

(Dr. Ong Siew Teng)  
Assistant Professor/Supervisor  
Department of Chemical Science  
Faculty of Science  
Universiti Tunku Abdul Rahman

Date:.....

---

(Dr. Hii Siew Ling)  
Associate Professor/Co-supervisor  
Department of Chemical Engineering  
Faculty of Engineering and Science  
Universiti Tunku Abdul Rahman

Date:.....

**FACULTY OF ENGINEERING AND SCIENCE  
UNIVERSITI TUNKU ABDUL RAHMAN**

Date: \_\_\_\_\_

**SUBMISSION OF FINAL YEAR PROJECT /DISSERTATION /THESIS**

It is hereby certified that **KHOO ENG CHEONG** (ID No. **08UEM01471**) has completed this final year project/ dissertation/ thesis\* entitled “REMOVAL OF BASIC DYES USING SUGARCANE BAGASSE” under supervision of Asst. Prof. Dr. Ong Siew Teng (Supervisor) from the Department of Chemical Science, Faculty of Science, and Associate Prof. Dr Hii Siew Ling (Co-supervisor) from Department of Chemical Engineering, Faculty of Engineering and Science.

I understand that University will upload softcopy of my final year project/ dissertation /thesis\* in pdf format into UTAR Institutional Repository, which may be made accessible to UTAR community and public.

Yours truly,

\_\_\_\_\_  
(KHOO ENG CHEONG)

\*Delete whichever not applicable

## DECLARATION

I hereby declare that the dissertation is based on my original work except for quotations and citations which have been duly acknowledged. I also declare that it has not been previously or concurrently submitted for any other degree at UTAR or other institutions.

Name: \_\_\_\_\_

Date: \_\_\_\_\_



## TABLE OF CONTENTS

	<b>Page</b>
<b>ABSTRACT</b>	<b>ii</b>
<b>ACKNOWLEDGEMENTS</b>	<b>iv</b>
<b>APPROVAL SHEET</b>	<b>v</b>
<b>SUBMISSION SHEET</b>	<b>vi</b>
<b>DECLARATION</b>	<b>vii</b>
<b>LIST OF TABLES</b>	<b>xii</b>
<b>LIST OF FIGURES</b>	<b>xv</b>
<b>LIST OF ABBREVIATIONS</b>	<b>xxii</b>
<b>CHAPTER</b>	
<b>1.0 INTRODUCTION</b>	<b>1</b>
1.1 Environmental Aspect	1
1.2 Dyes	2
1.3 Sugarcane Plant	3
1.3.1 Sugarcane Bagasse	5
1.4 Current Treatment of Textile Effluents	6
1.4.1 Coagulation	6
1.4.2 Oxidation	7
1.4.3 Biological Treatment	8
1.4.4 Adsorption Processes	8
1.4.5 Membrane Filtration	10
1.5 Statistical Analysis	11
1.6 Objectives	12
<b>2.0 LITERATURE REVIEW</b>	<b>13</b>
2.1 Natural Adsorbent	13
2.1.1 Batch Study	13
2.1.2 Column Study	17
2.2 Modified Adsorbent	20

2.2.1	Batch Study	20
2.2.2	Column Study	26
2.3	Industrial Waste	28
2.3.1	Batch Study	28
2.3.2	Column Study	32
2.4	Optimisation of Adsorption Process Using Response Surface Methodology (RSM)	33
<b>3.0</b>	<b>METHODOLOGY</b>	<b>38</b>
3.1	Preparation of Sorbent	38
3.2	Preparation of Dye Solution	38
3.3	Batch Studies	39
3.3.1	Effect of pH	39
3.3.2	Effect of Initial Dye Concentration and Contact Time	39
3.3.3	Effect of Agitation Rate	40
3.3.4	Study of Sorption Isotherm	40
3.3.5	Effect of Temperature	40
3.3.6	Effect of Particle Size	41
3.3.7	Effect of Sorbent Dosage	41
3.4	Chemical Modification of Surface Functional Groups	41
3.4.1	Esterification	41
3.5	Optimisation of Dye Adsorption	42
3.5.1	Plackett-Burman Design	42
3.5.2	Optimisation of Percentage Uptake	42
3.6	Column Study	43
3.6.1	Effect of Flow Rate	43
3.6.2	Effect of Influent Concentration	43
3.6.3	Effect of Bed Height	44
3.7	Instrumental Analysis	44
3.7.1	Fourier-Transform Infrared Spectroscopy	44

3.7.2	Scanning Electron Microscope (SEM) Analysis	44
3.7.3	Atomic Force Microscope (AFM) Analysis	50
<b>4.0</b>	<b>RESULTS AND DISCUSSIONS</b>	<b>46</b>
4.1	Comparison Study on the Uptake of Various Dyes by NSB	46
4.2	Fourier Transform Infrared (FT-IR) Analysis of Sorbent	48
4.3	Scanning Electron Microscopy (SEM)	48
4.4	Atomic Force Microscopy (AFM)	51
4.5	Sorption Mechanism	52
4.6	Batch Studies	59
4.6.1	Effect of pH	59
4.6.2	Effect of Initial Concentration and Contact Time	62
4.6.3	Kinetic Study	69
4.6.4	Effect of Agitation Rate	78
4.6.5	Boundary Layer Effect	84
4.6.6	Intraparticle Diffusion	92
4.6.7	Sorption Isotherm	94
4.6.8	Effect of Temperature	113
4.6.9	Effect of Particle Size	117
4.6.10	Effect of Sorbent Dosage	119
4.7	Optimisation Studies	122
4.7.1	Plackett-Burman Design	122
4.7.2	Verification of Plackett-Burman Design Models	134
4.7.3	Response Surface Methodology Approach	135
4.7.3.1	Single Dye Solutions	135
4.7.3.2	Binary Dye Solutions	142
4.7.3.3	Verification of RSM Models	154
4.8	Column Studies	155
4.8.1	Effect of Flow Rate on Breakthrough Curve	155
4.8.2	Effect of Initial Dye Concentration on Breakthrough Curve	161

4.8.3	Effect of Bed Height on Breakthrough Curve	166
4.8.4	Thomas Model	171
4.8.5	The Belter and Chu Models	175
4.8.6	The Bed-Depth/Service Time Analysis (BDST) Model	184
4.8.7	Column Regeneration Studies	195
<b>5.0</b>	<b>CONCLUSION</b>	<b>212</b>
	<b>REFERENCES</b>	<b>215</b>

## LIST OF TABLES

Table		Page
1.1	Usage classification of dyes (Hunger, 2003)	4
4.1	Sorption capacities and regression coefficients of the effect of initial BB3, MB and BY11 in single and binary dye solutions	71
4.2	Empirical parameters for predicted $q_e$ , $k$ and $h$ from $C_o$	73
4.3	The values of $\beta_L S$ and regression coefficients for BB3, MB and BY11 in single and binary dye solutions	93
4.4	The parameters value of intraparticle diffusion model for BB3, MB and BY11 in single and binary dye solutions	95
4.5	Langmuir, Freundlich and BET constants for the sorption of all studied dye solutions	111
4.6	Shape of Isotherm	112
4.7	Values of $R_L$ for all the studied dye solutions	113
4.8	The values of $\Delta S^0$ , $\Delta H^0$ and $\Delta G^0$ for all studied dye solutions	117
4.9	The effect of particle size for all studied dye solutions	118
4.10	Plackett-Burman design and results for the removal of BB3 from single dye solution	123
4.11	Plackett-Burman design and results for the removal of MB from single dye solution	124
4.12	Plackett-Burman design and results for the removal of BY11 from single dye solution	125
4.13	Plackett-Burman design and results for the removal of BB3 from BB3-BY11 binary dye solution	126
4.14	Plackett-Burman design and results for the removal of BY11 from BB3-BY11 binary dye solution	127

4.15	Plackett-Burman design and results for the removal of MB from MB-BY11 binary dye solution	128
4.16	Plackett-Burman design and results for the removal of BY11 from MB-BY11 binary dye solution	129
4.17	Regression analysis (ANOVA) of Plackett-Burman for the removal of BB3 from single dye solution	130
4.18	Regression analysis (ANOVA) of Plackett-Burman for the removal of MB from single dye solution	130
4.19	Regression analysis (ANOVA) of Plackett-Burman for the removal of BY11 from single dye solution	131
4.20	Regression analysis (ANOVA) of Plackett-Burman for the removal of BB3 from BB3-BY11 binary dye solution	131
4.21	Regression analysis (ANOVA) of Plackett-Burman for the removal of BY11 from BB3-BY11 binary dye solution	132
4.22	Regression analysis (ANOVA) of Plackett-Burman for the removal of MB from MB-BY11 binary dye solution	132
4.23	Regression analysis (ANOVA) of Plackett-Burman for the removal of BY11 from MB-BY11 binary dye solution	133
4.24	Plackett-Burman model validation	134
4.25	The central composite design matrix for two coded independent variables and the observed response for single BB3 and MB	136
4.26	Regression analysis (ANOVA) for the removal of BB3 from single dye solution	137
4.27	Regression analysis (ANOVA) for the removal of MB from single dye solution	137
4.28	The central composite design matrix for four independent variables and the observed response (Binary BB3)	143
4.29	The central composite design matrix for three independent variables and the observed response (Binary MB)	144
4.30	Regression analysis (ANOVA) for the removal of BB3 from BB3-BY11 binary dye solution	146
4.31	Regression analysis (ANOVA) for the removal of MB from	147

	MB-BY11 binary dye solution	
4.32	Validation of model equations for all studied dye solutions	154
4.33	Calculated constants of Thomas model at different conditions using non-linear regression analysis for single BB3	172
4.34	Calculated constants of Thomas model at different conditions using non-linear regression analysis for single MB	173
4.35	Calculated constants of Thomas model at different conditions using non-linear regression analysis for binary BB3 of BB3-BY11	173
4.36	Calculated constants of Thomas model at different conditions using non-linear regression analysis for binary BY11 of BB3-BY11	174
4.37	Calculated constants of Thomas model at different conditions using non-linear regression analysis for binary MB of MB-BY11	174
4.38	Calculated constants of Thomas model at different conditions using non-linear regression analysis for binary BY11 of MB-BY11	175
4.39	Predicted breakthrough time based on the BDST constants for a new flow rate ( $C_o = 10$ mg/L)	194
4.40	Predicted breakthrough time based on the BDST constants for a new influent concentration ( $v = 10$ ml/min)	195
4.41	Adsorption process parameters for three adsorption-desorption cycles	211

## LIST OF FIGURES

<b>Figure</b>		<b>Page</b>
4.1	Comparative study on the percentage uptake of various dyes	47
4.2	Infrared spectra of NSB before and after sorption	49
4.3	SEM micrograph of NSB before (a), and after (b) BB3 adsorption, (c) MB adsorption, (d) BY11 adsorption, (e) BB3-BY11 adsorption and (f) MB-BY11 adsorption	50
4.4	AFM micrograph of NSB before (a), and after (b) BB3 adsorption, (c) MB adsorption, (d) BY11 adsorption, (e) BB3-BY11 adsorption and (f) MB-BY11 adsorption	51
4.5	(a) Cellulose molecule, (b) principal sugar residues of hemicellulose, (c) phenylpropanoid units found in lignin (El-Hendawy, 2006)	53
4.6	Point-zero-charge ( $P_{zc}$ ) of NSB	55
4.7	Electrostatic attraction between MB and RDP surfaces (Al- Ghouti <i>et al.</i> , 2010)	56
4.8	Schematic models of (a) BB3, (b) MB and (c) BY11 and NSB surface	57
4.9	Schematic representation of MB and cotton fiber interaction (Kaewprasit <i>et al.</i> , 1998)	57
4.10	Comparative study on the percentage uptake of various dyes onto NSB and esterified-SB	58
4.11	Effect of pH on the sorption of BB3, MB and BY11 in single solutions onto NSB	60
4.12	Effect of pH on the sorption of BB3, MB and BY11 in binary solution onto NSB	61
4.13	Effect of contact time on the sorption of single BB3 solution onto NSB	63



4.14	Effect of contact time on the sorption of single MB solution onto NSB	64
4.15	Effect of contact time on the sorption of single BY11 solution onto NSB	65
4.16	Effect of contact time on the sorption of binary BB3-BY11 solution onto NSB	66
4.17	Effect of contact time on the sorption of binary MB-BY11 solution onto NSB	67
4.18	Comparison between the measured and pseudo-second order modeled time profiles for single BB3 sorption	75
4.19	Comparison between the measured and pseudo-second order modeled time profiles for single MB sorption	76
4.20	Comparison between the measured and pseudo-second order modeled time profiles for single BY11 sorption	77
4.21	Effect of agitation rate on the sorption of single BB3 onto NSB	79
4.22	Effect of agitation rate on the sorption of single MB onto NSB	80
4.23	Effect of agitation rate on the sorption of single BY11 onto NSB	81
4.24	Effect of agitation rate on the sorption of binary BB3-BY11 onto NSB	82
4.25	Effect of agitation rate on the sorption of binary MB-BY11 onto NSB	83
4.26	Effect of boundary layer on the sorption of single BB3 onto NSB	85
4.27	Effect of boundary layer on the sorption of single MB onto NSB	86
4.28	Effect of boundary layer on the sorption of single BY11 onto NSB	87
4.29	Effect of boundary layer on the sorption of binary BB3 of BB3-BY11 onto NSB	88
4.30	Effect of boundary layer on the sorption of binary BY11 of BB3-BY11 onto NSB	89
4.31	Effect of boundary layer on the sorption of binary MB of	90

	MB-BY11 onto NSB	
4.32	Effect of boundary layer on the sorption of binary BY11 of MB-BY11 onto NSB	91
4.33	Effect of intraparticle diffusion on the sorption of single BB3 onto NSB	96
4.34	Effect of intraparticle diffusion on the sorption of single MB onto NSB	97
4.35	Effect of intraparticle diffusion on the sorption of single BY11 onto NSB	98
4.36	Effect of intraparticle diffusion on the sorption of binary BB3 of BB3-BY11 onto NSB	99
4.37	Effect of intraparticle diffusion on the sorption of binary BY11 of BB3-BY11 onto NSB	100
4.38	Effect of intraparticle diffusion on the sorption of binary MB of MB-BY11 onto NSB	101
4.39	Effect of intraparticle diffusion on the sorption of binary BY11 of MB-BY11 onto NSB	102
4.40	Langmuir isotherm for BB3 and BY11 in single and binary dye solutions onto NSB	105
4.41	Langmuir isotherm for MB and BY11 in single and binary dye solutions onto NSB	106
4.42	Freundlich isotherm for BB3 and BY11 in single and binary dye solutions onto NSB	107
4.43	Freundlich isotherm for MB and BY11 in single and binary dye solutions onto NSB	108
4.44	BET isotherm for BB3 and BY11 in single and binary dye solutions onto NSB	109
4.45	BET isotherm for MB and BY11 in single and binary dye solutions onto NSB	110
4.46	Effect of temperature on the sorption of BB3, MB and BY11 in single dye solutions onto NSB	114

4.47	Effect of temperature on the sorption of BB3, MB and BY11 in binary dye solutions onto NSB	115
4.48	Effect of sorbent dosage on the sorption of BB3, MB and BY11 in single dye solutions onto NSB	120
4.49	Effect of sorbent dosage on the sorption of BB3, MB and BY11 in binary dye solutions onto NSB	121
4.50	3D surface plot for uptake of BB3 in single dye solution as a function of initial dye concentration and sorbent dosage	140
4.51	3D surface plot for uptake of MB in single dye solution as a function of initial dye concentration and sorbent dosage	141
4.52	3D surface plot for uptake of binary BB3 dye solution as a function of pH and initial dye concentration at contact time of 122.50 min and 0.16 g of sorbent dosage	148
4.53	3D surface plot for uptake of binary BB3 dye solution as a function of pH and dosage at contact time of 122.50 min and 100 mg/L of initial dye concentration	150
4.54	3D surface plot for uptake of binary BB3 dye solution as a function of contact time and dosage at pH 6.00 and 100 mg/L of initial dye concentration	151
4.55	3D surface plot for uptake of binary MB dye solution as a function of sorbent dosage and initial dye concentration at contact time of 122.50 min	153
4.56	Comparison of breakthrough curves between single and binary BB3 for the effect of flow rate	156
4.57	Comparison of breakthrough curves between single and binary MB for the effect of flow rate	157
4.58	Comparison of breakthrough curves between single BY11 and binary BY11 of BB3-BY11 for the effect of flow rate	158
4.59	Comparison of breakthrough curves between single BY11 and binary BY11 of MB-BY11 for the effect of flow rate	159
4.60	Comparison of breakthrough curves between binary BY11 of BB3-BY11 and MB-BY11 for the effect of flow rate	160

4.61	Comparison of breakthrough curves between single and binary BB3 for effect of influent concentration	162
4.62	Comparison of breakthrough curves between single and binary MB for effect of influent concentration	163
4.63	Comparison of breakthrough curves between single BY11 and binary BY11 of BB3-BY11 for effect of influent concentration	164
4.64	Comparison of breakthrough curves between single BY11 and binary BY11 of MB-BY11 for effect of influent concentration	165
4.65	Effect of bed height on breakthrough curve of single and binary BB3 solution	167
4.66	Effect of bed height on breakthrough curve of single and binary MB solution	168
4.67	Effect of bed height on breakthrough curve of single BY11 and binary BY11 of BB3-BY11 solution	169
4.68	Effect of bed height on breakthrough curve of single BY11 and binary BY11 of MB-BY11 solution	170
4.69	Comparison of the experimental and model fit breakthrough curves for single BB3 by NSB according to: Belter, Chu (-ve) and Chu (+ve)	177
4.70	Comparison of the experimental and model fit breakthrough curves for single MB by NSB according to: Belter, Chu (-ve) and Chu (+ve)	178
4.71	Comparison of the experimental and model fit breakthrough curves for single BY11 by NSB according to: Belter, Chu (-ve) and Chu (+ve)	179
4.72	Comparison of the experimental and model fit breakthrough curves for binary BB3 of BB3-BY11 by NSB according to: Belter, Chu (-ve) and Chu (+ve)	180
4.73	Comparison of the experimental and model fit breakthrough curves for binary BY11 of BB3-BY11 by NSB according to: Belter, Chu (-ve) and Chu (+ve)	181

4.74	Comparison of the experimental and model fit breakthrough curves for binary MB of MB-BY11 by NSB according to: Belter, Chu (-ve) and Chu (+ve)	182
4.75	Comparison of the experimental and model fit breakthrough curves for binary BY11 of MB-BY11 by NSB according to: Belter, Chu (-ve) and Chu (+ve)	183
4.76	BDST plots of single BB3 at flow rate of 10 mL/min and influent concentration of 10 mg/L	186
4.77	BDST plots of single MB at flow rate of 10 mL/min and influent concentration of 10 mg/L	187
4.78	BDST plots of single BY11 at flow rate of 10 mL/min and influent concentration of 10 mg/L	188
4.79	BDST plots of binary BB3 of BB3-BY11 at flow rate of 10 ml/min and influent concentration of 10 mg/L	189
4.80	BDST plots of binary BY11 of BB3-BY11 at flow rate of 10 ml/min and influent concentration of 10 mg/L	190
4.81	BDST plots of binary MB of MB-BY11 at flow rate of 10 ml/min and influent concentration of 10 mg/L	191
4.82	BDST plots of binary BY11 of MB-BY11 at flow rate of 10 ml/min and influent concentration of 10 mg/L	192
4.83	Breakthrough curve for adsorption of single BB3 by NSB during three regeneration cycles	197
4.84	Elution curves for single BB3 column using 0.1 M HCl during three regeneration cycles	198
4.85	Breakthrough curve for adsorption of single MB by NSB during three regeneration cycles	199
4.86	Elution curves for single MB column using 0.1 M HCl during three regeneration cycles	200
4.87	Breakthrough curve for adsorption of single BY11 by NSB during three regeneration cycles	201
4.88	Elution curves for single BY11 column using 0.1 M HCl during three regeneration cycles	202

4.89	Breakthrough curve for adsorption of binary BB3 of BB3-BY11 by NSB during three regeneration cycles	203
4.90	Elution curves for binary BB3 of BB3-BY11 column using 0.1 M HCl during three regeneration cycles	204
4.91	Breakthrough curve for adsorption of binary BY11 of BB3-BY11 by NSB during three regeneration cycles	205
4.92	Elution curves for binary BY11 of BB3-BY11 column using 0.1 M HCl during three regeneration cycles	206
4.93	Breakthrough curve for adsorption of binary MB of MB-BY11 by NSB during three regeneration cycles	207
4.94	Elution curves for binary MB of MB-BY11 column using 0.1 M HCl during three regeneration cycles	208
4.95	Breakthrough curve for adsorption of binary BY11 of MB-BY11 by NSB during three regeneration cycles	209
4.96	Elution curves for binary MB of MB-BY11 column using 0.1 M HCl during three regeneration cycles	210

## LIST OF ABBREVIATIONS

AB1	Acid Black 1
AB15	Acid Blue 15
AB92	Acid Blue 92
AFM	Atomic Force Microscope
ANOVA	Analysis of variance
AR151	Acid Red 151
$\beta_L$	External mass transfer coefficient
B	BET constant expressive of the energy interaction with surface
BB3	Basic Blue 3
BET	Brunauer-Emmett-Teller
BG4	Basic Green 4
BR46	Basic Red 46
BV	Basic Violet
BV1	Basic Violet 1
BV10	Basic Violet 10
BY11	Basic Yellow 11
BY28	Basic Yellow 28
C	The intercept
$C_o$	Initial dye concentration
$C_t$	Dye concentration design
CCD	Central composition design

CR	Congo Red
CV	Crystal Violet
D	Dye molecule
DIC	Diisopropylcarbodiimide
DR23	Direct Red 23
DR80	Direct Red 80
$\text{erf}(x)$	Error function of $x$
F	Influent linear velocity
FT-IR	Fourier-Transform Infrared Spectroscopy
$\Delta G^0$	Standard free energy
GB	Germactive (Reactive) Black HFGR
GR	Germacion (Procion) Red H-E7B
GTB	Gemazol Turquoise Blue-G
$h (k_2q_e^2)$	The initial sorption rate
$\Delta H^0$	Standard enthalpy
HBT	1-hydroxybenzotriazole
HCl	Hydrochloric acid
JLP	Jackfruit leave powder
$k_1$	The rate constant of pseudo-first order sorption
$k_2$	The rate constant of pseudo-second order kinetics
$K_a$	Constant related to the energy of the sorbent
$K_B$	Rate constant in BDST model
$K_f$	Freundlich constant for sorption capacity
$k_p$	Intraparticle diffusion rate constant



$k_{Th}$	Thomas rate constant
MB	Methylene Blue
MF	Microfiltration
MG	Malachite Green
$n$	Freundlich constant for intensity
$N_o$	Sorption capacity
NaOH	Sodium hydroxide
PAC	Powdered activated carbon
Pb	Plumbum
PCSB	Formaldehyde pre-treated sugarcane bagasse
PCSBC	Sulphuric acid pre-treated sugarcane bagasse
PCSD	Formaldehyde treated-sawdust
PCSDC	Sulphuric acid treated-sawdust
$pH_{pzc}$	pH of point zero charge
PLP	Pineapple leave powder
PS	Pineapple stem
$q_e$	The amount of dyes sorbed at equilibrium
$q_m$	Maximum sorption capacity
$q_t$	The amount of dyes sorbed at time $t$
$R$	Gas constant
$R_L$	Dimensionless separation factor
$R^2$	Regression coefficient
RB5	Reactive Black 5

RBB	Remazol Black B
RDP	Raw date pits
RO	Reverse osmosis
RO16	Reactive Orange 16
ROr	Reactive Orange
RSM	Response Surface Methodology
$\sigma$	Standard deviation
S	Specific surface area for the mass transfer
SEM	Scanning Electron Microscope
$\Delta S^0$	Standard entropy
SB	Standard entropy
STL	Spent tea leave
t	Time
T	Absolute temperature
UF	Ultrafiltration
$V_{\text{eff}}$	Effluent volume
v	Flow rate
x	Amount of sorbent
Z	Bed depth of column

## CHAPTER 1

### INTRODUCTION

#### 1.1 Environmental Aspect

The demand of synthetic dyes in dyeing industries showed a dramatic growth in the past few decades. Dyes or colouring matter was used in almost every industry from textile to food industries to colour their products. The World Bank estimates that 17 to 20 % of industrial water pollution comes from textile dyeing and treatment. Without proper treatment, effluent discharged from dyeing industries are highly coloured and can cause problems to the environment. The presence of dyes in water sources even in trace amount is aesthetically unacceptable as it is the easiest recognised pollutants in waste water. Most of dyes are toxic, mutagenic and carcinogenic which poses hazard to aquatic life as well as other living organisms (Gregory *et al.*, 1991). In addition, many dyes are difficult to degrade, as they are generally stable to light, oxidizing agent and are resistant to aerobic digestion (Mckay and Sweeny, 1980). Due to the serious environment impacts and increase of public awareness in environmental protection, there is a need to remove these pollutants before it is discharge into the aqueous environment.

Synthetic dyes were considered harmful due to the chemicals used to produce it were highly toxic, carcinogenic, or even explosive. For example, Anililine, basis of Azo dyes, were considered as deadly poison (giving off

carcinogenic amine) and highly flammable (Brit, 2008). Acute exposure to Methylene Blue (basic dye) was found to cause increase heart rate, cyanosis, Heinz body formation, vomiting and shock. In addition, Methylene Blue was also found to be mutagenic to *Micrococcus aureus*, *Salmonella typhimurium* and *Escherichia coli* (Little, 1990). A study done in 1985 revealed that 21 people out of 414 workers (such as dye-house operators, dye workers, mixers, weighers and laboratory staff) who were exposed to reactive dye powders, were identified as having allergic reactions, including occupational asthma, due to one or more reactive dyes (Hunger, 2003; Platzek, 1997).

## **1.2 Dyes**

Dyes or colouring substances is considered as one of the significant pollutants and it is stated as 'visible pollutant'. About  $10 \times 10^3$  of different commercial dyes and pigment was estimated exist and over  $70 \times 10^4$  tonnes are produced annually worldwide (Garg *et al.*, 2004). An approximately 12 % of synthetic dyes were lost during manufacturing and processing operations, and about 20 % of these dyes enter the industrial wastewater (Hema and Arivoli, 2007; Essawy *et al.*, 2008). The textile industry contributes about 22 % of the total volume of industrial wastewater generated in the country (Hameed and El-Khaiary., 2008). Dyes residues are usually discharge with or without treatment to the aquatic environment causing serious water pollution as it contains various organic compounds and toxic substances.

Dyes contain chromophore (-C=C-, -C=N-, -C=O-, -N=N-, -NO<sub>2</sub> and quinod rings), and auxochromes (-NH<sub>3</sub>, -COOH, -SO<sub>3</sub>H and -OH) which cause or intensify the colour of the chromophore by altering the overall energy of the electron system. Dyes can be classified into several categories according to their usage such as reactive, disperse, direct, vat, sulphur, cationic, acid and solvent dyes (Hunger, 2003). The classification dyes according their usage is shown in Table 1.1.

### **1.3 Sugarcane Plant**

Sugarcane is a member of Gramineae (grasses) family with scientific name of *Saccharum officianrum*. It is a C<sub>4</sub> plant with a high rate of photosynthesis (its rates lies around 150-200 % above the average for other plants). It can be characterised by segmented stems, blade-like leaves and production by seeds (Barnes, 1974). Sugarcane plant originated from New Guinea where it has been known since about 6000 BC and then spread along human migration routes. Sugarcane is common in tropical and subtropical countries throughout the world. Brazil, Philippine and China are the three largest sugarcane plantation countries in the world. It offers one of the most cost-effective renewable resources among those renewable energy options that are readily available in developing countries.

The main usage of sugarcane is to produce sugar, which can then be used in an infinite numbers of products. The sugar produced by sugarcane, sucrose, is used as a sweetening agent for food and in the manufacture of

Table 1.1: Usage classification of dyes (Hunger, 2003)

Class	Principal substrates	Method of application	Chemical types
Acid	nylon, wool, silk, paper, inks and leather	Usually from neutral to acidic dyebaths	Azo (including premetallised), anthraquinone, triphenylmethane, azine, xanthene, nitro and nitroso
Basic	Paper, polyacrylonitrile, modified nylon, polyester and inks	Applied from acidic dyebaths	cyanine, hemicyanine, diazahemicyanine, diphenylmethane, triarylmethane, azo, azine, xanthene, acridine, oxanine and anthraquinone
Direct	cotton, rayon, paper, leather and nylon	Applied from neutral or slightly alkaline baths containing additional electrolyte	Azo, phthalocyanine, stilbene and oxanine
Disperse	Polyester, polyamide, acetate, acrylic and plastics	Fine aqueous dispersions often applied by high temperature/pressure or lower temperature carrier methods; dye may be padded on cloth and baked on or thermofixed	Azo, anthraquinone, styryl, nitro and benzodifuranone
Reactive	cotton, wool, silk and nylon	Reactive site on dye reacts with functional group on fiber to bind dye covalently under influence of heat and pH (alkaline)	Azo, anthraquinone, phthalocyanine, formazan, oxanine and basic
Solvent	plastics, gasoline, varnishes lacquers, stains, inks, fats, oils and waxes	Dissolution in the substrate	Azo, triphenylmethane, anthraquinone and phthalocyanine
Sulphur	cotton and rayon	Aromatic substrate vatted with sodium sulphide and reoxidised to insoluble sulphur-containing products on fiber	Indeterminate structures
Vat	cotton, rayon and wool	Water-insoluble dyes solubilised by reducing with sodium hydrogensulphide, then exhausted on fiber and reoxidised	Anthraquinone (including polycyclic quinines) and indigoids

foodstuff. Although the usage of sugar in human diet is controversial, sucrose supplies about 13 % of all energy that is derived from foods (Escalona, 1952). Sugarcane also consist a considerable amount of leaves surrounding the stalks, which have the function of assimilating carbon dioxide through photosynthesis. At harvest time, the leaves along with the tops of the stalks are either burnt or cut off, and hence are sometimes referred as ‘cane trash’.

### **1.3.1 Sugarcane Bagasse**

Sugarcane bagasse is a fibrous residue that remains after the stalks are crushed for juice. It consists of water, fibers and trace amount of soluble solids. It primarily compose of lignin (20-30 %), cellulose (40-45 %) and hemicelluloses (30-35 %) (Peng *et al.*, 2009). Generally, bagasse is a waste product in sugar industry which incurs additional disposal cost. Therefore, most of the mill utilise it in the boiler as fuel for steam production which is used to power the milling process. The surplus of the bagasse is used in the industry to produce ethanol, paper, building materials and livestock feed. In addition, it can also be used to produce various important enzymes such as cellulose, xylanase, amylase, inulinase and lipase (Parameswaran, 2009). In Brazil, about 40 % of the automobiles are designed to burn pure ethanol and the rest use gasohol (which is produced by bagasse), as a result of the Brazilian Fuel Alcohol Program, one of the largest commercial biomass energy projects in the world.

## **1.4 Current Treatment of Textile Effluents**

Several approaches have been used to remove dyes from wastewater such as coagulation, oxidation, biological treatments, adsorption and membrane filtration.

### **1.4.1 Coagulation**

Coagulation is one of the techniques used to treat textile wastewater. The principle of the process is the addition of coagulant followed by a generally rapid chemical association between the waste and the coagulant. Then the formed coagulants subsequently precipitate and removed. There are various commercially available coagulants such as calcium, iron or aluminium salts, and polymers with multiple charged sites.

However, this method consist a few difficulties. The process can be expensive causing the user for paying chemicals whose only purpose is to be thrown away. In addition, the solids waste produced increase the cost of disposal. Dyes which have high water solubility will resist coagulation and larger additions of the coagulants may be required in order to achieve reasonable removal of pollutants (Hardin, 2007).



### 1.4.2 Oxidation

Oxidation treatments are one of the most commonly applied method to treat textile waste as they require low quantities and short reaction time. In this process, the dye molecules are oxidized and decomposed to smaller molecules such as aldehyde, carboxylate, sulphate and nitrogen. Chlorine, hydrogen peroxide and ozone are some of the commercially available oxidants.

Water soluble dyes (reactive, acid, direct and metal complex dyes) are decolourised readily by chlorine (in the form of sodium hypochloride). However, this method is not suitable for water insoluble dyes such as disperse and vat dyes, as they resist to decolourised (Namboodri *et al.*, 1994a; Namboodri *et al.*, 1994b). In addition, the decolourisation of reactive dyes will require long reaction time, while metal complex dye solution will remain partially coloured. This method will also produce organochlorine compounds including toxic trihalomethane as side reaction.

Hydrogen peroxide is used to treat textile effluent as it generates free radicals which will form dimers and trimers with organic molecules and ultimately result in the formation of water insoluble oligomers (Yamazaki *et al.*, 1960). Hydrogen peroxide is readily available and easily mixed with water. However, long reaction time is needed for effective result and the cost of equipment for storage itself is a major drawback.

### **1.4.3 Biological Treatment**

Biological treatment is a method used in treating textile industry waste. In this process, dyes were degraded into simpler compounds and are finally mineralised to water and carbon dioxide by variety of aerobic and anaerobic organisms (McMullan *et al.*, 2001). It can be done in the presence of oxygen (aerobic degradation) or without oxygen (anaerobic degradation). Wood-rotting fungus, *Rhizopus oryzae*, *Eubacterium* sp. and *Proteus vulgaris* are some of the micro-organisms used in this treatment.

The decolourisation process can be affected by various factors such as concentration of pollutants, initial pH and effluent temperature. To achieve successful biotreatment, the micro-organisms must be kept healthy and active. Type and concentration of potentially toxic substances also must be kept at a level that does not cause any serious damage to the micro-organism population (Kandelbauer *et al.*, 2007). Although biological treatments are suitable for some dyes, some of them are recalcitrant to biological breakdown (Crips *et al.*, 1990), such as triphenylmethane and phthalocyanine dyes.

### **1.4.4 Adsorption Processes**

Adsorption is a process of binding molecules or particles onto the external surface of solid or internal surface if the material is porous in a very thin layer. The binding to the solid are usually weak and reversible. This

process can occur in two ways which are physisorption and chemisorption. Physisorption is a type of adsorption which the forces are intermolecular forces (van der Waals forces) of the same kind as those responsible for the imperfection of real gases and the condensation of vapours, and which do not involve a significant change in the electronic orbital patterns of the species involved (Everett and Koopal, 2002). The adsorbed molecules are not affixed to a specific site at the surface of adsorbent but are free to undergo translational movement within the interface. It is predominant at low temperature and is characterised by relatively low energy of adsorption. Chemisorption is adsorption which the forces involved is valence forces of the same kind as those operating in the formation of chemical compounds (Everett and Koopal, 2002). Chemisorption is favoured at high temperature because chemical reactions proceed more rapidly at an elevated temperature.

Several adsorbent had been used in this process such as activated sludge, clay, fly-ash and activated carbon. In adsorption using activated sludge, concentration of sludge, water-hardness and dwell time must be taken into consideration because these factors can affect the optimum adsorption of colour. Activated carbon is applicable in a wide range of pH, however it remains as an expensive adsorbent and has high regeneration cost while being exhausted (Han *et al.*, 2008). These disadvantages increase the importance of finding more economical sorbent for the removal of various dyes from the effluents.

### 1.4.5 Membrane Filtration

Membrane filtration is a technique which is used to separate solids from liquid by flowing the mixture through a medium which only the liquid can pass through. The membrane acted as a barrier which only allow one component of mixture to permeate the membrane freely while hinder the permeation of other components. Cellulose acetate, polysulfone and polyvinylidenedifluoride are some of the industrial membrane materials. This technique consist four membrane processes which are reverse osmosis (RO), nanofiltration (NF), ultrafiltration (UF) and microfiltration (MF) (Wagner, 2001). MF is suitable to remove colloidal dyes from the exhausted dye bath, while, UF is effective as single-step treatment of secondary textile wastewater. NF is capable in separating salts and low molecular weight (<1000) organic compounds, with an appreciable softening effect. RO is apply to remove ions and larger species from dye bath effluents. The permeate produced is usually colourless and low in total salinity (Chakraborty *et al.*, 2003).

Membrane filtration is a quick method with low spatial requirement. In addition, the permeate and some of the concentration compounds, including non-reactive dyes can be reused (Buckley, 1992). The drawback of this technique are flux decline and membrane fouling, require frequent cleaning and regular replacement of the membranes. Another disadvantage is that the generated dye concentrate require further process, for instance by ozonation (Wu and Wang, 2001). The capital cost of membrane filtration is also rather

high (Hao *et al.*, 2000). The treatment of textile wastewater using filtration technique is widely applied in South Africa.

### **1.5 Statistical Analysis**

Conventional and classical methods of studying a process by maintaining other factors involved at an unspecified constant level does not describe the combined effect of all the factors involved (Ravikumar *et al.*, 2006). In addition, it is a time consuming method and does not guarantee the determination of optimal conditions (Rajendran *et al.*, 2007). These limitations of conventional methods can be eliminated by introducing statistically experiment design such as Plackett-Burman design and Response Surface Method (RSM).

Plackett-Burman design composed of a specific fraction  $2^P$  factorial design, where the levels of the factors are denoted by +1 (if the factor is at high level) and -1 (if the factor is at low level). A complete replicate of this design requires  $2 \times 2 \times \dots \times 2 = 2^P$  observations (Roger, 1985; Montgomery, 2004). Plackett-Burman design determines the most important variables for further optimisation and gave unbiased estimates of linear of all variables with maximum accuracy for a given number of observations (Rajendran *et al.*, 2007). Several advantages of utilising factorial design are increase in efficiency; each variable is screened in the presence of all other variables, as opposed to conventional methods, and decrease in the number of experiments as the

number of experiments in conventional method is often larger, (Motola and Agharkar, 1992).

RSM optimise all the affecting parameters collectively (Murat, 2002). The main objective of RSM is to determine the optimum operational conditions of the system or to determine a region that satisfies the operational specifications (Myers and Montgomery, 2002). The application of statistical experimental design techniques in adsorption process development improved product yields, reduced process variability, closer confirmation of output response to nominal and target requirements, and reduced development time and overall costs (Annadurai *et al.*, 2003).

## **1.6 Objectives**

The aims of this research are:

- To prepare an inexpensive and efficient sorbent for the removal of commercial dyes from aqueous solution
- To identify type of dyes resulting the greatest adsorption onto sugarcane bagasse
- To study the parameter that influence the sorption of these dyes under batch and continuous flow conditions
- To identify and optimise the operating conditions for dye removal using Plackett-Burman (PB) and Response Surface Methodology (RSM)

## CHAPTER 2

### LITERATURE REVIEW

#### 2.1 Natural Adsorbent

##### 2.1.1 Batch Study

The removal of Basic Violet 10 (BV10), Basic Violet 1 (BV1) and Basic Green 4 (BG4) from aqueous solution using sugarcane dust as adsorbent was studied by Ho *et al.* (2005). Three equilibrium isotherms, namely Langmuir, Freundlich and Redlich-Peterson isotherms, were used to describe their experimental data. The  $R^2$  values of Langmuir isotherm linear plot for BV10, BV1 and BG4 were 0.966, 0.930 and 0.983, respectively. The  $R^2$  values of BV1, BG4 and BV10 for Freundlich isotherm were 0.961, 0.985 and 0.876, respectively. Redlich-Peterson isotherm showed a better fit compared to the Langmuir isotherm and Freundlich isotherm. The Langmuir monolayer saturation sorption for BV1, BG4 and BV10 were 50.4 mg/g, 20.6 mg/g and 13.9 mg/g, respectively.

Removal of cationic dye from aqueous solution using pineapple stem (PS) was studied by Hameed *et al.* (2009a). They found that the amount of Methylene Blue (MB) dye adsorbed in mg/g increased with increasing dye concentration. They also reported that as the pH value increased, the dye uptake increased. Langmuir and Freundlich isotherm models were applied and

experimental data fitted better in Langmuir isotherm with maximum sorption capacity of 119.05 mg/g. In adsorption kinetics study, pseudo-second-order kinetic correlated well with experimental data. This suggested that the dye uptake is a kind of chemisorption process.

The ability of spent tea leaves (STL) to remove basic dye from aqueous solution was investigated by Hameed (2009b). In this study, MB was selected as the targeted dye. The optimum dosage for MB removal was at 3.50 g of STL and the dye uptake changed slightly over pH range of 2 to 9. The amount of MB adsorbed per unit mass of adsorbent increased with increasing initial dye concentration. The initial concentration provides an important driving force to overcome all mass transfer resistance of the MB between the aqueous and solid phase. Hence, a higher initial concentration of dye will enhance the adsorption process. In isotherm study, Langmuir, Freundlich and Temkin models were used, and the equilibrium data were best described by Langmuir isotherm model with maximum sorption monolayer adsorption capacity of 300.052 mg/g of STL. The kinetics of the adsorption process followed pseudo-second-order kinetic model which suggested a chemisorption process. The plots of intraparticle diffusion model were not linear over the whole time range which indicated there were more than one process affecting the adsorption process.

Pavan *et al.* (2008) studied the removal of MB dye from aqueous solutions by adsorption using yellow passion fruit peel as adsorbent. It was observed that an alkaline pH was favourable for the adsorption of MB and the maximum adsorption was achieved at 56 hours of contact time. The long



contact time required to reach equilibrium may be resulted from the diffusion processes of the dye into porous structure of the adsorbent.

Weng *et al.* (2009) investigated the removal of MB from aqueous solution by adsorption onto pineapple leaf powder (PLP). MB adsorption increased as the initial MB concentration increased. The driving force of the concentration was stronger as the MB concentration was higher, thus increased the adsorption capacity. From intra-particle diffusion study, it was observed that the adsorption process was controlled by multi-steps process which involved adsorption on the external surface and diffusion into the internal pores of PLP. In addition, the amount of MB adsorbed increased with increasing pH. The equilibrium data were fitted into Langmuir isotherm and the maximum sorption capacity was found to be increased with increasing pH. The maximum sorption capacity of PLP was reported as  $8.88 \times 10^{-4}$  mol/g at pH 7.5 and 24°C. The adsorption of MB onto PLP was found to be spontaneous and exothermic.

Equilibrium and kinetic studies for Basic Yellow 11 (BY11) removal by *Sargassum binderi* was conducted by Tan *et al.* (2009). It was reported that the removal of BY11 was not pH dependent and the uptake of BY11 increased as the sorbent dosage increased while the initial dye concentration decreased. The equilibrium data obeyed Freundlich isotherm which indicated that heterogeneous sorption occurred. It was also observed that the adsorption process followed pseudo-second-order kinetic which suggested the adsorption process was controlled by chemisorption.

Oliveira *et al.* (2008) evaluated untreated coffee husks as potential biosorbent for treatment of dye contaminated waters. The effects of solution temperature, pH, biosorbent dosage and contact time on MB uptake were studied. The experimental data obeyed Langmuir isotherm model with maximum sorption capacity of 90.00 mg/g (at 30°C). In thermodynamic study, it was confirmed that sorption of MB by coffee husks was endothermic and decreased randomness at the solid-solute interface during biosorption.

Gupta *et al.* (2006) studied the adsorption of hazardous dye, Erythrosine, over hen feathers. The parameters studied included the effect of pH, concentration of dye, temperature and dosage of adsorbent. The optimum pH range for removal of Erythrosine was reported at pH 3 – 8. It also showed that as the temperature increased, the adsorption of dye increased. The result was successfully fitted into Langmuir and Freundlich isotherms with high regression values.

Orange peel was used as sorbent in a study by Ardejani *et al.* (2006) for the removal of Direct Red 23 (DR23) and Direct Red 80 (DR80) from textile effluent. Results obtained were successfully fitted to the Langmuir non-linear adsorption isotherm. The maximum sorption capacity was recorded as 10.718 mg/g and 21.052 mg/g with correlation coefficients of 0.9762 and 0.9997 for DR23 and DR80, respectively. In another study by Arami *et al.*, (2005), orange peel was also used for the removal of dyes from coloured textile waste water. The experiment data were analysed using Langmuir and Freundlich isotherms and the experimental data fitted better into Langmuir model compared to

Freundlich model. Maximum sorption capacities were recorded as 10.718 mg/g and 21.052 mg/g for DR23 and DR80, respectively. It was also observed that acidic pH was favourable for adsorption of dyes onto orange peel.

Single and binary chromium (VI) and Remazol Black B (RBB) biosorption properties of *Phormidium* sp. was studied by Aksu *et al.* (2009). The removal of both pollutants was pH-dependent and highest removal was recorded at pH 2.0. It was proposed that pH affected the interaction between the sorbent and sorbates which due to the different functional groups might have different ionization potentials. The sorption for both pollutants showed an exothermic character which due to weakened physical bonding between the Cr(VI) and/or dye ions and active sites of biosorbent with increasing temperature. In isotherm study, both pollutants in single and binary systems fitted well in Langmuir and Freundlich isotherm models. The maximum sorption capacities for Cr(VI) was recorded as 24.3 mg/g in single and 31.2 mg/g in binary systems. The enhancement in maximum sorption capacity was observed in binary system. This might due to synergistic adsorption onto the biosorbent.

### **2.1.2 Column Study**

Han *et al.* (2007) studied the biosorption of MB from aqueous solution by rice husk using fixed-bed column. The breakthrough curve was affected by pH, influent concentration, flow rate and existed salt. Results showed that, the

breakthrough curves shifted from left to right when the pH of the influent increased. It was observed that breakthrough occurred faster with higher flow rate. In this study, two models were applied namely, Thomas and BDST models. From BDST modeling, the adsorption performance at other operating conditions for adsorption of MB onto rice husk can be predicted by the BDST equation. By applying Thomas model, lower influent concentration and higher flow rate were unfavourable to the adsorption of MB on rice husk column.

Biosorption of Acid Blue 15 (AB15) using fresh water macroalga *Azolla filiculoides* was investigated by Padmesh *et al.* (2006). The dye biosorption was favoured at increasing bed height and initial dye concentration, while the maximum dye biosorption was achieved at minimum flow rate. The optimum conditions for AB15 uptake were reported at 25 cm of bed height, 5 mL/min of flow rate and 100 mg/L of initial dye concentration. BDST and Thomas models were applied and both models were valid.

Han *et al.* (2008) conducted the study of the use of rice husk for the adsorption of Congo Red (CR) from aqueous solution in column mode. The effect of several important parameters such as pH, flow rate, flow rate, initial dye concentration, existing salt and bed depth were studied. Studies showed that biosorption of CR was initial dye concentration, bed depth and flow rate dependent. In this study, several models were applied. From the application of Thomas model, a less favourable adsorption of CR was observed at higher flow rate and lower influent concentration. A better column performance was obtained when the initial dye concentration increased, due to the increase of

driving force for biosorption. Thus, Thomas model was suitable for adsorption processes where the external and internal diffusions will not be the limiting step. From Adam-Bohart model, the model was valid for the relative concentration region up to 0.5 but a large discrepancies between the experimental and predicted curves was observed above this level. Yoon-Nelson model cannot predict the experimental data due to the low  $R^2$  values and large least of sum square. BDST model was reported adequately describe the adsorption of CR onto rice husk.

Han *et al.* (2009) studied the adsorption of MB by phoenix tree leaf powder in fixed-bed column. It was observed that the breakthrough time increased as the initial dye concentration and flow rate decreased, while the bed depth increased. Several models such as Thomas, Adam-Bohart, Yoon-Nelson, Clark and BDST models were applied to the experimental data. Thomas and Clark models were found suitable to describe the whole breakthrough curve, while Adam-Bohart model was used to predict the initial part of dynamic process. In addition, the data were in good agreement with BDST model.

Continuous fixed bed biosorption of reactive dyes by dried *Rhizopus arrhizus* was studied by Aksu *et al.* (2007). The targeted dyes were Germacion (Procion) Red H-E7B (GR), Gemazol Turquoise Blue-G (GTB) and Germactive (Reactive) Black HFGR (GB). From the experimental results, the total amount of dye sorbed decreased when flow rate increased, and increased when initial dye concentration for each dyes increased. The column biosorption capacities

were reported as 1007.8 mg/g, 823.8 mg/g and 635.7 mg/g for GR, GTB and GB, respectively, at initial dye concentration of 750 mg/L and flow rate of 0.8 mL/min. Thomas and Yoon-Nelson were applied and both models were found suitable to describe the whole dynamic behaviour of the column with respect to flow rate and initial dye concentration.

Uddin *et al.* (2009) studied the adsorption of MB from aqueous solution by jackfruit (*Artocarpus heterophyllus*) leaf powder (JLP). The efficiency of JLP to remove MB was investigated under several parameters such as flow rate, bed depth and initial dye concentration. The adsorbed amount and equilibrium uptake decreased with increasing flow rate, and increased with increasing initial dye concentration. BDST and Thomas models were applied and both models were in very good agreement with the experimental results. In addition, point of zero charge ( $\text{pH}_{\text{pzc}}$ ) of JLP was determined as 3.9.

## **2.2 Modified Adsorbent**

### **2.2.1 Batch Study**

Methyl Red removal from aqueous solution by using treated sugarcane bagasse was conducted by Azhar *et al.* (2006). The sugarcane bagasse was pre-treated with formaldehyde (PCSB) and sulphuric acid (PCSBC). The experiment was also conducted with commercial powdered activated carbon (PAC) to compare the performance of PCSB and PCSBC. PCSB showed the

dye adsorption changed significantly over the pH value of 4 to 7 and the percentage uptake remained constant at the pH range of 7 to 10. Almost the same pattern was obtained for PCSBC. The percentage of dye removal for PCSBC increased from 54.9 to 96.6 as the adsorbent dosage increased from 0.002 g/L to 0.010 g/L. PCSB also showed increment from 17.5 % to 74.5 % for the same increment in adsorbent dosage. The study showed that the adsorption efficiency of these 3 adsorbents was PAC > PCSBC > PCSB. The optimum pH range for the removal for both PCSBC and PCSB was from pH 7 to 10.

Junior *et al.* (2007) studied the adsorption for heavy metal ion from aqueous single metal solution by chemically modified sugarcane bagasse. In this study, chelating function (carboxylic acid and amine) was introduced to the sugarcane bagasse by modifying it with succinic anhydride, 1,3-diisopropylcarbodiimide (DIC) and triethylenetetramine. It was observed that the equilibrium time for  $\text{Cu}^{2+}$ ,  $\text{Cd}^{2+}$  and  $\text{Pb}^{2+}$  were less than 50 minutes, and the maximum removal for  $\text{Cu}^{2+}$ ,  $\text{Cd}^{2+}$  and  $\text{Pb}^{2+}$  were achieved when the solution was above pH 5.5, 6.0 and 5.0, respectively. Based on the regression coefficient obtained, Langmuir isotherm provided a better fitting compared to Freundlich isotherm. The maximum sorption capacities obtained for  $\text{Cu}^{2+}$ ,  $\text{Cd}^{2+}$  and  $\text{Pb}^{2+}$  were 139, 313 and 313 mg/g, respectively.

The removal of reactive dye from aqueous solutions by adsorption onto activated carbon prepared by sugarcane bagasse pith was studied by Amin (2008). The activated carbon used were prepared from bagasse pith by

chemical activation with 28 %  $\text{H}_3\text{PO}_4$  (AC1), 50 %  $\text{ZnCl}_2$  (AC2) followed by pyrolysis at  $600^\circ\text{C}$  and physical activation at  $600^\circ\text{C}$  in absence of air (AC3). The percentage removal of Reactive Orange (ROr) decreased as the initial dye concentration increased for all the AC due to the insufficient of available active sites as the dye concentration increased. The percentage of removal for all AC was rapid at the beginning and gradually decreased with time and finally attained equilibrium. The maximum uptake was reported after one hour of shaking time while the optimum removal pH for ROr was obtained at pH 1. The adsorption data fitted well in both Langmuir and Freundlich isotherm models. In kinetic study, the author found that the adsorption of ROr onto AC fitted well in pseudo-second-order model and the adsorption data was controlled by external mass transfer and intraparticle diffusion.

Krishnan and Anirudhan (2008) conducted the kinetic modeling of cobalt(II) adsorption onto bagasse pith based sulphurised activated carbon. The sorbent (SAC) used in this study was prepared by activating the carbonised sugarcane bagasse with  $\text{H}_2\text{S}$  and  $\text{SO}_2$ . The optimum pH for Co(II) removal was observed over pH range of 4.5 to 8.5. The percentage uptake of Co(II) was higher at higher temperature, indicated that the endothermic nature of adsorption. The experiment data fitted well in Langmuir isotherm with maximum sorption capacity of 153.85 mg/g at  $30^\circ\text{C}$ .

Adsorption of polluting substances on activated carbons prepared from rice husk and sugarcane bagasse had been studied by Kalderis *et al.* (2008). The sorbent (ACs) was prepared by chemical impregnated of rice husk and



sugarcane bagasse with  $ZnCl_2$  and carbonised at  $700^\circ C$ . These ACs provided a good sorption capacities for phenol, arsenic and humic acid. Phenol showed the highest uptake with removal of 80 % at equilibrium time of 4 hours. In the treatment of landfill leachate, 30 g/L of AC was capable to remove 70 % and 60 % of COD and colour, respectively.

Wong *et al.* (2009) studied the removal of basic and reactive dyes using quarterised sugarcane bagasse. In this study, the removal of Basic Blue 3 (BB3) and Reactive Orange 16 (RO16) were studied in single and binary systems. The effect of pH was found to be strongly affecting the sorption of dye and the optimum pH was determined in the range of 6 – 8. The equilibrium data followed pseudo-second-order kinetic model which indicated that the rate limiting step may be chemisorption involving valency forces through sharing or exchange of electrons between the sorbent and sorbate. In isotherm study, all the systems obeyed Langmuir and Freundlich isotherm models with maximum sorption capacities of 5.58 mg/g, 37.59 mg/g, 22.73 mg/g and 34.48 mg/g for single BB3, binary BB3, single RO16 and binary RO16, respectively. In addition, the sorption of BB3 was found favourable at lower temperature, and the optimum dosage was determined as 0.10 g.

Ong *et al.* (2007) studied the removal of basic and reactive dyes using ethylenediamine modified rice hull. Dyes used in this study were BB3 and RO16 in both single and binary systems. Various important parameters such as pH, initial dye concentration, sorption isotherm, agitation rate, particle size and sorbent dosage were investigated by using batch adsorption studies. The results

showed that the sorption of targeted dyes were pH and concentration dependent. The favourable pH for uptake of BB3 was reported at higher pH while uptake of RO16 was favoured at lower pH. At low pH, the carboxyl groups on the surface of rice hull were predominantly protonated, hence incapable of binding BB3. Meanwhile, a reverse trend was observed for the removal of RO16 where the uptake was enhanced at lower pH. The amine groups on the surface of rice hull were protonated at lower pH, therefore increased the electrostatic charge attractions between the negatively charged RO16 molecules and positively charged sorption sites. In isotherm study, the equilibrium data fitted well in both Langmuir and Freundlich isotherms with maximum sorption capacities of 3.29 mg/g and 24.88 mg/g for BB3 and RO16, respectively, in single dye solutions. An enhancement of 4.5 and 2.4 fold were reported for BB3 and RO16, respectively, in binary dye systems.

The use of raw and activated date pits as potential adsorbents for dye containing water was investigated by Banat *et al.* (2003). In this study, the effects of activation temperature, solution temperature, solution pH, adsorbent particle size and solution salinity of MB removal were studied. Dye removal was observed increased with increasing pH, however decreased with an increase in solution temperature. Adsorption process was found to be exothermic. The experimental data were fitted into Langmuir isotherm and the calculated maximum sorption capacities were 80.29 mg/g, 12.94 mg/g and 17.27 mg/g for raw date pits, activated date pits at 500°C and activated date pits at 900°C, respectively.

The adsorption behaviour of cationic dyes on citric acid esterifying wheat straw was conducted by Gong *et al.* (2008). The removal of MB and Crystal Violet (CV) were found to be better at value beyond pH 4. The equilibrium data were fitted into Langmuir isotherm model with maximum sorption capacities of 312.50 mg/g and 227.27 mg/g for MB and CV, respectively. Adsorption kinetic study showed that the kinetic data conformed well to the pseudo-second-order rate kinetic model. In addition, the adsorption of dyes was spontaneous and endothermic.

Garg *et al.* (2004) studied the removal of Malachite Green (MG) dye from aqueous solution by adsorption using *Prosopis cineraria* sawdust treated with formaldehyde and sulphuric acid. Commercially available coconut based carbon (GAC) was used to evaluate the performance of the formaldehyde treated-sawdust (PCSD) and sulphuric acid treated-sawdust (PCSDC). The parameters studied were the effect of surface charge, initial pH, initial dye concentration, adsorbent mass and contact time on the dye removal. Results showed that at low pH (2 – 5), adsorption of MG by PCSDC and PCSD was unfavourable due to the negatively charged sites and the presence of excess H<sup>+</sup> ions which competed with dye cations for the adsorption sites. The adsorption efficiency was in the order of GAC > PCSDC > PCSD.

Kardivelu *et al.*, (2003) utilised various agricultural wastes for activated carbon preparation and application for the removal of dyes and metal ions from aqueous solutions. The activated carbon used in this study were prepared by agricultural solid wastes, silk cotton hull, coconut tree sawdust, sago waste,

maize cob and banana pith. An appreciable amount of dyes and metal ions can be adsorbed within a very short time.

Jumasiah *et al.* (2005) studied the adsorption of basic dye (Basic Blue 9) onto palm kernel shell activated carbon. Three isotherms were used to analyse the experimental data, namely Langmuir, Freundlich and Redlich-Peterson isotherm. The experimental data fitted best in Redlich-Peterson isotherm followed by Langmuir and Freundlich models. The regression coefficient for Redlich-Peterson, Langmuir and Freundlich isotherms were 0.9996, 0.9979 and 0.8011, respectively. The Langmuir monolayer saturation sorption was recorded as 311.72 mg/g.

### **2.2.2 Column Study**

The removal of Acid Blue 92 (AB92) and Basic Red 29 (BR29) using *Euphorbia antiquorum L* activated carbon had been studied by Sivakumar and Palanisamy (2009). The removal efficiency of AB92 and BR29 were strongly dependent on influent concentration, bed height and flow rate. The column performances were analysed using Thomas and Yoon-Nelson models, and Yoon-Nelson model described the adsorption behaviour of targeted dyes more reasonably compared to Thomas model with higher correlation coefficients and lower standard deviation. The adsorption capacity increased with increase in influent concentration and decrease with increase in flow rate and bed height.

Lee *et al.* (2008) investigated the removal of BB3 and RO16 in single and binary systems using ethylenediamine modified rice hull (MRH). The breakthrough time was found increased with decreasing influent dye concentration and sharper breakthrough curves were obtained as the dye concentration increased. For binary dye solutions, effluent concentrations greater than influent concentrations were obtained. This showed that BB3 was displaced from the column after initial sorption. In addition, typical 'S' shape of breakthrough curve was obtained for BB3 while a rapid initial breakthrough was observed in both single and binary systems of RO16 before effective sorption took place. In the effect of bed depth, a longer service time before breakthrough occurs was observed at higher bed depth. When varying the flow rate, a small effect on the breakthrough profiles of BB3 was reported, but this effect was more evident in the breakthroughs of RO16. BDST model was applied and a deviation was observed which was due to the presence of more than one rate-limiting steps in the sorption process.

Ahmad and Hamed (2010) studied the fixed-bed adsorption of Reactive Black onto granular activated carbon prepared from bamboo waste. The adsorption system was found performed better with lower influent concentration, lower flow rate and higher bed height. The highest bed capacity of 39.02 mg/g was reported using 100 mg/L influent concentration, 80 mm bed height and 10 mL/min of flow rate. Adam-Bohart, Thomas and Yoon-Nelson models were used to fit the adsorption data, and the results fitted well to Thomas and Yoon-Nelson models with high  $R^2$ .

## 2.3 Industrial Waste

### 2.3.1 Batch Study

Batch study of liquid-phase adsorption of MB using cedar sawdust and crushed brick had been investigated by Hamdaoui (2006). The experimental data were modeled with Langmuir, Freundlich, Elovich and Temkin isotherm models, and the adsorption of MB obeyed the Langmuir isotherm model with maximum sorption capacity of 142.36 mg/g and 96.61 mg/g for cedar sawdust and crushed brick, respectively. From Temkin model, the reaction of adsorption was determined as exothermic. The optimum pH value for dye adsorption for both adsorbents was observed at pH 7 and the dye adsorption decreased at higher pH values of 9.51 – 11.0.

A study of Direct Blue 71 dye from aqueous solution by using palm ash as adsorbent was conducted by Ahman *et al.* (2006). The equilibrium data fitted well into Freundlich isotherm in the range of 50 to 600 mg/L of initial dye concentration. The increase in agitation time and concentration led to an increment of dye adsorbed. Equilibrium adsorption capacity was reported as 400.01 mg/g at 30°C. In another study by Isa *et al.*, (2006), palm ash was used to remove Disperse Blue and Disperse Red from aqueous solution. The experimental data showed that acidic pH was favourable for both dyes and the equilibrium time was found to be 60 minutes for both dyes. Adsorption of both dyes was analysed using Langmuir and Freundlich isotherms, however Langmuir model provided a better fit.

Batzias and Sdiras (2006) conducted a simulation of dye adsorption by beech sawdust as affected by pH. Freundlich isotherm was used to estimate the adsorption capacity. The model indicated that an increase in pH enhanced the adsorption behaviour. The lower adsorption of MB in acidic pH can be attributed to the presence of  $H^+$  ions that compete with the dye cations for adsorption sites. As the pH increases, the amount of positively charged sites decreases and the amount of negatively charged increases. Due to the electrostatic attraction, the negatively charged sites favoured the adsorption of MB cations. Increment in initial pH from 8.0 to 11.5 increased the amount of dye adsorbed.

A study of unburned carbon as low-cost adsorbent for treatment of MB-containing wastewater has been conducted by Wang *et al.* (2005). In this study, fly ash, natural zeolite and unburned carbon derived from coal fly ash were used as the low-cost adsorbent. Initially the uptake of dye increases rapidly, then levels off gradually and finally approaches equilibrium. This was due to the strong attractive forces between the dye molecules and the adsorbent. The results showed that the adsorption was influenced by initial dye concentration, temperature, pH and particle size. The adsorption of MB onto activated carbon increased with increasing initial dye concentration, temperature and pH. MB and other cationic dyes produce an intense molecular cation ( $C^+$ ) and reduced ions ( $CH^+$ ). At higher pH,  $OH^-$  on the adsorbent surface favoured the adsorption of cationic dye molecules was proposed. The adsorption dropped with increasing particle size. The decreasing in dye adsorption as the particle size increased was probably due to the decrease in surface area.

Another similar study had been conducted by Wang and Li (2005) with Rhodamine B as the selected dye. Two sorption isotherms were used to describe the experimental data, namely Langmuir and Freundlich isotherms. Langmuir model fitted better with dye adsorption capacities of  $9.7 \times 10^{-5}$ ,  $11.4 \times 10^{-4}$  and  $1.5 \times 10^{-4}$  mol/g at the temperature of 30, 40 and 50°C, respectively. The favourability and the shape of the isotherm of adsorption were studied by calculating the dimensionless separation factor ( $R_L$ ). The value of  $R_L$  indicates the type of the isotherm to be either unfavourable ( $R_L > 1$ ), linear ( $R_L = 1$ ), favourable ( $0 < R_L < 1$ ) or irreversible ( $R_L = 0$ ). The  $R_L$  values obtained indicate the sorption was favourable.

Adsorption of basic dyes from single and binary component systems onto bentonite was investigated by Turabik (2008). The studied dyes were Basic Red 46 (BR46) and Basic Yellow 28 (BY28). The adsorption of both dyes in single system were not pH dependent. The uptake of both dyes increased slightly when the temperature increased. For the effect of initial dye concentration, the individual adsorption uptake of dyes in binary component system were lower than those in single component system. The total dye adsorption uptake of bentonite binary system were also found lower than expected total adsorption uptake that calculated by considering the total concentration of each dye in single solutions. Therefore, the author suggested that the binary mixture exhibited inhibitory (antagonistic) adsorption. In isotherm study, multi-component Freundlich model was found agreed reasonably well except for high initial dye concentrations.



Wang and Ariyanto (2007) investigated the competitive adsorption of MG and Plumbum (Pb) ions on natural ions zeolite. The removal of both MG and  $Pb^{2+}$  was pH-dependent. A sharp increase in adsorption was observed at pH 5 and pH 7 for MG and  $Pb^{2+}$ , respectively. A reduce in adsorption of MG and  $Pb^{2+}$  was noticed in binary system which suggested a competitive adsorption. However, the total adsorption of natural zeolite was higher in the binary system than that of any MG and  $Pb^{2+}$  in single systems. A higher adsorption rate of  $Pb^{2+}$  than MG was recorded in binary system due to the difference in electronic structure and molecular size. The adsorption phenomenon depends on the charge density of cations and it was proposed that a higher charge density of ions will lead a higher ion exchange rate.

Wang and Li (2007) conducted the kinetic modeling and mechanism of dye adsorption on unburned carbon in fly ash. Several important parameters such as effect of particle size, pH, temperature and kinetic modeling which affect the nature of adsorption were studied. Larger particle of unburned carbon reduced the adsorption capacity which showed that the external transport limits that rate of adsorption. In the effect of pH, adsorption of Acid Black 1 (AB1) decreased with increasing pH while adsorption of Basic Violet (BV) showed an increase trend with increasing pH. In addition, the adsorption for both dyes were favourable at higher temperature. In the kinetic modelling, the adsorption data obeyed pseudo-second-order model and the mechanism consist of two process (external and internal diffusion), where external diffusion was the dominate process.

### 2.3.2 Column study

Teng and Lin (2005) studied the removal of basic dye from water using pristine and HCl-activated montmorillonite in fixed beds. The break point occurred faster with increasing flow rate and influent concentration, however, increased in bed height showed opposite result. Two-parameter mathematical model was used to analyse the results and it fitted the model reasonably well. The breakthrough curve displayed a symmetrical shape of adsorption process. The mechanism controlling the adsorption of basic dye was found to be liquid-film diffusion for pristine clay and intraparticle diffusion for HCl-activated montmorillonite. In addition, the adsorption capacity of HCl-activated montmorillonite was four times greater than pristine clay due to increase in the surface area during acidification process.

The removal of reactive azo dyes in fixed-bed reactors using modified organo-zeolite surface was conducted by Benkli *et al.* (2005). The sorbent was modified using quaternary amine and the dyes studied were Reactive Black 5, Red 239 and Yellow 176. The sorption of all dyes was flow rate dependent and flow rate of 25 mL/min exhibited the best performance for Yellow 176 removal. The order of dye removal by modified zeolite was reported in following manner: Reactive Black 5 > Yellow 176 > Red 239. It was proposed that bilayer formation favours the interaction of anionic dyes and quaternary amine on cationic zeolite surface.

Goshadrou and Moheb (2011) studied the continuous fixed bed adsorption of Acid Blue 92 by exfoliated graphite. The graphite used was treated with mixture of sulphuric and nitric acid, and thermal treatment. The experimental data was reasonably described by Langmuir and Radke-Prausnitz isotherm models with maximum sorption capacity of 6.0 mg/L. Breakthrough time increased with increasing in sorbent dosage, however it decreased with increasing flow rate and influent concentration. In addition, axially dispersed assumption, Langmuir isotherm and LDG mass transfer resistance were used to model the data. A good agreement between experimental and modeled curves was observed.

#### **2.4 Optimisation of Adsorption Process Using Response Surface Methodology (RSM)**

The optimisation of basic dye removal by oil palm fibre-based activated carbon using response surface methodology was studied by Hameed *et al.* (2008). The effect of different preparation methods for activated carbon; varying in activation temperature, activation time and chemical impregnation ratio on MB uptake were studied using central composition design (CCD) method. The activation temperature and chemical impregnation ratio was found significantly affects the MB uptake with chemical impregnation ratio showing the greatest effect on the response. Meanwhile, carbon yield was greatly affected by activation temperature. The optimum conditions for the AC preparation were reported at 862°C of activation temperature, 1 hr of activation time and chemical impregnation ratio of 3:1 (KOH:char). In addition, the

equilibrium data followed Langmuir isotherm with maximum monolayer adsorption capacity of 400 mg/g.

Murugesan *et al.* (2007) conducted the optimisation of decolourisation of Reactive Black 5 (RB5) by laccase using response surface methodology approach. Four different factors were studied namely dye concentration, enzyme concentration, 1-hydroxybenzotriazole (HBT) concentration and incubation time. Box-Behnken design was used to analyse the experimental results to obtain an empirical model for the best response. From the analysis of variance (ANOVA) results, the predicted response fitted well with those of the experimental response with  $R^2$  value of 0.999.  $P$  value less than 0.01 showed that the model was statistically significant. Maximum decolourisation of RB5 (84.33 %) was achieved at the optimum conditions of dye concentration (62.5 mg/L), enzyme (2.5 U/mL), HBT (15mM) and time (36 hours).

Ravikumar *et al.* (2006) studied the application of response surface methodology to optimise the process variables for Reactive Red and Acid Brown dye removal using a novel adsorbent. The adsorbent used was prepared by pyrolysing a mixture of carbon and flyash at 1:1 ratio. The combine effect of pH, temperature, particle size and time on the dye adsorption and optimised the operating conditions were studied using response surface methodology. By using the same adsorbent and approach, Ravikumar *et al.* (2005) studied the removal of Acid Blue 158 and MB. They reported that the optimum pH, temperature, particle size and time were found to be 2.20, 27.80°C, 0.0565 mm and 245 min, respectively for Acid Blue 158. For MB, the optimum operation

conditions were found at pH 13.40, temperature of 28.45°C, particle size of 0.0555 mm and 230 min.

Response surface methodological approach for the decolourisation of simulated dye effluent using *Aspergillus fumigatus fresenius* was conducted by Sharma *et al.* (2009). The target dye was Acid Red 151 (AR151). CCD matrix and RSM was applied to evaluate the interactive effects of temperature, pH and initial dye concentration on the removal of AR151. The  $R^2$  and the adjusted  $R^2$  of the model were found very high which advocated a high correlation between the observed and the predicted values. The lack-of-fit term was not significant indicated that the quadratic model was statistically significant for the response. The optimum conditions for the removal of AR151 was reported at initial dye concentration of 150 mg/L , pH 5.5 and temperature of 30°C with AR151 decolourisation of 85%.

Azila *et al.* (2008) investigated the biosorption of lead, Pb(II), onto immobilised cells of *Pycnopus sanguineus* using RSM. Three variables were studied namely, initial concentration, pH and biomass loading. The optimum point of the combined effects was analysed using RSM approach. From the ANOVA of the model,  $R^2$  was 0.9691 and the lack-of-fit was 0.1284 which indicated that the quadratic model was valid. The optimum conditions was reported at 200 mg/L of Pb(II) ions, pH 4 and 10.0 g/L of biosorbent to achieve the removal of 97.7 %.

Khattar and Shailza (2009) studied the optimisation of  $\text{Cd}^{2+}$  removal by the cyanobacterium *Synechocystis pevalekii* using the response surface methodology. In this study, three-level Box-Behnken factorial design were used to optimise the pH, biomass and metal concentration for  $\text{Cd}^{2+}$  removal. The model was reported valid with  $R^2$  value of 0.99, model  $F$ -value of 86.40 and low  $p$ -value ( $F < 0.001$ ). Contour plot was applied to further understand the relationship between the response and the experimental levels of each factor. The optimum conditions were reported at pH 6.48, biomass concentration of 0.24 mg protein/mL and metal concentration of  $5\mu\text{g/mL}$  with  $\text{Cd}^{2+}$  removal of  $4.27\mu\text{g/mL}$ .

Application of response surface methodology for optimisation of cadmium biosorption in aqueous solution by *Saccharomyces cerevisiae* was conducted by Ghorbani *et al.*, (2008). In this study, initial pH, initial cadmium concentration and sorbent dosage were optimised. From the ANOVA results, the quadratic model was found highly significant with high  $R^2$  (0.9867). The optimum cadmium uptake of 8.56 mg/g was obtained at initial cadmium ions concentration of 30 mg/L and sorbent dosage of 1.6 g/L. In addition, the equilibrium data obeyed pseudo-second-order model and maximum sorption capacity calculated based on Langmuir isotherm was 8.17 mg/g.

Removal of nickel(II) from aqueous solution by adsorption on agricultural waste biomass using a response surface methodological approach was conducted by Garg *et al.*, (2008). In this study, the biomass used was sugarcane bagasse and the factors studied were the effect of pH, adsorbent

dosage and agitation speed. Quadratic model was significant with very high  $R^2$  (close to 1) and adjusted  $R^2$  values, and the non-significant value of lack-of-fit term. The maximum removal of nickel was evaluated using RSM. The optimum conditions for maximum removal of nickel at concentration of 50 mg/L were found to be pH at 7.52, adsorbent dosage of 1500 mg/L and stirring speed of 150 rpm.

## **CHAPTER 3**

### **METHODOLOGY**

#### **3.1 Preparation of Sorbent**

The sugarcane bagasse was collected from a sugarcane juice hawker at Wangsa Maju, Setapak. The bagasse was cut into small pieces and boiled for 3 hours to remove the sugar residue in the bagasse. After the boiling process, the bagasse was washed several times with tap water and rinsed with distilled water before sun dried. The dried bagasse was ground to pass through a 3 mm size sieve and labelled as natural sugarcane bagasse (NSB).

#### **3.2 Preparation of Dye Solution**

The dyes being studied were Basic Blue 3 (BB3), Methylene Blue (MB) and Basic Yellow 11 (BY11). For each dye, 1000 mg/L of standard dye solutions were prepared as stock solution and subsequently diluted when necessary. All prepared dye solutions were kept in dark to prevent light degradation.



### **3.3 Batch Studies**

All the batch experiments were carried out in duplicate and the results given are the average. A control (without sorbent) was simultaneously carried out to ascertain that the sorption was by sorbent and not by the wall of the container. At the end of the experiment the sorbent-sorbate mixture was centrifuged at  $3 \times 10^3$  rpm for phase separation. The supernatant was analysed for its dye concentration using UV-Visible Spectrophotometer (Perkin Elmer Lambda 35 UV-Vis Spectrophotometer). The measurements were made at the wavelength corresponding to maximum absorption; for BY11,  $\lambda_{\text{max}} = 412$  nm; for BB3,  $\lambda_{\text{max}} = 654$  nm and for MB,  $\lambda_{\text{max}} = 664$  nm.

#### **3.3.1 Effect of pH**

0.10 g of sorbent was added to 20 mL of 100 mg/L dye solutions at pH 2, 3, 4, 5, 6, 7, 8, 9 and 10. The desired pH value was adjusted by dropwise addition of hydrochloric acid (HCl) and sodium hydroxide (NaOH), prior to the experiment. The solutions were then agitated for 4 hours at the speed of 150 rpm.

#### **3.3.2 Effect of Initial Dye Concentration and Contact Time**

0.10 g of sorbent was added to 20 mL of 50 mg/L dye solution and shaken at 150 rpm for various time intervals at 5, 10, 15, 30, 60, 120, 180, 240,

300, 360 and 420 minutes. The above steps were repeated using dye concentrations of 100, 150 and 200 mg/L dye solutions.

### **3.3.3 Effect of Agitation Rate**

The influence of different agitation rate on the dye adsorption was conducted by agitating 0.10 g of sorbent in 20 mL of 100 mg/L dye solution at various speeds of 100, 150 and 200 rpm. The mixture was shaken at various time intervals of 5, 10, 15, 30, 60, 120, 180, 240, 300, 360 and 420 minutes.

### **3.3.4 Study of Sorption Isotherm**

Sorption isotherm was studied by agitating 0.10 g of sorbent with 20 mL of 50 mg/L dye solution for 4 hours at 150 rpm. The concentration of dye solution was varied from 50 – 300 mg/L.

### **3.3.5 Effect of Temperature**

The effect of temperature on the dye adsorption was carried out by agitating 0.10 g of sorbent with 100 mg/L dye solution at temperature of 30, 40, 50, 60 and 70°C. The mixture was shaken at 150 rpm for 4 hours.

### **3.3.6 Effect of Particle Size**

The sorbent was sieved into several particle sizes, <300 micron, 300 – 600 micron and >600 micron, For each group of particle size, 0.10 g of sorbent was added to 20 mL of 100 mg/L dye solution and agitated at 150 rpm for 4 hours to study the dye uptake.

### **3.3.7 Effect of Sorbent Dosage**

The effect of sorbent dosage on dye sorption was accessed by agitating 20 mL of 100 mg/L dye solution using 0.05, 0.10, 0.15 and 0.20 g of NSB for 4 hours at 150 rpm.

## **3.4 Chemical modification of Surface Functional Groups**

### **3.4.1 Esterification**

2.0 g of sorbent was added to mixture of 150 mL of methanol with few drops of concentrated hydrochloric acid. Then the mixture was heated at 60°C and stirred for 48 hours. The modified sorbent was then rinsed with distilled water and dried.

### 3.5 Optimisation of Dye Adsorption

#### 3.5.1 Plackett-Burman Design

Plackett-Burman design was used to evaluate the effect of various variables that influence the percentage uptake of dyes. In this study, 5 assigned variables (pH, contact time, initial dye concentration, sorbent particle size and sorbent dosage) were screened in 12 experimental designs generated by Design Expert Version 7.1.3 software. The statistical analysis of the data was carried out using the same software.

#### 3.5.2 Optimisation of Percentage Uptake

In this study, central composite design (CCD) model was used. The variables studied were obtained from the result of Plackett-Burman study and the percentage uptake of dye was optimised using following cubic equation:

$$Y = \beta_o + \sum_{i=1}^2 \beta_i X_i + \sum_{i=1}^2 \beta_{ii} X_i^2 + \sum_{i=1}^2 \beta_{iii} X_i^3 + \sum_{i=1}^1 \sum_{j=i+1}^2 \beta_{ij} X_i X_j + \sum_{i=1}^1 \sum_{j=i+1}^2 \beta_{ijj} X_i X_j^2 + \sum_{i=1}^1 \sum_{j=i+1}^2 \beta_{ijj} X_i^2 X_j$$

where  $\beta_o$ ,  $\beta_i$ ,  $\beta_{ii}$ ,  $\beta_{iii}$ ,  $\beta_{ij}$ ,  $\beta_{ijj}$  and  $\beta_{ijj}$  are the constant coefficients, and  $X_i$ , and  $X_j$  are the independent variables. All the experimental design and statistical analysis of the data were carried out by using Design Expert Version 7.1.3 software.

### **3.6 Column Study**

Continuous flow sorption experiments were performed in a glass column (1 cm interval diameter). Sorbent was packed into the glass column followed by running distilled water through the column prior to the dye solutions to achieve hydraulic equilibrium. Next, the column was fed with dye solution and the eluants were collected at 10 mL fractions. The flow rate was controlled by using peristaltic pump.

#### **3.6.1 Effect of Flow Rate**

The effect of different flow was studied using flow rate of 7, 10 and 15 mL/min. The bed height was fixed at height of 12 cm (0.5 g) and the influent concentration was remained constant at 10 mg/L.

#### **3.6.2 Effect of Influent Concentration**

The effect of different influent concentrations in the breakthrough curve was studied using dye concentration of 5, 10, 15 and 20 mg/L. The column was packed with 1.00 g of sorbent and the flow rate was maintained and regulated at 10 mL/min.

### **3.6.3 Effect of Bed Height**

The column was packed with 0.50 g (12 cm), 0.75 g (18 cm) and 1.00 g (24 cm) of sorbent. The column was fed with 10 mg/L of dye solution and the flow rate was maintained at 10 mL/min.

## **3.7 Instrumental Analysis**

### **3.7.1 Fourier-Transform Infrared Spectroscopy**

The functional groups of NSB before and after sorption were determined using Perkin-Elmer FTIR, Spectrum RX1 at wave number range of 400 – 4000  $\text{cm}^{-1}$ . The sample disk was prepared by mixing KBr powder with dried biosorbent, then ground and compressed into pellet before it was analysed.

### **3.7.2 Scanning Electron Microscope (SEM) Analysis**

The surface morphology of NSB before and after sorption was studied using SEM which equipped with energy dispersive X-ray Spectrometer (SEM-EDX)-JOEL JSM-6400.

### **3.7.3 Atomic Force Microscope (AFM) Analysis**

The surface morphology of NSB before and after sorption was studied using AFM (Park System, XE-70).

## CHAPTER 4

### RESULTS AND DISCUSSIONS

#### 4.1 Comparative Study on the Uptake of Various Dyes by NSB

The NSB was used to adsorb various dyes in order to determine which dyes showed the greatest percentage uptake. The experiments were carried out by agitating 0.10 g of NSB in 20 mL of 25 mg/L of each dye solution at 150 rpm for 7 hours..

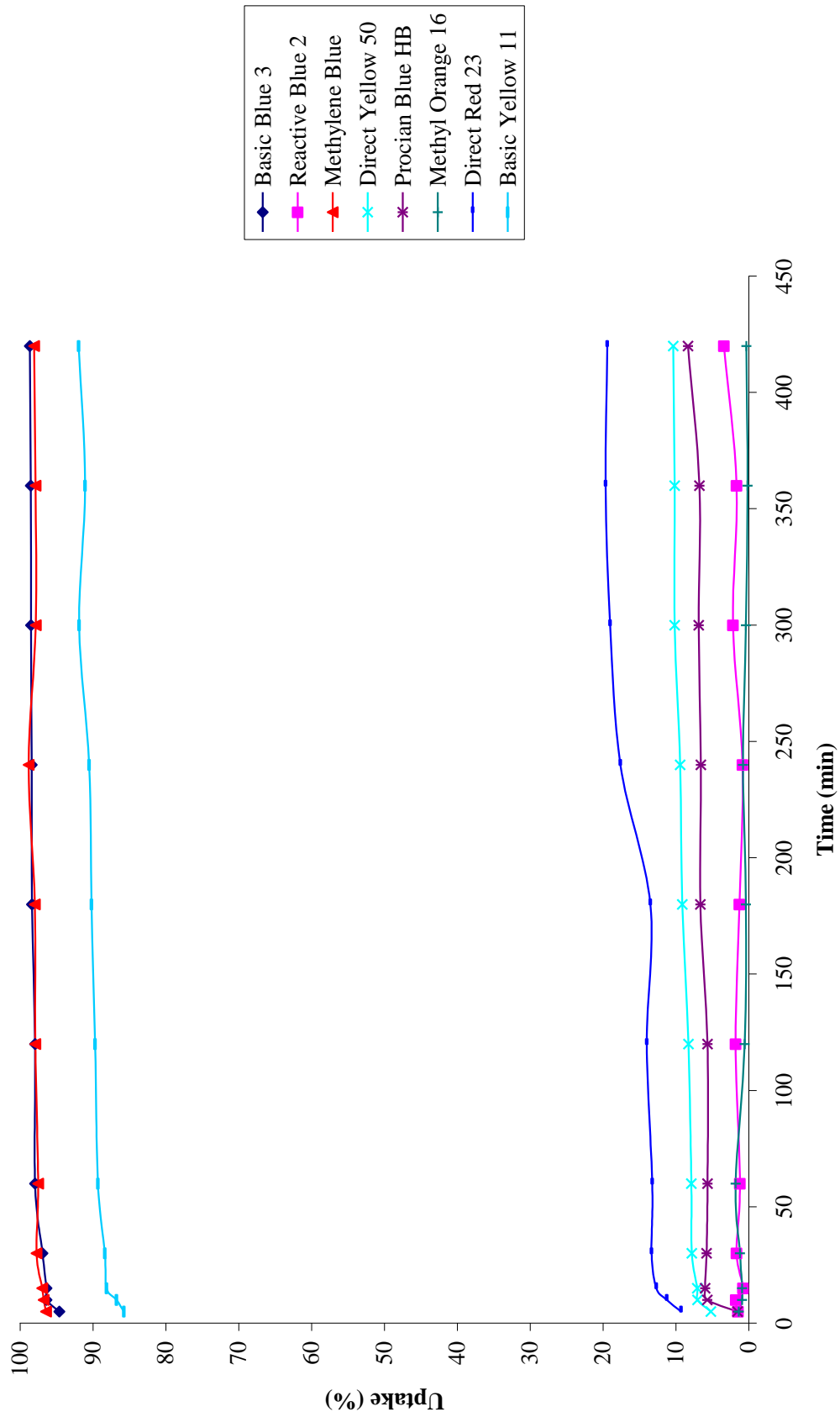
The percentage of dye uptake was calculated using the following equation:

$$\% \text{ uptake of dye} = \left( \frac{C_o - C_t}{C_o} \right) \times 100 \quad (1)$$

where  $C_o$  is the initial dye concentration and  $C_t$  is the dye concentration (mg/L) at time  $t$ .

Figure 4.1 shows the comparative study on the percentage uptake of various dyes. From the data obtained, BB3, MB and BY11 showed the highest percentage uptake. Therefore, BB3, MB and BY11 were used as the targeted dyes in single and binary solutions for the following studies.





Condition: 0.1 g of sorbent in 20 mL of 100 mg/L dye solution at 150 rpm for 4 hours at room temperature of  $25 \pm 2^\circ\text{C}$

Figure 4.1: Comparative study on the percentage uptake of various dyes

## 4.2 Fourier Transform Infrared (FT-IR) Analysis of Sorbent

The FT-IR analysis was used to study the changes in the functional groups of NSB before and after sorption. Figure 4.2 shows that there is no significant difference in the functional groups present in NSB before and after sorption. NSB shows absorption in the region of  $3200 - 3600 \text{ cm}^{-1}$  indicates the existence of free and intermolecular bonded hydroxyl groups. The peak observed at  $2905 \text{ cm}^{-1}$  can be assigned to stretching vibration of C-H group. Peaks around  $1720 \text{ cm}^{-1}$  were due to the C=O group and around  $1620 \text{ cm}^{-1}$  corresponded to C=C or asymmetric and symmetric stretching C=O vibrations. A strong C-O band was observed at  $1051 \text{ cm}^{-1}$  was due to  $-\text{OCH}_3$  group, showing the presence of lignin structure in the NSB (Garg *et al*, 2008). The peak at  $610 \text{ cm}^{-1}$  was due to the bending modes of aromatic compounds.

## 4.3 Scanning Electron Microscopy

Scanning Electron Microscope was used to study the morphology of NSB before and after sorption. Figure 4.3 shows that there is no significance difference in the surface morphology of NSB before and after sorption. In addition, it is observed that the NSB was non-porous material due to the lack of pores and cavities.

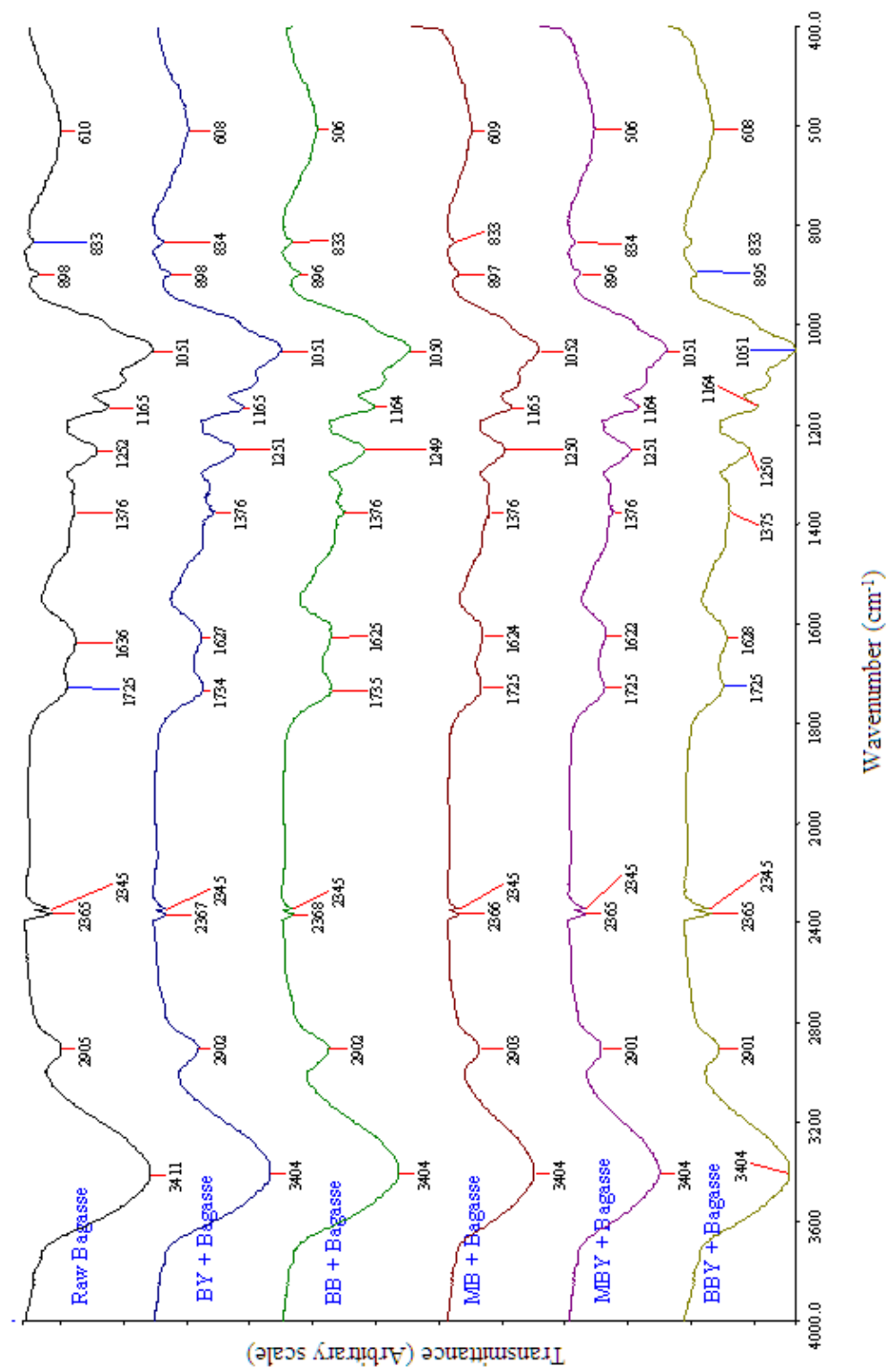
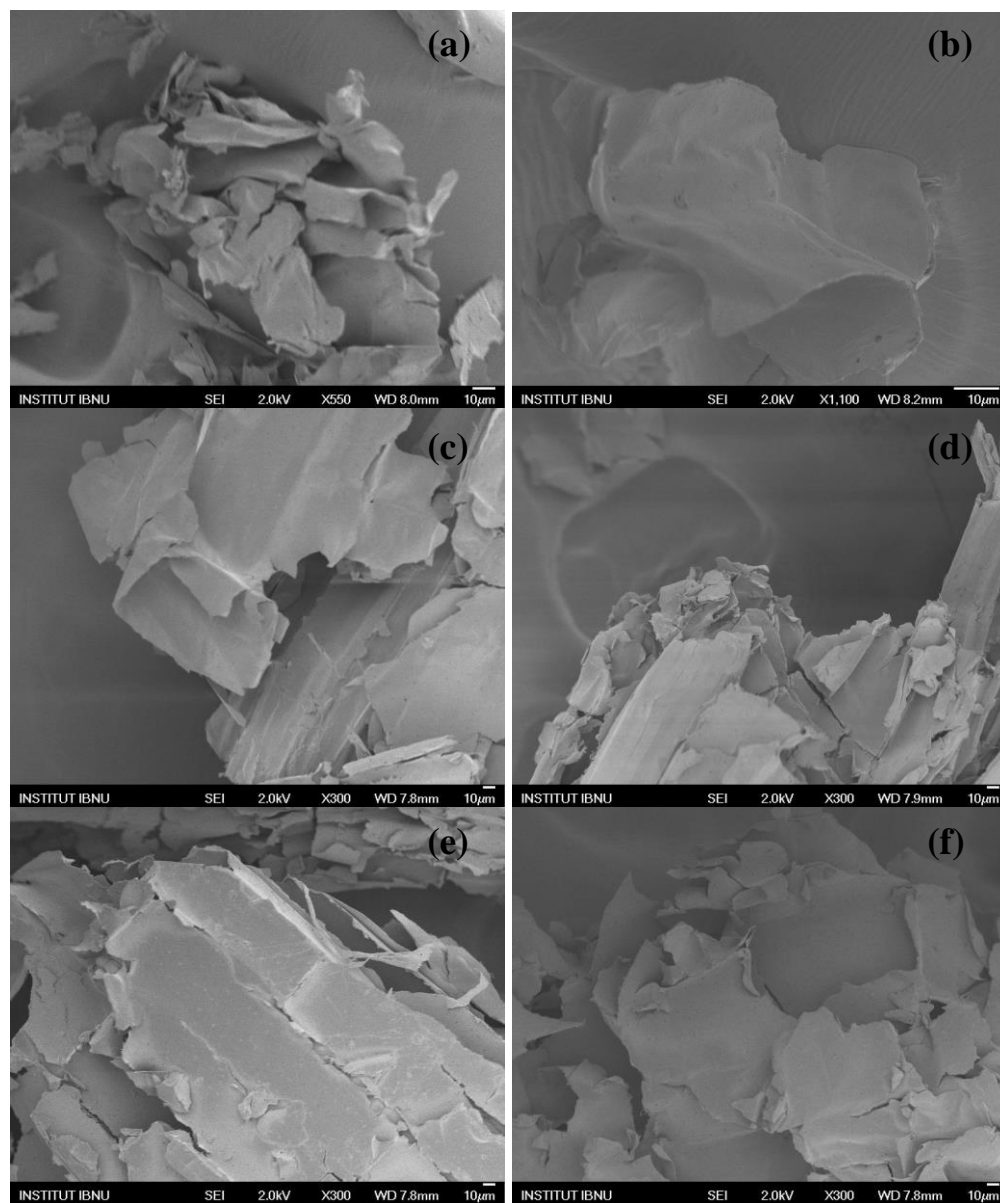


Figure 4.2: Infrared spectra of NSB before and after sorption



**Figure 4.3: SEM micrograph of NSB before (a), and after (b) BB3 adsorption, (c) MB adsorption, (d) BY11 adsorption, (e) BB3-BY11 adsorption and (f) MB-BY11 adsorption**

#### 4.4 Atomic Force Microscopy

Figure 4.4 shows the surface morphology of NSB before and after sorption. The surface morphology of NSB before sorption exhibited flat smooth plateau like structure with average grain length of 2.802  $\mu\text{m}$ . Meanwhile, all sorbed NSB showed pellet like structure with average grain length ranging from 0.890 to 0.975  $\mu\text{m}$ . The change in the surface morphology might be due to the binding of the dye molecules to the surface of the sorbent.

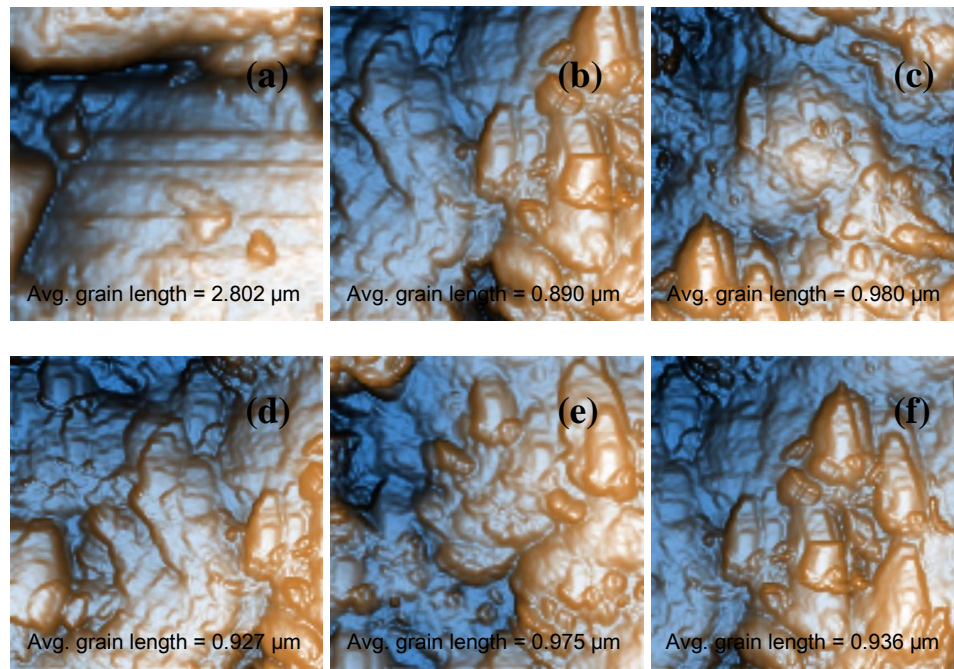


**Figure 4.4: AFM micrograph of NSB before (a), and after (b) BB3 adsorption, (c) MB adsorption, (d) BY11 adsorption, (e) BB3-BY11 adsorption and (f) MB-BY11 adsorption**

#### 4.5 Sorption Mechanism

Sugarcane bagasse consists of mainly cellulose (40%), hemicelluloses (24%) and lignin (25%) (Sun and Cheng, 2002). Cellulose is a linear polymer with  $\beta$ -D-glucopyranose units and non-water soluble. Hemicellulose is a low molecular weight chemically ill-defined polysaccharide, thus it can be dissolved in water (El-Hendawy, 2006). Both cellulose and hemicelluloses consist majority of oxygen functional groups such as hydroxyl, ether and carbonyl which exist in lignocellulosic material (Figure 4.5). Meanwhile, lignin is a complex, systematically polymerised, highly aromatic substance, and acts as a cementing matrix holding between and within cellulose and hemicelluloses units (Al-Ghouti *et al.*, 2010).

According to Simoncic *et al.* (2008), the polysaccharide-bound hydroxyl groups may still allow the surface of relatively pure cellulose to be classified as acidic although they do not significantly release protons in the pH range up to about 12. This conclude that the cellulose may still be negatively charge at neutral pH, hence capable to bind to positively charged dye's molecules. In addition, the dissociation of carboxylic acid groups associated with hemicellulose, certain extractions and other components of cellulosic surface contributes negatively surface charge (Hubbe and Rojas, 2008). In another study, Shigo (2001) stated that cellulose has many oxygen and hydrogen units as part of its makeup. Because

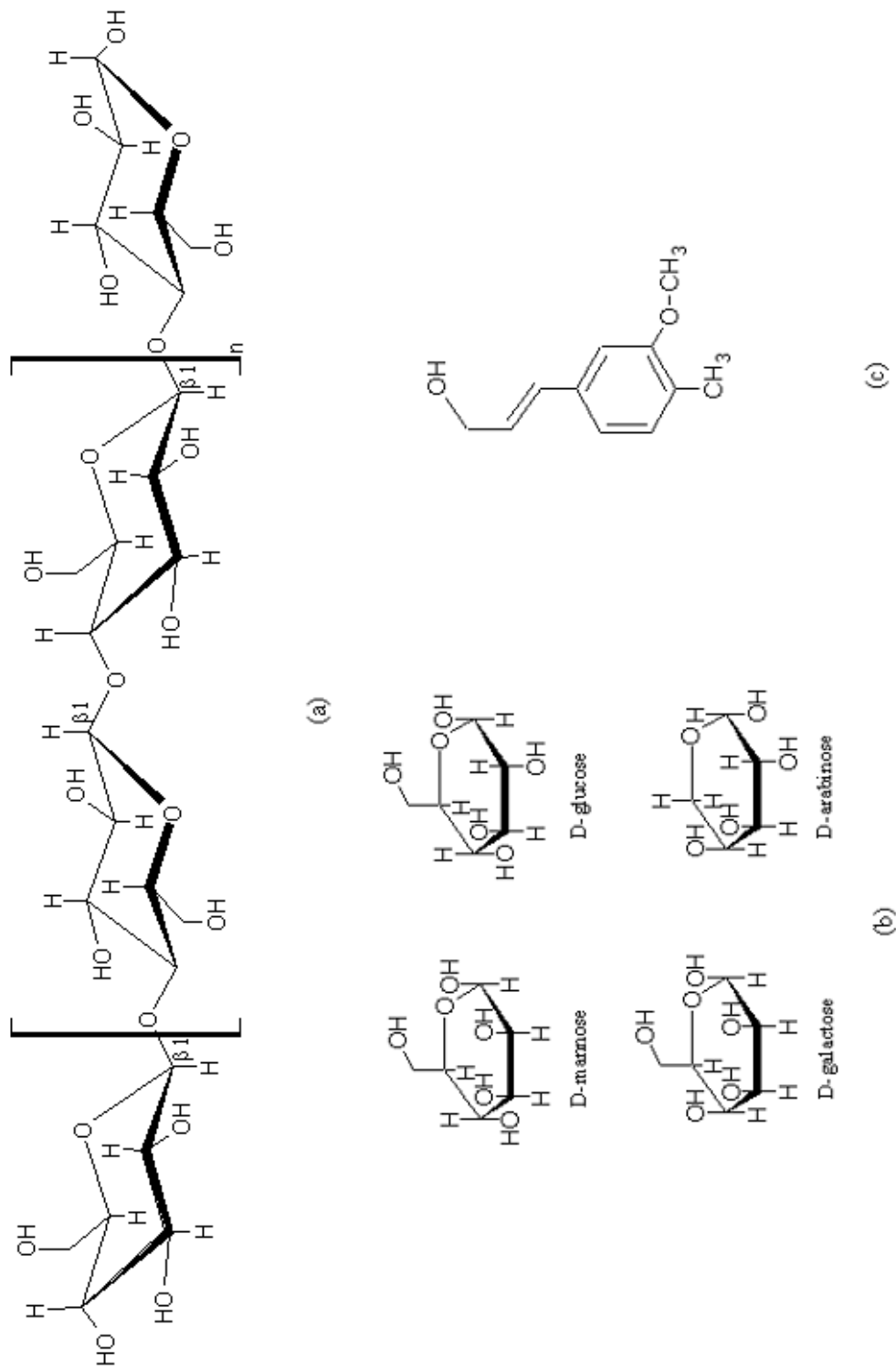
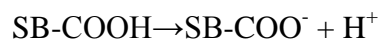


**Figure 4.5: (a) Cellulose molecule, (b) principal sugar residues of hemicellulose, (c) phenylpropanoid units found in lignin (El-Hendawy, 2006)**

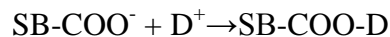
oxygen has a weak negatively charge, the site could be potential bonding site for a positive charge atom or molecule.

Figure 4.6 shows the pH of point of zero charge ( $\text{pH}_{\text{pzc}}$ ) of NSB and the  $\text{pH}_{\text{pzc}}$  determined was pH 5. This indicated that NSB carried negatively charge at neutral pH. The sorption mechanism is postulated as below:

Deprotonation



Binding of dye cation



where, SB and D represent the surface of NSB and dye molecule, respectively.

The steps involve are deprotonation of the bagasse forming negatively charge sites followed by the binding of the dye cations. When the pH of the dye solution is high enough, the NSB can release protons thus acquired a net negative charge which favours the adsorption of basic dyes. In a study by Al-Ghouti *et al.* (2010) on the removal of heavy metals and dyes using date pits, they proposed that there were electrostatic attraction between MB cations and the cellulose-O<sup>-</sup> on the raw date pits (RDP) surface (Figure 4.7).



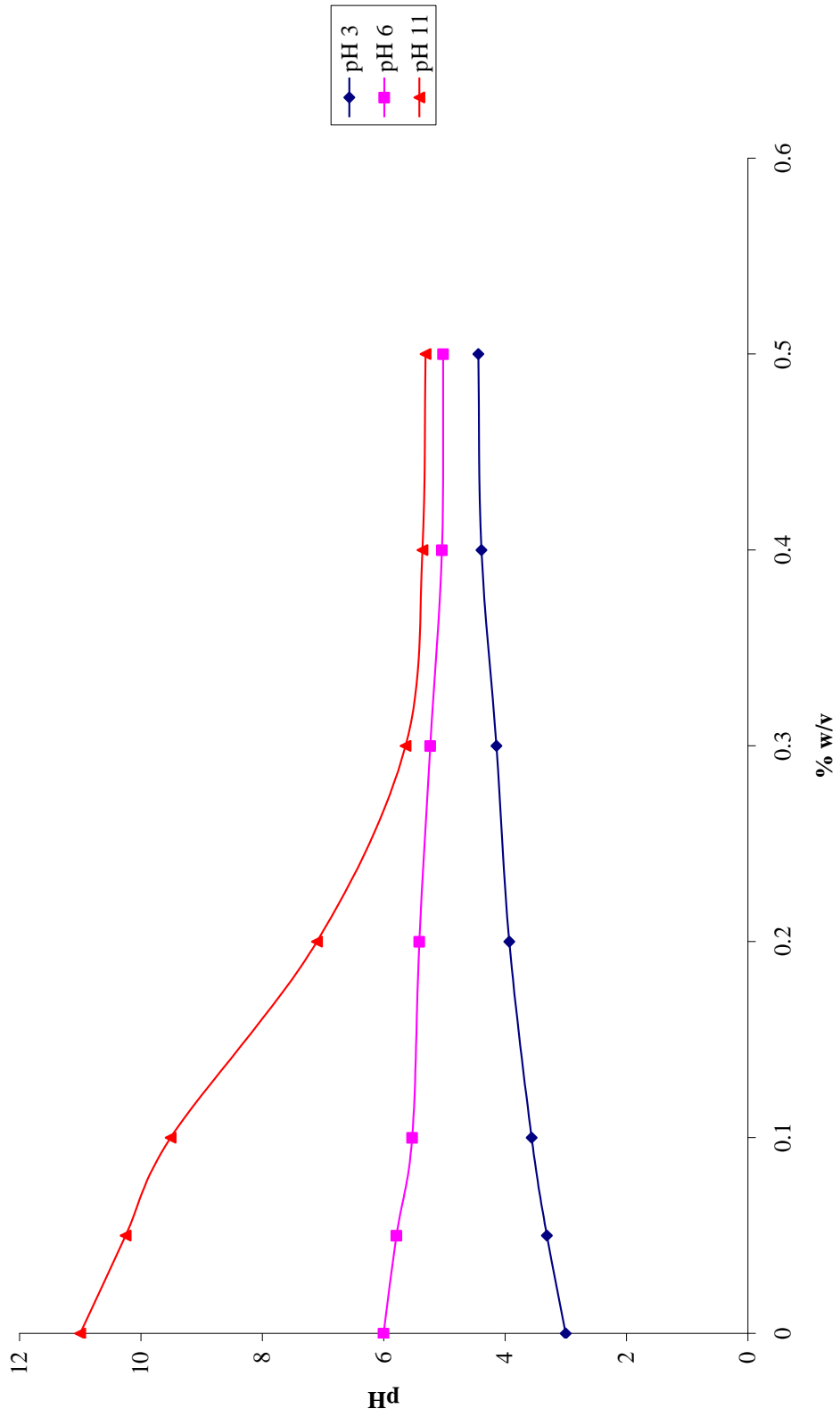


**Figure 4.6: Point-zero-charge (P<sub>zc</sub>) of NSB**

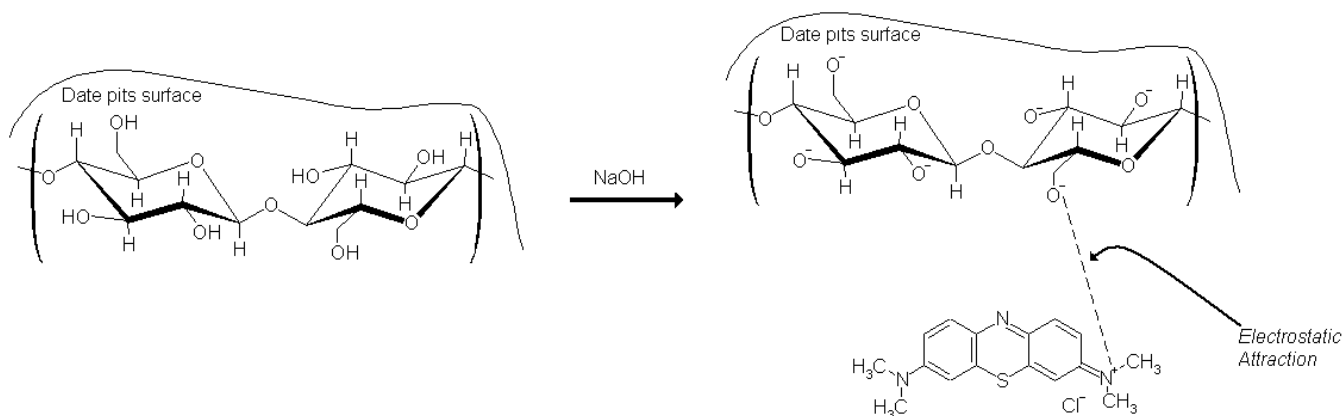


**Figure 4.7: Electrostatic attraction between MB and RDP surfaces (Al-Ghouti *et al.*, 2010)**

The binding of BB3, MB and BY11 may also be due to the formation of surface hydrogen bonds between the hydroxyl groups on NSB surface and the nitrogen atoms of the dyes (Figure 4.8). A study by Kaewprasit *et al.* (1998) assumed that a complete monolayer adsorption of MB onto the surface of the cotton fiber was formed through hydrogen bond between the cotton fibers surface and the nitrogen and sulphur of MB molecules (Figure 4.9).

Esterification of NSB is carried out and the dye adsorption using esterified-SB shows a reduction in percentage uptake for all dye solutions compared to NSB (Figure 4.10). This might be due to the esterification of  $-OH$  and  $-COOH$  functional groups on the sorbent thus impeding the deprotonation process.

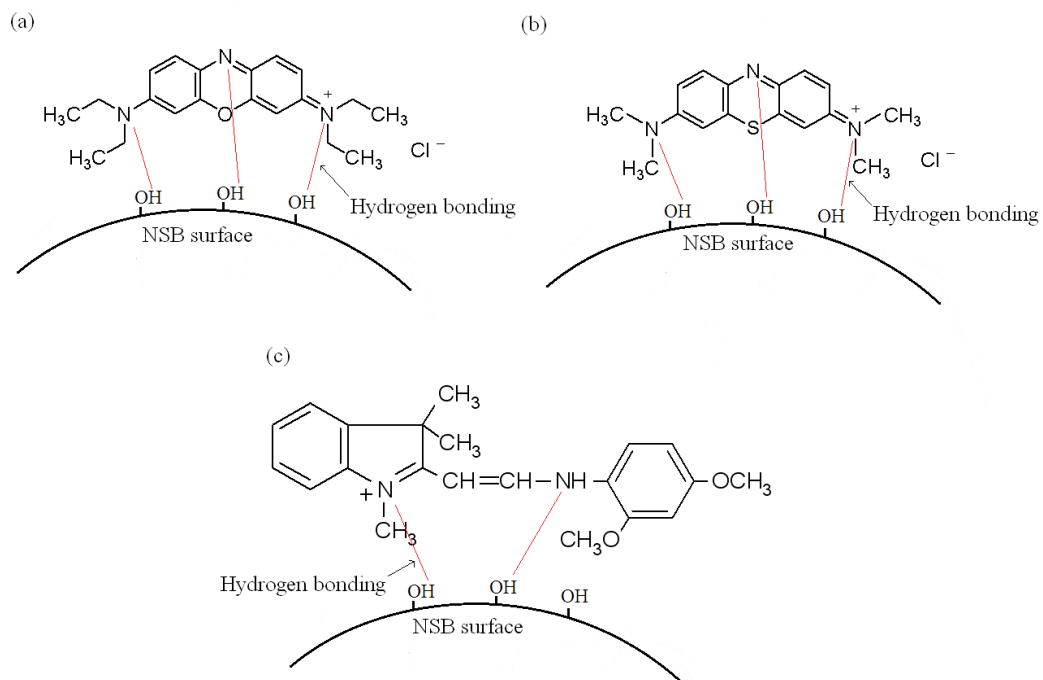


**Figure 4.8: Schematic models of (a) BB3, (b) MB and (c) BY11 and NSB surface**

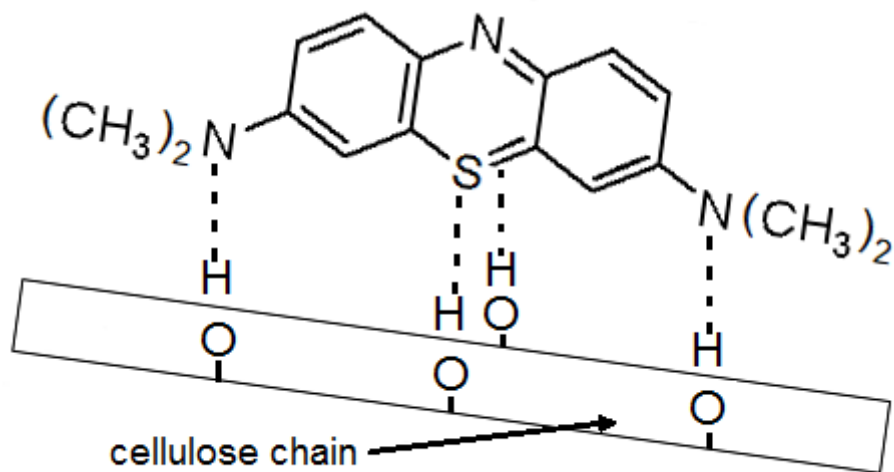
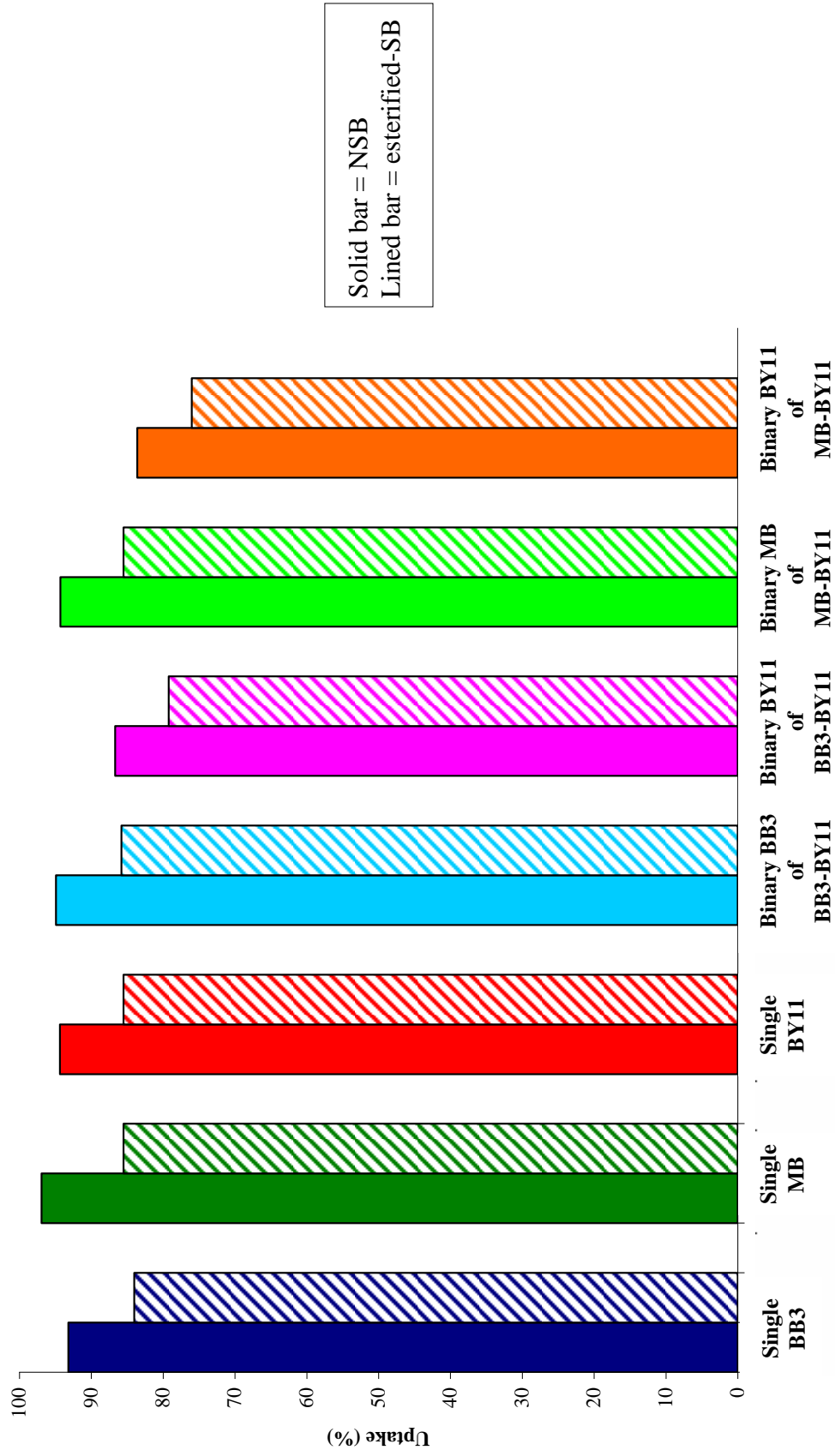


**Figure 4.9: Schematic representation of MB and cotton fiber interaction (Kaewprasit *et al.*, 1998)**



**Condition:** 0.1 g of sorbent in 20 mL of 50 mg/L dye solution at 150 rpm for 4 hours at room temperature of  $25 \pm 2^\circ\text{C}$

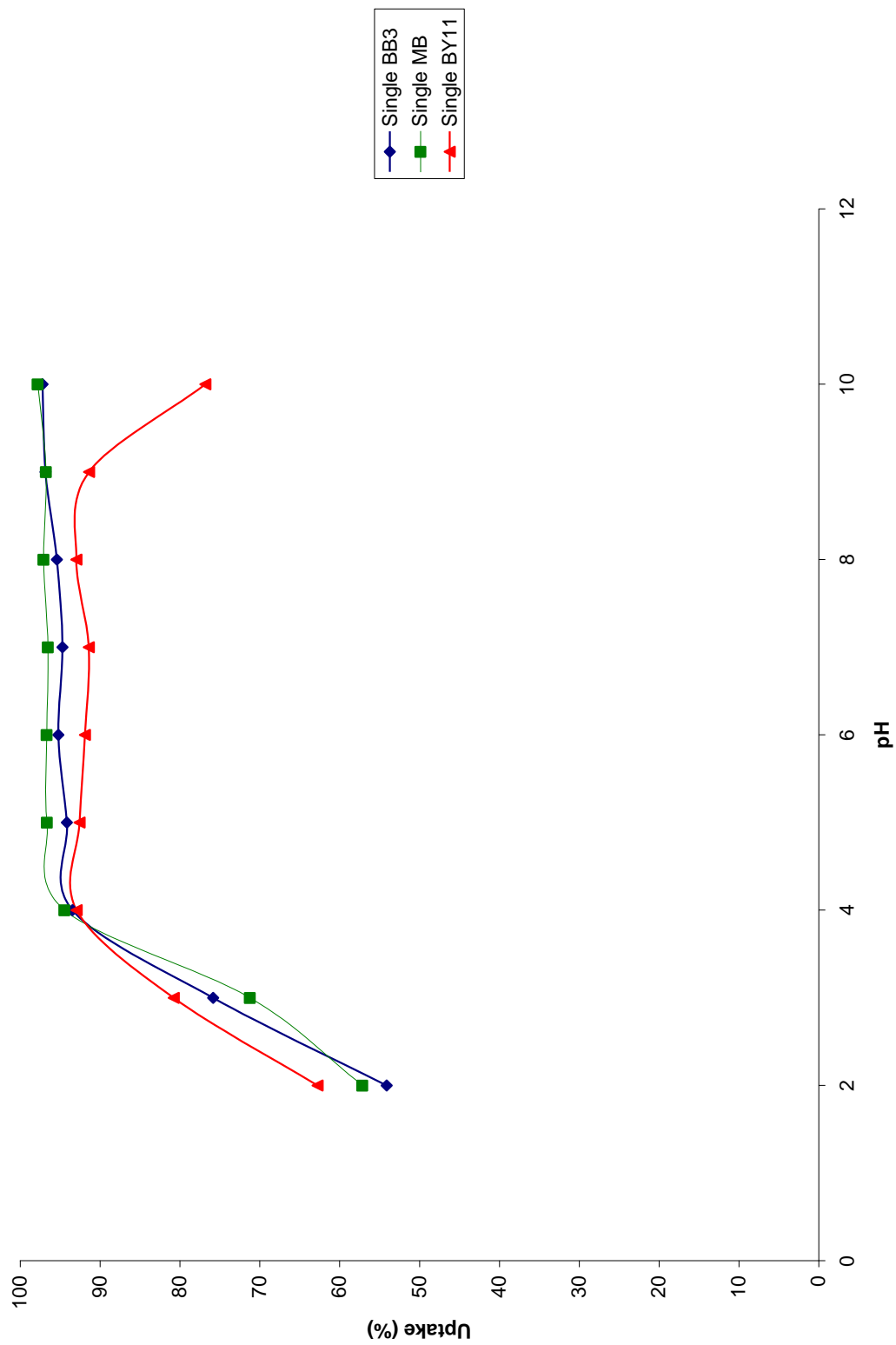
**Figure 4.10: Comparative study on the percentage uptake of various dyes onto NSB and esterified-SB**

## 4.6 Batch Studies

### 4.6.1 Effect of pH

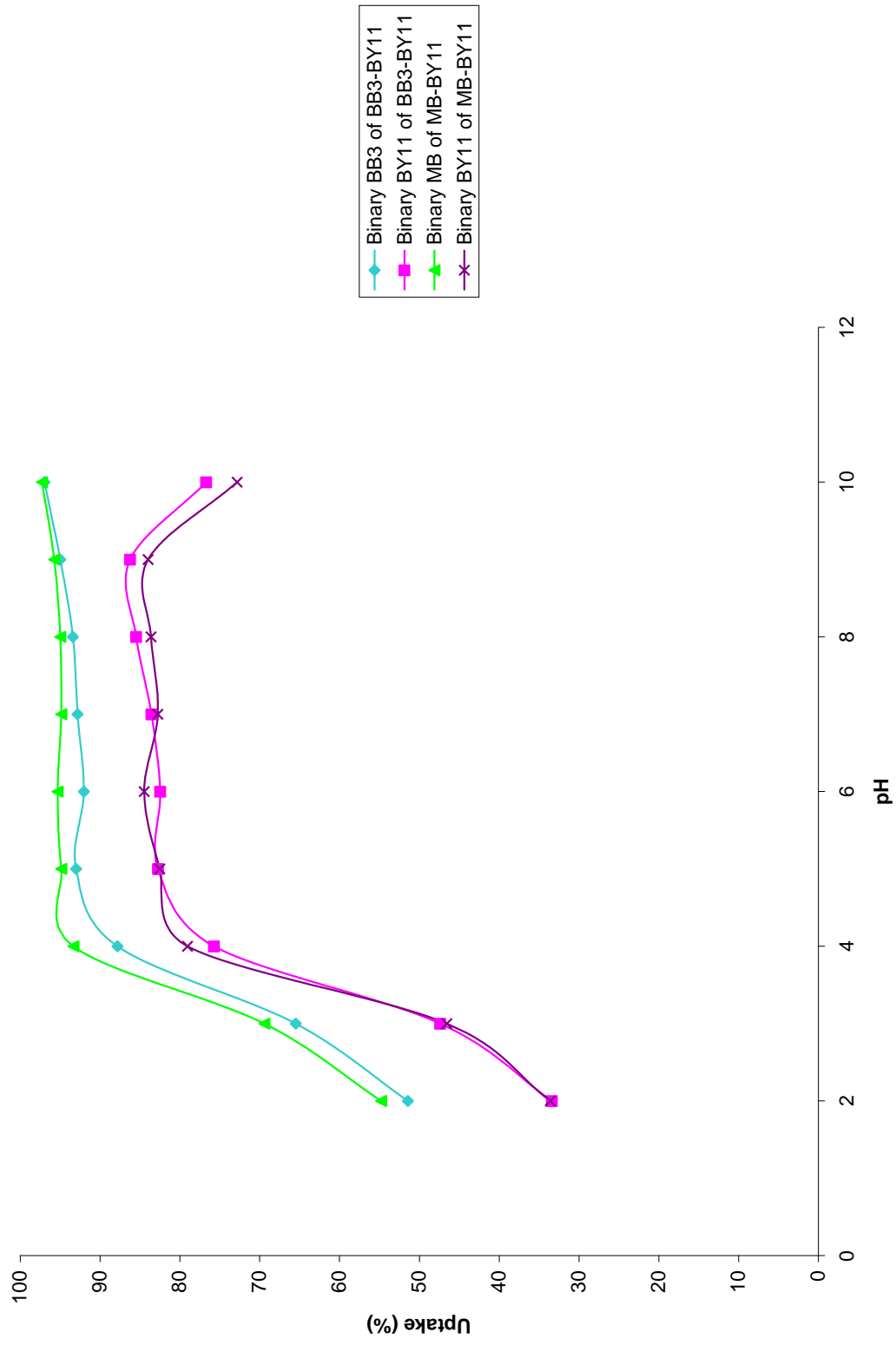
Figures 4.11 and 4.12 show the effect of pH on the uptake of BB3, MB and BY11 on NSB for both single and binary solutions, respectively. The lowest uptake for all dye solutions was observed at pH 2. As the pH of the initial dye solutions increased, the percentage uptake increased. A sharp increase in percentage uptake was observed between pH 2 to 4. The percentage uptake remained almost constant over the pH range of 4 to 9. However a slight drop in percentage uptake of BY11 was observed for both single and binary solutions at pH 10.

With increasing pH, the number of positively charged sites decreased and the number of negatively charged sites increased. This favours the sorption of basic dyes due to electrostatic attraction, which resulting an increase in percentage uptake (Namasivayam *et al.*, 2001). In addition, the excess of  $H^+$  ions in the solution at lower pH will also compete with the dye cations for the available binding sites. Therefore, lower solution pH does not favour the sorption of positively charged dye cations. A slight drop in percentage uptake of BY11 in single and binary solutions might due to the occurrence of another mode of



**Condition:** 0.1 g of sorbent in 20 mL of 100 mg/L dye solution at 150 rpm for 4 hours at room temperature of  $25 \pm 2^\circ\text{C}$

**Figure 4.11: Effect of pH on the sorption of BB3, MB and BY11 in single solutions onto NSB**



**Condition:** 0.1 g of sorbent in 20 mL of 100 mg/L BB3 dye solution at 150 rpm for 4 hours at room temperature of  $25 \pm 2^\circ\text{C}$

**Figure 4.12: Effect of pH on the sorption of BB3, MB and BY11 in binary solution onto NSB**

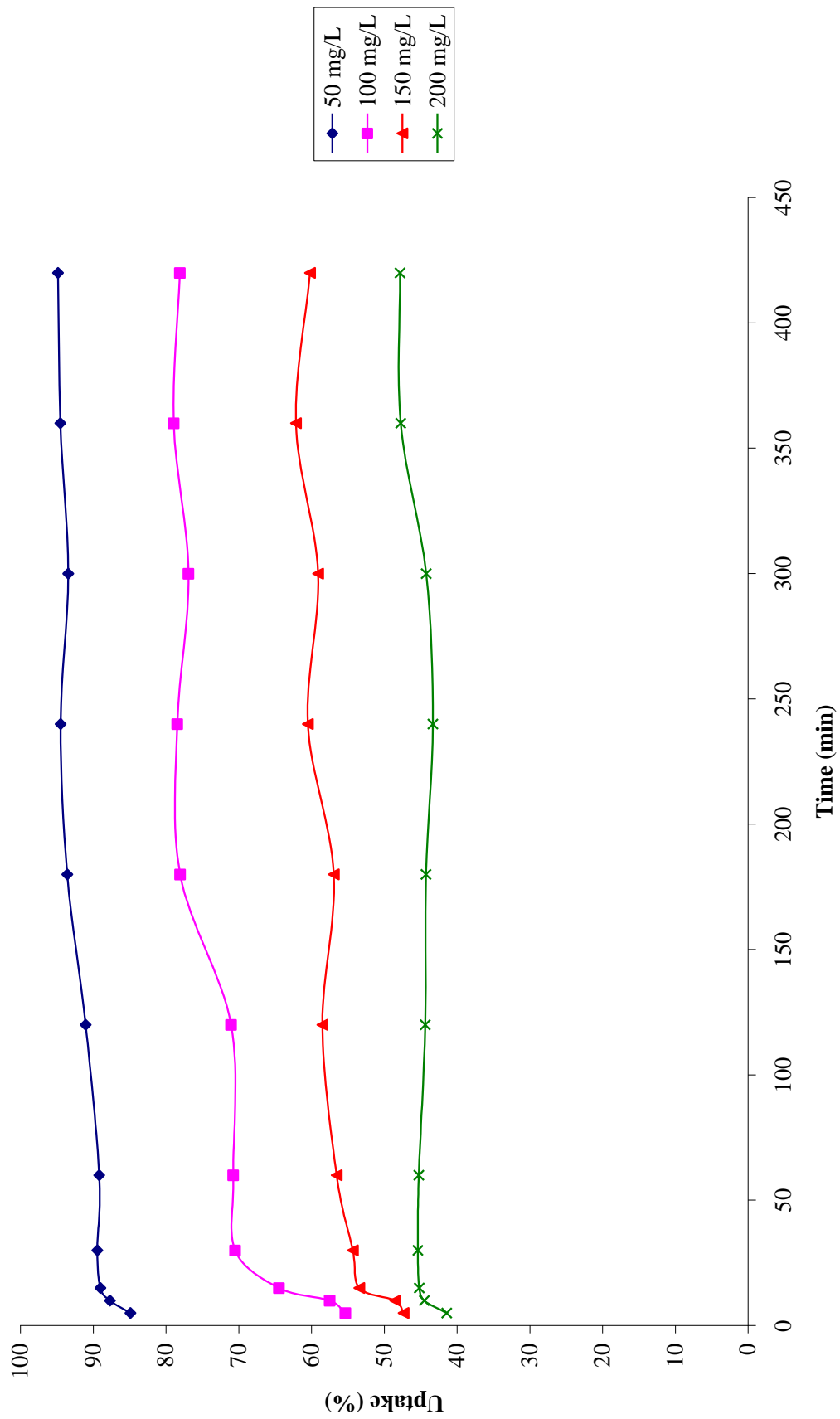
sorption, such as ion exchange or chelation (Hamdaoui, 2006). There is also a possibility that the NSB might be subjected to hydrolysis, which creates positively charged sites which is not favorable for removing cationic species (Garg *et al.*, 2004).

In a previous work done by Ong *et al.* (2007) in the removal of basic and reactive dyes using ethylenediamine modified rice hull, they proposed that at low pH of dye solution, the carboxyl groups on the biosorbent surface which are responsible for binding the dye cations are predominantly protonated, therefore lead to a lower uptake of the dyes. As the pH of the dye increased, sorption became favourable due to the deprotonation of the carboxyl groups, resulted in an increase of available binding sites.

#### **4.6.2 Effect of Initial Concentration and Contact Time**

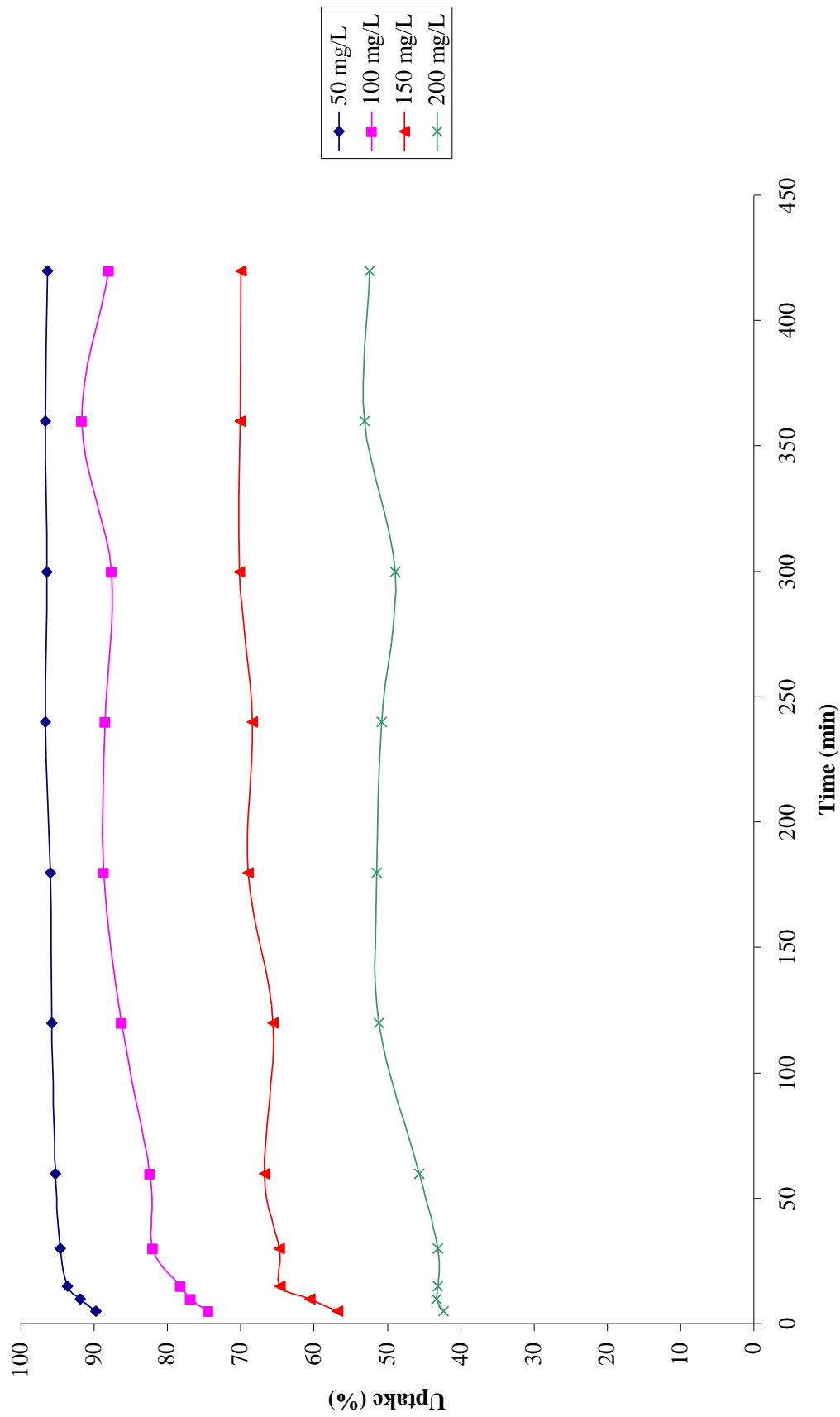
The effect of contact time on various initial dye concentrations on the percentage uptake of BB3, MB and BY11 in single and binary solutions by NSB are shown in Figures 4.13 – 4.17. The uptake for all the dyes increased rapidly at the first 15 minutes and gradually attained equilibrium after 60 minutes of agitation time. After first hour of agitation, the percentage uptake of dyes remained almost constant until the seventh hour, irrespective of dye concentrations.





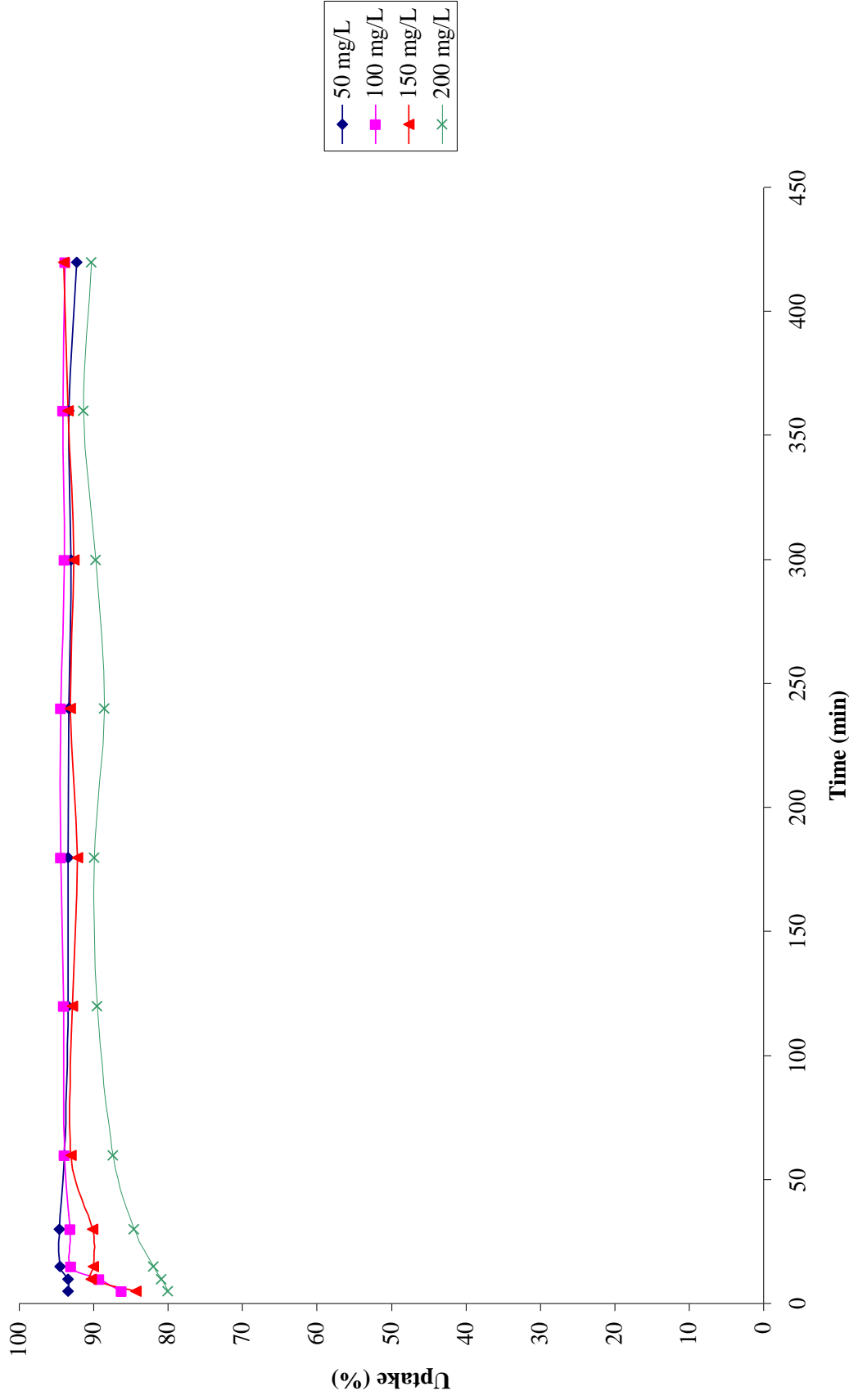
**Condition:** 0.1 g of sorbent in 20 mL of 50, 100, 150 and 200 mg/L BB3 dye solution at 150 rpm for 7 hours at room temperature of  $25 \pm 2^\circ\text{C}$

**Figure 4.13: Effect of contact time on the sorption of single BB3 solution onto NSB**



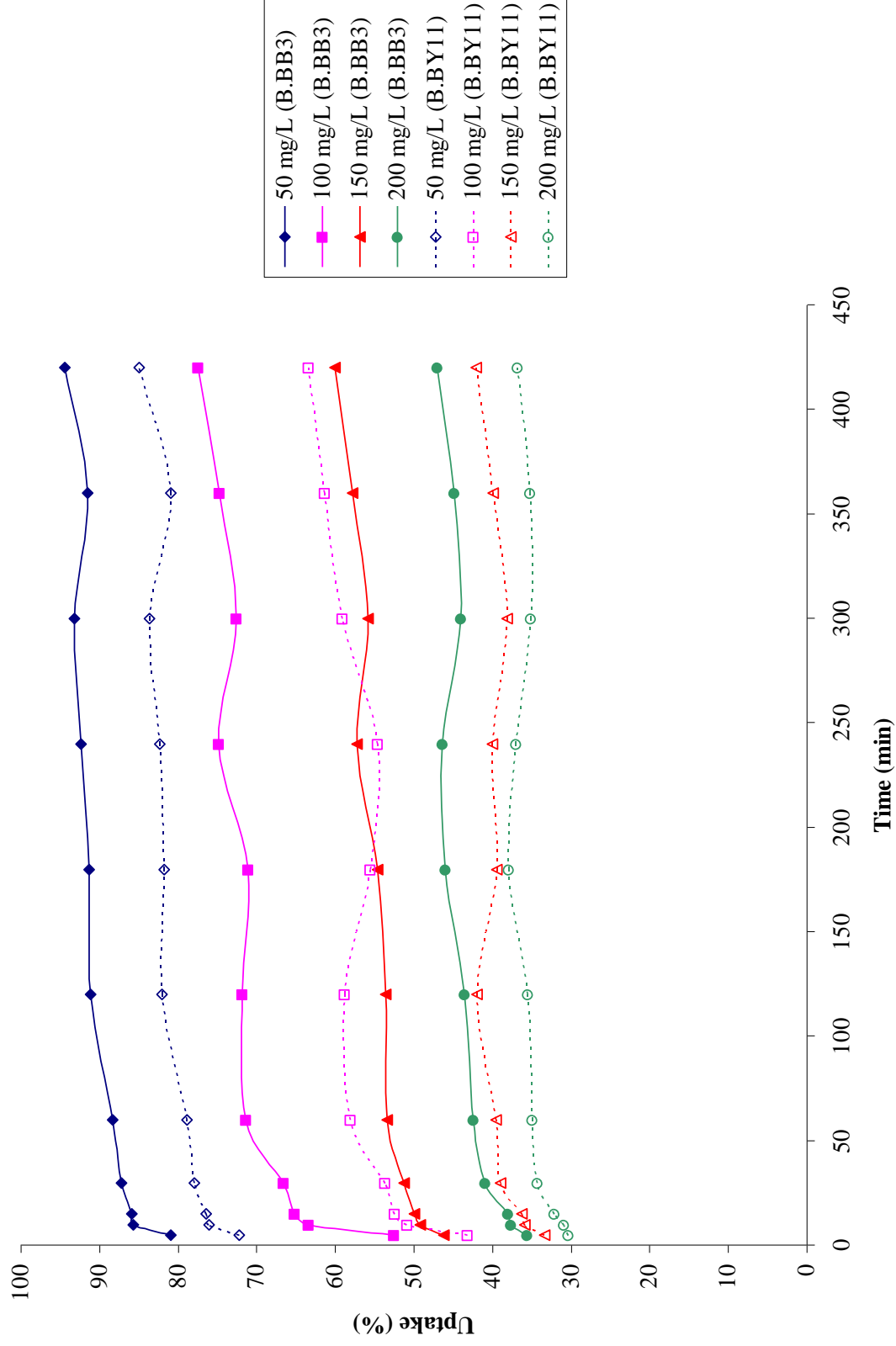
**Condition:** 0.1 g of sorbent in 20 mL of 50, 100, 150 and 200 mg/L MB dye solution at 150 rpm for 7 hours at room temperature of  $25 \pm 2^\circ\text{C}$

**Figure 4.14: Effect of contact time on the sorption of single MB solution onto NSB**



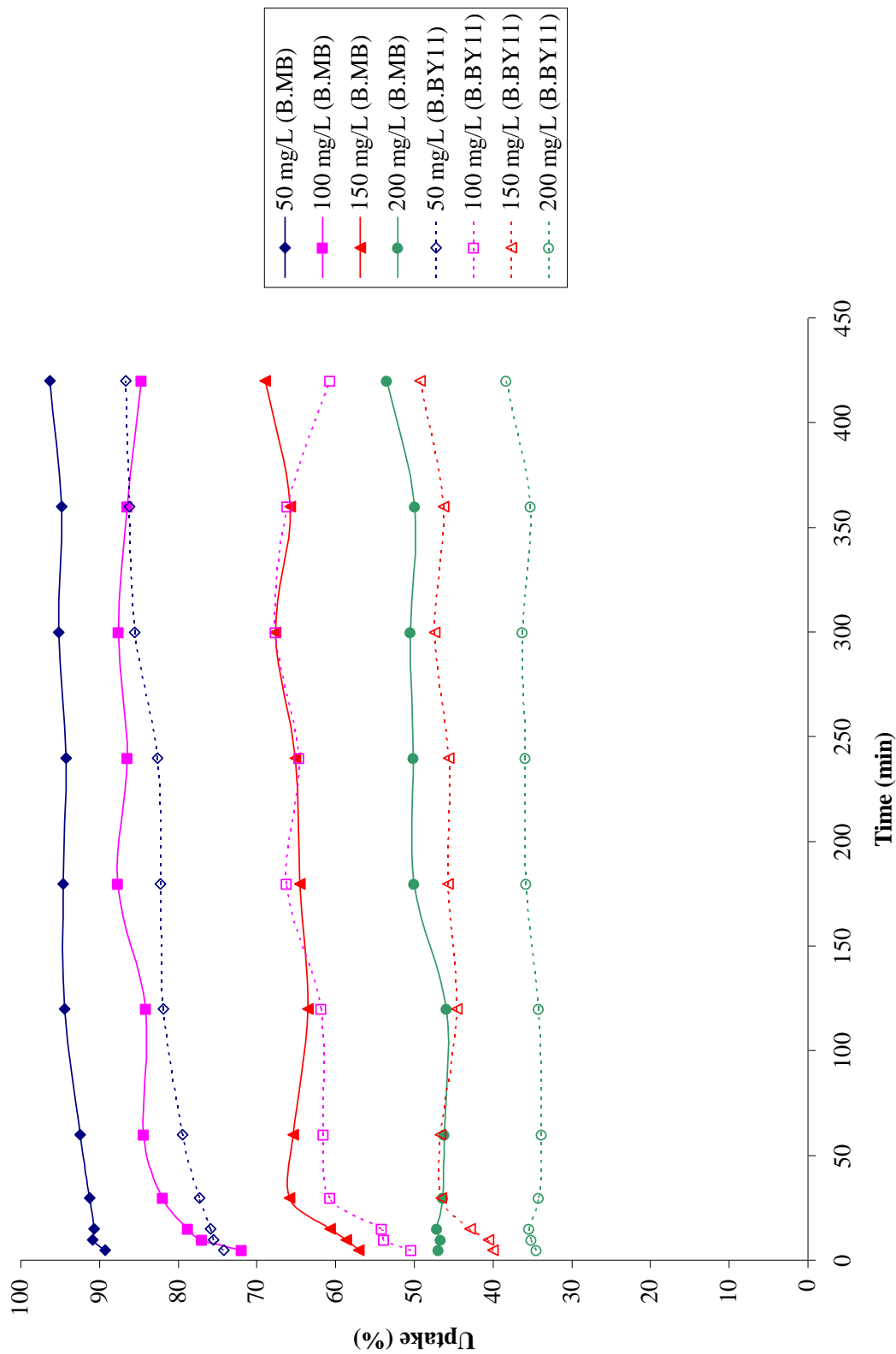
**Condition:** 0.1 g of sorbent in 20 mL of 50, 100, 150 and 200 mg/L BY11 dye solution at 150 rpm for 7 hours at room temperature of  $25 \pm 2^\circ\text{C}$

**Figure 4.15: Effect of contact time on the sorption of single BY11 solution onto NSB**



**Condition:** 0.1 g of sorbent in 20 mL of 50, 100, 150 and 200 mg/L BB3 and BY11 dye solution at 150 rpm for 7 hours at room temperature of  $25 \pm 2^\circ\text{C}$

**Figure 4.16: Effect of contact time on the sorption of binary BB3-BY11 solution onto NSB**



**Condition:** 0.1 g of sorbent in 20 mL of 50, 100, 150 and 200 mg/L MB and BY11 dye solution at 150 rpm for 7 hours at room temperature of  $25 \pm 2^\circ\text{C}$

**Figure 4.17: Effect of contact time on the sorption of binary MB-BY11 solution onto NSB**

The rapid uptake at the initial stage showed that there were still plenty of readily accessible sites. It was also suggested that a strong attractive force occurred between the dye molecules and the sorbent. As the experiment proceeds, saturation occurred, resulting in the percentage uptake to be remained almost constant. This may also be due to the deficient in the number of available sorption sites at the end of the sorption process. Malik (2003) proposed that in the process of dye sorption, initially dye molecules have to first encounter the boundary layer effect, then adsorb onto the surface and finally diffuse into the porous structure of the adsorbent. This phenomenon will take a relatively longer contact time. The time profile of dye uptake is a single, smooth and continuous curve leading to saturation, suggesting the possible monolayer coverage of dye on the surface of the adsorbent.

A decrease in percentage uptake for all the dye solutions was observed as the initial dye concentration increased from 50 mg/L to 200 mg/L. This was due to the increase of the ratio of the dye's cations to the dosage of the adsorbent. A similar trend was observed in the study of the removal of basic and reactive dyes using quarterised sugar cane bagasse done by Wong *et al.*, (2009). They found that the percentage of dye removal decreased with increasing initial dye concentration. From their results, for RO16, 80 % dye removal was recorded for 50 mg/L, and then dropped to 60 % when the dye concentration increased to 150 mg/L. Similar observation was observed for BB3. The equilibrium time for BB3 and RO16 was recorded at 120 minutes and 180 minutes, respectively.

### 4.6.3 Kinetic Study

The kinetic of the dye sorption on NSB were examined using pseudo-first and pseudo-second order equation. According to Abd. El-Rahman *et al.* (2006), the process of dye sorption involved multisteps mechanism, consist of (i) diffusion across the liquid film surrounding the solid particles (a process controlled by an external mass transfer coefficient), (ii) diffusion within the particle itself assuming a pore diffusion mechanism (intraparticle diffusion) and (iii) physical or chemical sorption at a site.

The kinetics of the dye sorption on NSB was examined using the following equations [Lagergren, (1898); Ho and McKay, (1999); Ho and McKay, (2000)]:

$$\log (q_e - q_t) = \log q_e - \frac{k_1 t}{2.303} \quad (\text{pseudo- first order}) \quad (2)$$

and

$$\frac{t}{q_t} = \frac{1}{h} + \frac{t}{q_e} \quad (\text{pseudo- second order}) \quad (3)$$

where,

$q_e$  = the amount of dyes sorbed at equilibrium (mg/g)

$q_t$  = the amount of dyes sorbed at time  $t$  (mg/g)

$k_1$  = the rate constant of pseudo-first order sorption (1/min)

$h$  ( $k_2 q_e^2$ ) = the initial sorption rate (mg/g min)

$k_2$  = the rate constant of pseudo-second order kinetics (g/mg min)

The values of sorption capacities and regression coefficients for all dye solutions are shown in Table 4.1. Based on the correlation coefficients with both models, pseudo-second order kinetics exhibited a better correlation with the experimental data for all the solutions studied. In addition, for the whole range of concentrations studied, the equilibrium sorption capacities calculated based on pseudo-first order kinetic model gave large deviation compared to those determined experimentally (Table 4.1). Pseudo-first order kinetic model does not fit well to the whole range of contact time in many cases and is generally applicable over the initial stage of the sorption processes. In many cases, pseudo-second order kinetic model correlates well to sorption study (Wan Ngah *et al.*, 2004). Thus, the dye solutions studied are more appropriately described by pseudo-second order model which is based on the assumption that the rate limiting step may be chemical sorption or chemisorption involving valency forces through sharing or exchange of electron between sorbent and sorbate (Ho and McKay, 2000).

The values of  $q_e$ ,  $k_2$  and  $h$  against  $C_0$  in the corresponding linear plots of the pseudo-second order equation were regressed to obtain the expressions for these values in terms of the initial dye concentration. Each of these parameters can be expressed as a function of  $C_0$  for BB3, MB and BY11 (Ho and Mckay, 2000).



Table 4.1: Sorption capacities and regression coefficients of the effect of initial BB3, MB and BY11 in single and binary dye solutions

Dye systems	Initial concentration (mg/L)	Pseudo-first order		Pseudo-second order		Experimental Sorption capacities (mg/g)
		Sorption capacities (mg/g)	R <sup>2</sup>	Sorption capacities (mg/g)	R <sup>2</sup>	
BB3 (Single)	100	7.005	0.722	15.926	0.999	15.783
	200	22.798	0.336	18.450	0.996	17.013
MB (Single)	100	3.946	0.753	18.051	0.999	17.828
	200	21.662	0.754	21.598	0.998	21.003
BY11 (Single)	100	1.682	0.324	18.797	1.000	18.854
	200	6.717	0.731	36.232	0.999	35.381
Binary BB3-BY11	100	7.432	0.693	15.093	0.999	14.815
	200	23.818	0.688	18.939	0.999	19.012
BY11	100	10.088	0.636	12.092	0.994	10.631
	200	25.633	0.468	15.674	0.999	15.953
MB	100	4.264	0.520	17.094	0.999	17.163
	200	20.361	0.816	21.882	0.998	21.159
Binary MB-BY11	100	8.827	0.479	12.642	0.997	12.749
	200	25.316	0.560	15.699	0.998	15.284

$$q_e = \frac{C_o}{A_q C_o + B_q} \quad (4)$$

$$k_2 = \frac{C_o}{A_k C_o + B_k} \quad (5)$$

$$h = \frac{C_o}{A_h C_o + B_h} \quad (6)$$

where,  $A_q$ ,  $B_q$ ,  $A_k$ ,  $B_k$ ,  $A_h$  and  $B_h$  are constant related to the respective equations. The values of these constants are shown in Table 4.2. The generalised predictive models for BB3, MB and BY11 in single and binary sorbed at any initial concentration and contact time within the given range with relationship of  $q_e$ ,  $C_o$  and  $t$  can be represented as follows by substituting the various values in the pseudo-second order kinetic equation.

For BB3-NSB solution:

in single dye solution

$$q_t = \frac{C_o t}{0.2614C_o - 1.3846 + (0.0330C_o + 3.5496)t} \quad (7)$$

in binary dye solution

$$q_t = \frac{C_o t}{0.3180C_o - 3.4782 + (0.0325C_o + 3.5976)t} \quad (8)$$

Table 4.2: Empirical parameters for predicted  $q_e$ ,  $k$  and  $h$  from  $C_o$

Dyes	$A_q$ (g/mg)	$B_q$ (g/L)	$A_k$ (mg min/g)	$B_k$ (mg <sup>2</sup> min/g L)	$A_h$ (g min/mg)	$B_h$ (g min/L)
BB3 (Single)	$3.300 \times 10^{-2}$	3.550	105.312	$-4.145 \times 10^3$	0.261	- 1.385
MB (Single)	$2.160 \times 10^{-2}$	3.999	105.422	$-5.209 \times 10^3$	0.218	- 8.706
BY11 (Single)	$-3.000 \times 10^{-4}$	5.435	65.342	$-4.001 \times 10^3$	0.092	- 8.265
Binary BB3-BY11	BB3	3.598	121.617	$-4.839 \times 10^3$	0.318	- 3.478
	BY11	$5.030 \times 10^{-2}$	3.361	42.190	$-2.806 \times 10^2$	10.200
Binary MB-BY11	MB	$2.320 \times 10^{-2}$	3.952	113.620	0.204	- 5.658
	BY11	$4.820 \times 10^{-2}$	3.396	57.763	0.114	15.171

For MB-NSB solution:

in single solution

$$q_t = \frac{C_o t}{0.2177C_o - 8.0760 + (0.0216C_o + 3.9993)t} \quad (9)$$

in binary solution

$$q_t = \frac{C_o t}{0.2037C_o - 5.6582 + (0.0232C_o + 3.9519)t} \quad (10)$$

For BY11-NSB system:

in single solution

$$q_t = \frac{C_o t}{0.0924C_o - 8.2648 + (-0.0003C_o + 5.4347)t} \quad (11)$$

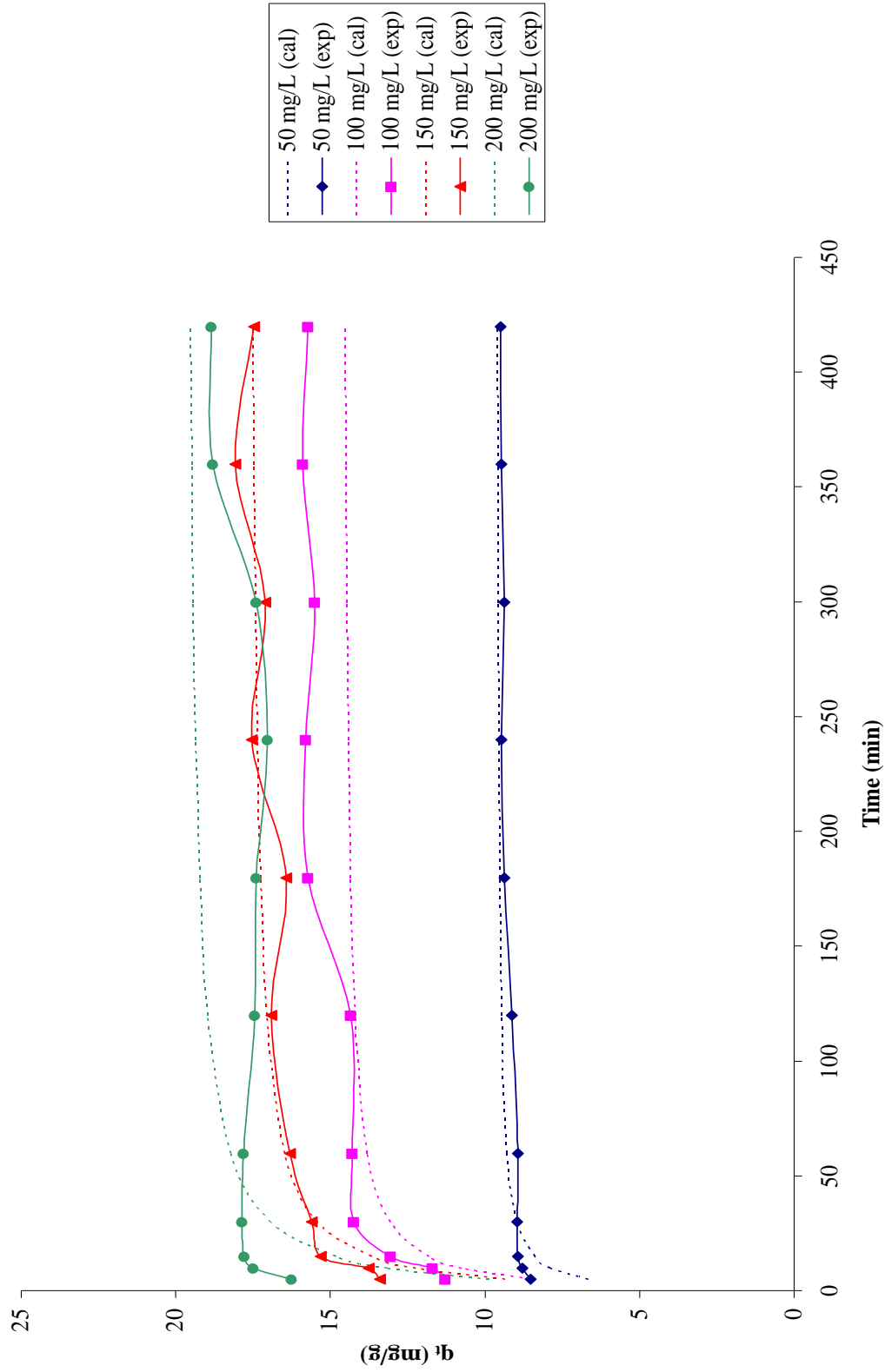
in BB3-BY11 binary solution

$$q_t = \frac{C_o t}{0.1749C_o - 10.2000 + (0.0503C_o + 3.3613)t} \quad (12)$$

in MB-BY11 binary solution

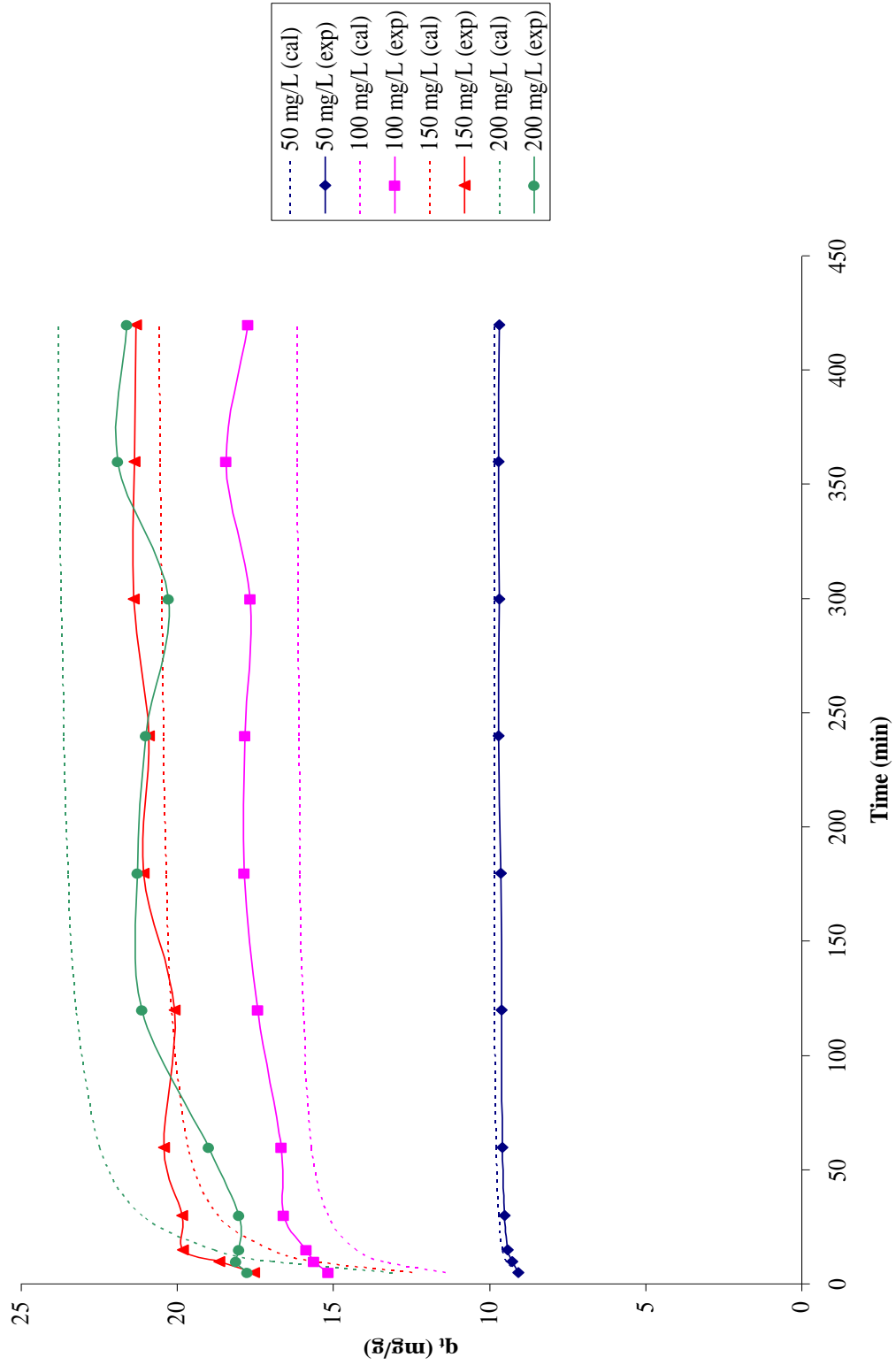
$$q_t = \frac{C_o t}{0.1135C_o - 15.1710 + (0.0482C_o + 3.3960)t} \quad (13)$$

The theoretical model derived for BB3, MB and BY11 sorption in single dye solutions by NSB were applied to the uptake of these dyes and the results were compared to the experimental values in Figures 4.18-4.20. From the plots, it is clear that the theoretically generated curves agreed well with the experimental values, however deviation was observed at concentration of 200 mg/L for single BB3 and MB. This might due to the saturation of NSB thus did not obey the theoretical curves.



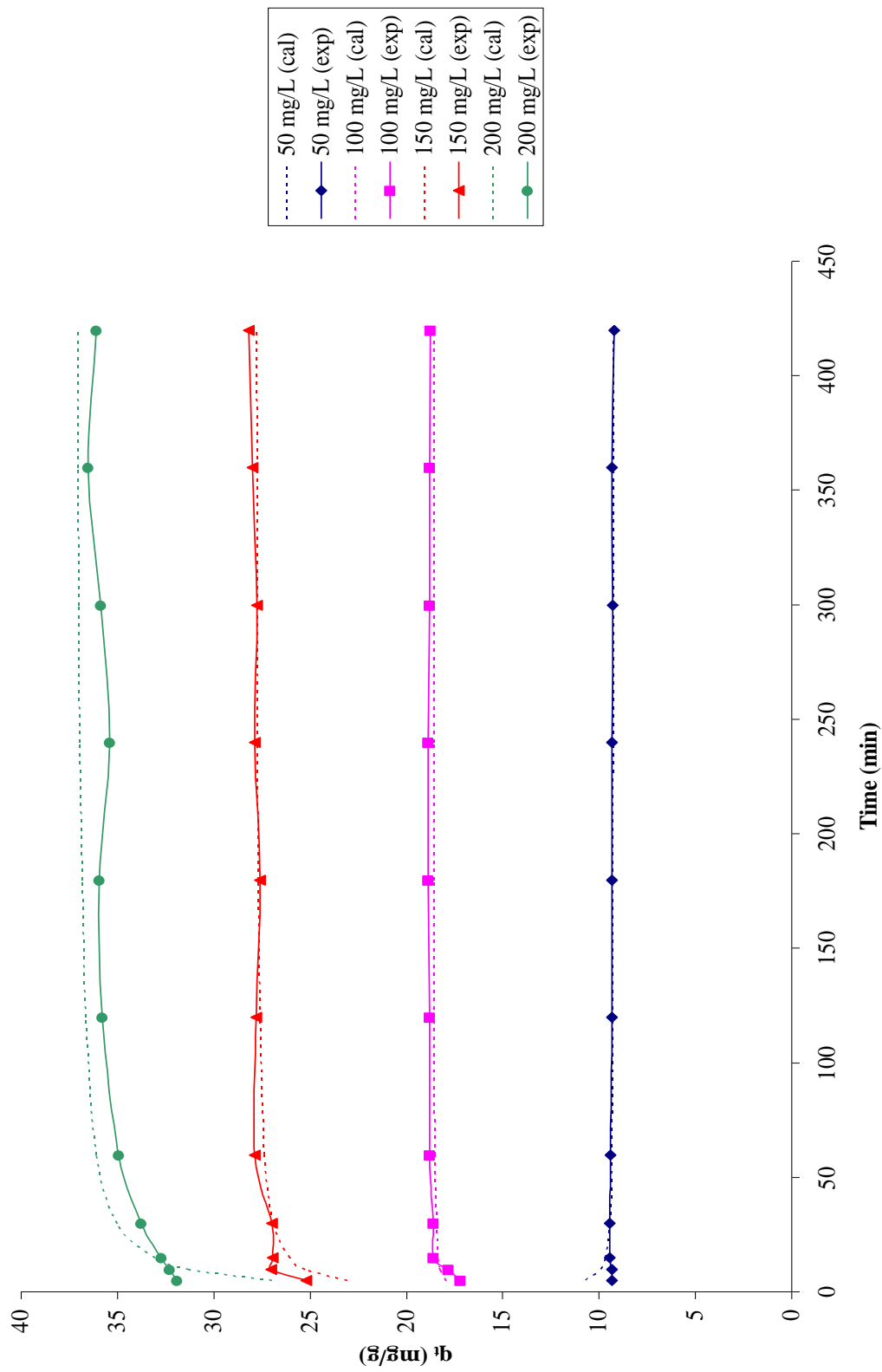
**Condition:** 0.1 g of sorbent in 20 mL of 50, 100, 150 and 200 mg/L single BB3 dye solution at 150 rpm for 7 hours at room temperature of  $25 \pm 2^\circ\text{C}$

**Figure 4.18: Comparison between the measured and pseudo-second order modeled time profiles for single BB3 sorption**



**Condition:** 0.1 g of sorbent in 20 mL of 50, 100, 150 and 200 mg/L single MB dye solution at 150 rpm for 7 hours at room temperature of 25±2°C

**Figure 4.19:** Comparison between the measured and pseudo-second order modeled time profiles for single MB sorption



**Condition:** 0.1 g of sorbent in 20 mL of 50, 100, 150 and 200 mg/L single BY11 dye solution at 150 rpm for 7 hours at room temperature of  $25 \pm 2^\circ\text{C}$

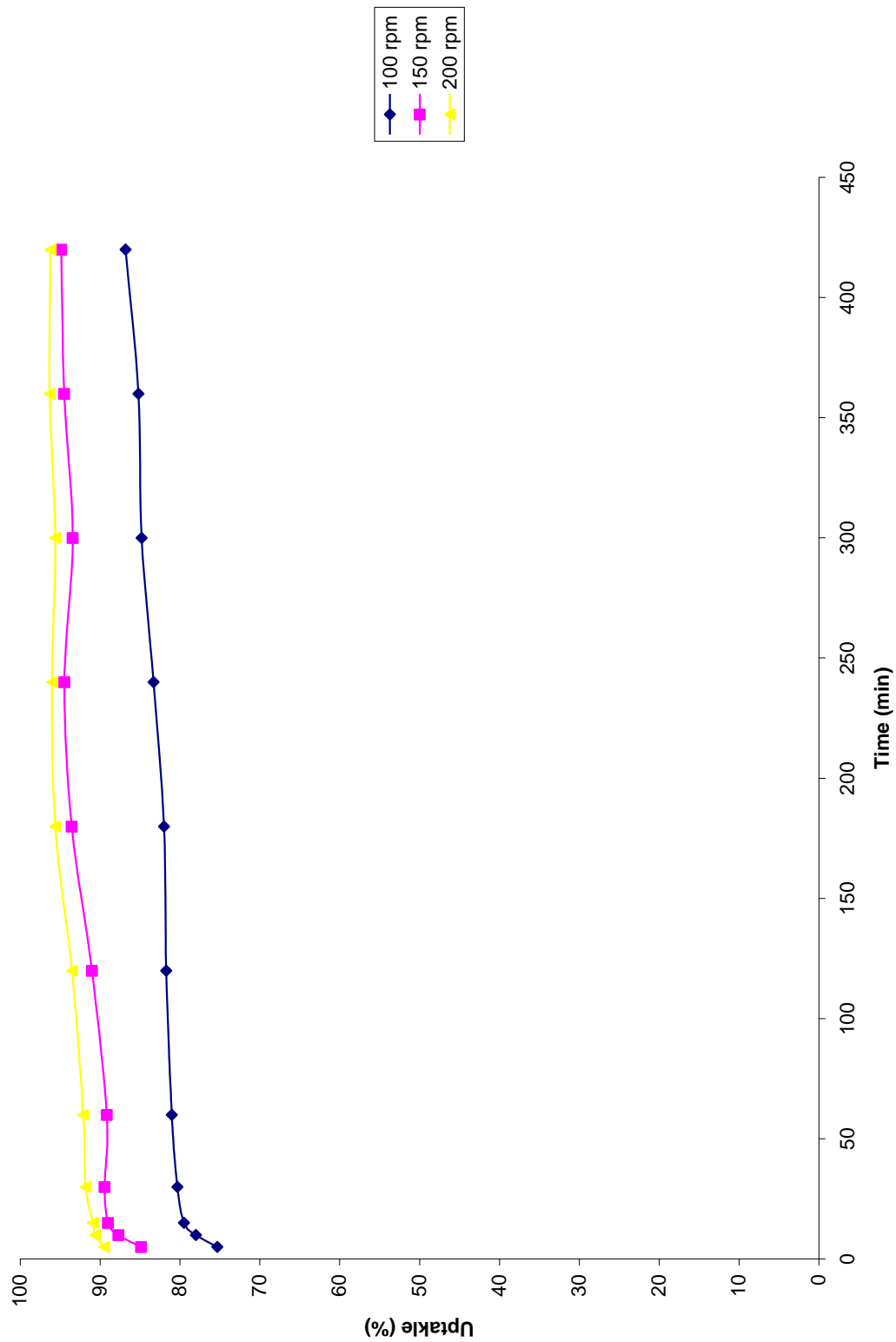
**Figure 4.20: Comparison between the measured and pseudo-second order modeled time profiles for single BY11 sorption**

#### 4.6.4 Effect of Agitation Rate

Agitation is an important factor in sorption process, which influences the distribution of the solute in the bulk solution and the formation of the external boundary layer (Batzias and Sdiras, 2007). Figures 4.21 – 4.25 show the effect of agitation rate on the percentage uptake of BB3, MB and BY11 in single and binary solutions. The results indicated that the percentage uptake was dependent on the agitation rate, whereby a higher agitation rate resulted in higher uptake of dyes. It was observed that the percentage uptake increased rapidly as the agitation speed increased from 100 to 150 rpm and minimal increment was recorded as the agitation speed increased from 150 to 200 rpm for all the dye solutions.

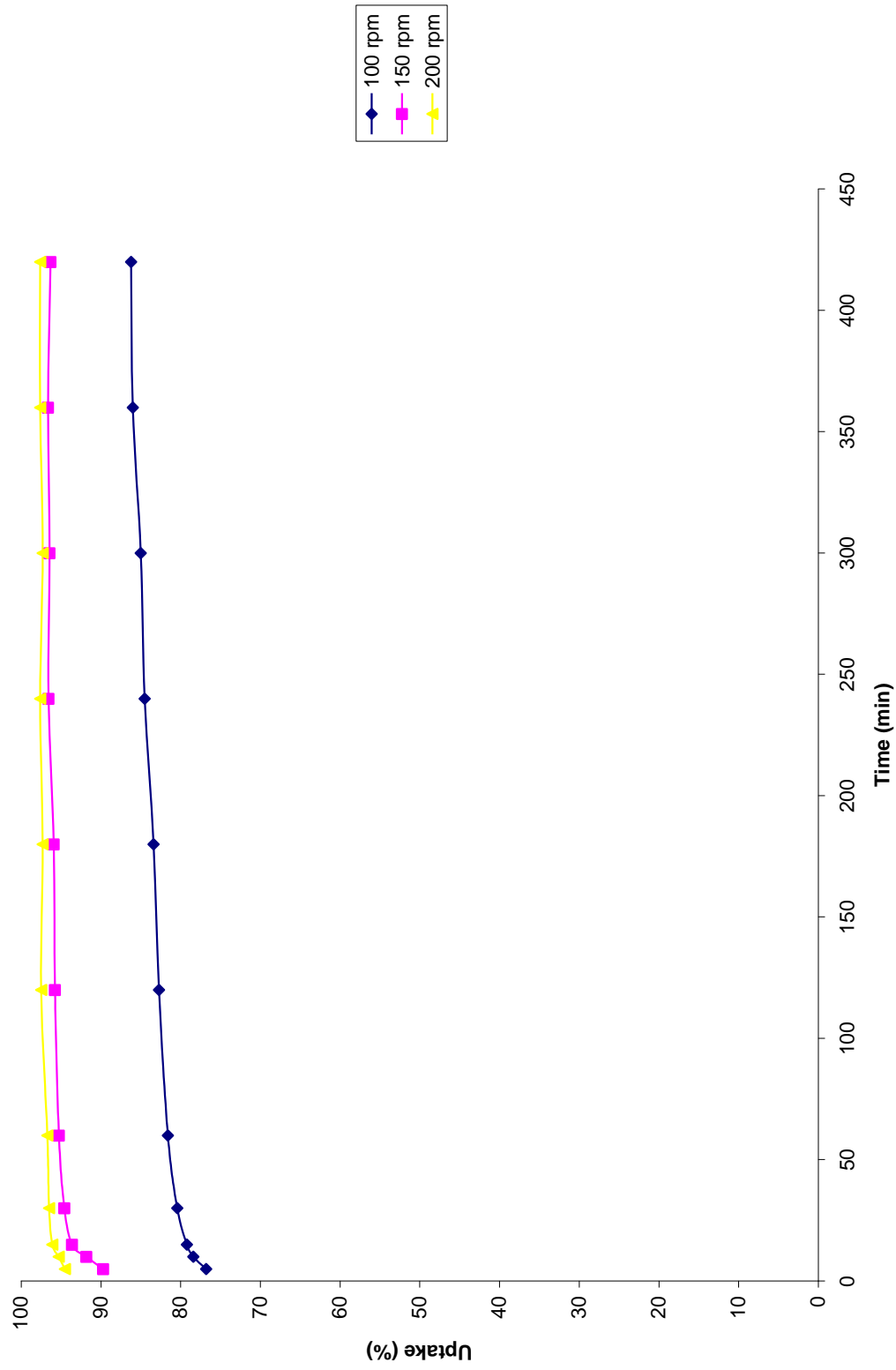
The non-negligible effect in percentage uptake as the agitation rate increased from 100 to 150 rpm confirming that the influence of external diffusion on the sorption kinetic control plays a significant role. On the other hand, the minimal increment in percentage uptake in the range of 150 to 200 rpm indicated that external mass transfer was not the sole rate limiting factor in a well agitated system, and implied that intraparticle diffusion resistance need to be included in the analysis of overall sorption (Batzias and Sdiras, 2004).





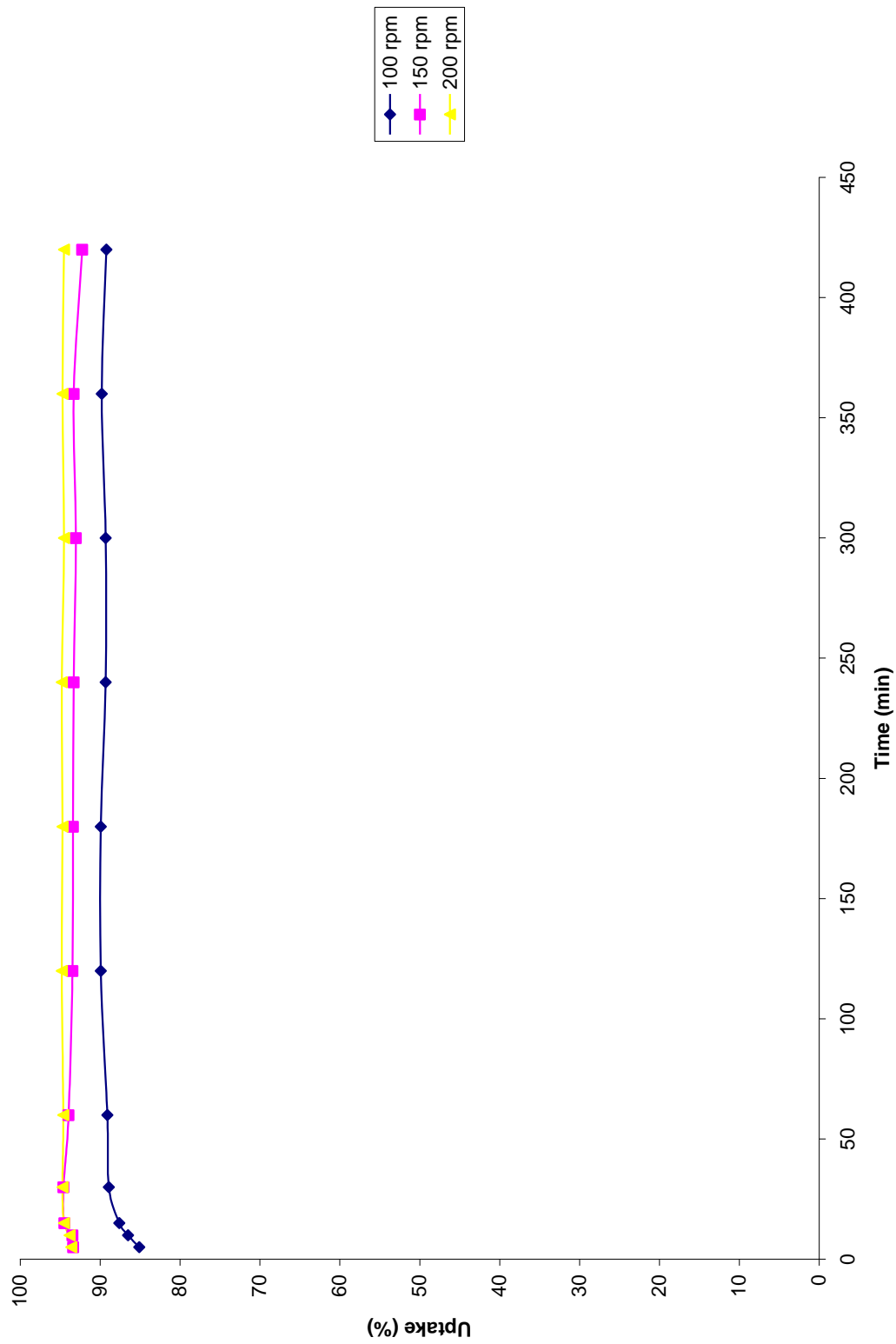
**Condition:** 0.1 g of sorbent in 20 mL of 100 mg/L BB3 single dye solution at 50, 100 and 150 rpm for 4 hours at room temperature of  $25 \pm 2^\circ\text{C}$

**Figure 4.21: Effect of agitation rate on the sorption of single BB3 onto NSB**



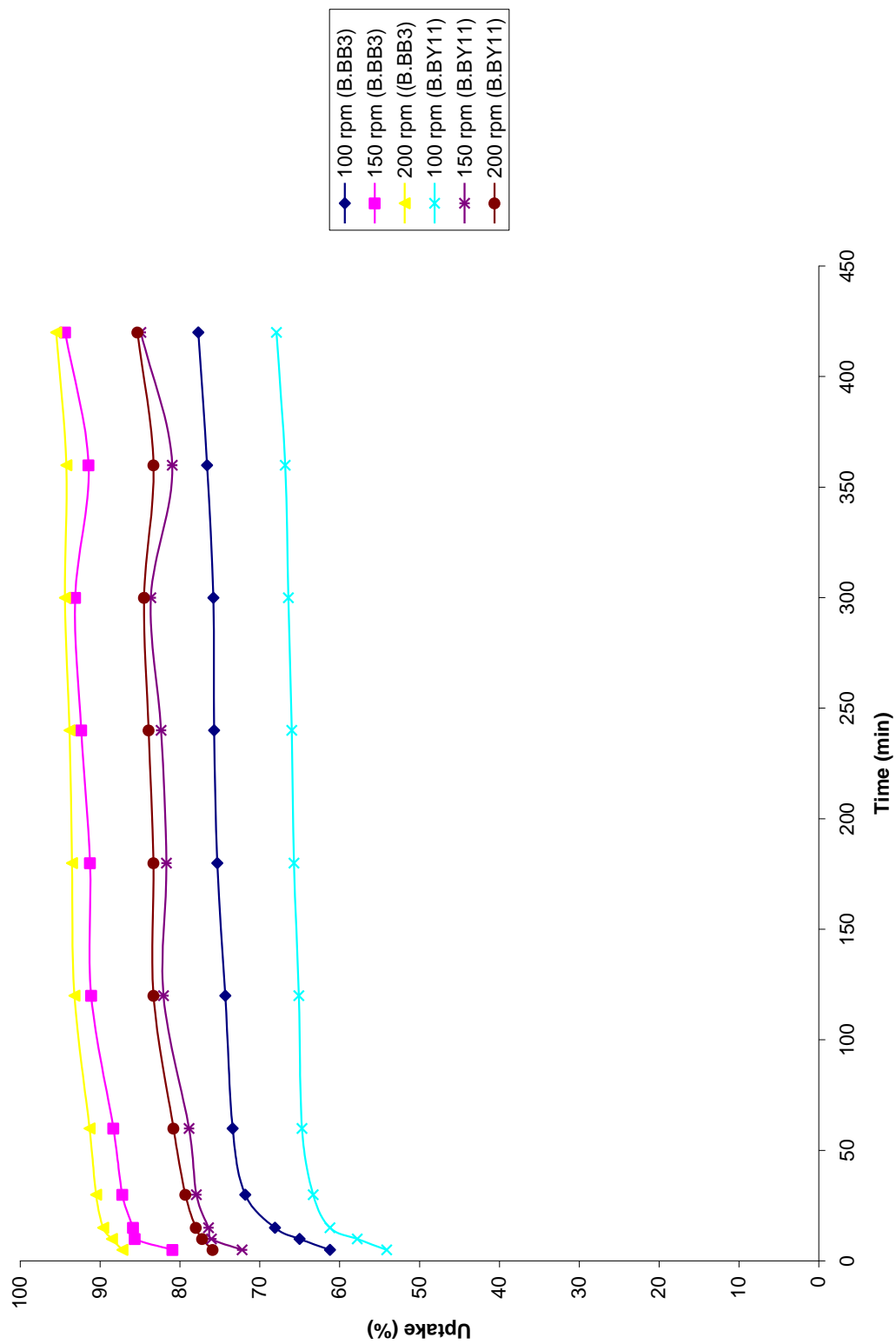
**Condition:** 0.1 g of sorbent in 20 mL of 100 mg/L MB single dye solution at 50, 100 and 150 rpm for 4 hours at room temperature of  $25 \pm 2^\circ\text{C}$

**Figure 4.22: Effect of agitation rate on the sorption of single MB onto NSB**



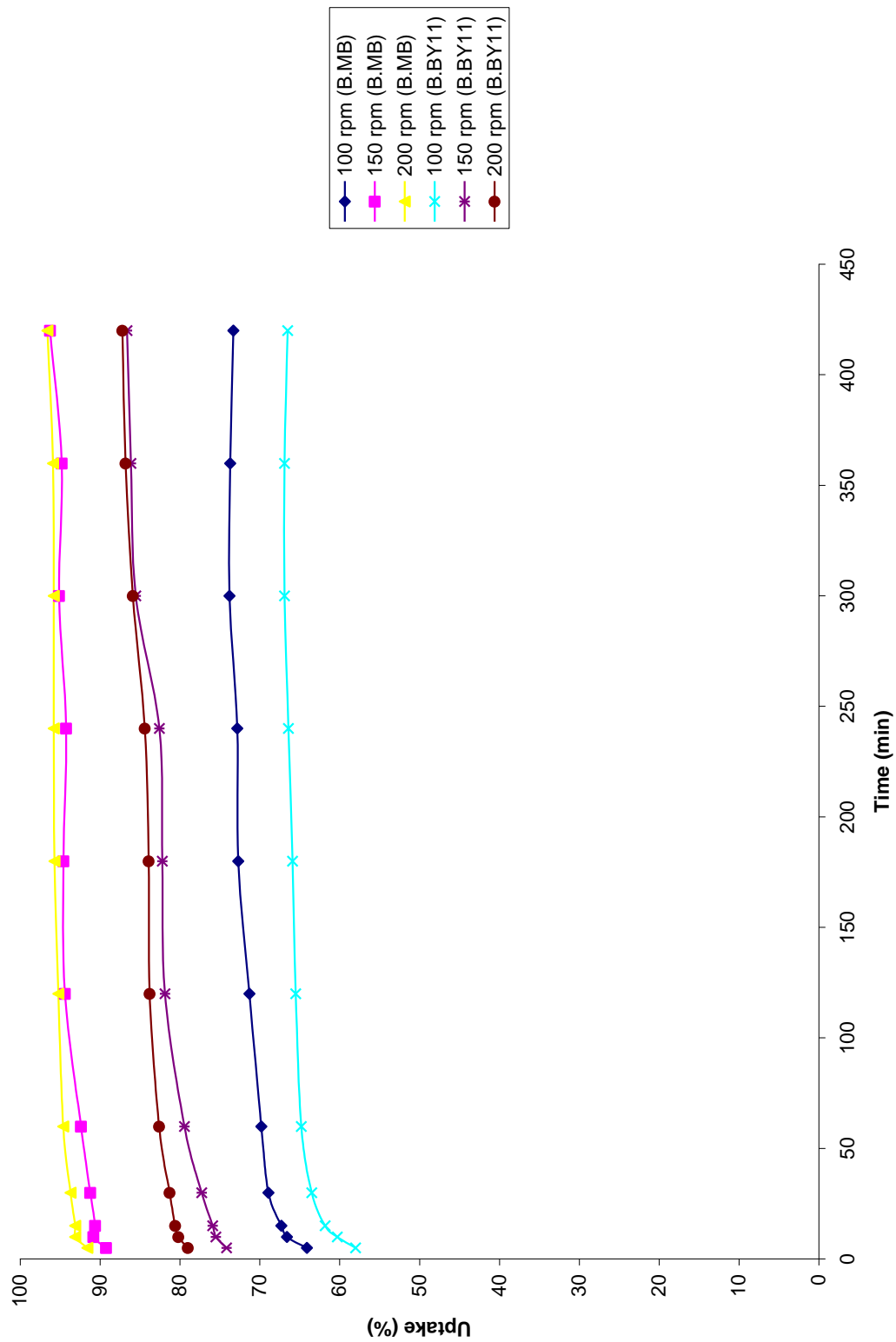
**Condition:** 0.1 g of sorbent in 20 mL of 100 mg/L BY11 single dye solution at 50, 100 and 150 rpm for 4 hours at room temperature of  $25\pm 2^\circ\text{C}$

**Figure 4.23: Effect of agitation rate on the sorption of single BY11 onto NSB**



**Condition:** 0.1 g of sorbent in 20 mL of 100 mg/L BB3 and BY11 binary dye solution at 50, 100 and 150 rpm for 4 hours at room temperature of  $25 \pm 2^\circ\text{C}$

**Figure 4.24: Effect of agitation rate on the sorption of binary BB3-BY11 onto NSB**



**Condition:** 0.1 g of sorbent in 20 mL of 100 mg/L MB and BY11 binary dye solution at 50, 100 and 150 rpm for 4 hours at room temperature of  $25 \pm 2^\circ\text{C}$

**Figure 4.25: Effect of agitation rate on the sorption of binary MB-BY11 onto NSB**

In a study conducted by Shiau and Pan (2004) on the sorption of basic dyes from aqueous solution by various adsorbents, a similar trend was observed. From the results, the percentage uptake of dyes was found to be increased with increasing agitation rate which implied that the transfer rate of a solute to a particle in liquid sorption system is affected by liquid film thickness surrounding the particle and this film thickness is dependent on the agitation speed.

#### 4.6.5 Boundary Layer Effect

External mass transfer or boundary layer diffusion of a system can be characterised by the initial rate of solute sorption. The boundary layer effect was determined using the following equation:

$$\left[ \frac{d(C_t / C_o)}{dt} \right]_{t=0} = -\beta_L S \quad (14)$$

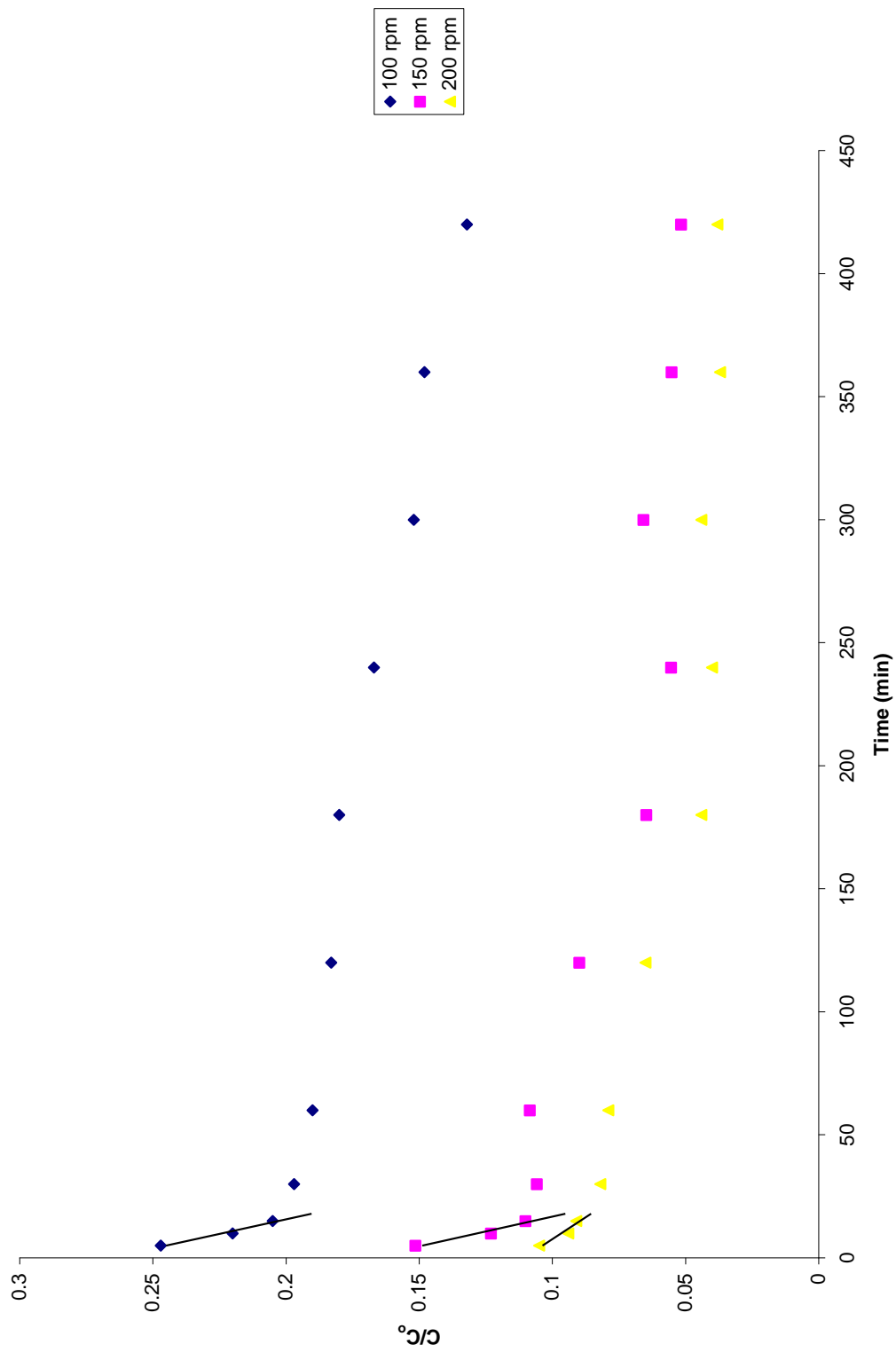
where,  $\beta_L$  = external mass transfer coefficient (cm/min)

$C_t$  = solute concentration at any time of  $t$  (mg/L)

$C_o$  = initial solute concentration (mg/L)

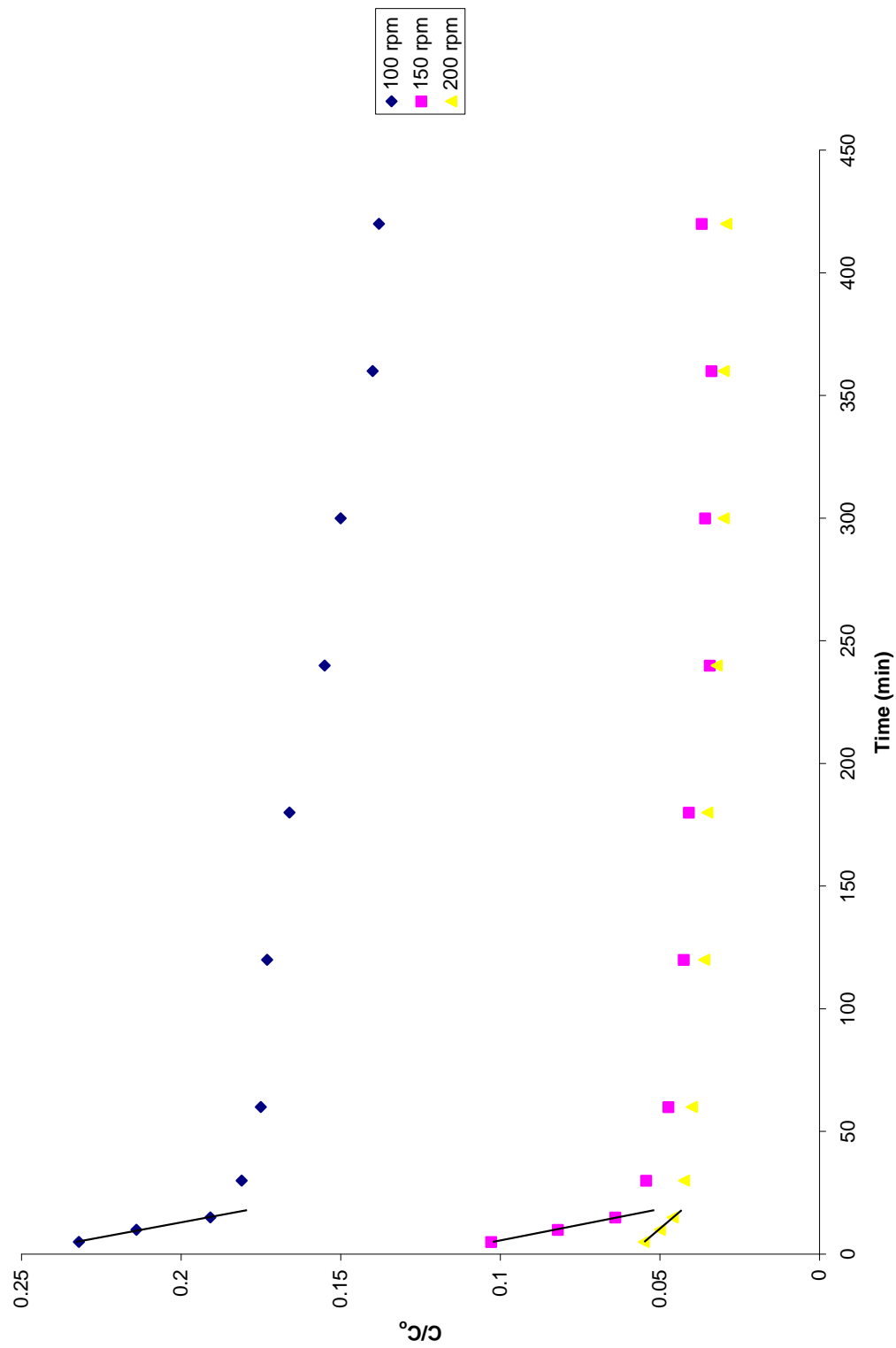
$S$  = specific surface area for the mass transfer

The external mass transfer coefficients can be determined from the slope as  $t \rightarrow 0$ . Figures 4.26 to 4.32 exhibit the  $C_t/C_o$  against time for all studied dye solutions for agitation rate and the  $\beta_L S$  values was calculated from the slope of the



**Condition:** 0.1 g of sorbent in 20 mL of 100 mg/L single BB3 dye solution at 50, 100 and 150 rpm for 4 hours at room temperature of  $25 \pm 2^\circ\text{C}$

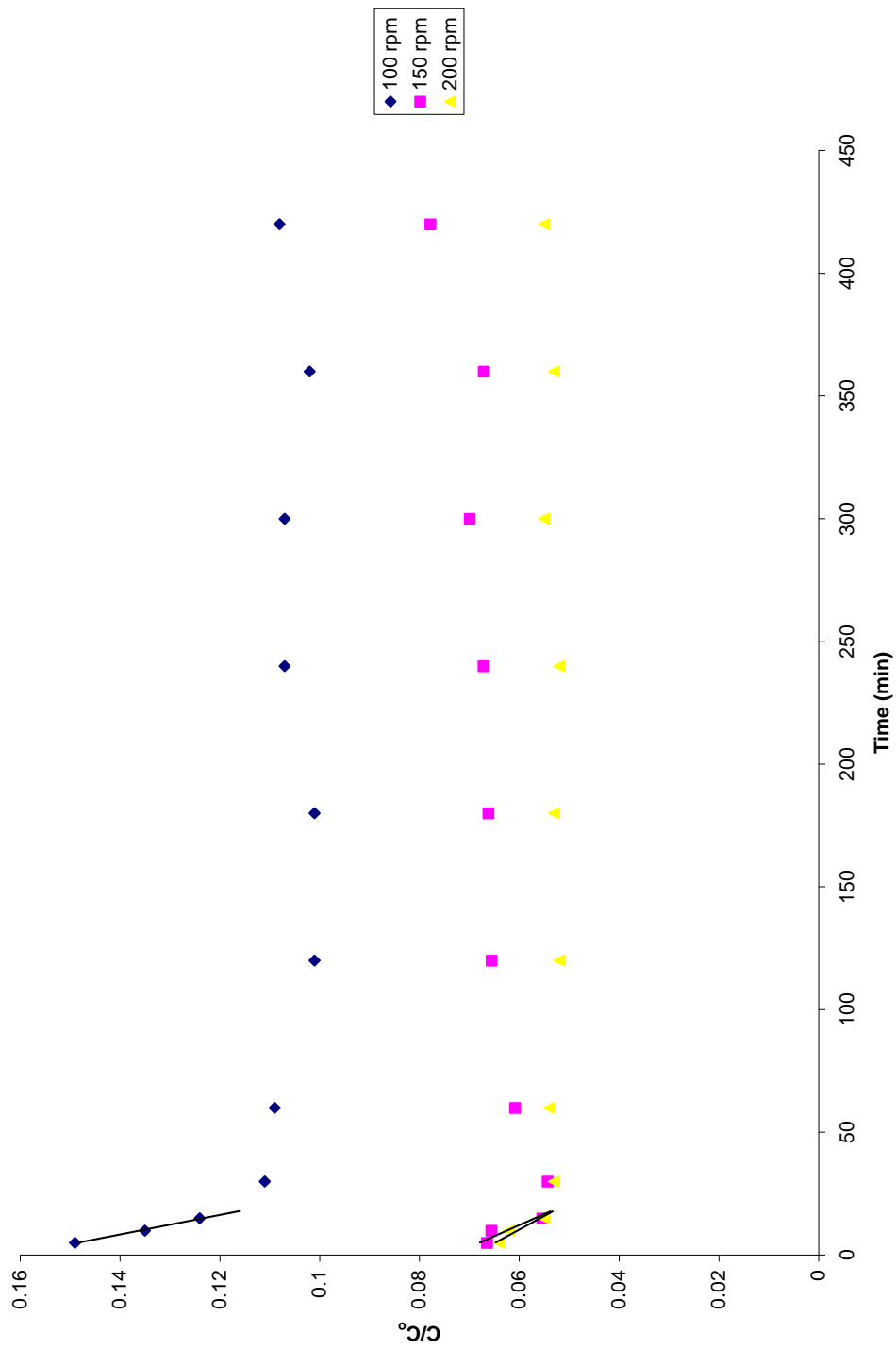
**Figure 4.26: Effect of boundary layer on the sorption of single BB3 onto NSB**



**Condition:** 0.1 g of sorbent in 20 mL of 100 mg/L single MB dye solution at 50, 100 and 150 rpm for 4 hours at room temperature of  $25 \pm 2^\circ\text{C}$

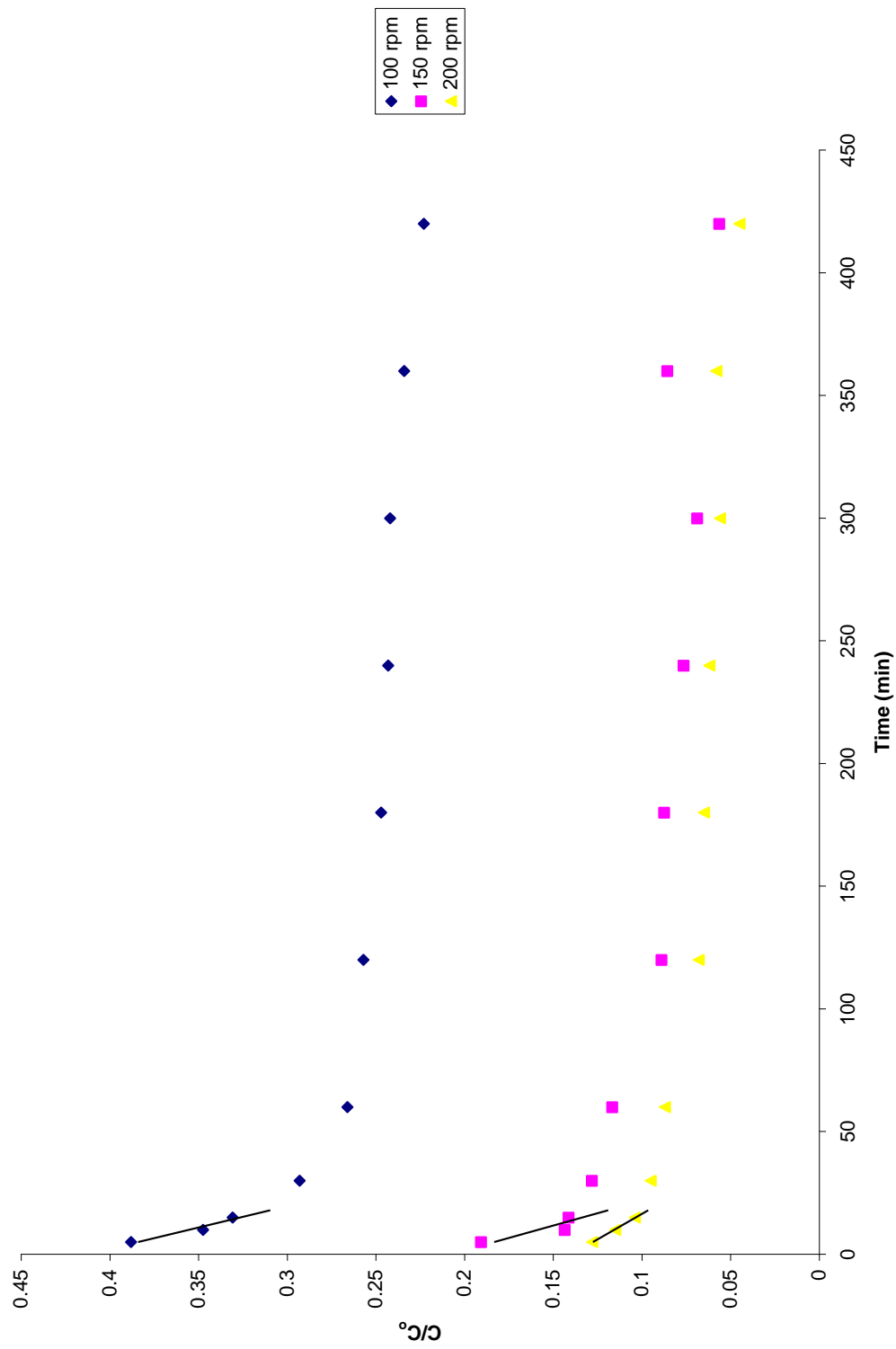
**Figure 4.27: Effect of boundary layer on the sorption of single MB onto NSB**





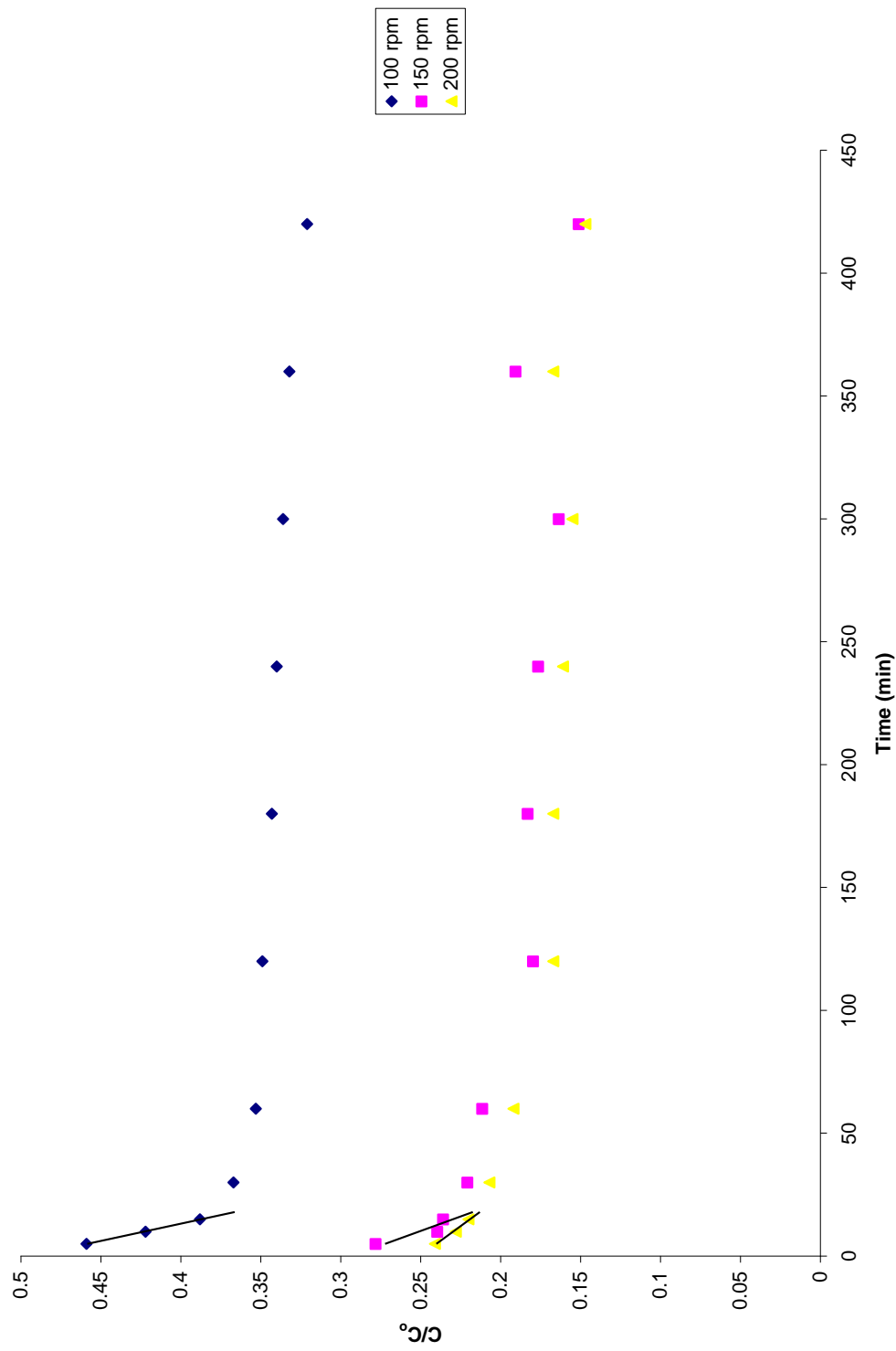
**Condition:** 0.1 g of sorbent in 20 mL of 100 mg/L single BY11 dye solution at 50, 100 and 150 rpm for 4 hours at room temperature of  $25 \pm 2^\circ\text{C}$

**Figure 4.28: Effect of boundary layer on the sorption of single BY11 onto NSB**



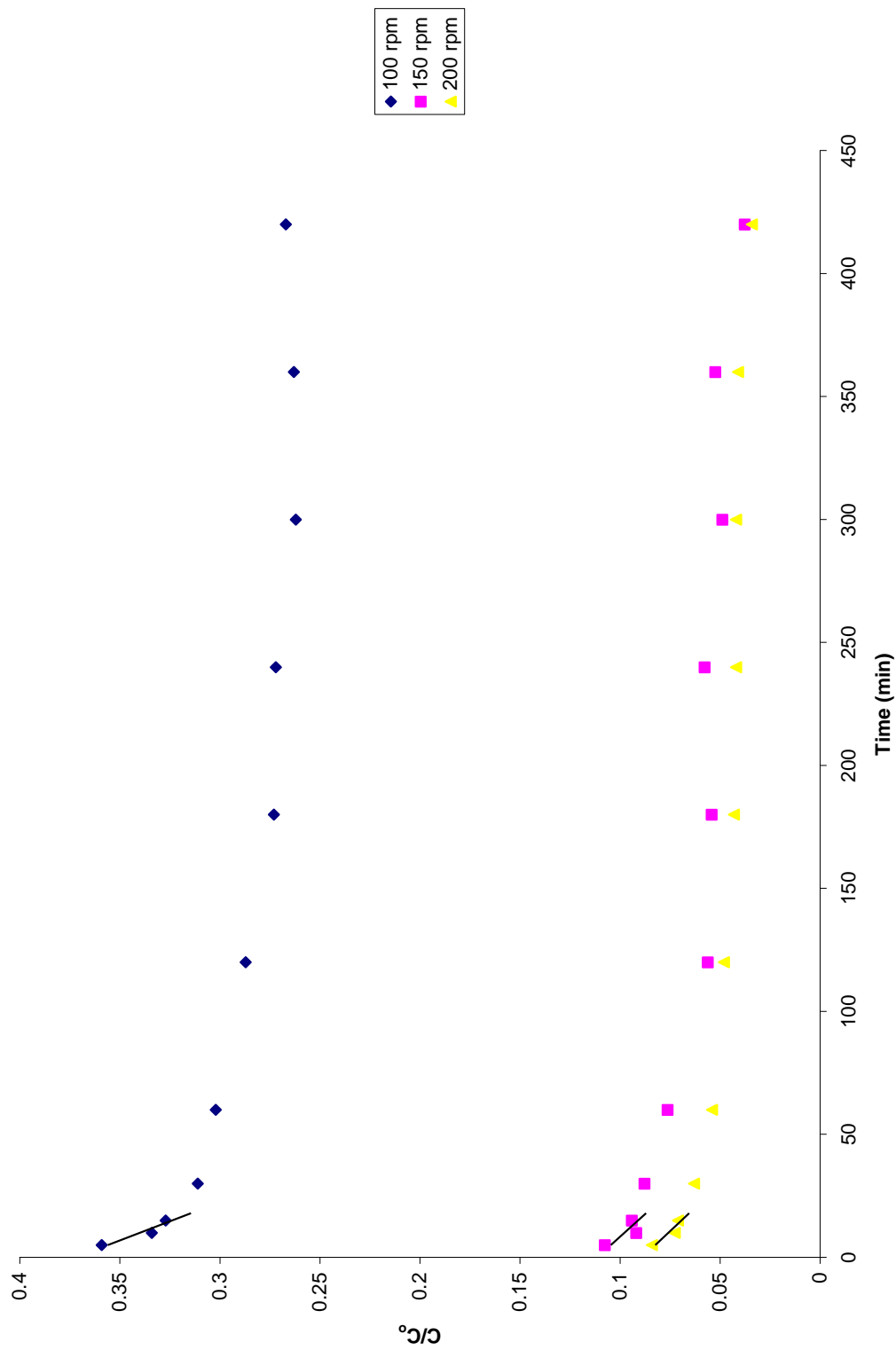
**Condition:** 0.1 g of sorbent in 20 mL of 100 mg/L binary BB3 of BB3-BY11 dye solution at 50, 100 and 150 rpm for 4 hours at room temperature of  $25 \pm 2^\circ\text{C}$

**Figure 4.29: Effect of boundary layer on the sorption of binary BB3 of BB3-BY11 onto NSB**



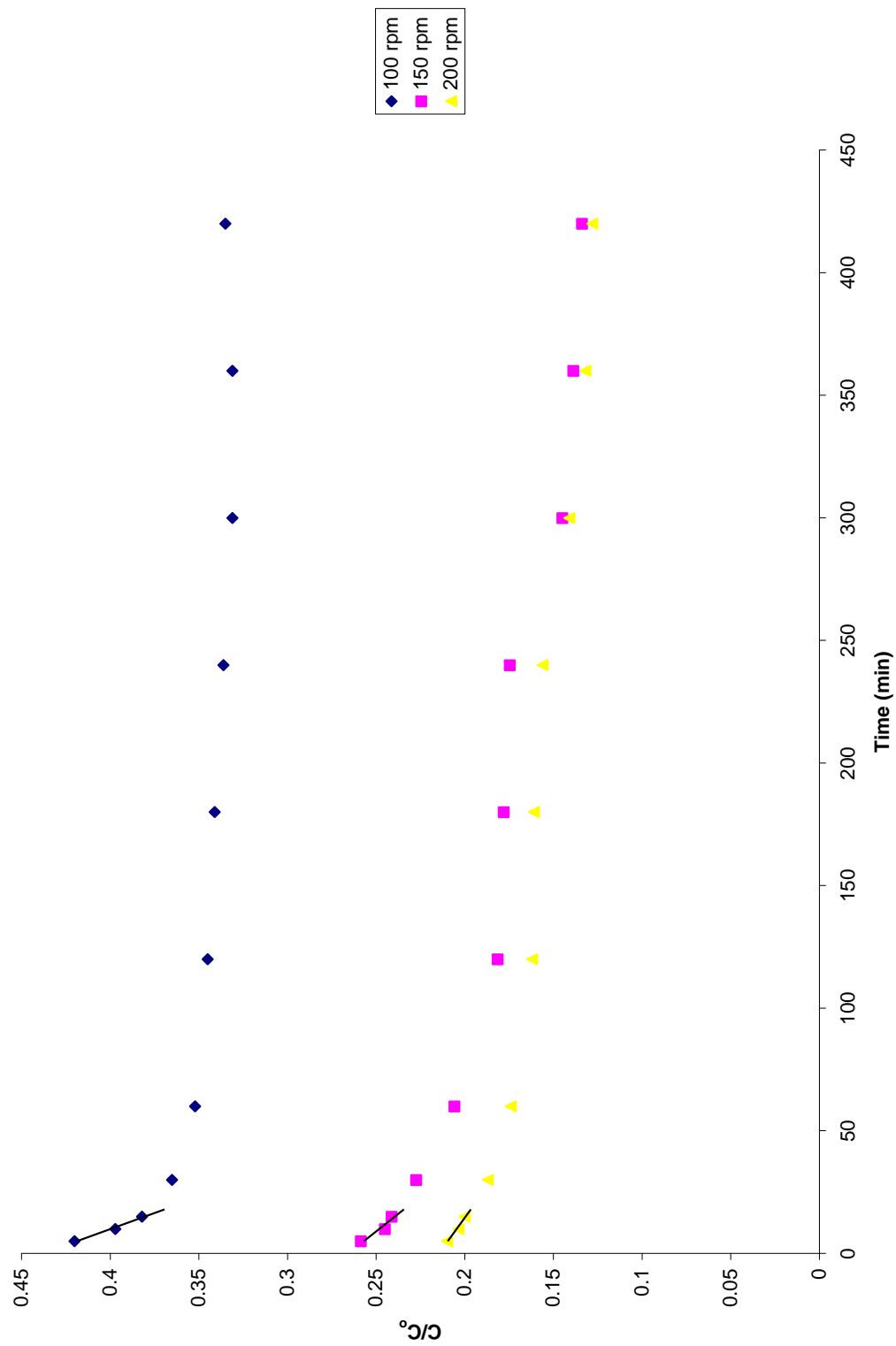
**Condition:** 0.1 g of sorbent in 20 mL of 100 mg/L binary BY11 of BB3-BY11 dye solution at 50, 100 and 150 rpm for 4 hours at room temperature of  $25 \pm 2^\circ\text{C}$

**Figure 4.30: Effect of boundary layer on the sorption of binary BY11 of BB3-BY11 onto NSB**



**Condition:** 0.1 g of sorbent in 20 mL of 100 mg/L binary MB of MB-BY11 dye solution at 50, 100 and 150 rpm for 4 hours at room temperature of  $25 \pm 2^\circ\text{C}$

**Figure 4.31: Effect of boundary layer on the sorption of binary MB of MB-BY11 onto NSB**



**Condition:** 0.1 g of sorbent in 20 mL of 100 mg/L binary BY11 of MB-BY11 dye solution at 50, 100 and 150 rpm for 4 hours at room temperature of  $25 \pm 2^\circ\text{C}$

**Figure 4.32: Effect of boundary layer on the sorption of binary BY11 of MB-BY11 onto NSB**

initial steep portions of each curves. Table 4.3 showed the calculated external mass transfer ( $\beta_L S$ ) and regression coefficients ( $R^2$ ) for each dye solution. It was observed that the  $\beta_L S$  decreased as the agitation rate increased. Higher  $\beta_L S$  values indicate the increase of the external mass transfer resistance (Akkaya and Özer, 2005). This trend confirmed the results of the effect of agitation rate where increase in agitation rate increased the percentage uptake.

#### 4.6.6 Intraparticle Diffusion

The adsorbate species are most likely transported from bulk of the solution into the solid phase through an intra-particle diffusion/transport process, which is frequently the rate-limiting step (Batziar and Sidiaras, 2007). To determine the diffusion mechanism, intraparticle diffusion model based on the theory proposed by Weber and Morris, (1963) was tested against the experimental results using following equation:

$$q_t = k_p t^{1/2} + C \quad (15)$$

where,

$q_t$  = the amount of dye adsorbed at time  $t$  (mg/g)

$k_p$  = intraparticle diffusion rate constant

$C$  = the intercept

Table 4.3: The values of  $\beta_{LS}$  and regression coefficients for BB3, MB and BY11  
in single and binary dye solutions

Dye solutions		Stirring speed (rpm)	$\beta_{LS}$ (cm/min)	$R^2$
Single BB3		50	0.0042	0.9735
		100	0.0041	0.9557
		150	0.0014	0.9018
Single MB		50	0.0041	0.9947
		100	0.0039	0.9982
		150	0.0016	1.0000
Single BY11		50	0.0025	0.9952
		100	0.0011	0.8094
		150	0.0009	0.9067
Binary BB3-BY11	BB3	50	0.0057	0.9452
		100	0.0049	0.7841
		150	0.0024	0.9977
	BY11	50	0.0071	0.9994
		100	0.0042	0.8153
		150	0.0013	0.9275
BinaryMB- BY11	MB	50	0.0032	0.9046
		100	0.0014	0.6319
		150	0.0013	0.8407
	BY11	50	0.0038	0.9854
		100	0.0011	0.9260
		150	0.0010	0.9709

Table 4.4 showed the  $k_p$  and C values which calculated from the slope and intercept of the linear plot of  $q_t$  against  $t^{1/2}$  (Figures 4.33 – 4.39). According to Wang *et al.* (2005), the plot might present in multilinearity, which indicates that two or more steps occur. The first sharper portion is the external surface sorption or instantaneous sorption stage. The second portion is the gradual sorption stage, where the intraparticle diffusion is rate controlled. The third portion is the final equilibrium stage where intraparticle diffusion starts to slow down due to extremely low solute concentrations in the solution. From the figures, two linear portions were determined for all studied dye solutions. In addition, all the plots did not pass through the origin which showed that although intraparticle diffusion was involved in the sorption process; however it was not the only rate controlling step. Similar dual or multiple linear plots were also reported by Gong *et al.* (2008) in the removal of cationic dyes using modified wheat straw.

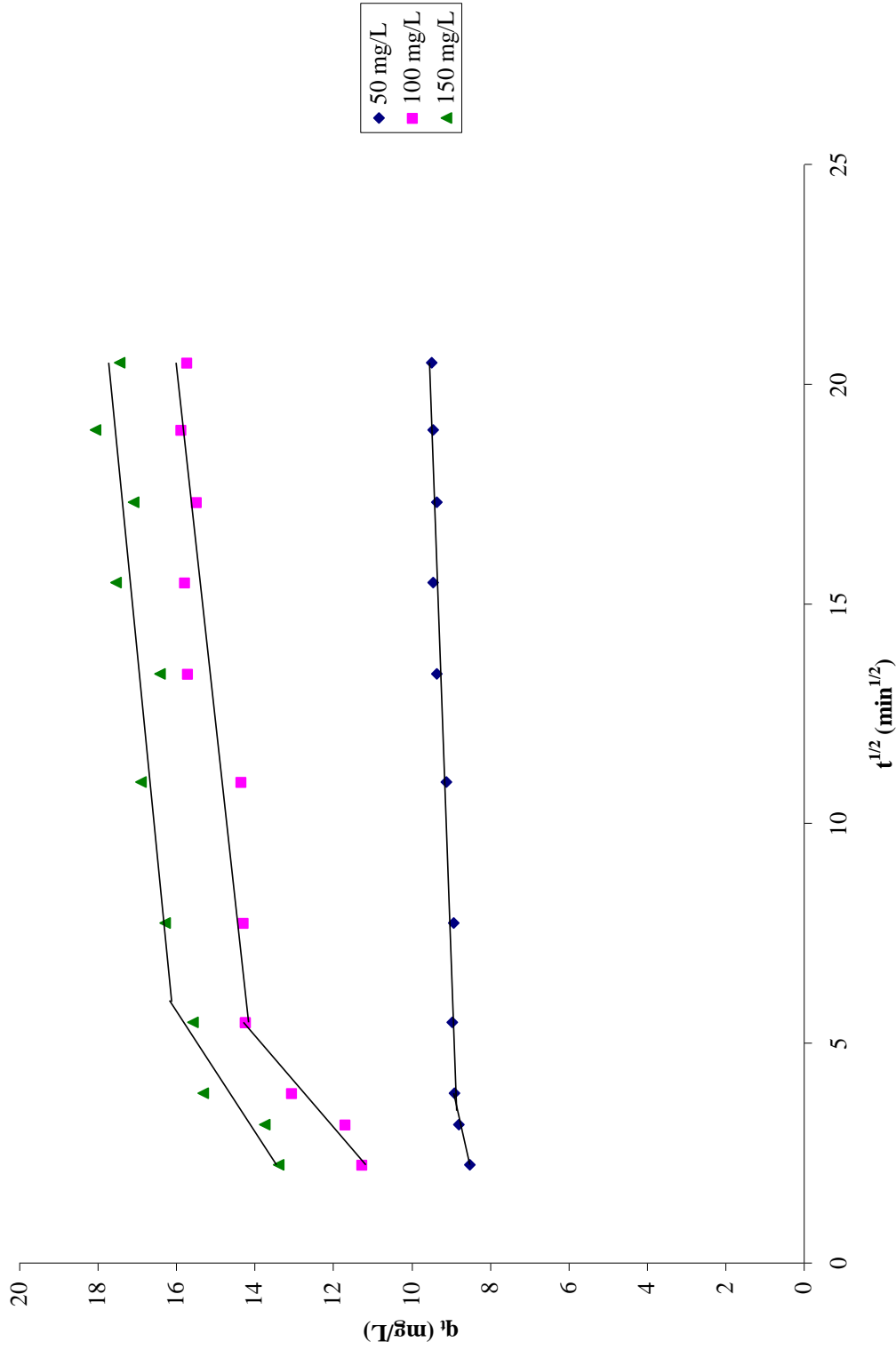
#### **4.6.7 Sorption Isotherm**

Sorption isotherms are the basic requirements for the design of the sorption systems (Lee *et al.*, 2008). Among various sorption isotherms, Langmuir, Freundlich and Brunauer-Emmett-Teller (BET) isotherm models were used to model the equilibrium data for BB3, MB and BY11 in single and binary solutions.



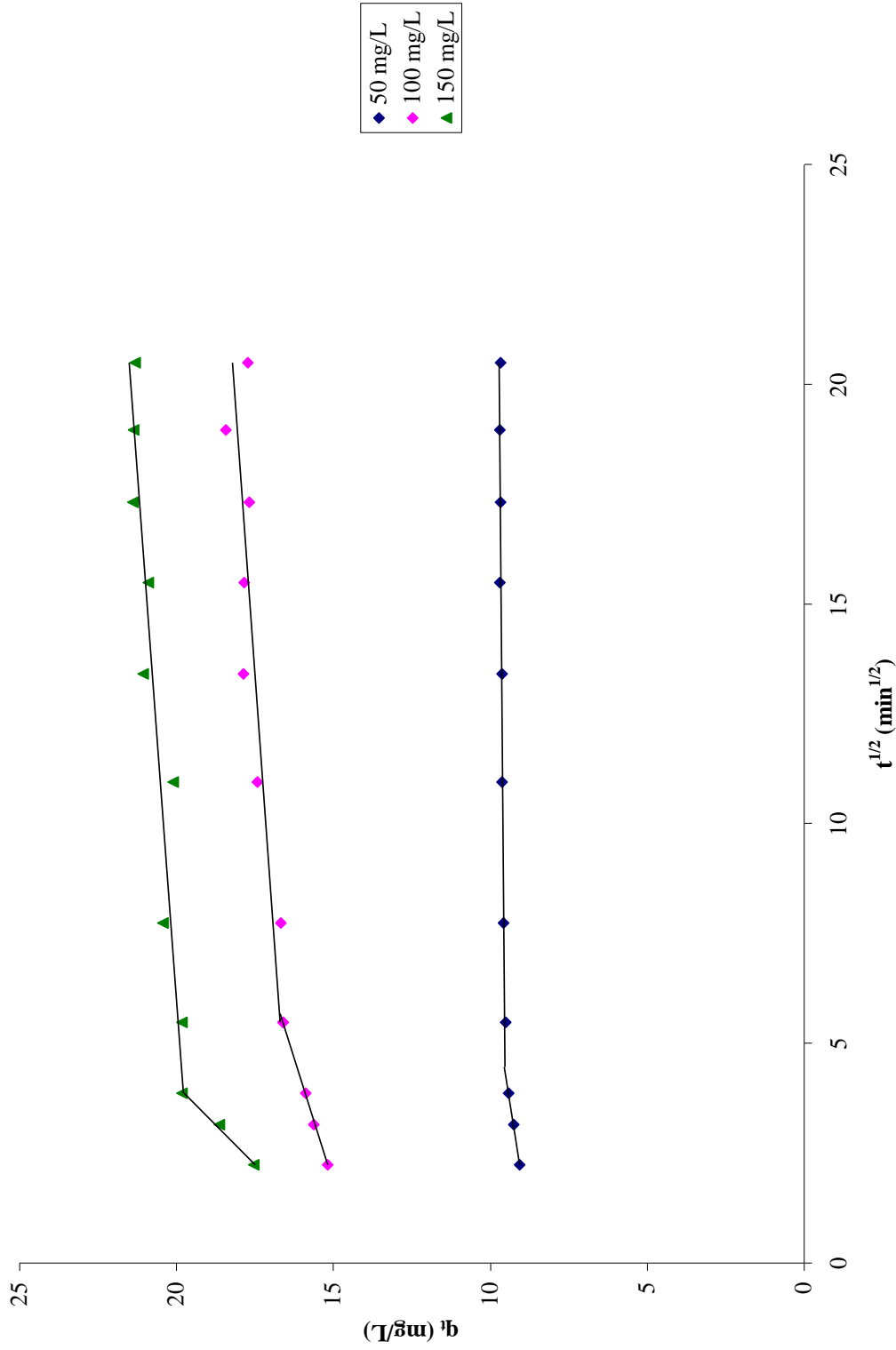
Table 4.4: The parameters value of intraparticle diffusion model for BB3, MB and BY11 in single and binary dye solutions

Dye solutions		Initial concentration (ppm)	$k_{p1}$ (mg/g min <sup>0.5</sup> )	$C_1$	$(R_1)^2$	$k_{p2}$ (mg/g min <sup>0.5</sup> )	$C_2$	$(R_2)^2$
Single BB3		50	0.2515	7.9589	0.9816	0.0403	8.7106	0.8844
		100	0.9631	9.0114	0.9551	0.1235	13.482	0.7811
		150	0.7298	11.813	0.8234	0.1107	15.455	0.6329
Single MB		50	0.2160	8.5783	0.9989	0.0112	9.4756	0.8513
		100	0.4737	14.197	0.9984	0.1006	16.137	0.7513
		150	1.3775	14.403	0.9912	0.1044	19.361	0.8390
Single BY11		50	0.0666	9.1532	0.7465	-0.0118	9.4834	0.8236
		100	0.8425	15.262	0.9788	0.0071	18.669	0.2132
		150	1.9879	20.730	1.000	0.593	26.902	0.6963
Binary BB3-BY11	BB3	50	0.2872	7.6547	0.8430	0.0376	8.6695	0.8519
		100	1.6250	6.8323	0.9055	0.1093	12.853	0.7813
		150	0.7224	11.541	0.9323	0.1575	13.823	0.9863
	BY11	50	0.2678	6.6422	0.8704	0.0366	7.6385	0.7119
		100	1.1952	5.7475	0.9207	0.0763	10.041	0.7855
		150	0.5492	8.6810	0.8960	0.0507	11.181	0.6771
Binary MB-BY11	MB	50	0.0402	9.0649	0.8729	0.0186	9.2724	0.7719
		100	0.6171	12.984	0.9292	0.0350	16.532	0.7913
		150	0.7170	14.565	0.9807	0.0706	18.169	0.7022
	BY11	50	0.1075	7.2045	0.9463	0.0599	7.4606	0.9593
		100	0.6307	8.4125	0.9618	0.0696	11.537	0.7688
		150	0.6928	8.8188	0.9632	0.0562	12.262	0.7766



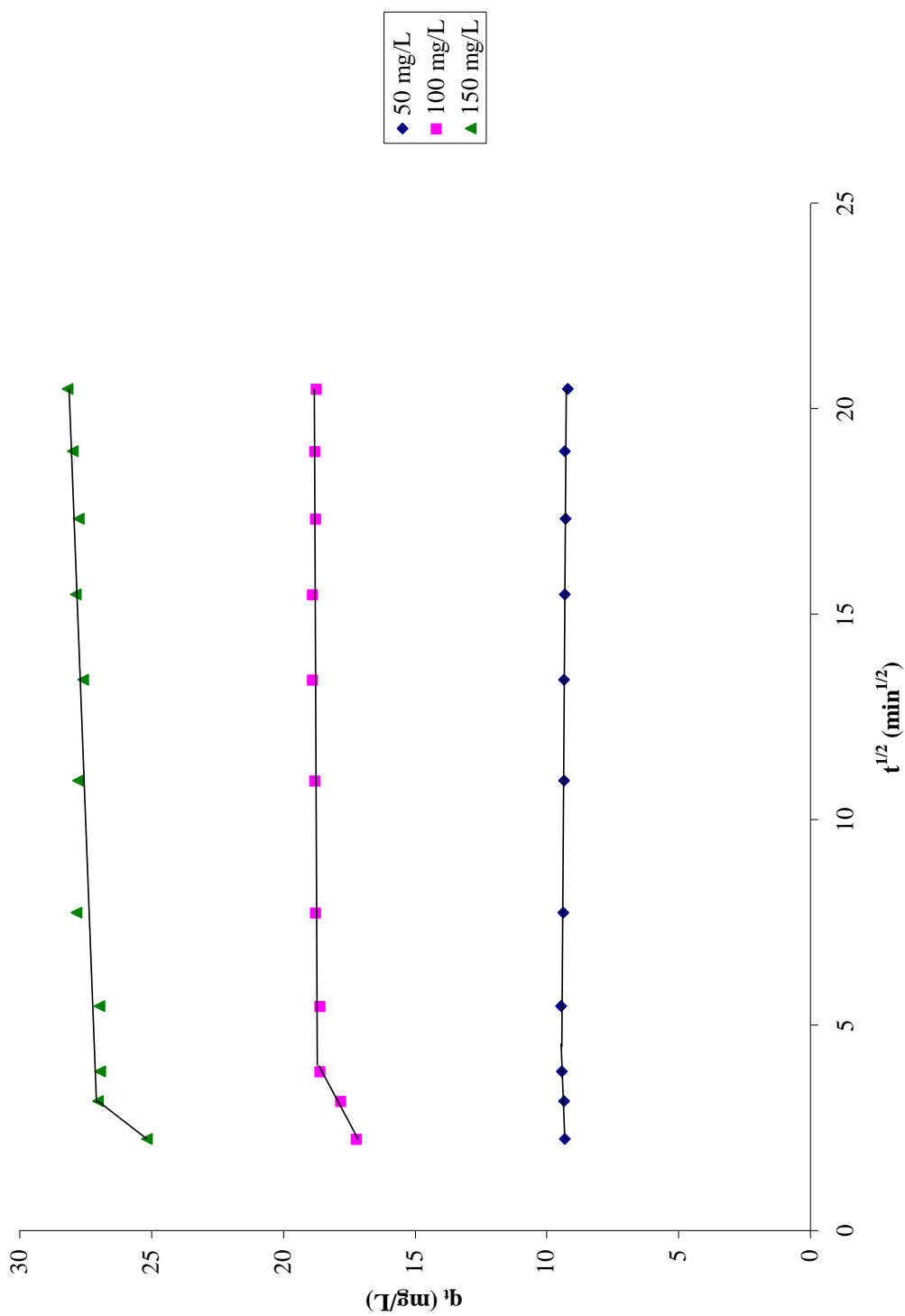
**Condition:** 0.1 g of sorbent in 20 mL of 50, 100 and 150 mg/L single BB3 dye solution at 150 rpm for 7 hours at room temperature of  $25 \pm 2^\circ\text{C}$

**Figure 4.33: Effect of intraparticle diffusion on the sorption of single BB3 onto NSB**



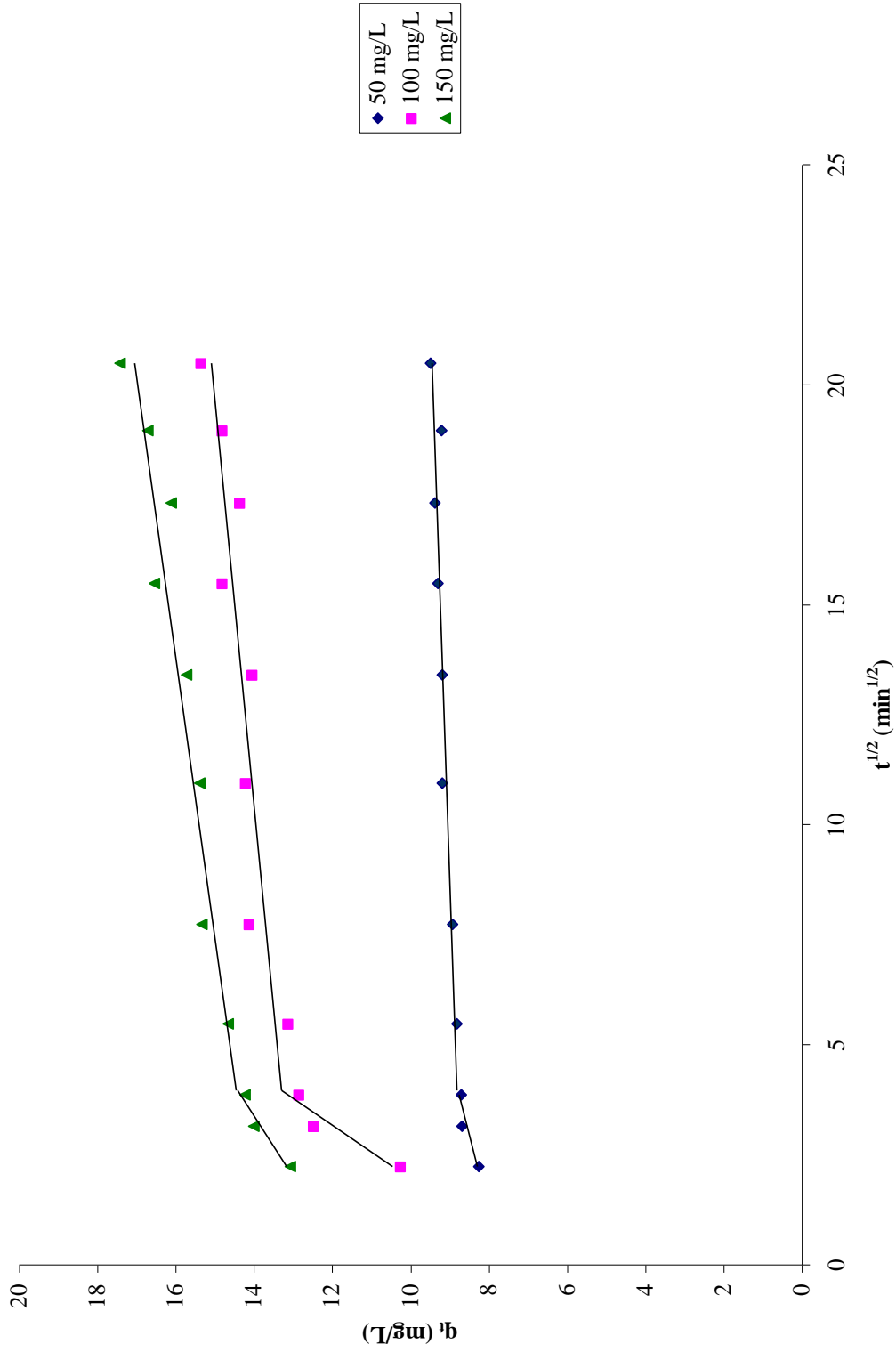
**Condition:** 0.1 g of sorbent in 20 mL of 50, 100 and 150 mg/L single MB dye solution at 150 rpm for 7 hours at room temperature of  $25 \pm 2^\circ\text{C}$

**Figure 4.34: Effect of intraparticle diffusion on the sorption of single MB onto NSB**



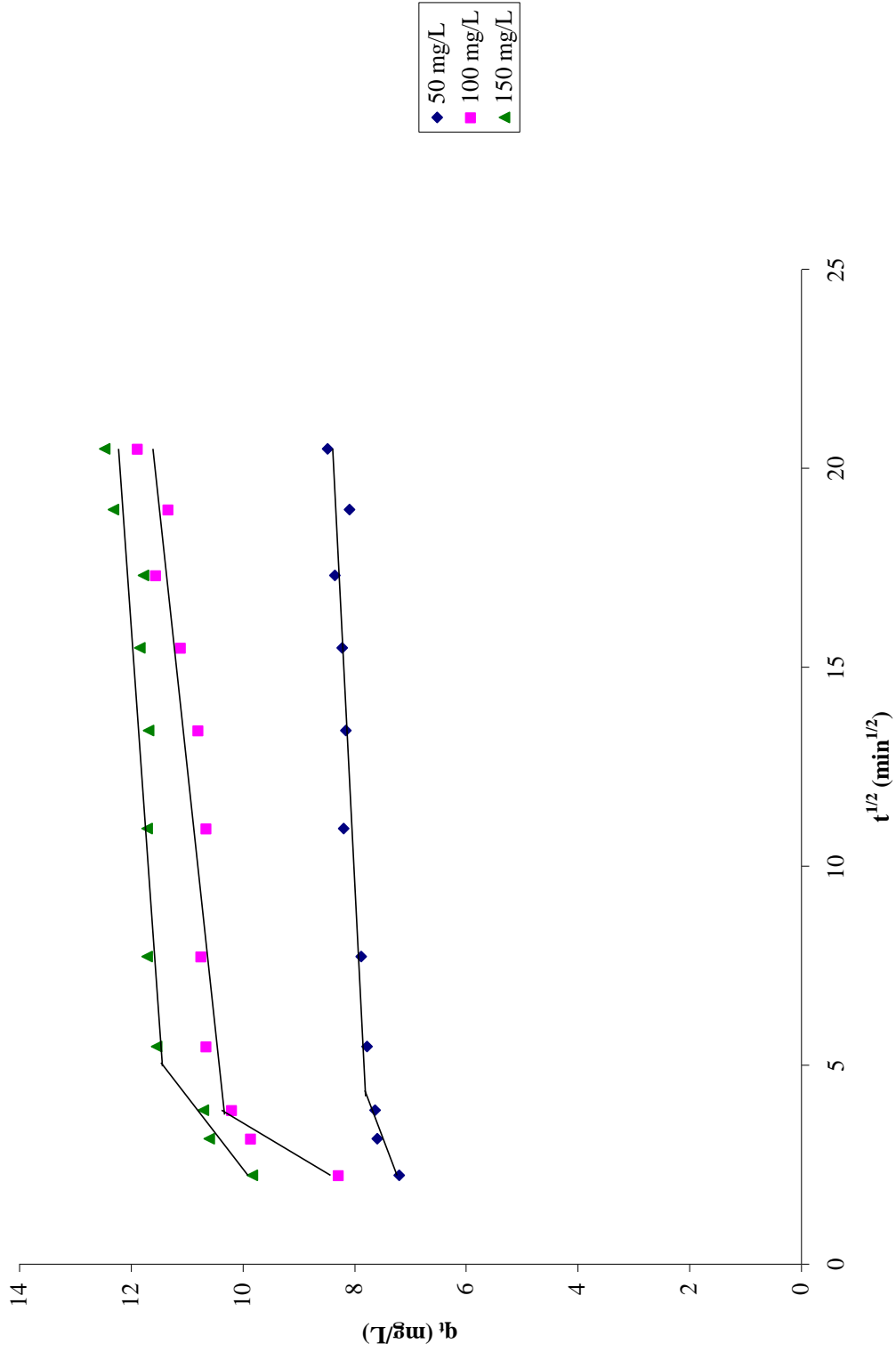
**Condition:** 0.1 g of sorbent in 20 mL of 50, 100 and 150 mg/L single BY11 dye solution at 150 rpm for 7 hours at room temperature of  $25 \pm 2^\circ\text{C}$

**Figure 4.35: Effect of intraparticle diffusion on the sorption of single BY11 onto NSB**



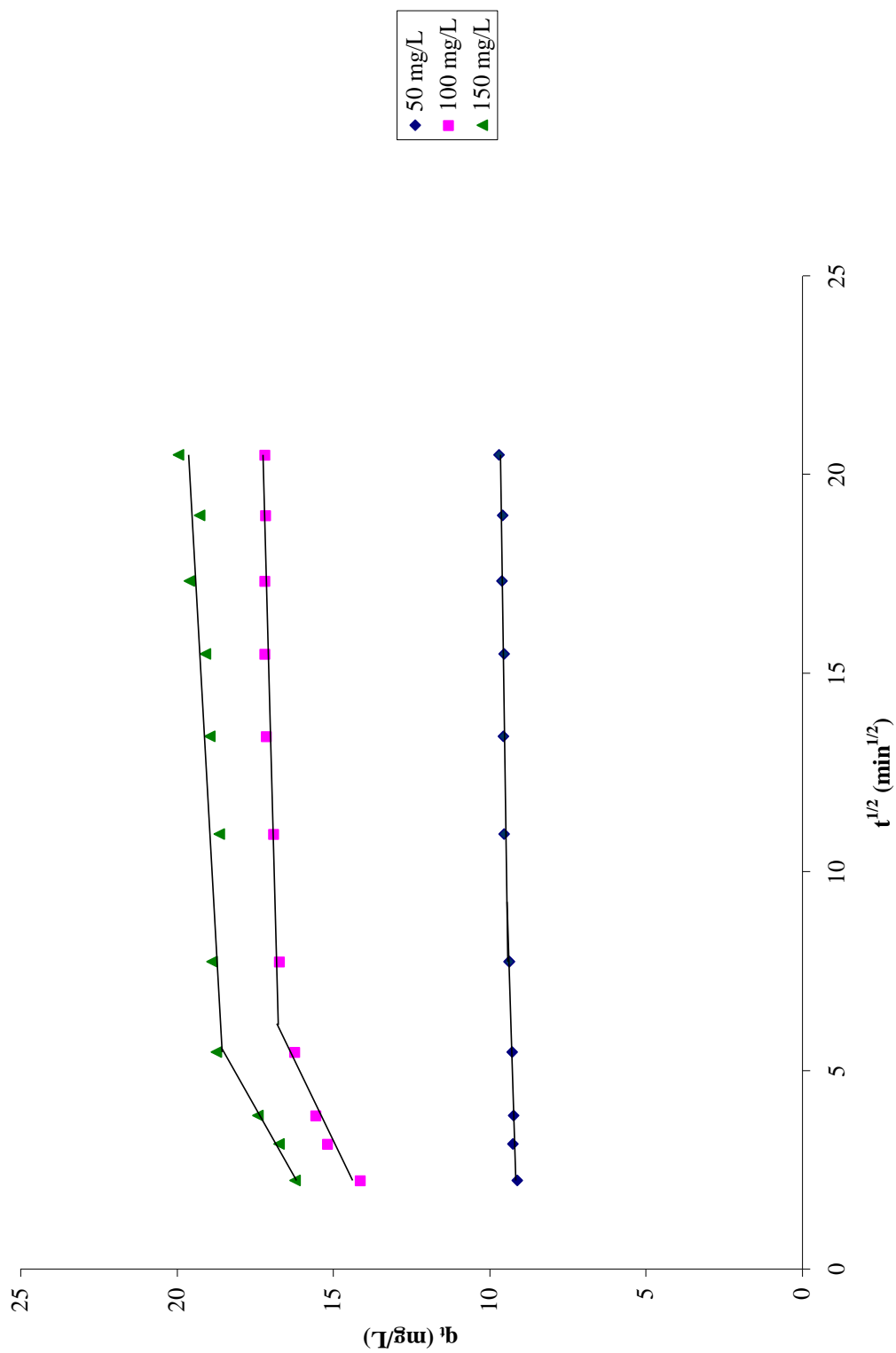
**Condition:** 0.1 g of sorbent in 20 mL of 50, 100 and 150 mg/L binary BB3 of BB3-BY11 dye solution at 150 rpm for 7 hours at room temperature of  $25 \pm 2^\circ\text{C}$

**Figure 4.36: Effect of intraparticle diffusion on the sorption of binary BB3 of BB3-BY11 onto NSB**



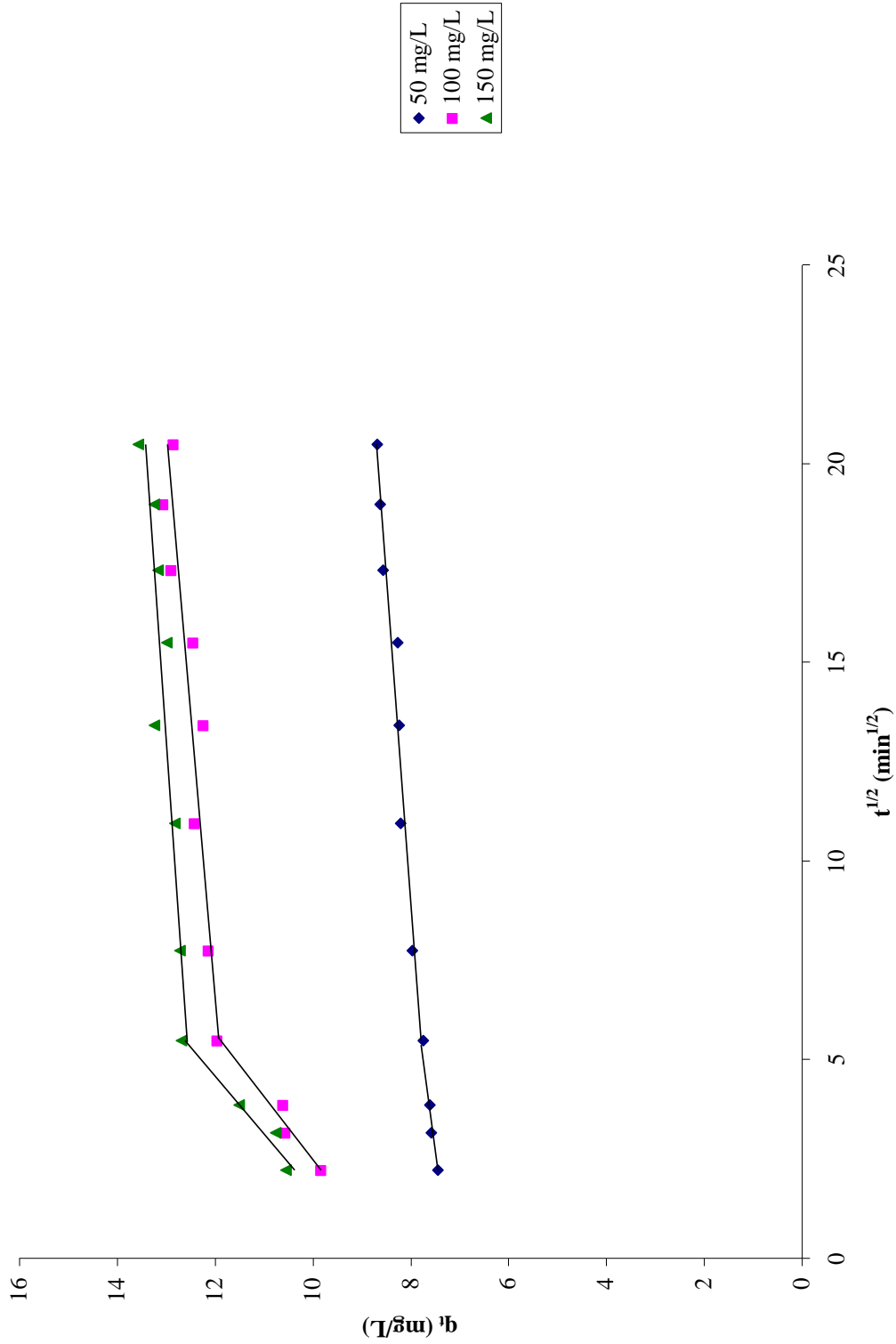
**Condition:** 0.1 g of sorbent in 20 mL of 50, 100 and 150 mg/L binary BY11 of BB3-BY11 dye solution at 150 rpm for 7 hours at room temperature of  $25 \pm 2^\circ\text{C}$

**Figure 4.37: Effect of intraparticle diffusion on the sorption of binary BY11 of BB3-BY11 onto NSB**



**Condition:** 0.1 g of sorbent in 20 mL of 50, 100 and 150 mg/L binary MB of MB-BY11 dye solution at 150 rpm for 7 hours at room temperature of  $25 \pm 2^\circ\text{C}$

**Figure 4.38: Effect of intraparticle diffusion on the sorption of binary MB of MB-BY11 onto NSB**



**Condition:** 0.1 g of sorbent in 20 mL of 50, 100 and 150 mg/L binary BY11 of MB-BY11 dye solution at 150 rpm for 7 hours at room temperature of  $25 \pm 2^\circ\text{C}$

**Figure 4.39: Effect of intraparticle diffusion on the sorption of binary BY11 of MB-BY11 onto NSB**



The linearised Langmuir equation is written as:

$$\frac{C_e}{q_e} = \frac{C_e}{q_m} + \frac{1}{K_a q_m} \quad (16)$$

whereas the linearised form of Freundlich model is shown as follows:

$$\log q_e = \log K_f + \frac{\log C_e}{n} \quad (17)$$

while the linearised form of BET model is given as follows:

$$\frac{C_e}{(C_o - C_e)(q_e)} = \left( \frac{1}{Bq_m} \right) + \left( \frac{B-1}{Bq_m} \right) \left( \frac{C_e}{C_o} \right) \quad (18)$$

where,

$C_e$  = equilibrium concentration of the dye (mg/L)

$q_e$  = amount of dye sorbed at equilibrium (mg/g)

$q_m$  = maximum sorption capacity (mg/g)

$K_a$  = constant related to the energy of the sorbent (L/mg)

$n$  = Freundlich constant for intensity

$K_f$  = Freundlich constant for sorption capacity

$C_o$  = initial concentration of dye (mg/L)

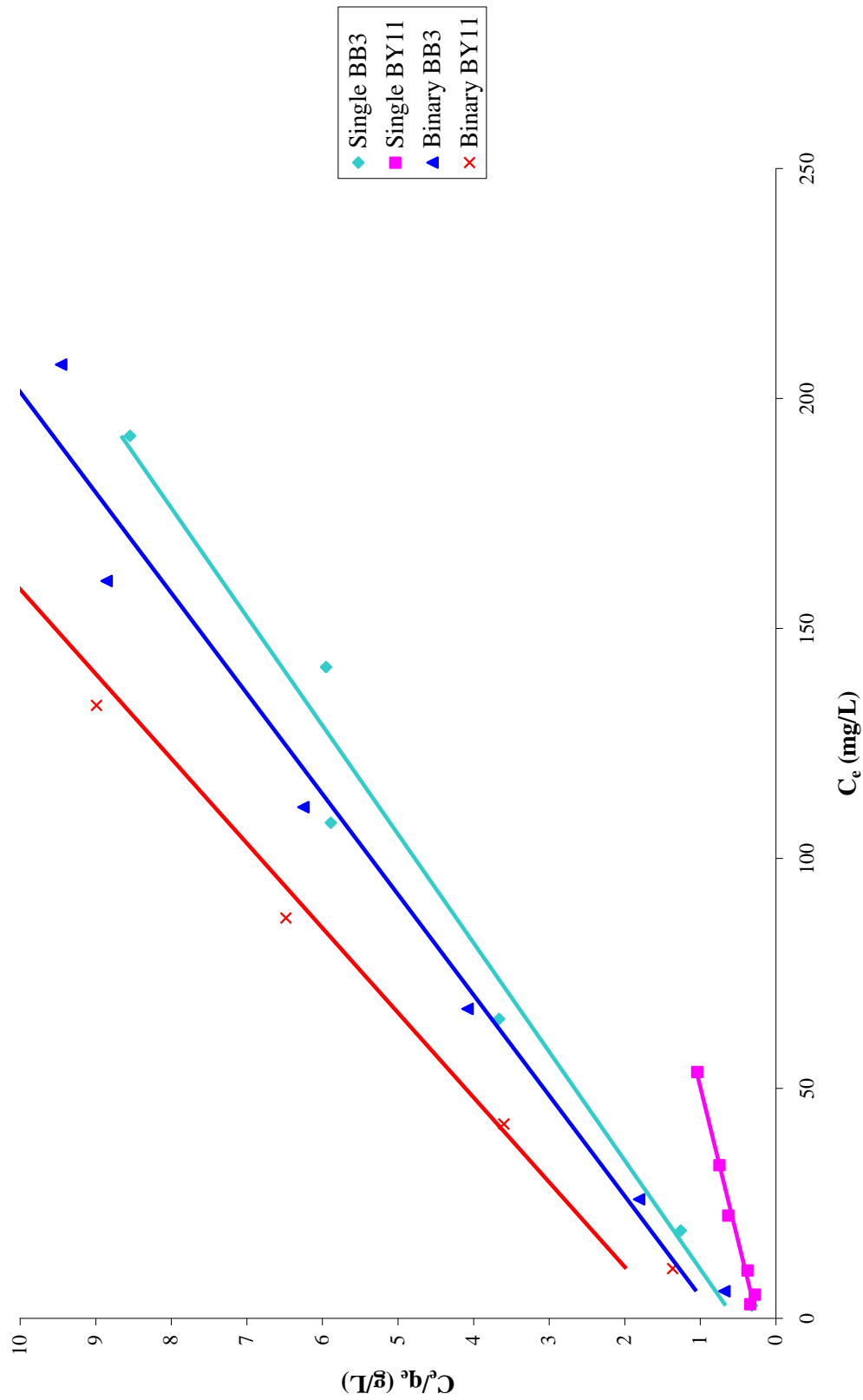
$B$  = BET constant expressive of the energy of interaction with surface

These three models were based on different assumptions. Langmuir model assumes that (i) sorption proceeds only until monolayer was formed, (ii) all binding sites are equivalent (surface is homogenous) and (iii) no lateral interaction between adsorbate molecules. Freundlich model was based on the

sorption on a heterogenous surface while the BET model was the modified Langmuir model which has same assumptions except it allows multilayer sorption.

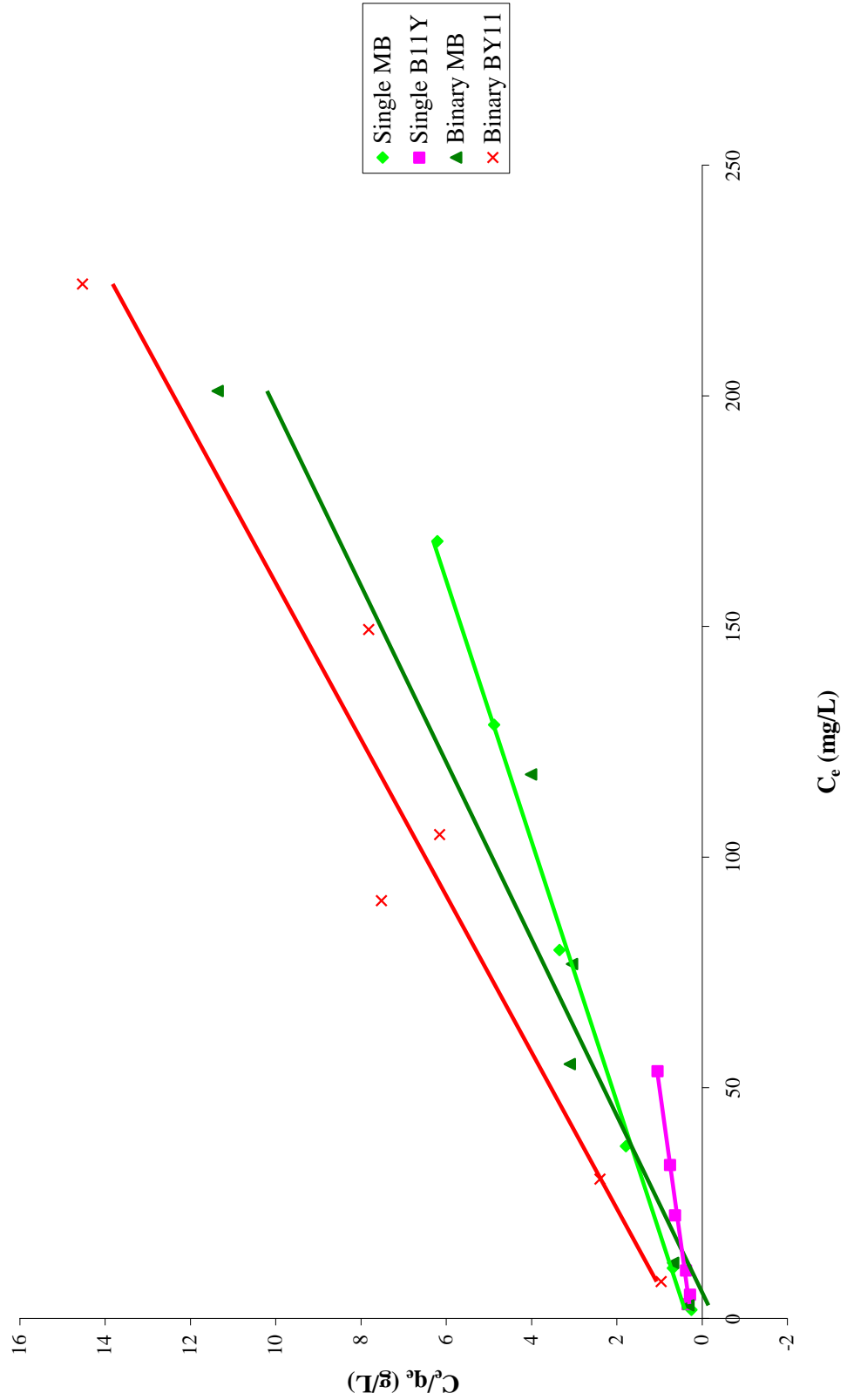
Langmuir, Freundlich and BET plots of BB3, MB and BY11 in single and binary dye solutions were shown in Figures 4.40 – 4.45. The calculated constants and regression values of these three isotherm models are listed in Table 4.5. Based on the data obtained, Langmuir model appeared to provide reasonable fitting for all the dye solutions. The  $q_m$  NSB for all the dye solutions were shown in Table 4.5. A decline in the maximum sorption capacity for binary dye solution was observed as compared to the single solution. This is most probably due to the competition between two types of dyes in the binary dye solutions for the sorption sites. In single dye solution, the  $q_m$  of BY11 was higher compared to BB3 and MB. This might be due to number of sorption site acquired by BY11 (Figure 4.8) was lower compared to BB3 and MB.

In addition, the decline in  $q_m$  of BY11 in both binary solutions compared to single BY11 solution was observed. This phenomenon might be due to different size of adsorbates. BB3 and MB have lower molecular size, thus they were more easily bind to the sorption sites in the binary solution compared to BY11, which was larger. The molecular conformation and dimension of adsorbate affect the adsorption, where planar molecules access and pack in the slit-shape pores more efficiently as compared to nonplanar molecule (Guo *et al.*, 2008).



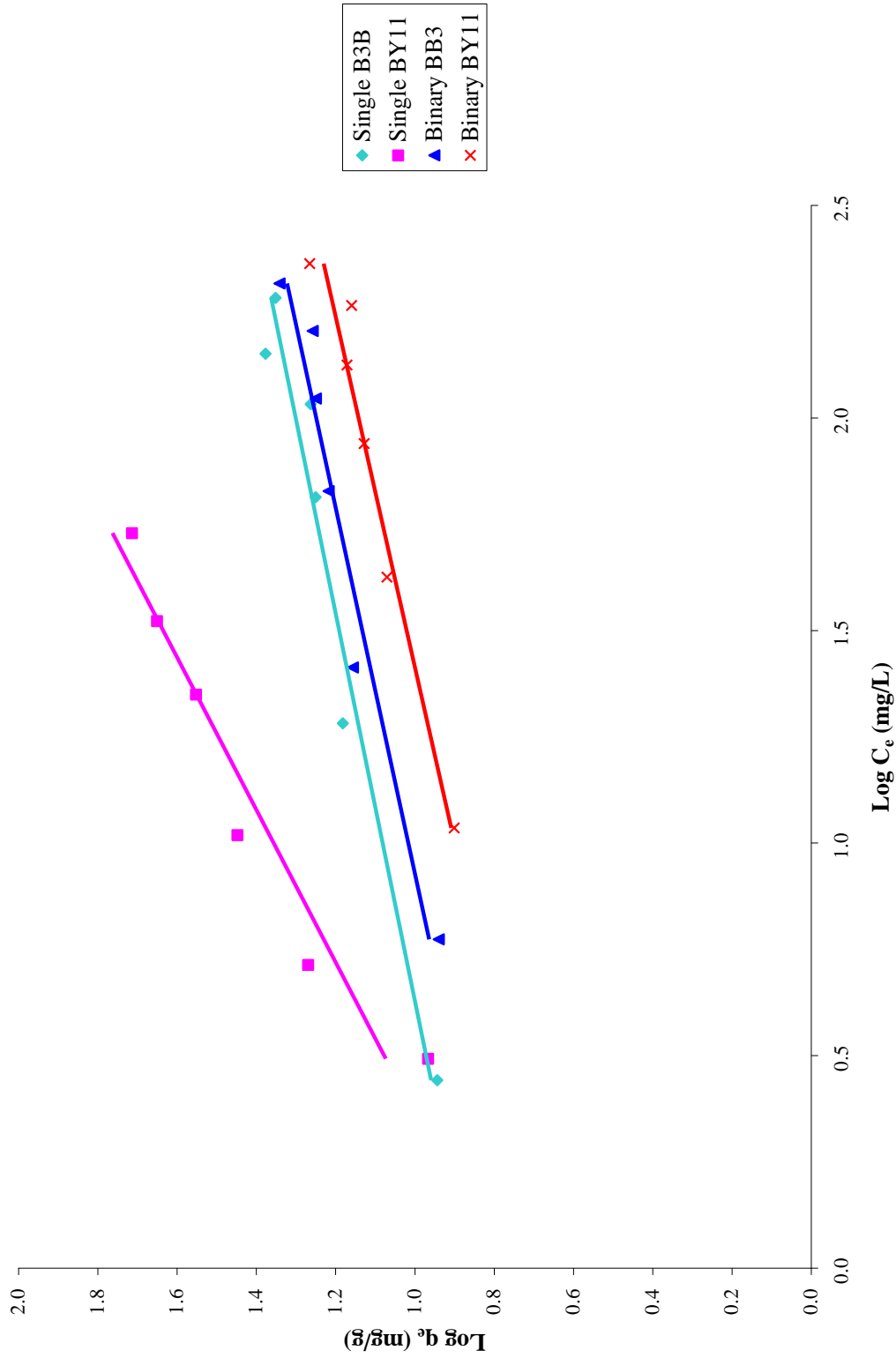
**Condition:** 0.1 g of sorbent in 20 mL of BB3 and BY11 in single and binary dye solutions at 150 rpm for 7 hours at room temperature of  $25 \pm 2^\circ\text{C}$

**Figure 4.40: Langmuir isotherm for BB3 and BY11 in single and binary dye solutions onto NSB**



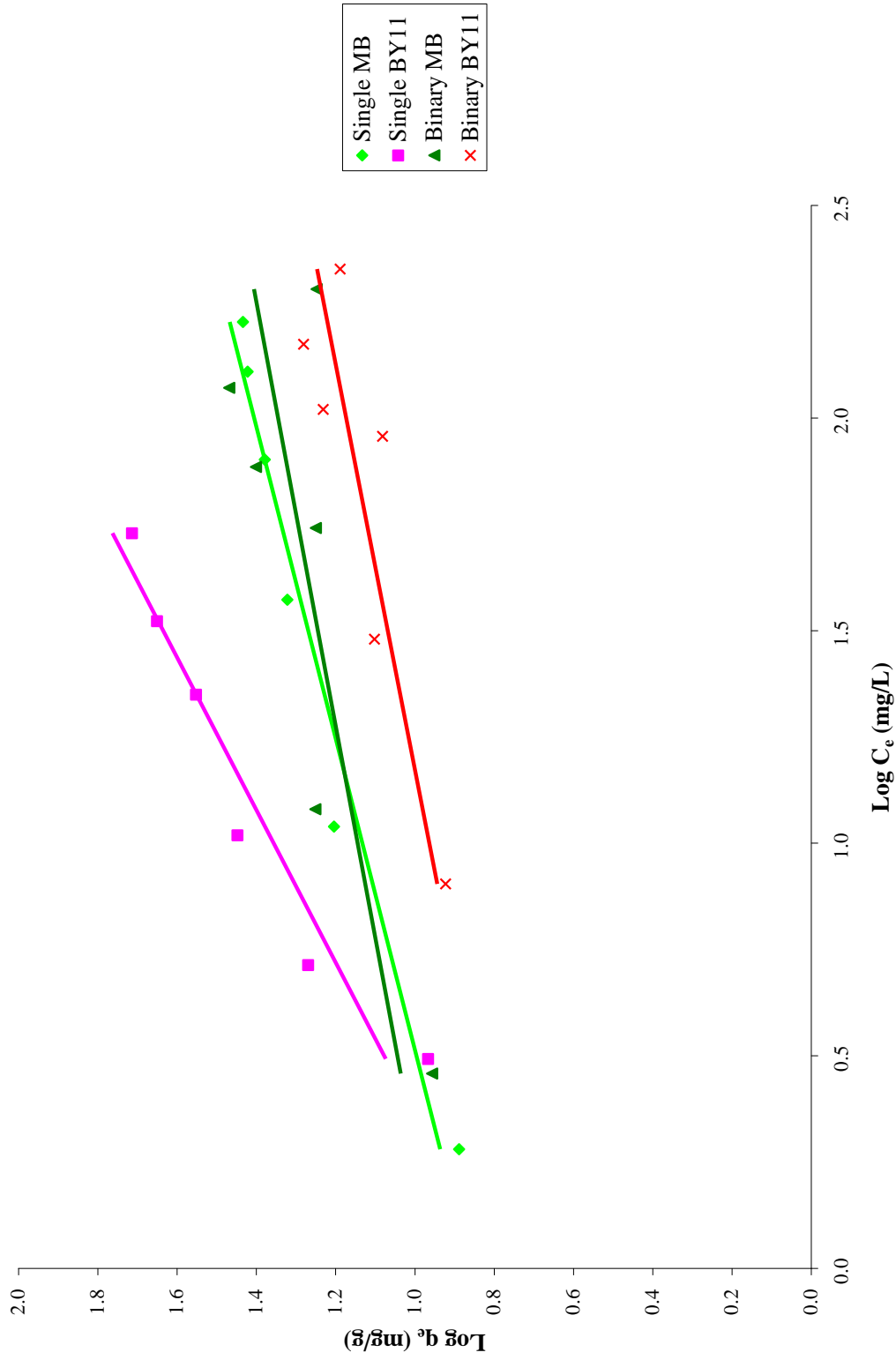
**Condition:** 0.1 g of sorbent in 20 mL of MB and BY11 in single and binary dye solutions at 150 rpm for 7 hours at room temperature of  $25 \pm 2^\circ\text{C}$

**Figure 4.41: Langmuir isotherm for MB and BY11 in single and binary dye solutions onto NSB**



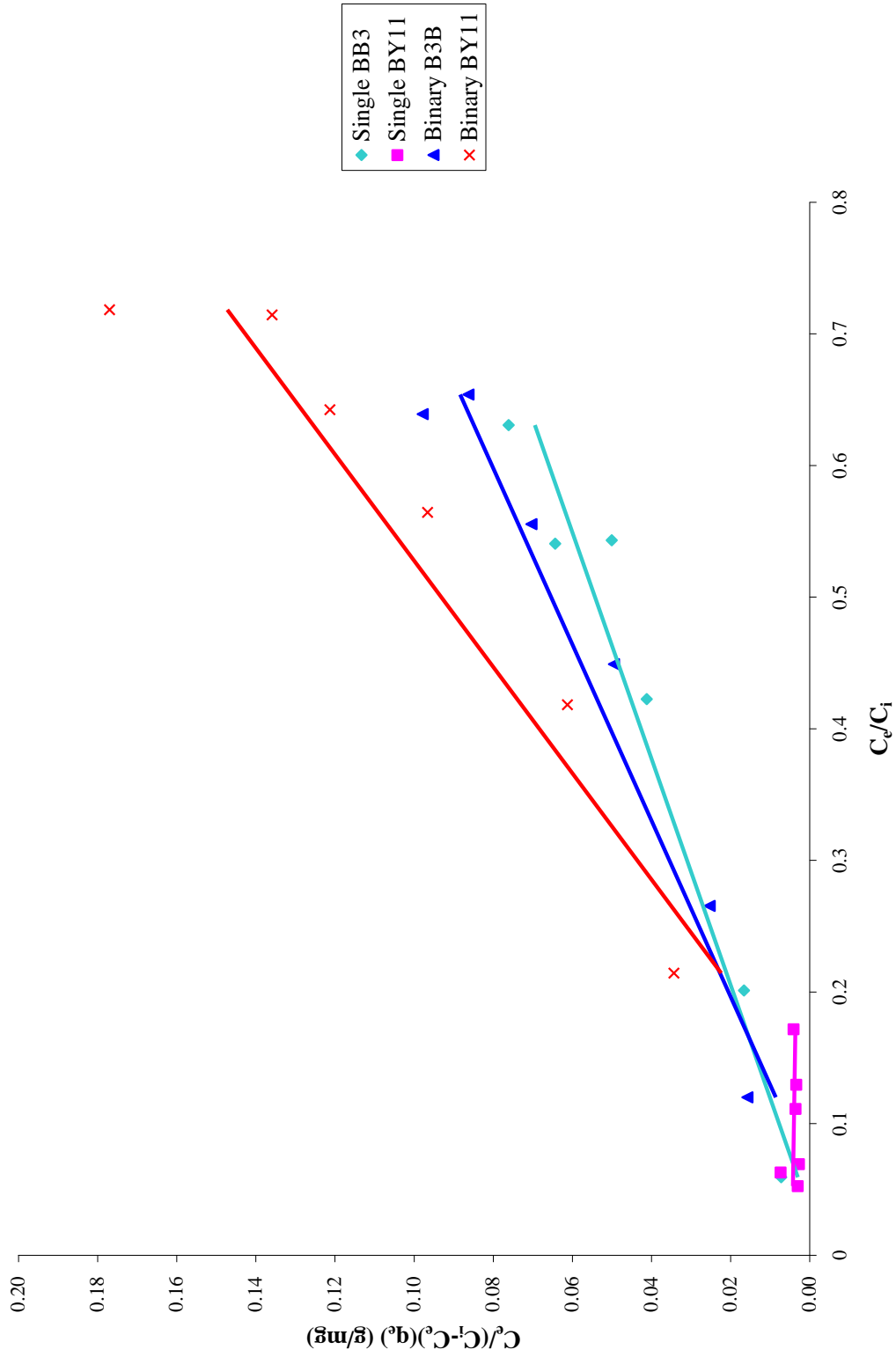
**Condition:** 0.1 g of sorbent in 20 mL of BB3 and BY11 in single and binary dye solutions at 150 rpm for 7 hours at room temperature of  $25 \pm 2^\circ\text{C}$

**Figure 4.42: Freundlich isotherm for BB3 and BY11 in single and binary dye solutions onto NSB**



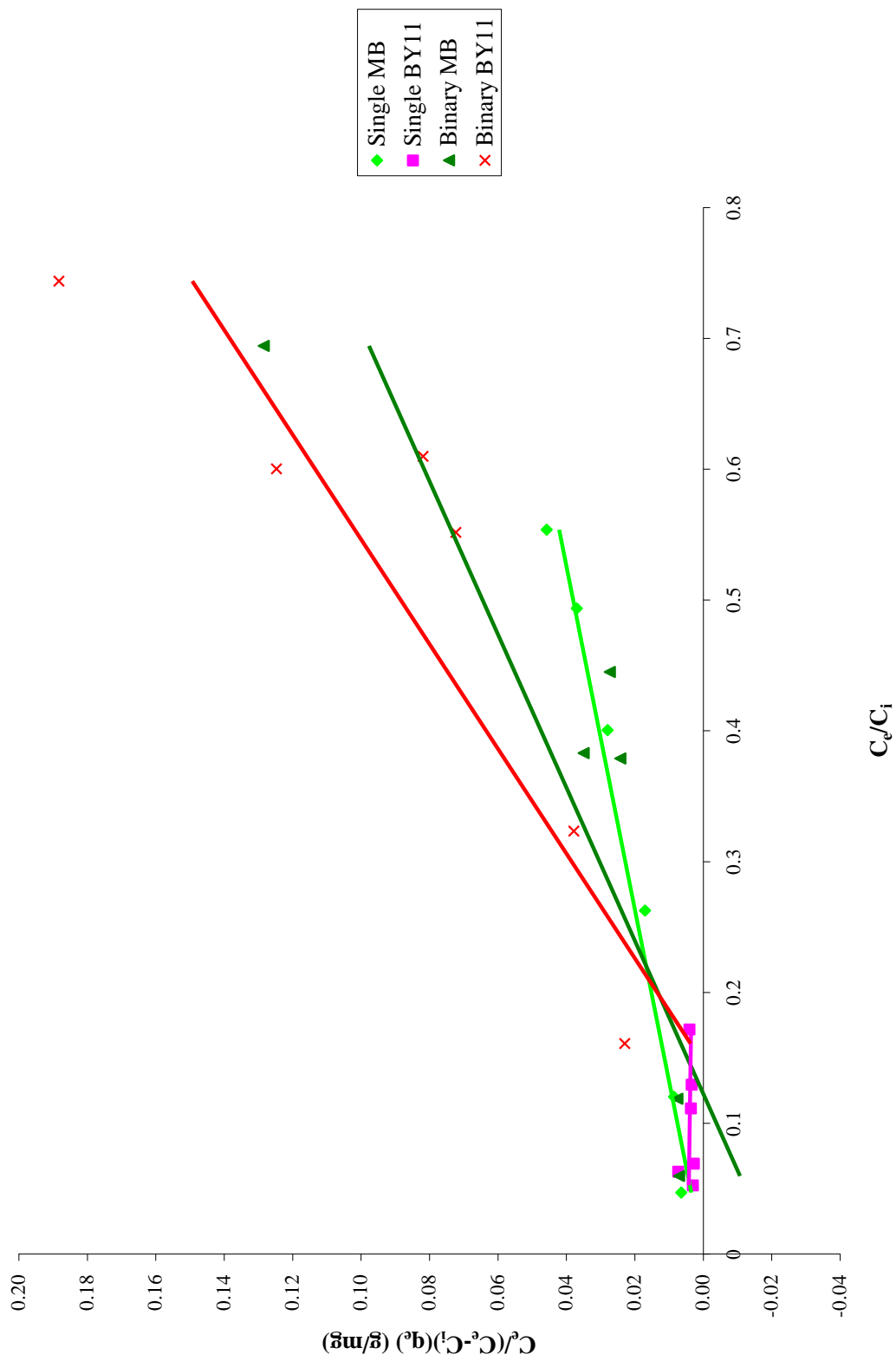
**Condition:** 0.1 g of sorbent in 20 mL of MB and BY11 in single and binary dye solutions at 150 rpm for 7 hours at room temperature of  $25 \pm 2^\circ\text{C}$

**Figure 4.43: Freundlich isotherm for MB and BY11 in single and binary dye solutions onto NSB**



**Condition:** 0.1 g of sorbent in 20 mL of BB3 and BY11 in single and binary dye solutions at 150 rpm for 7 hours at room temperature of  $25 \pm 2^\circ\text{C}$

**Figure 4.44: BET isotherm for BB3 and BY11 in single and binary dye solutions onto NSB**



**Condition:** 0.1 g of sorbent in 20 mL of MB and BY11 in single and binary dye solutions at 150 rpm for 7 hours at room temperature of  $25 \pm 2^\circ\text{C}$

**Figure 4.45: BET isotherm for MB and BY11 in single and binary dye solutions onto NSB**



Table 4.5: Langmuir, Freundlich and BET constants for the sorption of all studied dye solutions

Dye systems	Langmuir			Freundlich			BET		
	$q_m$ (mg/g)	$K_a$ (L/mg)	$R^2$	$K_f$	$n$	$R^2$	$q_m$ (mg/g)	B	$R^2$
Single BB3	23.641	0.077	0.9748	0.7268	4.554	0.9525	23.343	$1.071 \times 10^3$	0.9757
Single MB	28.249	0.106	0.9971	0.7231	3.663	0.9608	27.917	$1.791 \times 10^3$	0.9974
Single BY11	67.110	0.060	0.9835	0.6276	1.791	0.9331	66.578	$7.510 \times 10^2$	0.9837
Binary BB3-BY11	BB3	21.834	0.059	0.6077	4.303	0.9530	21.191	$5.243 \times 10^2$	0.9783
	BY11	18.416	0.039	0.9587	0.4535	0.9487	17.762	$2.815 \times 10^2$	0.9616
Binary MB-BY11	MB	26.178	0.097	0.7065	3.851	0.9229	18.671	$-1.339 \times 10^3$	0.9260
	BY11	21.142	0.028	0.9265	0.5664	0.7567	16.428	$8.696 \times 10^2$	0.9492

An essential character of Langmuir isotherm can be expressed in terms of a dimensionless constant separation factor,  $R_L$  (Wang *et al.*, 2005), which defined by the relationship of:

$$R_L = \frac{1}{1 + K_a C_0} \quad (19)$$

where,

$K_a$  = Langmuir constant (mL/mg)

$C_0$  = initial dye concentration

The  $R_L$  value shows the isotherm shape accordingly with a view to predict if sorption system is “favourable” or “unfavourable” by referring to Table 4.6.

Table 4.6: Shape of isotherm

<b><math>R_L</math> value</b>	<b>Type of isotherm</b>
$R_L > 1$	Unfavourable
$R_L = 1$	Linear
$0 < R_L < 1$	Favourable
$R_L = 0$	Irreversible

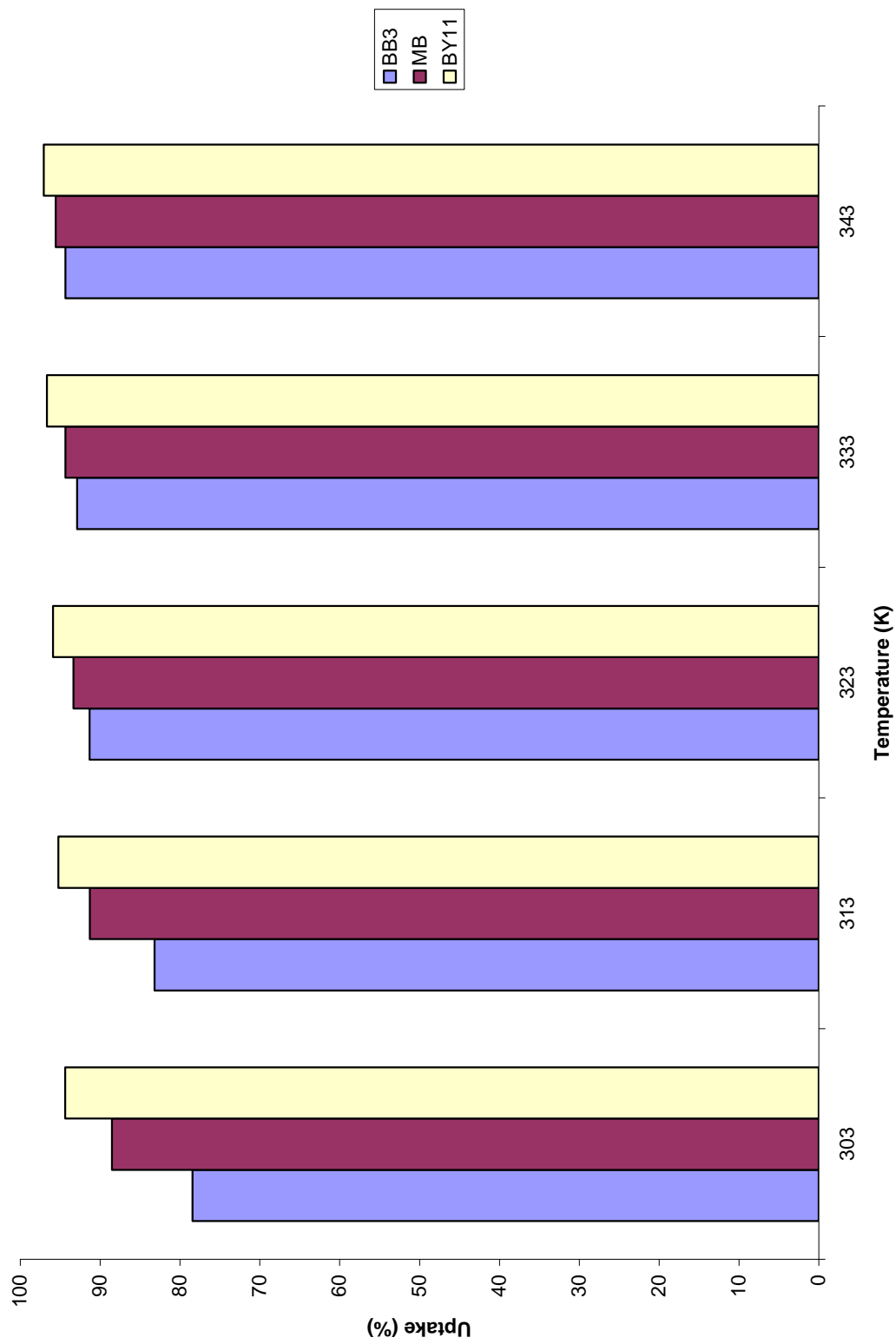
Table 4.7 showed the  $R_L$  values for all the dye solutions under study were in the range of  $0 < R_L < 1$ , which implied favourable sorption process.

Table 4.7: Values of  $R_L$  for all the studied dye solutions

$C_0$ (mg/L)	BB3 (Single)	MB (Single)	BY11 (Single)	Binary BB3-BY11		Binary MB-BY11	
				BB3	BY11	MB	BY11
50	0.199	0.159	0.249	0.254	0.339	0.172	0.417
100	0.111	0.086	0.142	0.145	0.204	0.094	0.263
150	0.077	0.059	0.100	0.102	0.146	0.065	0.192
200	0.078	0.045	0.077	0.078	0.113	0.049	0.151
250	0.047	0.036	0.062	0.064	0.093	0.040	0.125
300	0.040	0.030	0.052	0.054	0.079	0.033	0.106

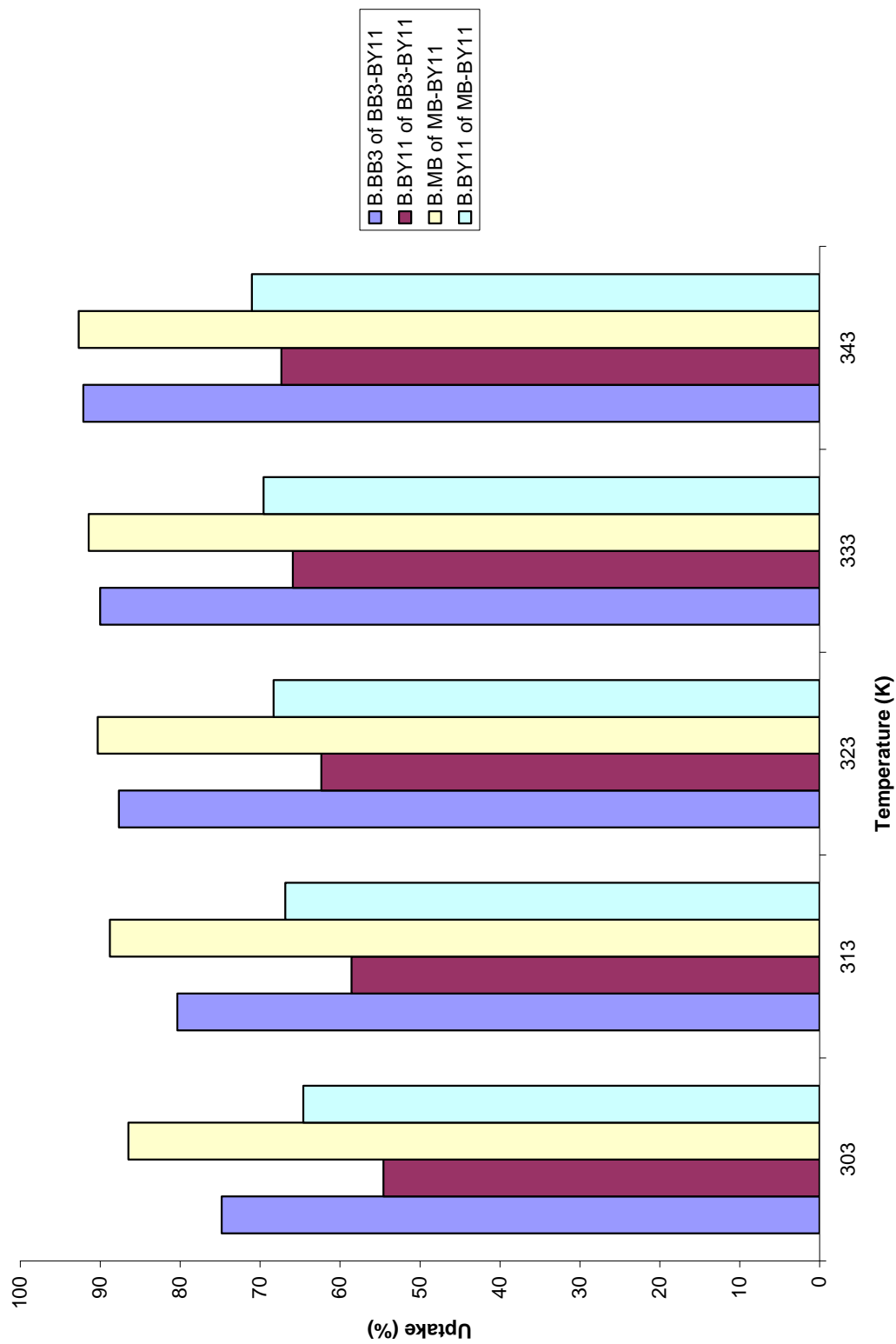
#### 4.6.8 Effect of Temperature

Figures 4.46 and 4.47 show the effect of temperature on the sorption of BB3, MB and BY11 in single and binary dye solutions. The temperature dependence of targeted dyes sorption onto NSB was studied under the temperature range of 303 K to 343 K. From the plots, the percentage uptake of all dye solutions increased as the temperature of the solution increased from 303 K to 343 K, indicating that the sorption process was endothermic. The increment in sorption might be due to the increased rate of diffusion of the adsorbate molecules



**Condition:** 0.1 g of sorbent in 20 mL of BB3, MB and BY11 in single dye solution at 150 rpm for 4 hours at 30, 40, 50, 60 and 70°C

**Figure 4.46: Effect of temperature on the sorption of BB3, MB and BY11 in single dye solutions onto NSB**



**Condition:** 0.1 g of sorbent in 20 mL of BB3, MB and BY11 in binary dye solution at 150 rpm for 4 hours at 30, 40, 50, 60 and 70°C

**Figure 4.47: Effect of temperature on the sorption of BB3, MB and BY11 in binary dye solutions onto NSB**

as the viscosity of the dye solution decreases with increase in temperature (Özdemir *et al.*, 2006).

The thermodynamic parameters of all studied dye solutions were calculated using following van't Hoff equation:

$$\ln\left(\frac{q_e}{C_e}\right) = \frac{\Delta S^\circ}{R} - \frac{\Delta H^\circ}{RT} \quad (20)$$

where,

$q_e/C_e$  = equilibrium constant (mL/g)

$\Delta S^\circ$  = standard entropy (J/molK)

$\Delta H^\circ$  = standard enthalpy (J/mol)

T = absolute temperature (K)

R = gas constant (8.314 J/molK)

The  $\Delta S^\circ$  and  $\Delta H^\circ$  values were determined from the slope and intercept, respectively, of linear plot of  $\ln(q_e/C_e)$  against  $1/T$ , and showed in Table 4.8. The thermodynamic parameter,  $\Delta G^\circ$ , was calculated using following Gibbs-Helmholtz equation:

$$\Delta G^\circ = \Delta H^\circ - T\Delta S^\circ \quad (21)$$

where,

$\Delta G^\circ$  = standard free energy (kJ/mol).

The negative values of  $\Delta G^\circ$  (Table 4.8) for all the dye solutions indicated that all the sorption processes were spontaneous, confirming the affinity of NSB

for the dyes. A similar phenomenon was reported by Weng *et al.* (2009) in the removal of Methylene Blue by pineapple leaf powder. The positive values of  $\Delta H^0$  indicated that the sorption processes of BB3, MB and BY11 in single and binary solutions were endothermic. The positive value of  $\Delta S^0$  indicated the increase of randomness at the interface of NSB-solution during the sorption process.

Table 4.8: The values of  $\Delta S^0$ ,  $\Delta H^0$  and  $\Delta G^0$  for all studied dye solutions

Dye solutions		$\Delta S^0$ (J/molK)	$\Delta H^0$ (J/mol)	$\Delta G^0$ (kJ/mol)				
				303 K	313 K	323 K	333 K	343 K
Single BB3		18.5456	3619	-2000	-2186	-2371	-2557	-2742
Single MB		12.3315	1493	-2244	-2367	-2490	-2614	-2767
Single BY11		9.7906	588	-2379	-2477	-2575	-2673	-2770
Binary BB3-BY11	BB3	19.0433	3862	-1909	-2099	-2289	-2480	-2670
	BY11	13.9697	2849	-1383	-1523	-1663	-1802	-1942
Binary MB-BY11	MB	11.5296	1307	-2186	-2301	-2417	-2532	-2647
	BY11	9.8500	1351	-1634	-1732	-1831	-1929	-2028

#### 4.6.9 Effect of Particle Size

The effect of particle size on the percentage uptake of BB3, MB and BY11 by NSB in single and binary dye solutions are shown in Table 4.9. From Table 4.9, the percentage uptake decrease as the particle size of the sorbent increase. The

lower uptake was probably due to the decrease in the surface area over the weight of the sorbent as the size increase. Small particle moves faster in solution thus there is more shear on their surface. This follows that the boundary layer thickness is thinner than that on the larger particles which caused a faster rate of sorption.

Table 4.9: The effect of particle size for all studied dye solutions

Particle size Dye solutions		% Uptake		
		< 300 micron	300 – 600 micron	> 600 micron
Single BB3		96.62	92.99	91.61
Single MB		95.99	94.81	94.12
Single BY11		96.70	95.71	92.30
Binary BB3-BY11	BB3	96.65	91.33	87.18
	BY11	89.36	81.43	76.53
Binary MB-BY11	MB	97.26	95.00	89.99
	BY11	87.49	82.59	75.24

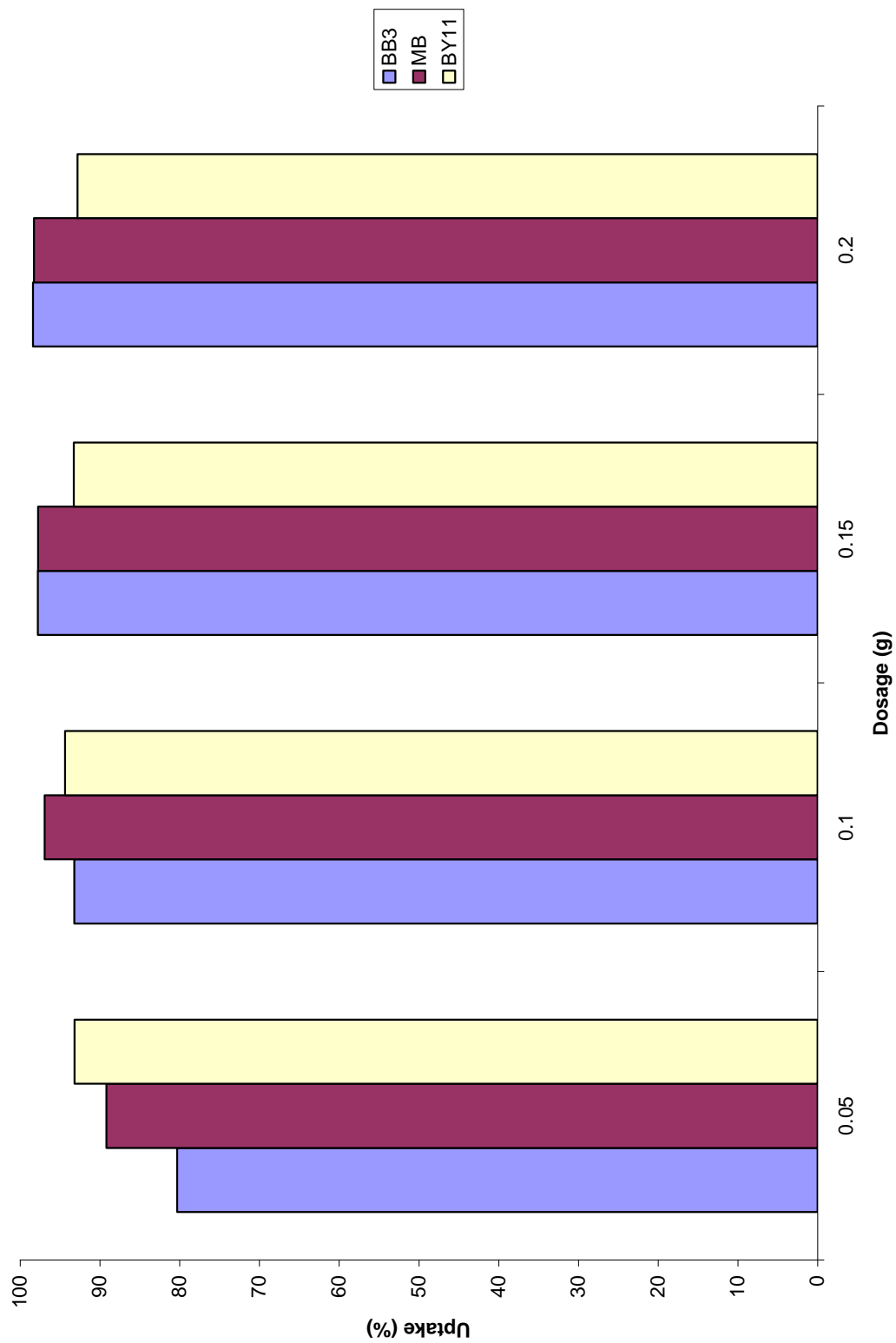
A similar observation was reported by Wang *et al.* (2005) on treatment of MB using unburned carbon. They proposed that the increase in dye sorption as the particle size decreases was probably due to the increase in surface area and also suggested that external transport limits the rate of sorption. In addition, similar trend were also reported in the removal of dyes by modified rice hull.



#### 4.6.10 Effect of Sorbent Dosage

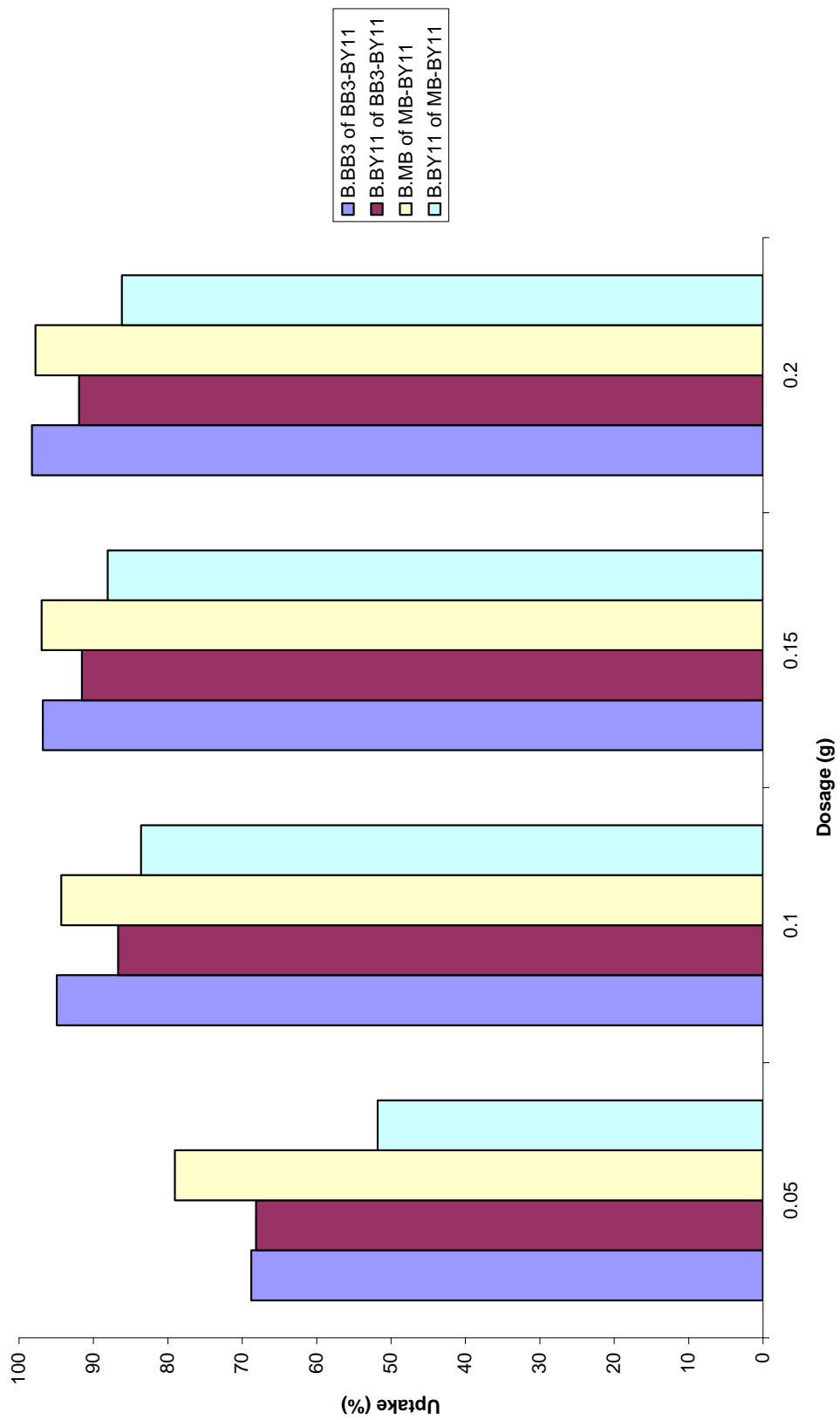
The effect of sorbent dosage on the percentage uptake of BB3, MB and BY11 in single and binary solutions were shown in Figures 4.48 and 4.49, respectively. Generally, the percentage uptake of the targeted dyes increased as the sorbent dosage increased from 0.05 g to 0.20 g. This phenomenon followed the expected trend where increasing sorbent dosage increases the percentage uptake of dye. A higher sorbent dosage can attribute to the increase of surface area and availability of sorption sites (Garg *et al.*, 2004; Fungaro *et al.*, 2009; Wong *et al.*, 2009).

The optimum dosage for all studied dyes was found to be 0.10 g of NSB. As the sorbent dosage increased above 0.10 g, only minimal increment in percentage uptake was observed. A similar behaviour was observed in a study by Hameed (2009) on the removal of methylene blue using papaya seeds.



**Condition:** 0.05, 0.10, 0.15 and 0.20 g of sorbent in 20 mL of BB3, MB and BY11 in single dye solution at 150 rpm for 4 hours at room temperature of  $25 \pm 2^\circ\text{C}$

**Figure 4.48: Effect of sorbent dosage on the sorption of BB3, MB and BY11 in single dye solutions onto NSB**



**Condition:** 0.05, 0.10, 0.15 and 0.20 g of sorbent in 20 mL of BB3, MB and BY11 in binary dye solution at 150 rpm for 4 hours at room temperature of  $25 \pm 2^\circ\text{C}$

**Figure 4.49: Effect of sorbent dosage on the sorption of BB3, MB and BY11 in binary dye solutions onto NSB**

## 4.7 Optimisation Studies

### 4.7.1 Plackett-Burman Design

Plackett-Burman design is an approach which can be used to evaluate the relative importance of various parameters that influence the percentage uptake in the sorption study. It is able to determine the most important parameters for further optimisation and provides unbiased estimates of linear of all variables with maximum accuracy for a given number of observation (Rajendran *et al.*, 2007). In this study, five factors which are most likely to affect the percentage uptake (pH, contact time, initial dye concentration, sorbent particle size and sorbent dosage) were screened in twelve experimental designs. Tables 4.10 to 4.16 show the design and the results for the removal of BB3, MB and BY11 in both single and binary dye solutions.

Analysis of variance (ANOVA) results of all the dye solutions under studied are presented in Tables 4.17 to 4.23. For single BB3 and MB dye solutions, both models were significant with *Prob>F* value of 0.0027 (Tables 4.17 and 4.18). Model terms were determined as significant when the value of *Prob>F* was less than 0.05. Both models of binary BB3 and MB also exhibited a significant model with *Prob>F* less than 0.05. Whereas, all the BY11 solutions models (single and binary) were insignificant. The *Prob>F* obtained were 0.5652,

0.6605 and 0.6482 for single BY11, binary BY11 of BB3-BY11 and binary BY11 of MB-BY11 dye solutions, respectively.

Table 4.10: Plackett-Burman design and results for the removal of BB3 from single dye solution

Experimental run	Variables					Observed response (%)	Predicted response (%)
	pH	Contact time	Particle size	Initial dye concentration	Sorbent dosage		
1	3.00	5.00	150.00	50.00	0.05	79.12	66.30
2	9.00	5.00	850.00	200.00	0.05	29.24	31.11
3	9.00	240.00	850.00	50.00	0.05	84.33	79.52
4	3.00	240.00	150.00	200.00	0.20	85.89	80.10
5	3.00	240.00	850.00	50.00	0.20	96.11	100.70
6	3.00	5.00	850.00	50.00	0.20	88.44	86.43
7	9.00	5.00	850.00	200.00	0.20	73.78	64.77
8	9.00	5.00	150.00	50.00	0.20	97.12	112.43
9	3.00	240.00	850.00	200.00	0.05	23.54	32.91
10	3.00	5.00	150.00	200.00	0.05	25.51	32.17
11	9.00	240.00	150.00	50.00	0.05	93.32	93.05
12	9.00	240.00	150.00	200.00	0.20	95.66	92.57

Table 4.11: Plackett-Burman design and results for the removal of MB from single dye solution

Experimental run	Variables					Observed response (%)	Predicted response (%)
	pH	Contact time	Particle size	Initial dye concentration	Sorbent dosage		
1	3.00	5.00	150.00	50.00	0.05	80.57	66.30
2	9.00	5.00	850.00	200.00	0.05	29.36	30.98
3	9.00	240.00	850.00	50.00	0.05	85.03	79.52
4	3.00	240.00	150.00	200.00	0.20	86.79	80.52
5	3.00	240.00	850.00	50.00	0.20	96.38	101.36
6	3.00	5.00	850.00	50.00	0.20	89.31	87.44
7	9.00	5.00	850.00	200.00	0.20	73.71	65.08
8	9.00	5.00	150.00	50.00	0.20	98.83	113.79
9	3.00	240.00	850.00	200.00	0.05	23.23	32.48
10	3.00	5.00	150.00	200.00	0.05	25.28	32.49
11	9.00	240.00	150.00	50.00	0.05	93.03	93.61
12	9.00	240.00	150.00	200.00	0.20	96.11	92.93

Table 4.12: Plackett-Burman design and results for the removal of BY11 from single dye solution

Experimental run	Variables					Observed response (%)	Predicted response (%)
	pH	Contact time	Particle size	Initial dye concentration	Sorbent dosage		
1	3.00	5.00	150.00	50.00	0.05	80.30	63.96
2	9.00	5.00	850.00	200.00	0.05	66.95	61.34
3	9.00	240.00	850.00	50.00	0.05	84.17	67.55
4	3.00	240.00	150.00	200.00	0.20	93.95	72.94
5	3.00	240.00	850.00	50.00	0.20	89.59	79.69
6	3.00	5.00	850.00	50.00	0.20	87.72	83.07
7	9.00	5.00	850.00	200.00	0.20	91.15	80.51
8	9.00	5.00	150.00	50.00	0.20	58.87	90.16
9	3.00	240.00	850.00	200.00	0.05	34.93	50.94
10	3.00	5.00	150.00	200.00	0.05	48.04	54.37
11	9.00	240.00	150.00	50.00	0.05	83.72	70.39
12	9.00	240.00	150.00	200.00	0.20	91.83	79.97

Table 4.13: Plackett-Burman design and results for the removal of BB3 from  
BB3-BY11 binary dye solution

Experimental run	Variables					Observed response (%)	Predicted response (%)
	pH	Contact time	Particle size	Initial dye concentration	Sorbent dosage		
1	3.00	5.00	150.00	50.00	0.05	70.05	61.75
2	9.00	5.00	850.00	200.00	0.05	30.01	31.39
3	9.00	240.00	850.00	50.00	0.05	83.93	79.44
4	3.00	240.00	150.00	200.00	0.20	85.87	79.98
5	3.00	240.00	850.00	50.00	0.20	96.01	100.40
6	3.00	5.00	850.00	50.00	0.20	88.33	84.78
7	9.00	5.00	850.00	200.00	0.20	73.70	66.44
8	9.00	5.00	150.00	50.00	0.20	96.99	110.89
9	3.00	240.00	850.00	200.00	0.05	23.39	32.92
10	3.00	5.00	150.00	200.00	0.05	25.49	29.32
11	9.00	240.00	150.00	50.00	0.05	93.40	91.46
12	9.00	240.00	150.00	200.00	0.20	95.66	94.07



Table 4.14: Plackett-Burman design and results for the removal of BY11 from  
BB3-BY11 binary dye solution

Experimental run	Variables					Observed response (%)	Predicted response (%)
	pH	Contact time	Particle size	Initial dye concentration	Sorbent dosage		
1	3.00	5.00	150.00	50.00	0.05	38.24	29.69
2	9.00	5.00	850.00	200.00	0.05	31.88	28.20
3	9.00	240.00	850.00	50.00	0.05	40.08	35.87
4	3.00	240.00	150.00	200.00	0.20	44.74	36.48
5	3.00	240.00	850.00	50.00	0.20	40.72	41.53
6	3.00	5.00	850.00	50.00	0.20	39.87	38.53
7	9.00	5.00	850.00	200.00	0.20	41.43	36.66
8	9.00	5.00	150.00	50.00	0.20	26.76	40.96
9	3.00	240.00	850.00	200.00	0.05	15.18	28.39
10	3.00	5.00	150.00	200.00	0.05	20.89	25.02
11	9.00	240.00	150.00	50.00	0.05	36.40	35.50
12	9.00	240.00	150.00	200.00	0.20	39.93	39.29

Table 4.15: Plackett-Burman design and results for the removal of MB from MB-BY11 binary dye solution

Experimental run	Variables					Observed response (%)	Predicted response (%)
	pH	Contact time	Particle size	Initial dye concentration	Sorbent dosage		
1	3.00	5.00	150.00	50.00	0.05	75.01	64.48
2	9.00	5.00	850.00	200.00	0.05	29.89	31.21
3	9.00	240.00	850.00	50.00	0.05	84.03	79.49
4	3.00	240.00	150.00	200.00	0.20	85.67	80.06
5	3.00	240.00	850.00	50.00	0.20	95.91	100.37
6	3.00	5.00	850.00	50.00	0.20	88.55	85.43
7	9.00	5.00	850.00	200.00	0.20	72.90	65.21
8	9.00	5.00	150.00	50.00	0.20	96.81	111.60
9	3.00	240.00	850.00	200.00	0.05	23.45	33.02
10	3.00	5.00	150.00	200.00	0.05	25.90	31.13
11	9.00	240.00	150.00	50.00	0.05	93.60	92.54
12	9.00	240.00	150.00	200.00	0.20	96.00	93.18

Table 4.16: Plackett-Burman design and results for the removal of BY11 from MB-BY11 binary dye solution

Experimental run	Variables					Observed response (%)	Predicted response (%)
	pH	Contact time	Particle size	Initial dye concentration	Sorbent dosage		
1	3.00	5.00	150.00	50.00	0.05	36.50	28.19
2	9.00	5.00	850.00	200.00	0.05	30.43	27.26
3	9.00	240.00	850.00	50.00	0.05	38.26	34.59
4	3.00	240.00	150.00	200.00	0.20	42.71	35.21
5	3.00	240.00	850.00	50.00	0.20	40.72	41.16
6	3.00	5.00	850.00	50.00	0.20	39.87	38.40
7	9.00	5.00	850.00	200.00	0.20	41.43	36.07
8	9.00	5.00	150.00	50.00	0.20	24.53	39.24
9	3.00	240.00	850.00	200.00	0.05	14.55	27.79
10	3.00	5.00	150.00	200.00	0.05	20.02	23.63
11	9.00	240.00	150.00	50.00	0.05	34.88	33.19
12	9.00	240.00	150.00	200.00	0.20	38.26	37.45

Table 4.17: Regression analysis (ANOVA) of Plackett-Burman for the removal of  
BB3 from single dye solution

Source	Degree of freedom	Sum of Square	Mean Square	<i>F</i> -value	Prob>F
Model	5	8521.37	1704.27	14.46	0.0027
pH	1	466.75	466.75	3.96	0.0937
Contact time	1	611.18	611.18	5.19	0.0630
Particle size	1	549.18	549.18	4.66	0.0742
Initial dye concentration	1	3495.94	3495.94	29.67	0.0016
Sorbent Dosage	1	3398.31	3398.31	228.84	0.0017
Residual	6	707.07	117.84		
Total	11	9228.44			

Table 4.18: Regression analysis (ANOVA) of Plackett-Burman for the removal of  
MB from single dye solution

Source	Degree of freedom	Sum of Square	Mean Square	<i>F</i> -value	Prob>F
Model	5	8744.01	1748.80	14.53	0.0027
pH	1	462.60	462.60	3.84	0.0976
Contact time	1	581.11	581.11	4.83	0.0703
Particle size	1	582.25	582.25	4.84	0.0701
Initial dye concentration	1	3628.53	3628.53	30.16	0.0015
Sorbent Dosage	1	3489.52	3489.52	29.00	0.0017
Residual	6	721.92	120.32		
Total	11	9465.94			

Table 4.19: Regression analysis (ANOVA) of Plackett-Burman for the removal of  
BY11 from single dye solution

Source	Degree of freedom	Sum of Square	Mean Square	<i>F</i> -value	Prob>F
Model	5	1696.75	339.35	0.84	0.5652
pH	1	148.16	148.16	0.37	0.5664
Contact time	1	169.97	169.97	0.42	0.5400
Particle size	1	0.41	0.41	1.02 x 10 <sup>-3</sup>	0.9756
Initial dye concentration	1	275.78	275.78	0.68	0.4397
Sorbent Dosage	1	1102.43	1102.43	2.74	0.1491
Residual	6	2416.88	402.81		
Total	11	4113.63			

Table 4.20: Regression analysis (ANOVA) of Plackett-Burman for the removal of  
BB3 from BB3-BY11 binary dye solution

Source	Degree of freedom	Sum of Square	Mean Square	<i>F</i> -value	Prob>F
Model	5	8600.89	1720.18	20.04	0.0011
pH	1	595.73	595.73	6.94	0.0388
Contact time	1	731.48	731.48	8.52	0.0267
Particle size	1	433.08	433.08	5.04	0.0658
Initial dye concentration	1	3155.44	3155.44	36.76	0.0009
Sorbent Dosage	1	3685.16	3685.16	42.93	0.0006
Residual	6	515.07	85.85		
Total	11	9115.96			

Table 4.21: Regression analysis (ANOVA) of Plackett-Burman for the removal of  
BY11 from BB3-BY11 binary dye solution

Source	Degree of freedom	Sum of Square	Mean Square	<i>F</i> -value	Prob>F
Model	5	331.37	66.27	0.67	0.6605
pH	1	23.62	23.62	0.24	0.6420
Contact time	1	26.96	26.96	0.27	0.6199
Particle size	1	0.41	0.41	4.17 x 10 <sup>-3</sup>	0.9506
Initial dye concentration	1	65.46	65.46	0.66	0.4465
Sorbent Dosage	1	214.92	214.92	2.18	0.1905
Residual	6	529.11	98.69		
Total	11	923.48			

Table 4.22: Regression analysis (ANOVA) of Plackett-Burman for the removal of  
MB from MB-BY11 binary dye solution

Source	Degree of freedom	Sum of Square	Mean Square	<i>F</i> -value	Prob>F
Model	5	8499.37	1699.87	16.99	0.017
pH	1	516.67	516.67	5.17	0.0634
Contact time	1	669.01	669.01	6.69	0.0414
Particle size	1	510.39	510.39	5.10	0.0647
Initial dye concentration	1	3336.64	3336.64	33.36	0.0012
Sorbent Dosage	1	3466.64	3466.64	34.66	0.0011
Residual	6	600.19	100.03		
Total	11	9099.56			

Table 4.23: Regression analysis (ANOVA) of Plackett-Burman for the removal of BY11 from MB-BY11 binary dye solution

Source	Degree of freedom	Sum of Square	Mean Square	F-value	Prob>F
Model	5	339.34	67.87	0.69	0.6482
pH	1	15.03	15.03	0.15	0.7089
Contact time	1	22.98	22.98	0.23	0.6454
Particle size	1	5.84	5.84	0.06	0.8153
Initial dye concentration	1	62.42	62.42	0.64	0.4553
Sorbent Dosage	1	233.08	233.08	2.38	0.1740
Residual	6	588.07	98.01		
Total	11	927.41			

The factors which will affect the percentage uptakes of dye were identified based on the value of *Prob>F* (model terms with value of *Prob>F* less than 0.05 will be identified as significant). Sorbent dosage and initial dye concentration were found out to be the factors which will affect the percentage uptake for single BB3 and MB. For binary BB3, pH, contact time, initial dye concentration and sorbent dosage were the model terms which were significant, while, particle size was not significant for the response (*Prob>F* = 0.0658). Meanwhile, for binary MB, contact time, initial dye concentration and sorbent dosage were the significant model terms. All the studied factors were not significant for single and both binary BY11 solutions.

#### 4.7.2 Verification of Plackett-Burman Design Models

In order to validate the models, function of desirability was applied. The experiment conditions to be verified were chosen based on the highest desirability. The experiment conditions as well as the predicted and experimental results for all dye solutions were shown in Table 4.24. The experimental values were in good agreement with the predicted values for all the dye solutions. The percentage errors were 1.73, 2.31, 5.33 and 3.80 for single BB3, single MB, binary BB3 and binary MB, respectively. The models of single and both binary BY11 solutions were not verified due to the insignificance of the models.

Table 4.24: Plackett-Burman model validation

Dye solution	Factors					Percentage uptake (%)	
	pH	Contact Time	Particle Size	Initial dye Concentration	Sorbent dosage	Predicted	Experimental
Single BB3	8.76	193.00	178.00	194.00	0.19	87.49	85.98
Single MB	8.76	193.00	178.00	56.00	0.06	90.65	88.56
Binary BB3	8.74	72.00	181.00	186.00	0.09	59.09	55.94
Binary MB	5.07	133.00	385.00	171.00	0.09	54.93	52.84



### 4.7.3 Response Surface Methodology Approach

#### 4.7.3.1 Single Dye Solutions

The important parameters which affect the percentage uptake of dyes were further studied using Response Surface Methodology (RSM) approach. Table 4.25 shows the result for the effect of initial dye concentration and sorbent dosage for single BB3 and MB dye solutions. Modified cubic model was used to describe the correlation between the two variables and the percentage uptake for single BB3 and MB were shown as follows as in terms of coded factors:

Single BB3 dye solution:

$$\begin{aligned} \% \text{ Uptake} = & 114.943 - 1.377A + 259.837B + 9.032AB + 0.004A^2 \\ & - 2376.894B^2 - 0.0292A^2B \end{aligned} \quad (22)$$

Single MB dye solution:

$$\begin{aligned} \% \text{ Uptake} = & 91.717 - 0.807A + 298.411B + 5.829AB + 0.002A^2 \\ & - 1836.390B^2 - 0.017A^2B \end{aligned} \quad (23)$$

where, A = initial dye concentration and B = sorbent dosage.

The results of analysis of variance (ANOVA) for both single BB3 and MB dye solutions were shown in Tables 4.26 and 4.27. From these tables, both of the

Table 4.25: The central composite design matrix for two coded independent variables and the observed response for single BB3 and MB

Experimental run	Coded values of variables		Single BB3		Single MB	
	A	B	Observed response (%)	Predicted response (%)	Observed response (%)	Predicted response (%)
1	-1.414	0	96.97	98.59	94.65	94.81
2	+1.414	0	71.57	71.99	57.78	58.86
3	0	-1.414	43.98	45.00	47.13	47.75
4	0	+1.414	94.63	95.66	91.92	92.55
5	-1	-1	79.95	78.50	77.50	77.21
6	1	-1	50.61	50.02	44.19	43.24
7	-1	1	97.36	95.92	95.49	95.19
8	1	1	87.39	86.80	79.28	78.33
9	0	0	82.13	83.70	80.31	80.28
10	0	0	82.88	83.70	82.40	80.28
11	0	0	85.08	83.70	79.85	80.28
12	0	0	85.11	83.70	80.93	80.28
13	0	0	83.30	83.70	78.89	80.28

Table 4.26: Regression analysis (ANOVA) for the removal of BB3 from single dye solution

Source	Degree of freedom	Sum of Square	Mean Square	F-value	P
Model	6	3148.85	524.81	186.06	< 0.0001
A	1	707.14	707.14	250.70	< 0.0001
B	1	1283.11	1283.11	454.90	< 0.0001
AB	1	93.76	93.76	33.24	0.0012
A <sup>2</sup>	1	4.42	4.42	1.57	0.2574
B <sup>2</sup>	1	310.88	310.88	110.22	<0.0001
A <sup>2</sup> B	1	38.05	38.05	13.49	0.0104
Residual	6	16.92	2.82		
Lack of fit	2	9.73	4.87	2.71	0.1805

R<sup>2</sup>: 0.9947, Adjusted R<sup>2</sup>: 0.9893, Predicted R<sup>2</sup>: 0.9236, Adequate precision: 43.483 and C.V.: 2.10 %

Table 4.27: Regression analysis (ANOVA) for the removal of MB from single dye solution

Source	Degree of freedom	Sum of Square	Mean Square	F-value	P
Model	6	3267.99	544.66	302.55	< 0.0001
A	1	1292.27	1292.27	717.84	< 0.0001
B	1	1003.46	1003.46	557.41	< 0.0001
AB	1	73.18	73.18	40.65	0.0007
A <sup>2</sup>	1	23.04	23.04	12.80	0.0117
B <sup>2</sup>	1	185.57	185.57	103.08	<0.0001
A <sup>2</sup> B	1	13.21	13.21	7.34	0.0351
Residual	6	10.80	1.80		
Lack of fit	2	3.96	1.98	1.16	0.4014

R<sup>2</sup>: 0.9967, Adjusted R<sup>2</sup>: 0.9934, Predicted R<sup>2</sup>: 0.9694, Adequate precision: 52.771 and C.V.: 1.76 %

models were found significant ( $P < 0.0001$ ) with model F-value of 186.06 and 302.55 for single BB3 and single MB, respectively. Coefficient of determination ( $R^2$ ) for single BB3 dye solution was recorded as 0.9947 while the rest (0.53 %) was explained as residues. Meanwhile, the  $R^2$  for single MB dye solution was reported as 0.9967. The relatively high  $R^2$  values for both models indicated that there were good agreements between the experimental and predicted values for both models. According to Chauchan *et al.* (2006), the closer the  $R^2$  to unity, the stronger the model and the better it predicts the response. In addition, the predicted multiple correlation coefficient (predicted  $R^2$ ) for both models was in reasonable agreement with the adjusted multiple correlation coefficient (adjusted  $R^2$ ).

The lack-of-fit observed for both single BB3 and MB models were 0.1805 and 0.4014, respectively. The lack of fit term is not significant, implies that both models were valid. Meanwhile, the coefficient of variance (C.V.) was recorded as 2.10% and 1.76% for single BB3 and single MB models, respectively. The precision and reliability of the conducted experiments is greater when the C.V. is lower (Kim *et al.*, 2008). Adequate precision indicates the signal to noise ratio and a ratio greater than 4 is desirable. A ratio of 43.483 and 52.771 were obtained for single BB3 and MB, respectively, showed an adequate signal. Therefore, both models can be used to navigate the design space. Table 4.26 shows all the coefficients of single BB3 were significant ( $P < 0.05$ ) except  $A^2$ ; however it cannot be eliminated in order to support the hierarchy model. For single MB

model, all the coefficients were significant except  $A^2B$ . Single BY11 were not further studied using RSM due to the insignificance of all the model terms at Plackett-Burman study.

The interaction between two factors and their optimum levels can be easily understood and located using response surface plot (Kim *et al.*, 2008). Figure 4.50 shows the 3D surface plot for BB3 dye solution of interaction between initial dye concentration and sorbent dosage. The maximum percentage uptake of BB3 dye was observed when initial dye concentration was at minimum point while sorbent dosage was at maximum point within the studied range. As the initial dye concentration increased the percentage uptake decreased. Decrease in percentage uptake at high initial dye concentration might be due to insufficient of available binding sites and increase in the ratio of the BB3's cations to the dosage of the adsorbent. Similar observation was observed in the removal of  $Cd^{2+}$  in Khattar and Shailza (2009) study. As the sorbent dosage in the plot increase, the percentage uptake increased. The higher uptake observed can be related to the increase of the availability of sorption sites (Garg *et al.*, 2004). The optimum values of experiment factors obtained were 50 mg/L of initial dye concentration and 0.13 g of sorbent dosage. At these optimum operational values, the model predicted 98.59 % uptake.

Figure 4.51 represents the 3D surface plot for MB dye solution of interaction between initial dye concentration and sorbent dosage. A similar

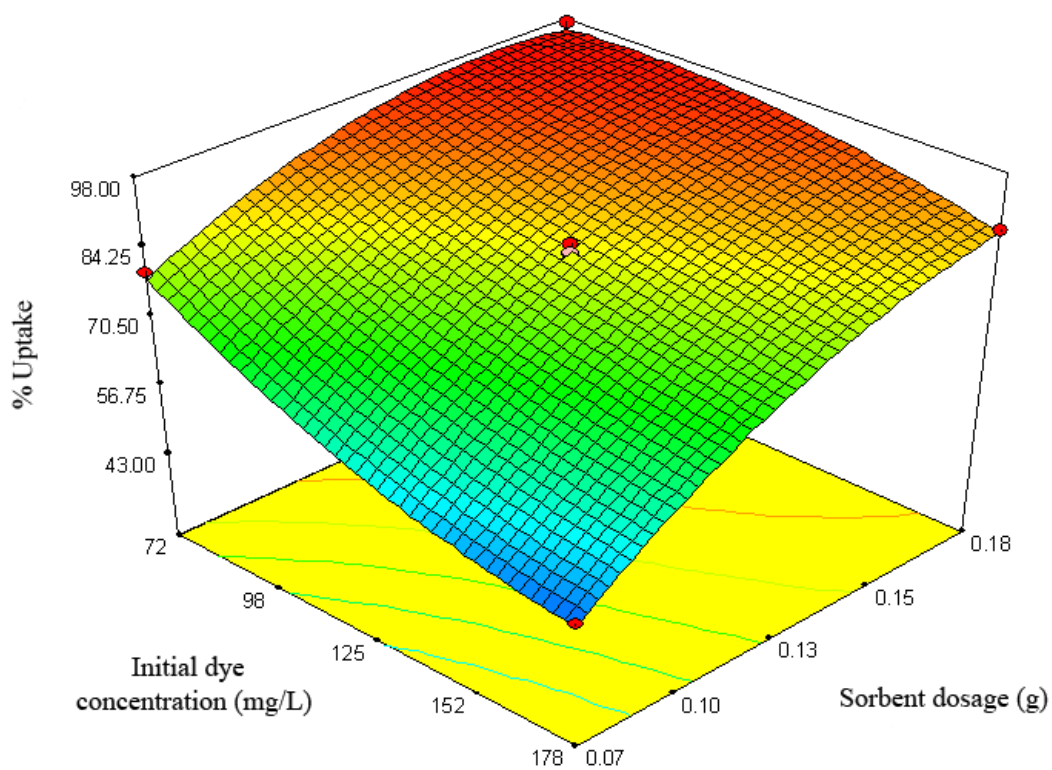


**Figure 4.50: 3D surface plot for uptake of BB3 in single dye solution as a function of initial dye concentration and sorbent dosage**

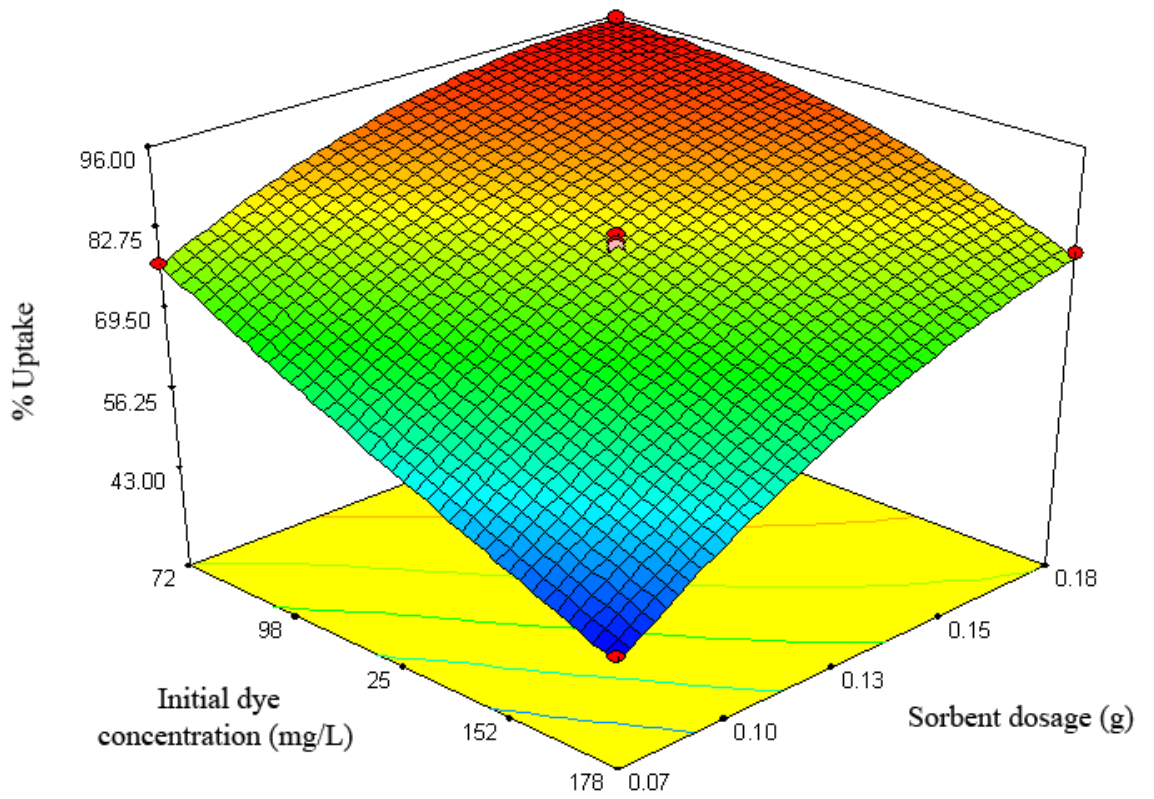


**Figure 4.51: 3D surface plot for uptake of MB in single dye solution as a function of initial dye concentration and sorbent dosage**

observation with BB3 dye solution was obtained. The maximum percentage uptake of MB dye was observed when the initial dye concentration was at minimum while sorbent dosage was at maximum. Optimum operational values were reported as 72 mg/L of initial dye concentration and 0.18 g of sorbent dosage. The model predicted 95.19 % uptake at these optimum operational values.

#### 4.7.3.2 Binary Dye Solutions

Tables 4.28 and 4.29 show the results of the effect of pH, contact time, initial dye concentrations and sorbent dosage on the percentage uptake of binary BB3, and the effect of contact time, initial dye concentration and sorbent dosage for binary MB dye solution. The modified cubic models that describe the correlation between the variables and the percentage uptake for both solutions were shown as follows:

Binary BB3 dye solution:

$$\begin{aligned} \% \text{ Uptake} = & 82.929 - 4.316A - 1.185B + 18.880C + 0.213D + 0.207AB \\ & + 206.820AC - 0.175AD - 0.288BC - 0.393A^2 + 0.00495B^2 \\ & - 1136.453C^2 - 18.162A^2C + 0.0162A^2D - 0.000819AB^2 \end{aligned} \quad (24)$$

Binary MB dye solution:

$$\begin{aligned} \% \text{ Uptake} = & 56.447 + 0.112B + 555.260C - 0.457D + 1.655CD - 2.627 B^2 \\ & - 1849.941C^2 \end{aligned} \quad (25)$$

where, A = pH, B = contact time, C = sorbent dosage and D = initial dye concentration



Table 4.28: The central composite design matrix for four independent variables  
and the observed response (Binary BB3)

Experimental run	Coded values of variables				Observed response (%)	Predicted response (%)
	A	B	C	D		
1	0	0	-2	0	46.82	46.61
2	0	0	0	-2	95.39	93.29
3	0	2	0	0	79.88	78.37
4	0	0	2	0	89.80	89.59
5	0	0	0	2	57.79	55.69
6	-2	0	0	0	53.63	53.42
7	0	-2	0	0	70.53	71.64
8	2	0	0	0	84.33	84.12
9	1	1	-1	1	61.35	61.79
10	-1	1	-1	1	48.84	50.33
11	1	-1	-1	1	57.05	57.03
12	-1	-1	-1	1	49.25	47.76
13	1	-1	1	1	76.15	75.72
14	1	1	1	1	77.51	77.93
15	-1	-1	-1	-1	65.34	65.33
16	-1	-1	1	1	67.90	68.94
17	-1	1	1	-1	87.58	88.01
18	1	1	-1	-1	77.44	76.81
19	1	1	1	-1	90.99	92.48
20	-1	1	-1	-1	69.42	69.85
21	1	-1	-1	-1	69.50	70.12
22	-1	-1	1	-1	86.48	86.04
23	-1	1	1	1	69.60	68.98
24	1	-1	1	-1	89.39	88.32
25	0	0	0	0	72.84	74.49
26	0	0	0	0	73.18	74.49
27	0	0	0	0	75.09	74.49
28	0	0	0	0	73.81	74.49
29	0	0	0	0	73.74	74.49
30	0	0	0	0	74.51	74.49

Table 4.29: The central composite design matrix for three independent variables and the observed response (Binary MB)

Experimental run	Coded values of variables			Observed response (%)	Predicted response (%)
	B	C	D		
1	0	0	-1.682	57.89	56.75
2	1.682	0	0	78.35	77.44
3	0	0	1.682	93.44	94.22
4	0	1.682	0	88.65	87.55
5	0	-1.682	0	42.97	42.61
6	-1.682	0	0	66.82	66.27
7	-1	-1	1	38.64	39.41
8	1	1	-1	92.66	95.06
9	-1	1	-1	90.27	88.41
10	1	-1	-1	76.60	74.92
11	1	1	1	78.45	79.35
12	1	-1	1	45.30	46.05
13	-1	1	1	71.46	72.71
14	-1	-1	-1	66.68	68.27
15	0	0	0	75.55	75.48
16	0	0	0	75.17	75.48
17	0	0	0	75.66	75.48
18	0	0	0	76.48	75.48
19	0	0	0	74.45	75.48
20	0	0	0	76.46	75.48

Tables 4.30 and 4.31 show the ANOVA tables for both binary BB3 and binary MB dye solutions. Both models were found significant ( $P < 0.0001$ ) with model F-value of 156.95 and 387.56 for binary BB3 and binary MB, respectively.  $R^2$  for both models exhibited a relatively high values showing that there were good agreements between the experimental and predicted values in both models. Meanwhile, the predicted  $R^2$  of binary BB3 (0.9653) and binary MB (0.9838) were in reasonable agreement with the adjusted  $R^2$  of both models. The lack-of-fit for binary BB3 and binary MB were found to be 0.0593 and 0.0529, respectively. This indicated that both models were valid as the lack-of-fit were not significant. Low C.V. values for binary BB3 (2.07%) and binary MB (1.95%) showed the good precision and reliability of the experiments. Adequate signal to noise ratio were also observed for both models, showing that both models can be used to navigate the design space. For binary BB3, all the coefficients were found significant ( $P < 0.05$ ) except AB, AC, BC,  $B^2$  and  $A^2D$ ; however it cannot be eliminated in order to support the hierarchy model. For binary MB, all the coefficients were significant. Binary BY11 for both dye solutions were not further studied using RSM approach due to the insignificance of all the studied factors at Plackett-Burman study.

Table 4.30: Regression analysis (ANOVA) for the removal of BB3 from BB3-BY11 binary dye solution

Source	Degree of freedom	Sum of Square	Mean Square	F-value	P
Model	14	4906.44	350.46	156.95	< 0.0001
A	1	471.15	471.15	211.00	< 0.0001
B	1	67.91	67.91	30.41	< 0.0001
C	1	923.63	923.63	413.64	< 0.0001
D	1	706.71	706.71	316.49	< 0.0001
AB	1	4.77	4.77	2.14	0.1646
AC	1	6.27	6.27	2.18	0.1146
AD	1	20.20	20.20	9.05	0.0088
BC	1	6.45	6.45	2.89	0.1098
A <sup>2</sup>	1	57.32	57.32	25.67	0.0001
B <sup>2</sup>	1	0.45	0.45	0.20	0.6585
C <sup>2</sup>	1	71.51	71.51	32.03	< 0.0001
A <sup>2</sup> C	1	12.52	12.52	5.61	0.0317
A <sup>2</sup> D	1	9.99	9.99	4.47	0.0516
AB <sup>2</sup>	1	95.82	95.82	42.91	< 0.0001
Residual	15	33.49	2.23		
Lack of fit	10	30.04	3.00	4.34	0.0593

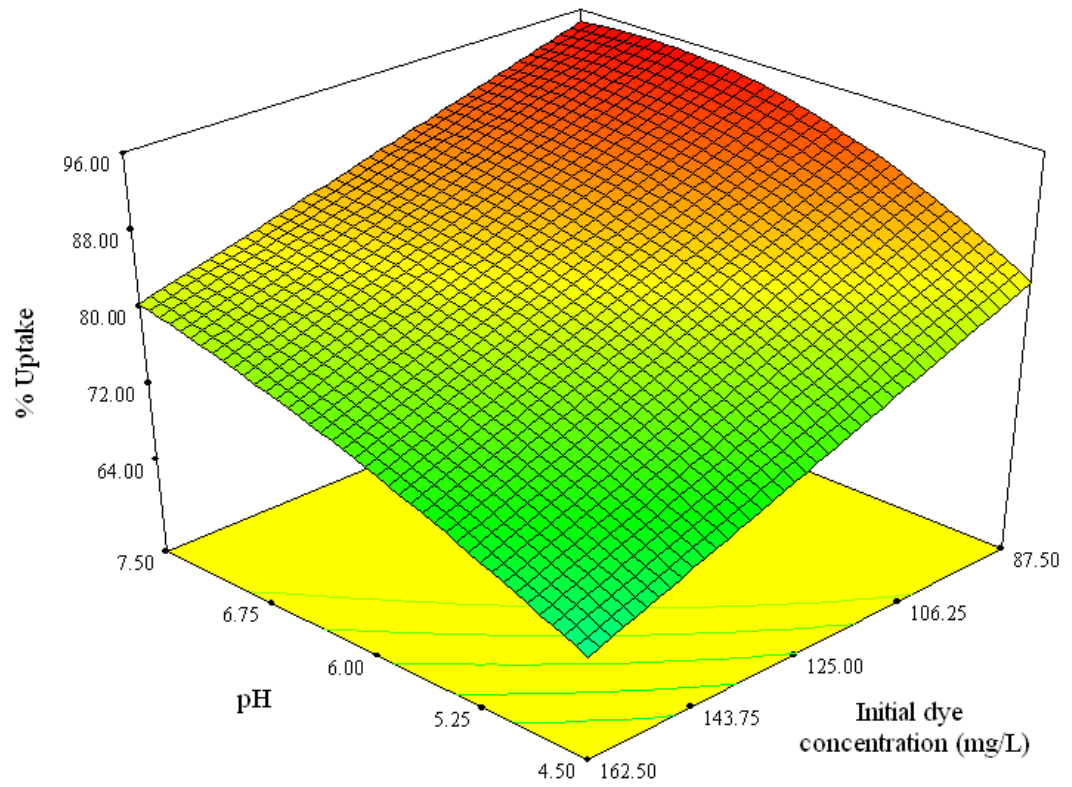
R<sup>2</sup>: 0.9932, Adjusted R<sup>2</sup>: 0.9869, Predicted R<sup>2</sup>: 0.9653, Adequate precision: 44.178 and C.V.: 2.07 %

Table 4.31: Regression analysis (ANOVA) for the removal of MB from MB-BY11 binary dye solution

Source	Degree of freedom	Sum of Square	Mean Square	F-value	P
Model	6	4580.77	763.46	387.56	< 0.0001
A	1	150.68	150.68	76.49	< 0.0001
B	1	2437.88	2437.88	1237.55	< 0.0001
C	1	1695.35	1695.35	860.62	< 0.0001
BC	1	86.62	86.62	43.97	< 0.0001
A <sup>2</sup>	1	23.93	23.93	12.15	0.0040
B <sup>2</sup>	1	197.00	197.00	100.01	< 0.0001
Residual	13	25.61	1.97		
Lack of fit	8	22.59	2.82	4.68	0.0529

R<sup>2</sup>: 0.9944, Adjusted R<sup>2</sup>: 0.9919, Predicted R<sup>2</sup>: 0.9838, Adequate precision: 67.018 and C.V.: 1.95 %

Figure 4.52 shows the 3D surface plot for binary BB3 dye solution of interaction between pH and initial dye concentration at contact time of 122.50 min and 0.16 g of sorbent dosage. The maximum percentage uptake of BB3 dye was observed when initial dye concentration was at minimum point while pH was at maximum point within the studied range. As the initial dye concentration increased the percentage uptake decreased. Decrease in percentage uptake at high initial dye concentration might be due to insufficient of available binding sites and increase in the ratio of the BB3's cations to the dosage of the adsorbent. Maximum percentage uptake was observed at higher pH was due to the increased of negatively charged sites as the pH of the dye solution increased. According to Hameed *et al.* (2009), the surface charge may be positively charged at lower pH,



**Figure 4.52: 3D surface plot for uptake of binary BB3 dye solution as a function of pH and initial dye concentration at contact time of 122.50 min and 0.16 g of sorbent dosage**

therefore making ( $H^+$ ) ions compete effectively with dye cations causing a decline in the percentage uptake.

Figure 4.53 exhibits the 3D surface plot for binary BB3 dye solution of interaction between pH and sorbent dosage at contact time of 122.50 min and initial dye concentration of 100 mg/L. Maximum percentage uptake was attained when both pH and sorbent dosage were at maximum level. At higher sorbent dosage, the percentage uptake was higher due to the increase of the sorbent sites against the available sorbate. Similar observation was reported by Ong *et al.*, 2007 in a study of removal of basic and reactive dyes. While at higher pH value, higher percentage uptake was obtained due to the increase in the negatively charged sites as the pH of the dye solution increased.

The interaction between contact time and sorbent dosage for binary BB3 dyes solution at pH 6 and initial dye concentration 100 mg/L (Figure 4.54) exhibited a quite similar plot with Figure 4.53. Maximum percentage uptake was observed when both contact time and sorbent dosage were at maximum point. Minimal changes in percentage uptake were observed as the contact time increased. This shows that the equilibrium time of sorption has been attained within the studied time frame and therefore percentage uptake remained almost constant. According to Ahmad *et al.* (2007), the time required to attain equilibrium was termed as equilibrium time, and the amount of dye adsorbed at

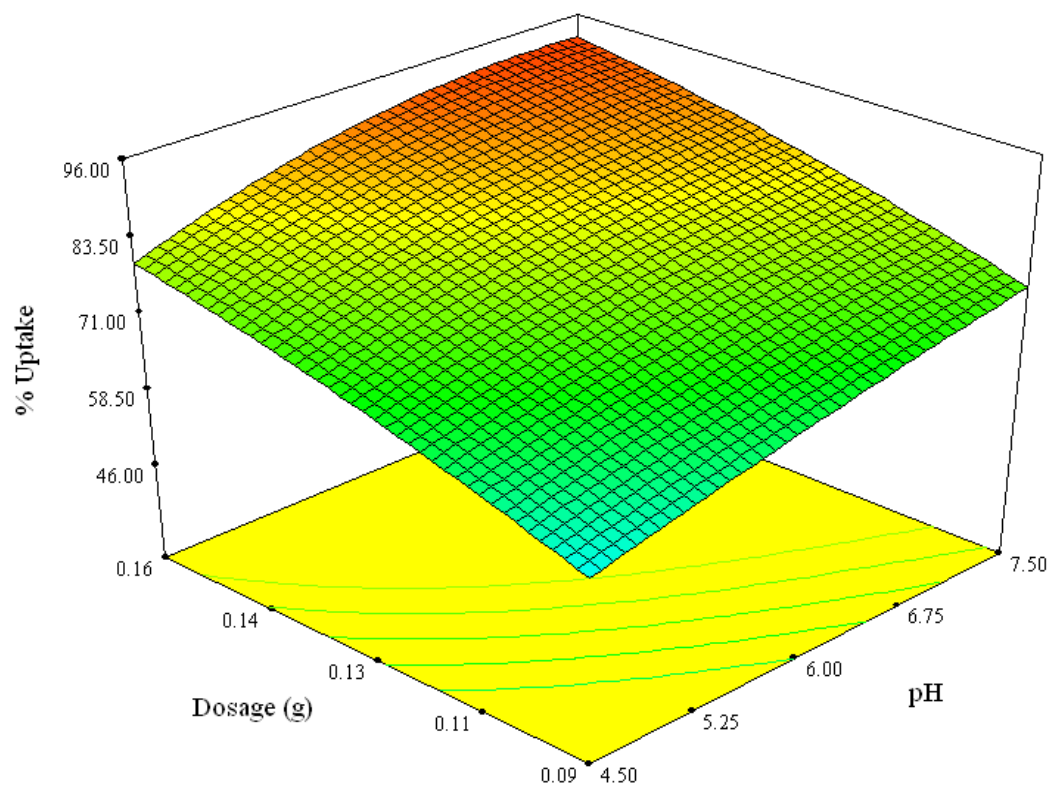


**Figure 4.53: 3D surface plot for uptake of binary BB3 dye solution as a function of pH and dosage at contact time of 122.50 min and 100 mg/L of initial dye concentration**



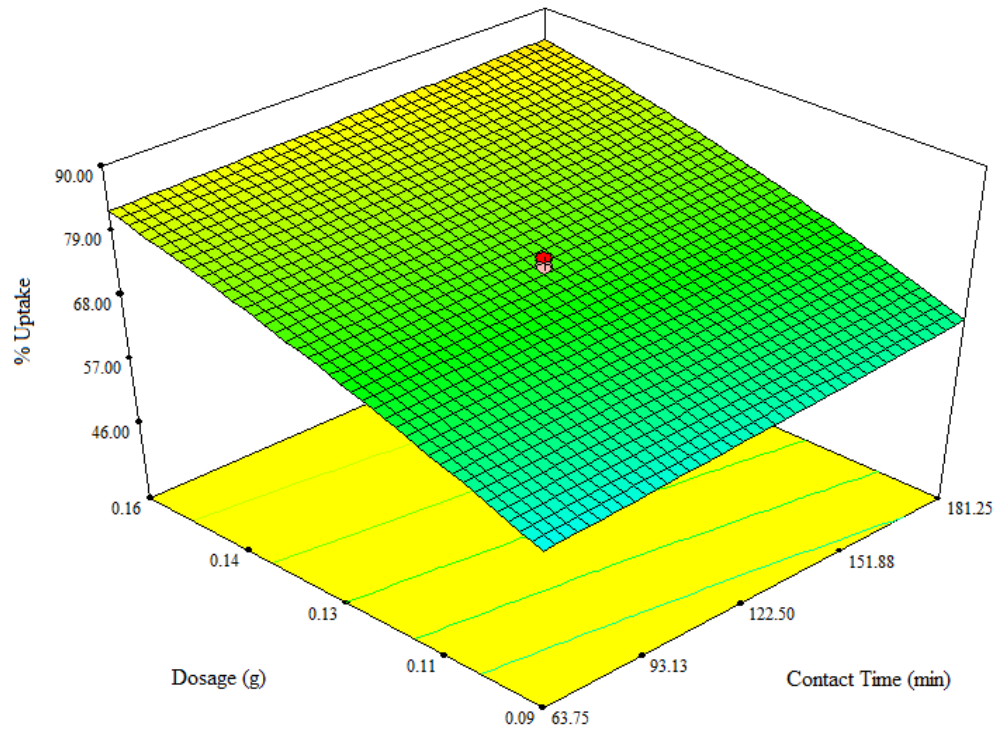


**Figure 4.54: 3D surface plot for uptake of binary BB3 dye solution as a function of contact time and dosage at pH 6.00 and 100 mg/L of initial dye concentration**

equilibrium time reflects the maximum sorption capacity of the adsorbent. The optimum values of experiment factors obtained were pH 6, 122.50 min of contact time, 0.09 g of sorbent dosage and 50 mg/L of initial dye concentration. At these optimum operational values, the model predicted 93.29% uptake.

Figure 4.55 represents the 3D surface plot for binary MB dye solution. The interaction between sorbent dosage and initial dye concentration for binary MB dye solution at contact time of 122.50 min showed a quite identical plot with Figure 4.52 as well. The maximum percentage uptake was obtained when the load of sorbent dosage was at maximum while the initial dye concentration at minimum. The percentage uptake increased as the dosage of sorbent increased. This was due to the increase of the binding sites as the sorbent dosage increased. Similar observation was reported by Tan *et al.* (2009) in the study of removal of Basic Yellow 11 using *Sargassum binderi* (a species of brown seaweed). Although the percentage uptake decreased with increasing initial concentration increased but the actual amount of dye adsorbed was increased. Similar observation was observed by Garg *et al.* (2004) in the removal of malachite green using an agro-industry waste (*Prosopis cineraria* sawdust). Optimum operational values were reported as 192.37 min of contact time, 0.17 g of sorbent dosage and 80.40 mg/L of initial dye concentration. The model predicted 95.06% uptake at these optimum operational values.

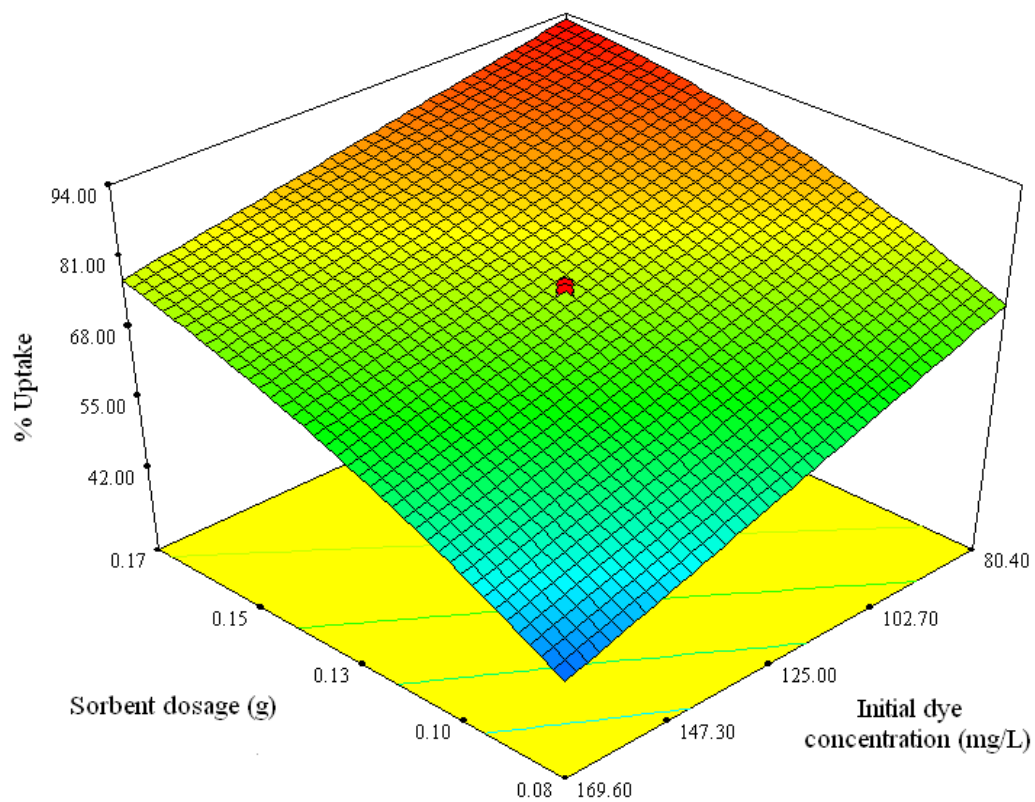


**Figure 4.55: 3D surface plot for uptake of binary MB dye solution as a function of sorbent dosage and initial dye concentration at contact time of 122.50 min**

### 4.7.3.3 Verification of RSM Models

In order to determine the validation of the model equations of all studied dye models, experiments were conducted based on the experimental conditions with the highest desirable which generated by design Expert v.7.1.3 software. Table 4.32 shows the experimental conditions as well as the predicted and experiments results. From the experimental results obtained, the percentage uptake for single BB3, single MB, binary BB3 and binary MB dye solutions were 95.96, 95.05, 94.22 and 91.85, respectively. All the models exhibited close results with the predicted results with percentage errors of 2.45, 1.48, 2.20 and 1.54 for single BB3, single MB, binary BB3 and binary MB, respectively. Thus, all models can be concluded as valid.

Table 4.32: Validation of model equations for all studied dye solutions

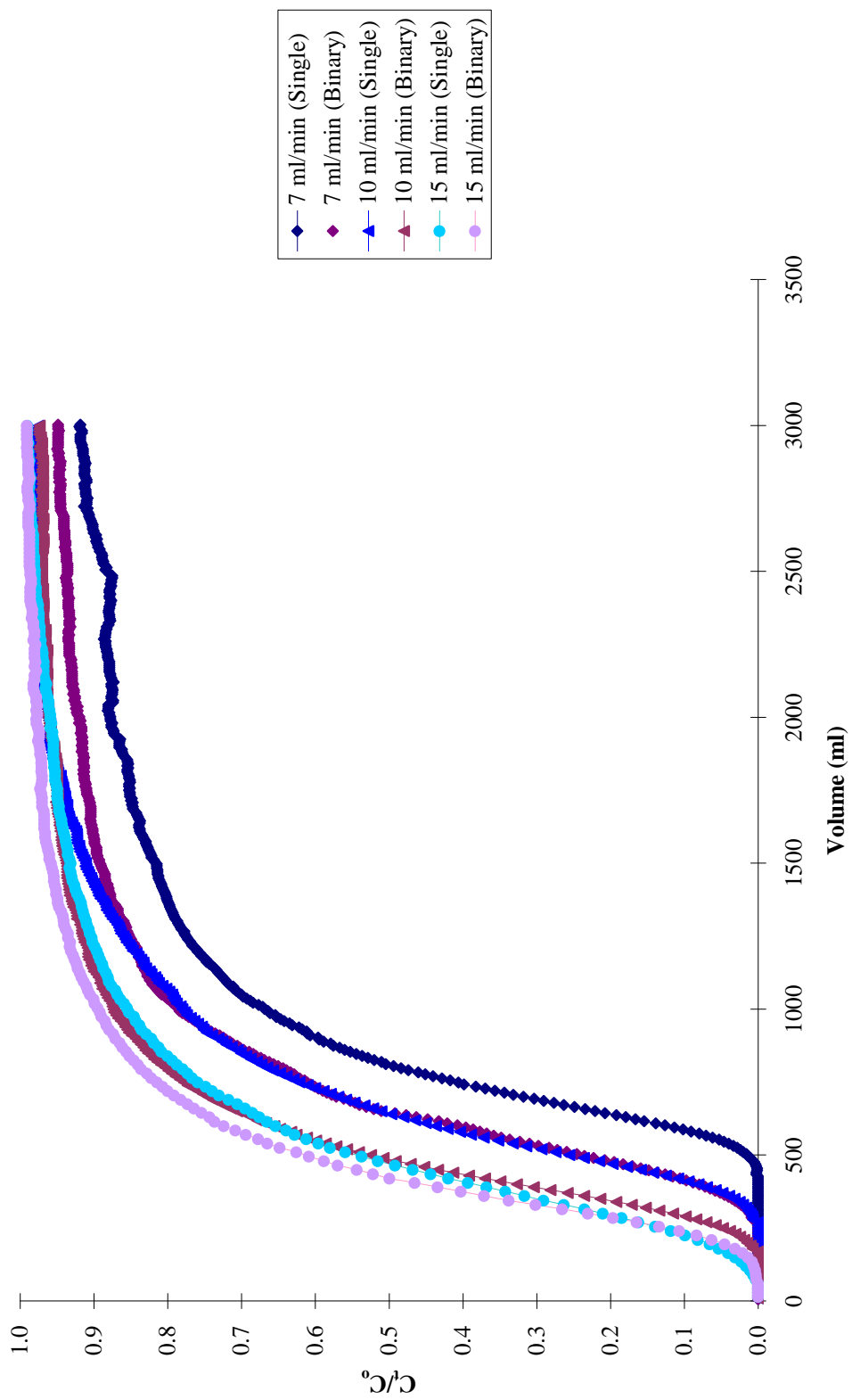
Dye solution	Factors				Percentage Uptake		Percentage error
	pH	Contact time (min)	Sorbent dosage (g)	Initial dye concentration (mg L <sup>-1</sup> )	Predicted	Observed	
BB3 (Single)	-	-	0.16	72.00	96.73	94.36	2.45
MB (Single)	-	-	0.17	72.00	95.26	93.85	1.48
Binary BB3	7.00	137.77	0.16	87.50	95.25	93.15	2.20
Binary MB	-	174.65	0.17	84.22	93.29	91.85	1.54

## 4.8 Column Studies

### 4.8.1 Effect of Flow Rate on Breakthrough Curve

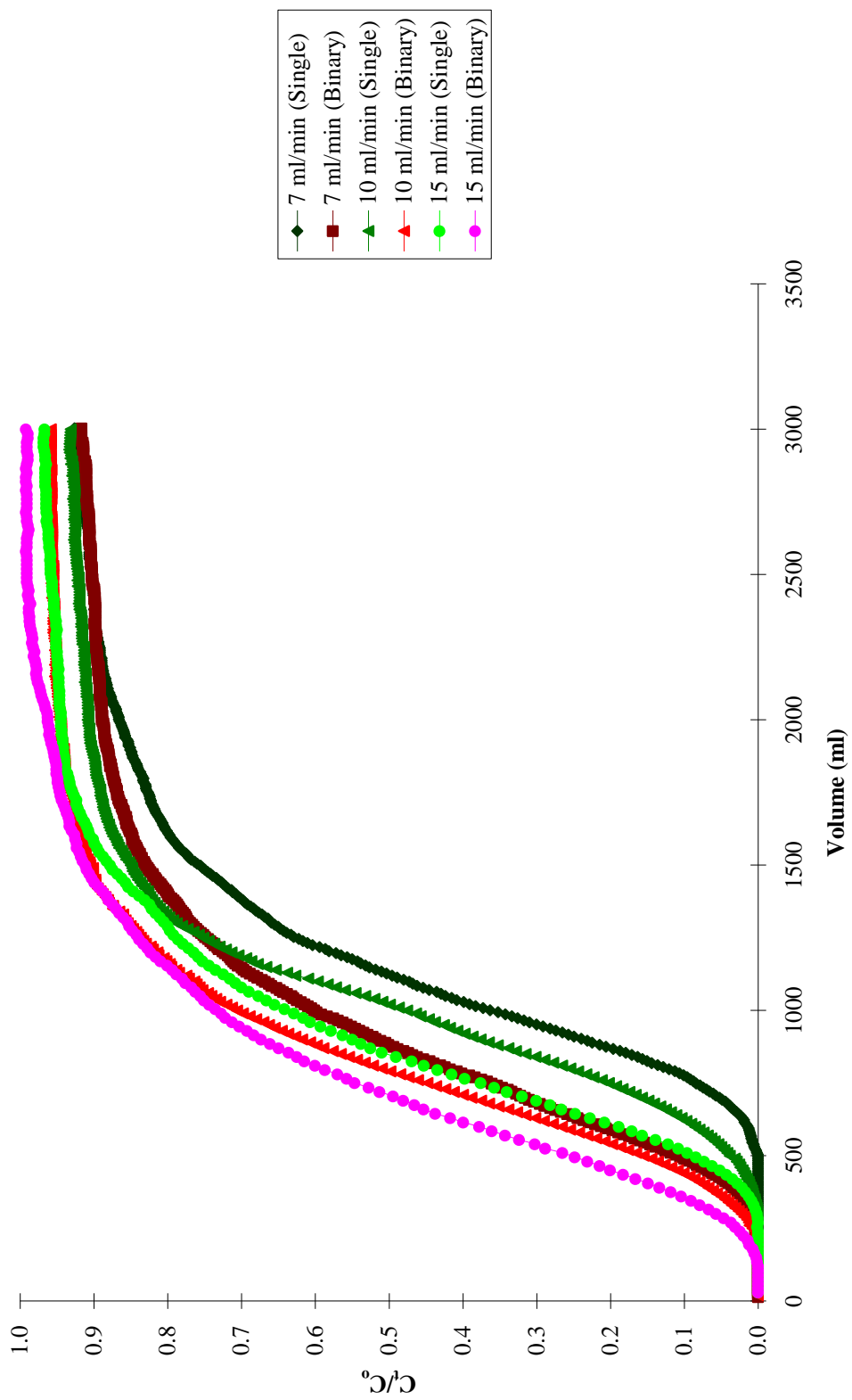
The effect of flow rate for the sorption of BB3, MB and BY11 in single and binary solutions by NSB are shown in Figures 4.56 – 4.60. In this study, the effects of three different flow rates were studied (7, 10 and 15 mL/min). Generally, a faster breakthrough was observed as the flow rate increased. An early breakthrough was observed at highest flow rate (15 mL/min), meanwhile the lowest flow rate (7 mL/min) exhibited a longer retention time for all the dye solutions. A rapid uptake was observed at the initial stage and decreased thereafter and finally reached saturation. A steeper breakthrough curve was also noticed as the flow rate increased. The contact time between the dye and the adsorbent was minimised at higher flow rate leading to an early breakthrough (Sivakumar and Palanisamy, 2009). A similar observation was reported by Han *et al.* (2007) in the removal of MB using rice husk. They found out that at low rate of influent introduction, MB had more time contact with the rice husk therefore resulted higher removal of MB ions in the column.

Figures 4.56 and 4.57 show the comparison of breakthrough curves between the single and binary BB3 and MB dye solutions. From Figure 4.56, breakthrough curves of binary BB3 showed a faster breakthrough compared to



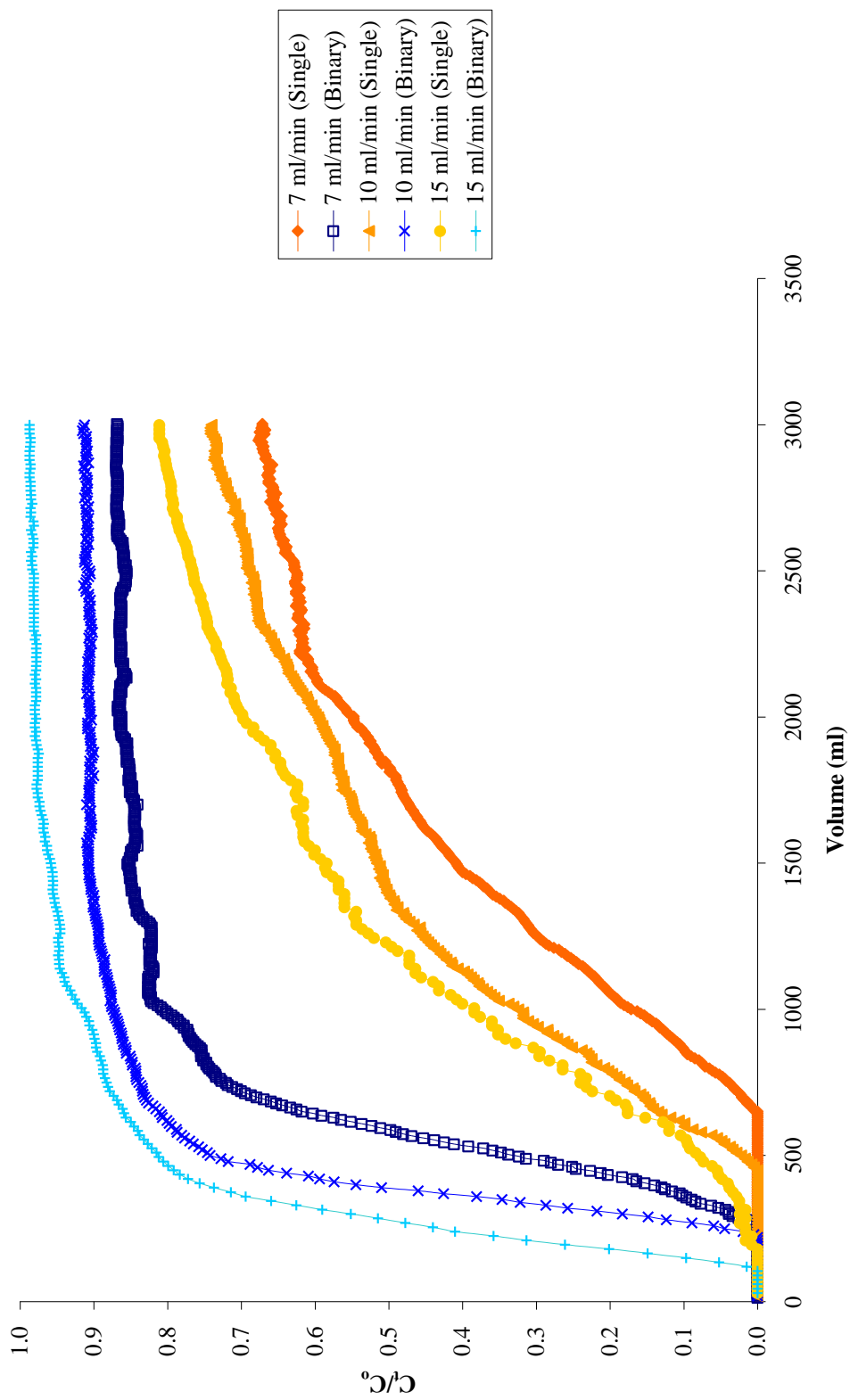
**Condition:** 10 mg/L of single and binary BB3 dye solution passing through 0.5 g of sorbent at flow rate of 7, 10 and 15 mL/min

**Figure 4.56:** Comparison of breakthrough curves between single and binary BB3 for the effect of flow rate



**Condition:** 10 mg/L of single and binary MB dye solution passing through 0.5 g of sorbent at flow rate of 7, 10 and 15 mL/min

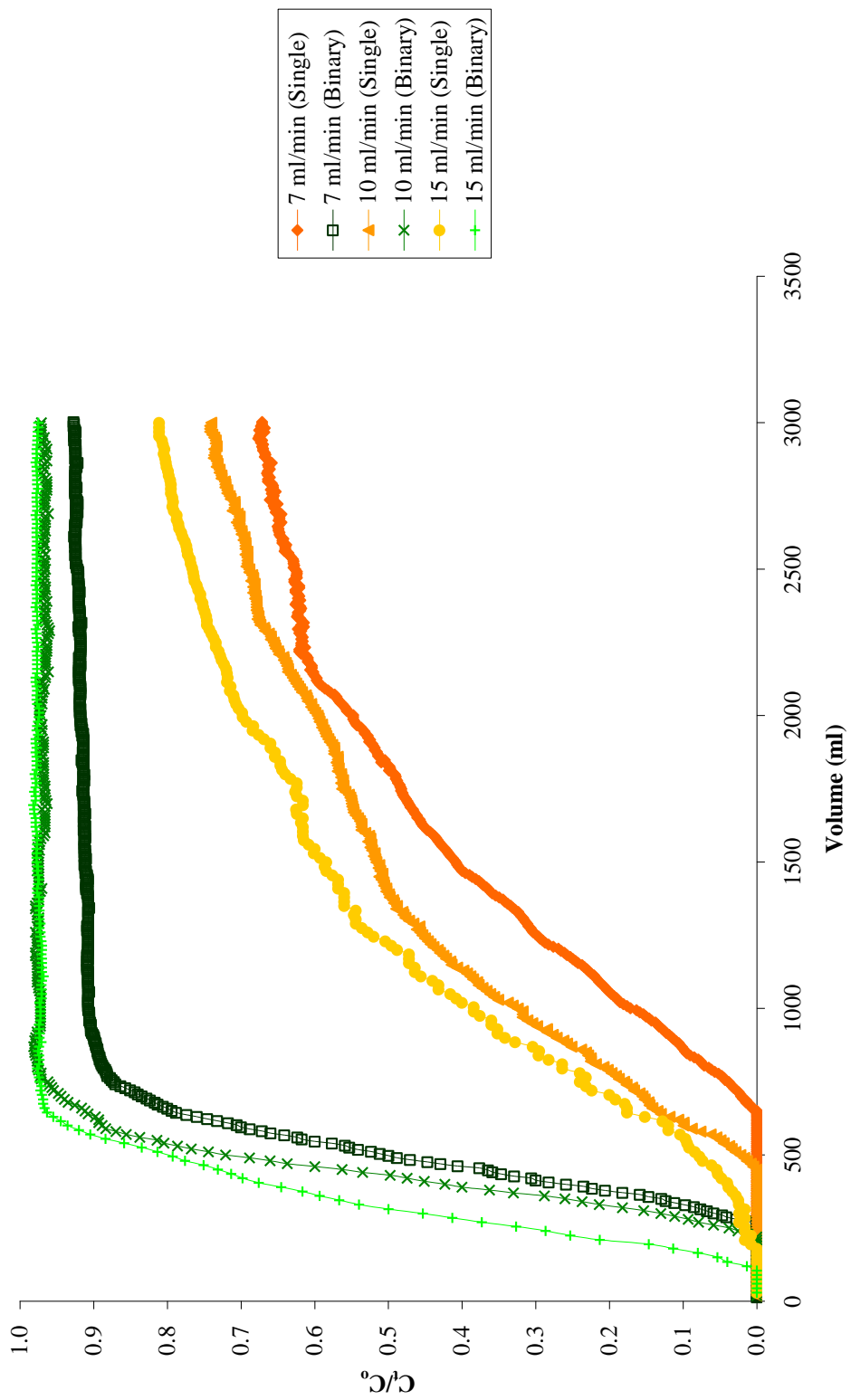
**Figure 4.57:** Comparison of breakthrough curves between single and binary MB for the effect of flow rate



Condition: 10 mg/L of single and binary BY11 dye solution passing through 0.5 g of sorbent at flow rate of 7, 10 and 15 mL/min

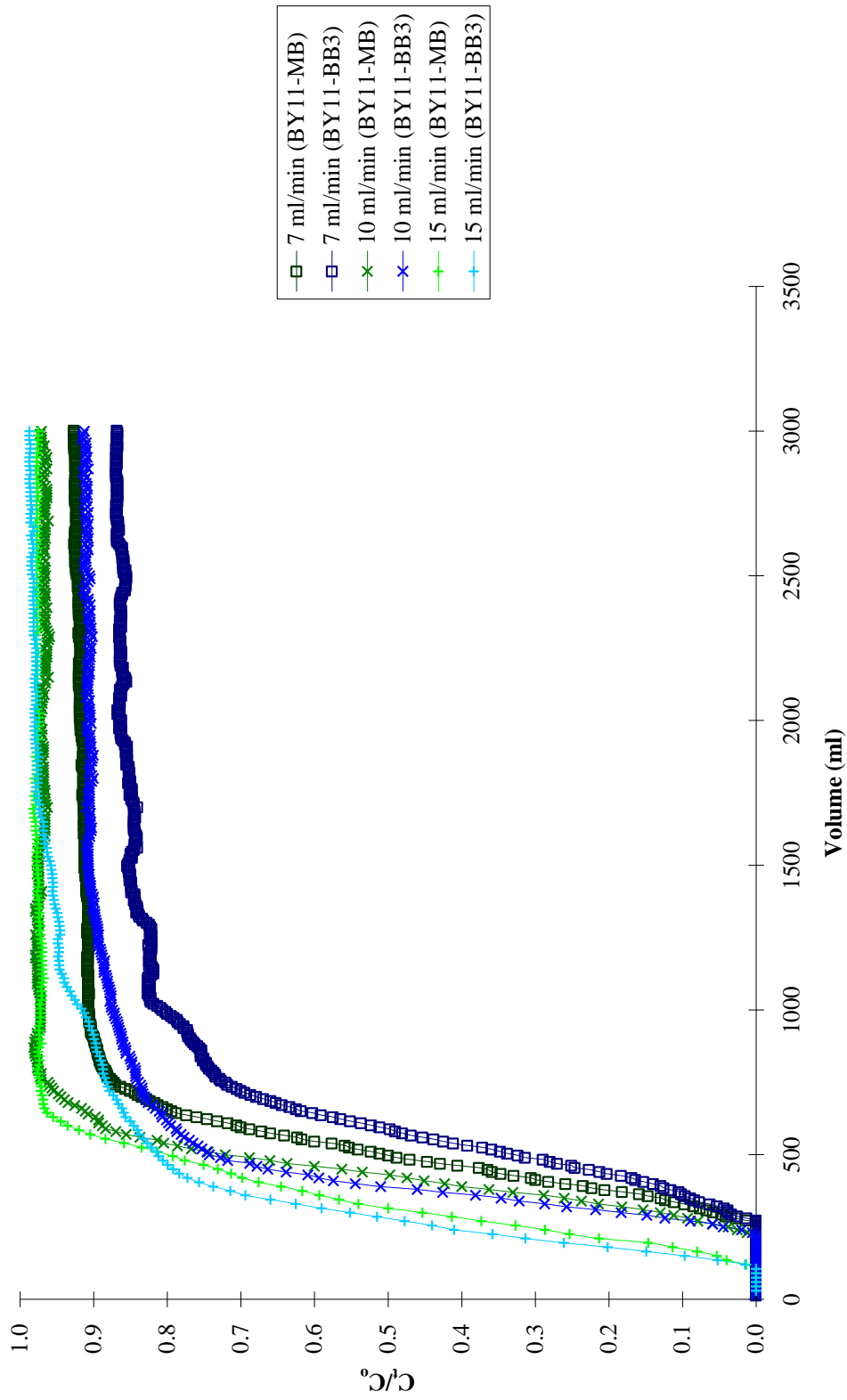
Figure 4.58: Comparison of breakthrough curves between single BY11 and binary BY11 of BB3-BY11 for the effect of flow rate





**Condition:** 10 mg/L of single and binary BY11 dye solution passing through 0.5 g of sorbent at flow rate of 7, 10 and 15 mL/min

**Figure 4.59:** Comparison of breakthrough curves between single BY11 and binary BY11 of MB-BY11 for the effect of flow rate



**Condition:** 10 mg/L of binary BY11 dye solution passing through 0.5 g of sorbent at flow rate of 7, 10 and 15 mL/min

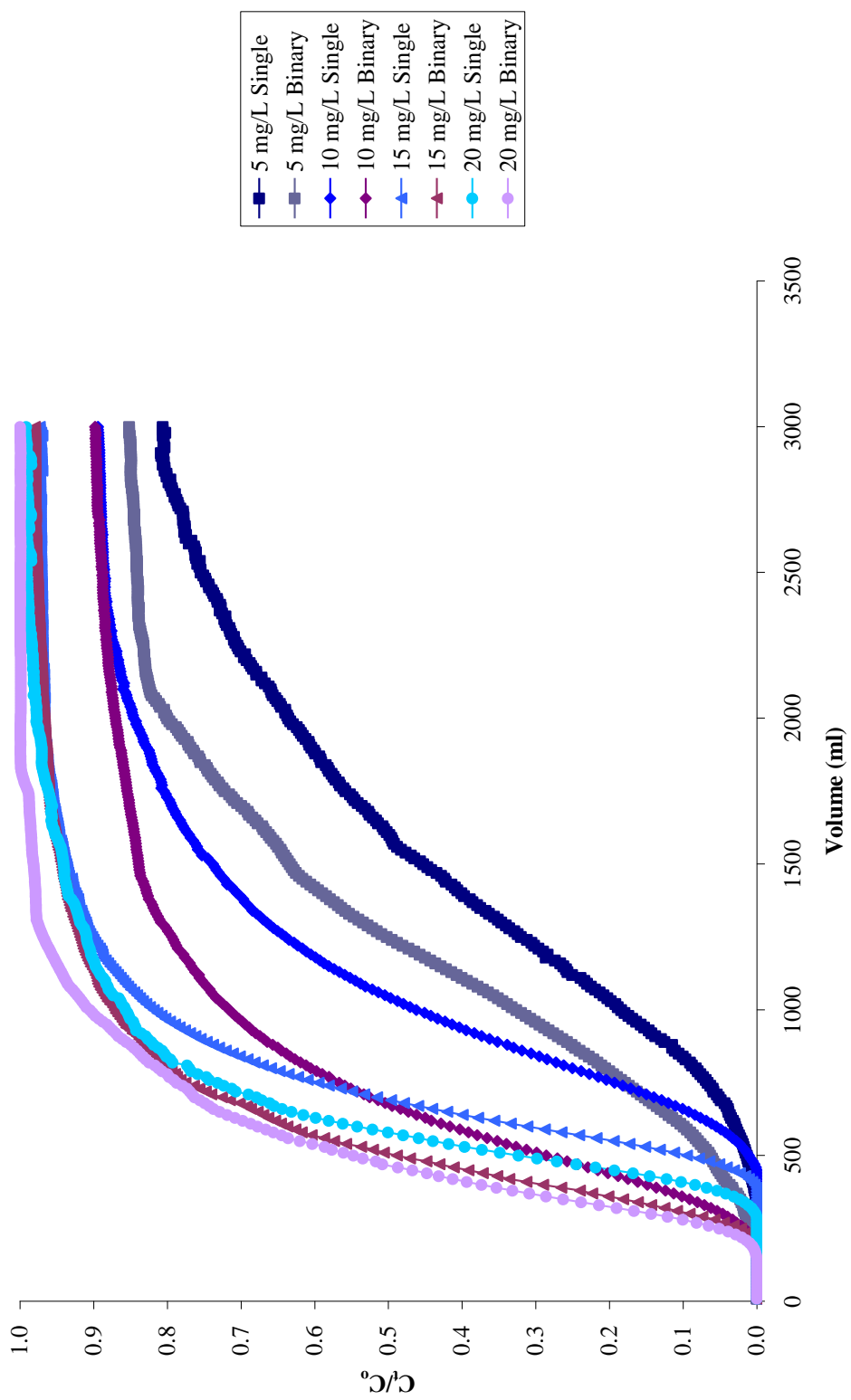
**Figure 4.60: Comparison of breakthrough curves between binary BY11 of BB3-BY11 and MB-BY11 for the effect of flow rate**

single BB3 at the same flow rate. This phenomenon can be explained by the competition of two different dyes in the binary solution for the available binding sites which lead to a faster breakthrough. Similar trend was observed for other dyes when they are in binary dye solution. In addition, single BY11 shows a slower breakthrough compared to other dyes. This might due to the higher affinity of BY11 cations toward the adsorbent compared to the other studied dyes.

Figure 4.60 shows the comparison of breakthrough curves between BY11 of BB3-BY11 and MB-BY11. It was noticed that the breakthrough of BY11 of MB-BY11 occurred faster as compared to BY11 of BB3-BY11 solution. This might due to the higher affinity of MB cations toward the adsorbent which lead to faster breakthrough of BY11 in the MB-BY11 binary solution.

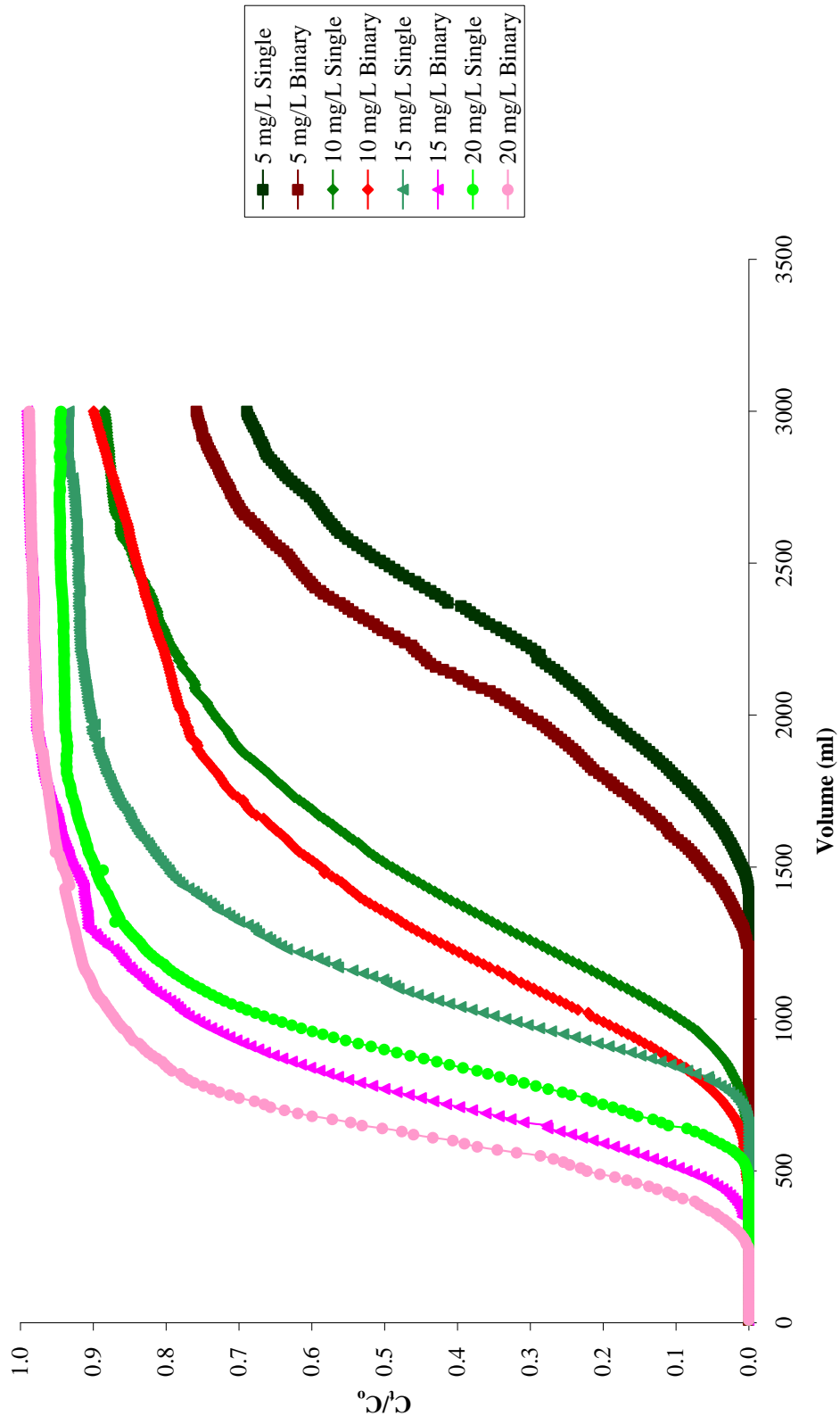
#### **4.8.2 Effect of Initial Dye Concentration on Breakthrough Curve**

The effect of initial dye concentration for sorption of BB3, MB and BY11 in single and binary dye solutions on NSB are shown in Figures 4.61 – 4.64. The initial dye concentrations studied were 5, 10, 15 and 20 mg/L at fixed flow rate (10 mL/min) and sorbent dosage (1.00 g). Overall, the breakthrough time increased with decreasing dye concentration for all studied solutions. The breakthrough curve shifted to left and steeper breakthrough curve was obtained as



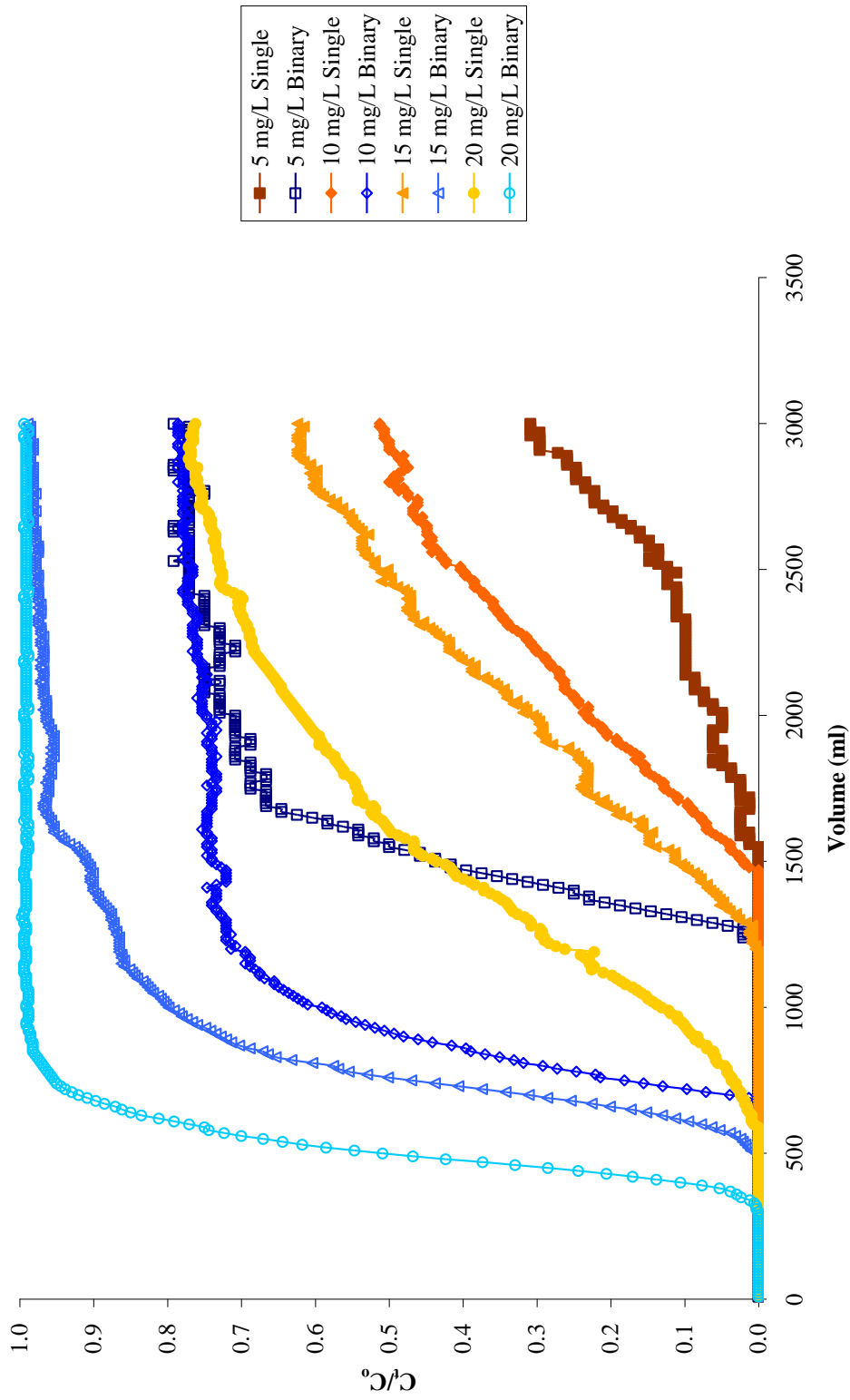
**Condition:** 5, 10, 15 and 20 mg/L of single and binary BB3 dye solution passing through 1.0 g of sorbent at flow rate of 10 mL/min

**Figure 4.61: Comparison of breakthrough curves between single and binary BB3 for effect of influent concentration**



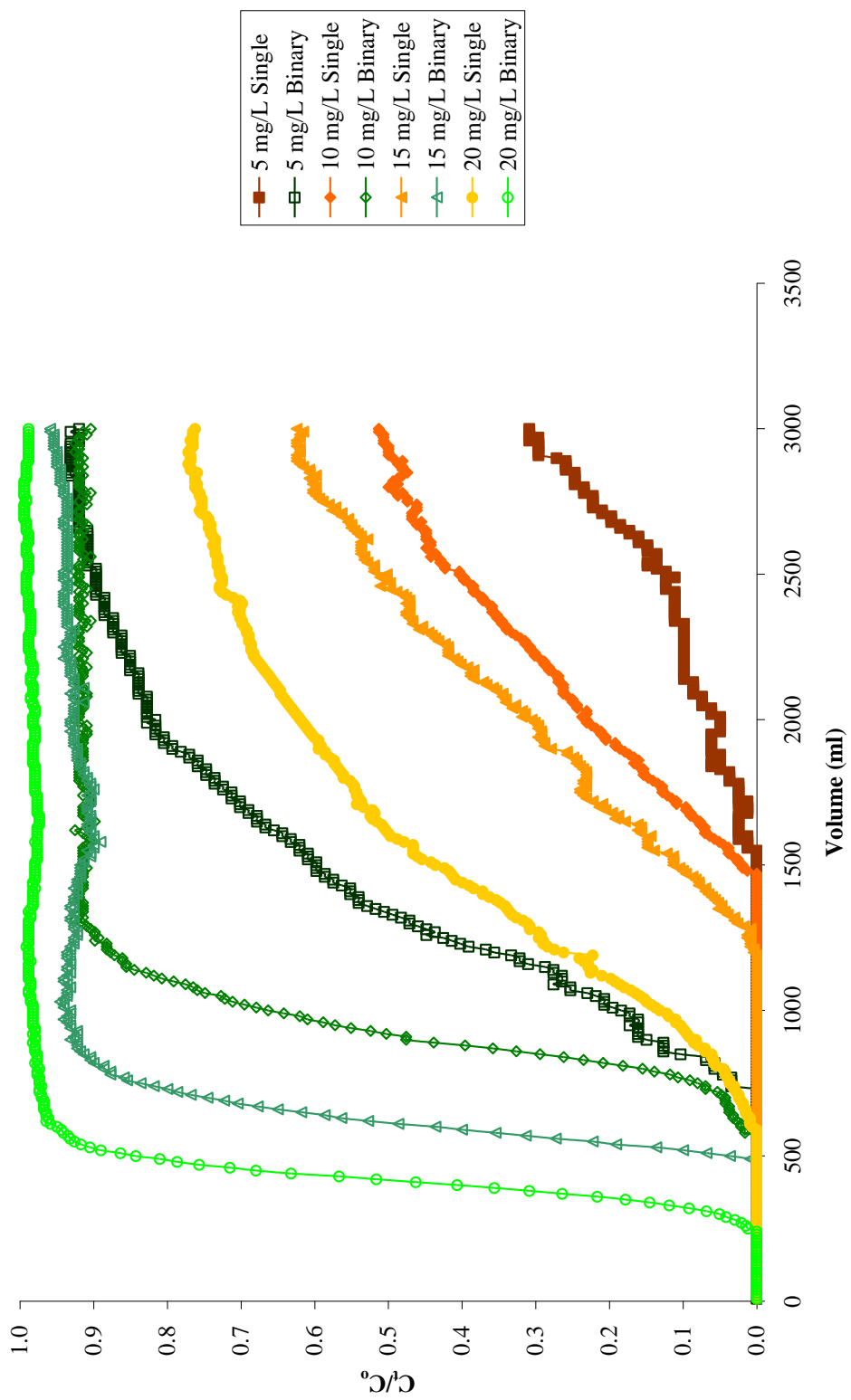
**Condition:** 5, 10, 15 and 20 mg/L of single and binary MB dye solution passing through 1.0 g of sorbent at flow rate of 10 mL/min

**Figure 4.62: Comparison of breakthrough curves between single and binary MB for effect of influent concentration**



**Condition:** 5, 10, 15 and 20 mg/L of single and binary BY11 dye solution passing through 1.0 g of sorbent at flow rate of 10 mL/min

**Figure 4.63: Comparison of breakthrough curves between single BY11 and binary BY11 of BB3-BY11 for effect of influent concentration**



**Condition:** 5, 10, 15 and 20 mg/L of single and binary BY11 dye solution passing through 1.0 g of sorbent at flow rate of 10 mL/min

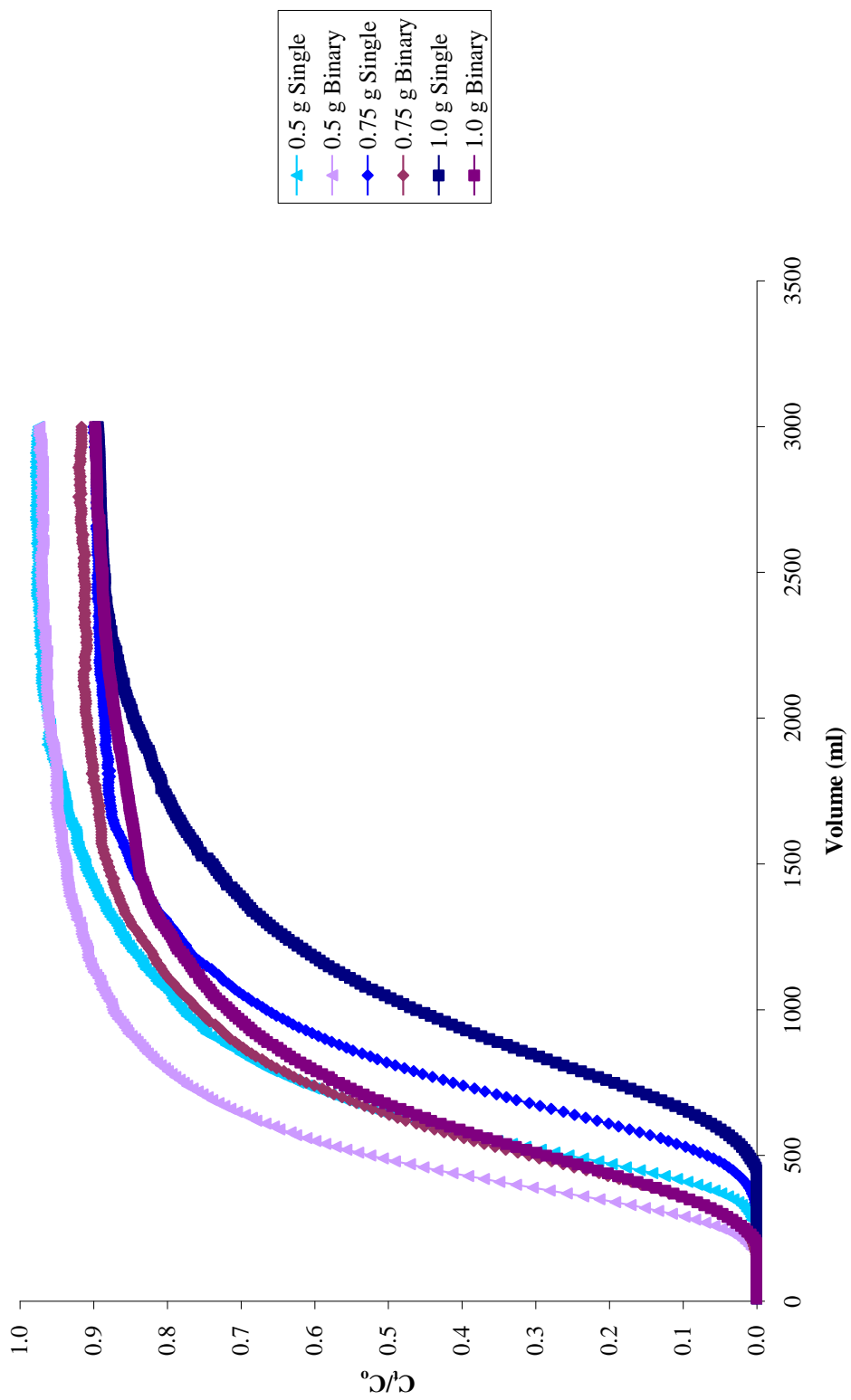
**Figure 4.64: Comparison of breakthrough curves between single BY11 and binary BY11 of MB-BY11 for effect of influent concentration**

the dye concentration increased. This indicates that the change in concentration gradient affects the saturation rate and breakthrough time (Ko *et al.*, 2000). In addition, as the influent concentration increases, the dye loading rate increases, so does the driving force for mass transfer, which resulted a decrease in the sorption zone length (Ko *et al.*, 2000).

### **4.8.3 Effect of Bed Height on Breakthrough Curve**

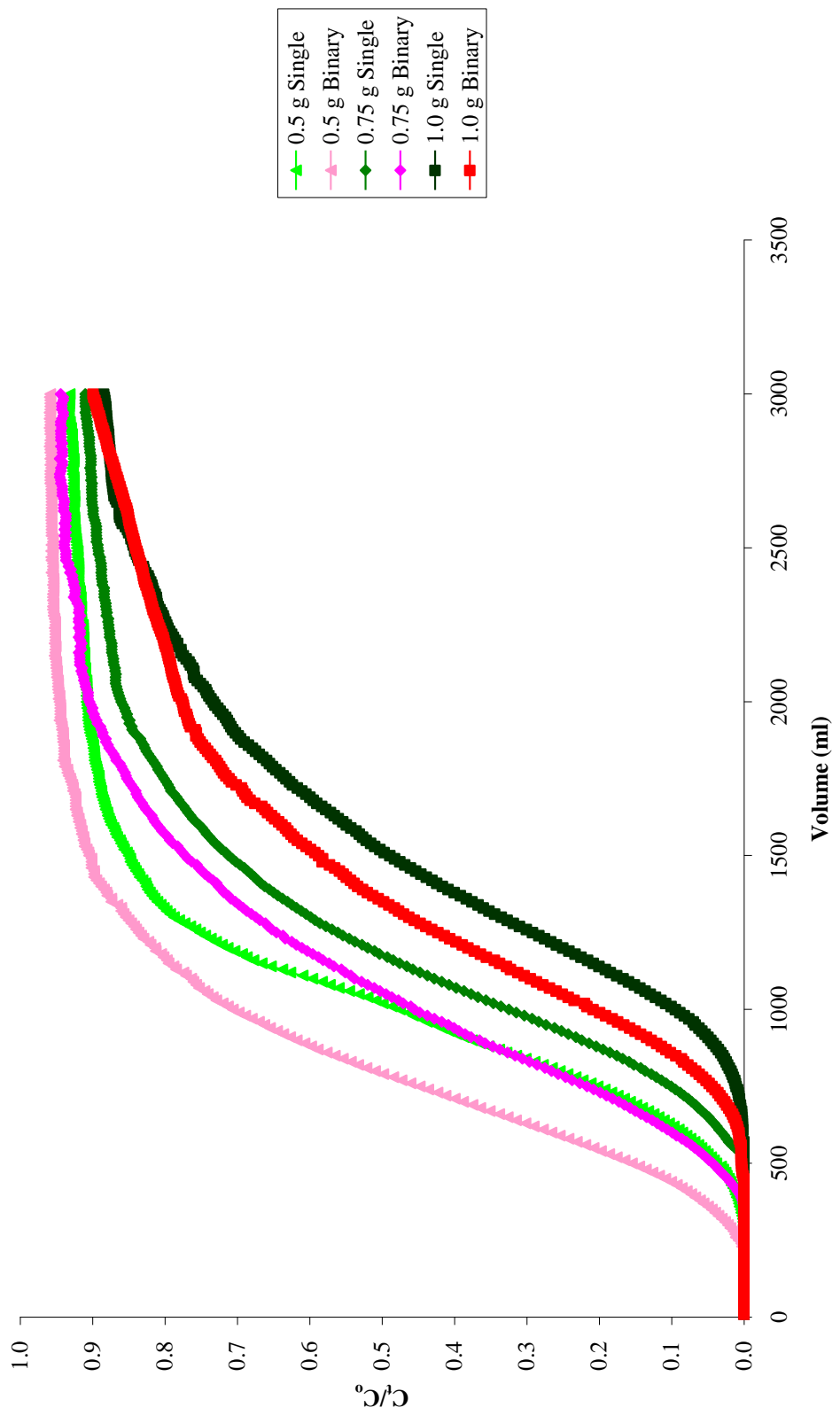
Figures 4.65 – 4.68 show the breakthrough curves at different bed height for single and binary BB3, MB and BY11 dye solutions. Higher removal efficiency of dye was observed as the bed height increases due to the increase in the contact time of dye cations with the adsorbent. The slope of breakthrough curve decreased when increase in bed height, which resulted in a broadened mass transfer zone (Han *et al.*, 2007). In addition, the longer retention time was observed at higher bed height. This was due to the increase in the availability of sorption sites. Similar observation was reported by Sivakumar and Palanisamy, (2009) in the study of removal of AB92 and BR29 using non-conventional adsorbent. They observed that the throughput volume of dye solution increased with increasing in bed height, due to the availability of more number of sorption sites.





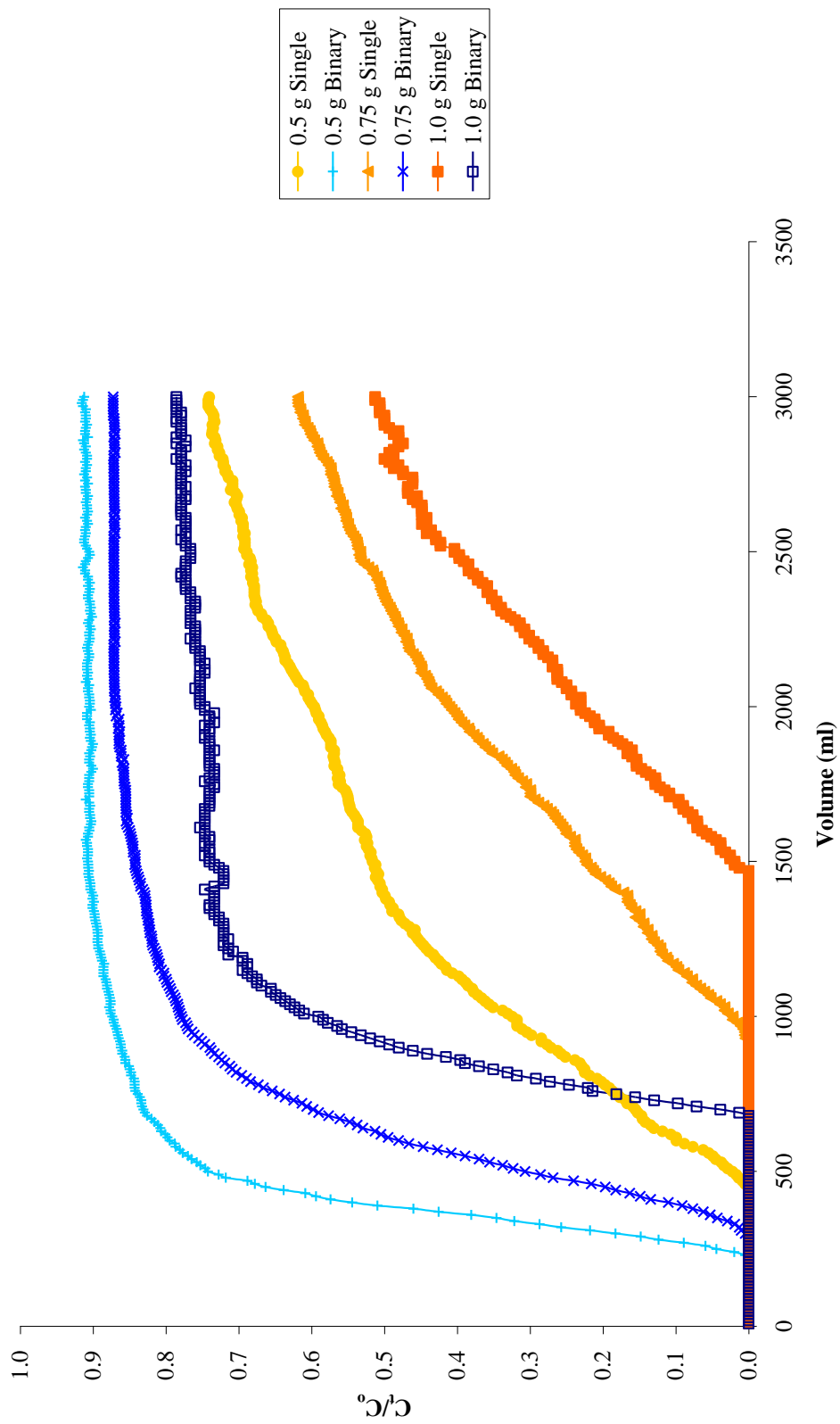
**Condition:** 10 mg/L of single and binary BB3 dye solution passing through 0.50, 0.75 and 1.0 g of sorbent at flow rate of 10 mL/min

**Figure 4.65: Effect of bed height on breakthrough curve of single and binary BB3 solution**



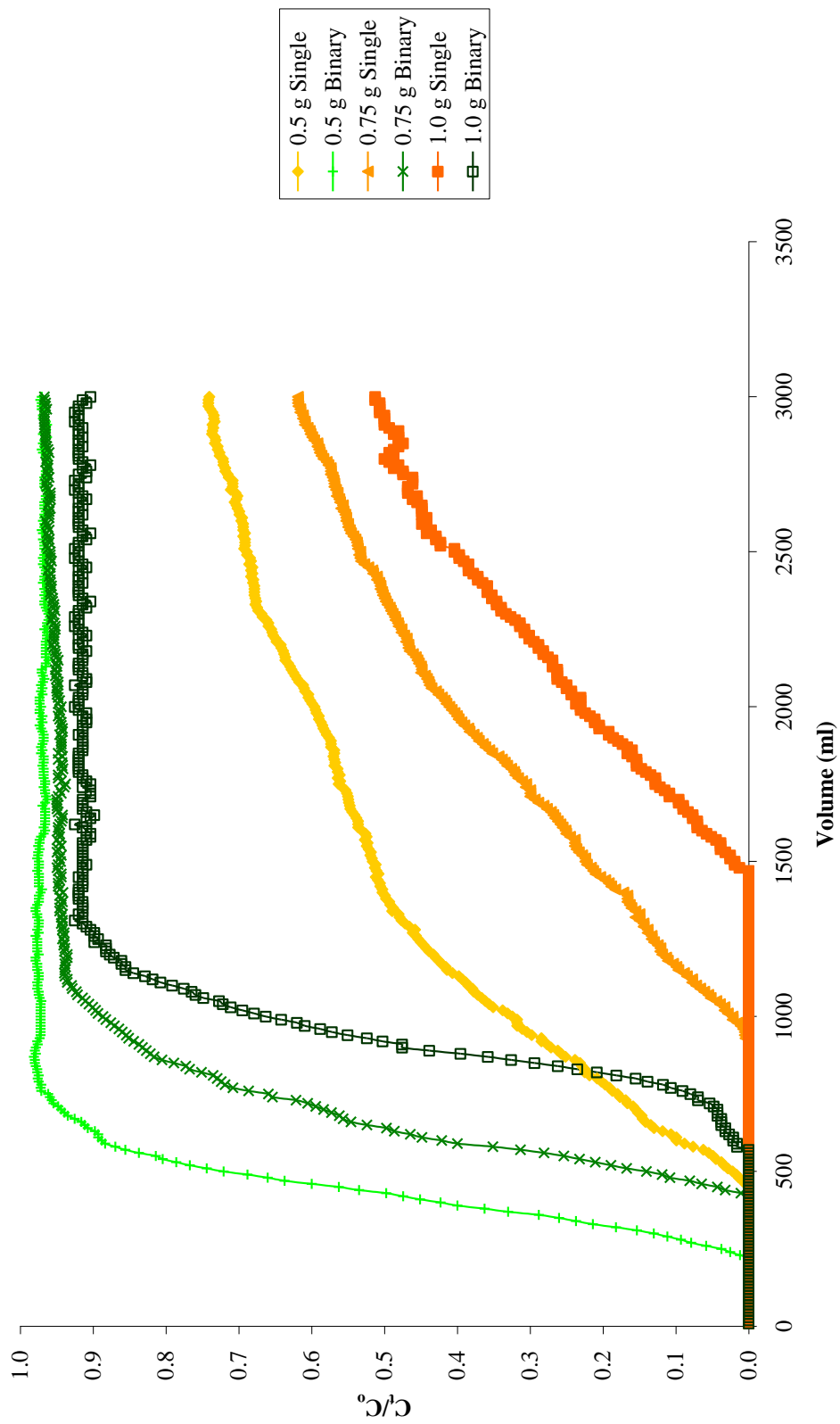
Condition: 10 mg/L of single and binary MB dye solution passing through 0.50, 0.75 and 1.0 g of sorbent at flow rate of 10 mL/min

Figure 4.66: Effect of bed height on breakthrough curve of single and binary MB solution



**Condition:** 10 mg/L of single and binary BY11 dye solution passing through 0.50, 0.75 and 1.0 g of sorbent at flow rate of 10 mL/min

**Figure 4.67: Effect of bed height on breakthrough curve of single BY11 and binary BY11 of BB3-BY11 solution**



**Condition:** 10 mg/L of single and binary BY11 dye solution passing through 0.50, 0.75 and 1.0 g of sorbent at flow rate of 10 mL/min

**Figure 4.68: Effect of bed height on breakthrough curve of single BY11 and binary BY11 of MB-BY11 solution**

#### 4.8.4 Thomas Model

Thomas model was used to calculate the sorption rate constant and the solid phase concentration of the dye on the sorbent from the continuous mode study. Thomas model is one of the most widely used kinetic models to evaluate column performance. The Thomas model equation was showed as:

$$\frac{C_t}{C_o} = \frac{1}{1 + \exp[k_{Th}(q_o x v - C_o V_{eff} / v)]} \quad (26)$$

where,

$C_t$  = effluent concentration at t (mg/L)

$C_o$  = influent dye concentration (mg/L)

$k_{Th}$  = Thomas rate constant (mL/min mg)

$q_o$  = equilibrium dye uptake per g of adsorbent (mg/g)

$x$  = amount of adsorbent (g)

$V_{eff}$  = effluent volume (mL)

$v$  = flow rate (mL/min)

Table 4.33 – 4.39 show that the Thomas model constants for all the studied dye solutions. For single BB3, the bed capacity,  $q_o$  and the Thomas rate constant,  $k_{Th}$ , increased as the influent concentration increased. The increase in  $q_o$  indicated that the driving force for biosorption was the difference between the dye on the sorbent and the dye in solution (Han *et al.*, 2006b). Therefore, higher influent concentration causes higher driving force gave better column performance. As the flow rate increase, the  $k_{Th}$  increase while the  $q_o$  decrease.

Meanwhile, as the bed height increased, both  $q_0$  and  $k_{Th}$  decreased. Thus, lower flow rate and higher influent concentration would increase the sorption of BB3 on NSB column. Similar observation was obtained for single MB, binary BB3 and binary MB. The  $k_{Th}$  and  $q_0$  for single BY11 does not show any consistent trend. This might be due to the shape of the breakthrough which does not exhibit a complete S-curve within the studied time frame.

Table 4.33: Calculated constants of Thomas model at different conditions using non-linear regression analysis for single BB3

$C_o$ (mg/L)	$v$ (mL/min)	$Z$ (cm)	$k_{Th}$ (mL/min mg)	$q_0$ (mg/g)	$R^2$
10	10	24	2.868	11.6741	0.967
20	10	24	3.538	12.461	0.987
10	7	12	2.680	26.559	0.959
10	10	12	4.912	14.329	0.983
10	15	12	7.449	7.049	0.981
10	10	18	3.938	12.060	0.972

Table 4.34: Calculated constants of Thomas model at different conditions using non-linear regression analysis for single MB

$C_o$ (mg/L)	$v$ (mL/min)	$Z$ (cm)	$k_{Th}$ (mL/min mg)	$q_0$ (mg/g)	$R^2$
10	10	24	2.611	12.626	0.980
20	10	24	3.018	18.666	0.993
10	7	12	2.509	34.392	0.982
10	10	12	4.340	20.826	0.991
10	15	12	6.376	12.117	0.991
10	10	18	3.140	16.846	0.981

Table 4.35: Calculated constants of Thomas model at different conditions using non-linear regression analysis for binary BB3 of BB3-BY11

$C_o$ (mg/L)	$v$ (mL/min)	$Z$ (cm)	$k_{Th}$ (mL/min mg)	$q_0$ (mg/g)	$R^2$
10	10	24	3.068	7.927	0.946
20	10	24	3.299	10.286	0.988
10	7	12	3.353	20.715	0.980
10	10	12	6.155	10.745	0.984
10	15	12	9.567	6.300	0.984
10	10	18	3.952	9.636	0.971

Table 4.36: Calculated constants of Thomas model at different conditions using non-linear regression analysis for binary BY11 of BB3-BY11

$C_o$ (mg/L)	$v$ (mL/min)	$Z$ (cm)	$k_{Th}$ (mL/min mg)	$q_0$ (mg/g)	$R^2$
10	10	24	1.945	12.136	0.809
20	10	24	7.929	10.221	0.998
10	7	12	3.187	18.921	0.944
10	10	12	8.976	8.558	0.973
10	15	12	13.491	4.121	0.970
10	10	18	3.945	9.582	0.941

Table 4.37: Calculated constants of Thomas model at different conditions using non-linear regression analysis for binary MB of MB-BY11

$C_o$ (mg/L)	$v$ (mL/min)	$Z$ (cm)	$k_{Th}$ (mL/min mg)	$q_0$ (mg/g)	$R^2$
10	10	24	2.511	14.773	0.972
20	10	24	3.745	13.201	0.994
10	7	12	2.324	27.467	0.977
10	10	12	4.477	16.627	0.993
10	15	12	6.183	10.159	0.991
10	10	18	3.313	14.917	0.990



Table 4.38: Calculated constants of Thomas model at different conditions using non-linear regression analysis for binary BY11 of MB-BY11

$C_o$ (mg/L)	$v$ (mL/min)	$Z$ (cm)	$k_{Th}$ (mL/min mg)	$q_0$ (mg/g)	$R^2$
10	10	24	9.274	9.432	0.995
20	10	24	10.631	8.375	0.999
10	7	12	6.516	14.797	0.991
10	10	12	13.298	8.646	0.998
10	15	12	15.863	4.505	0.995
10	10	18	8.500	9.025	0.994

#### 4.8.5 The Belter and Chu Models

The two parameter fixed bed sorption model (Belter *et al.*, 1988) and two subsequent modifications by Chu (Eq. 28) were used to fit the data obtained from the fixed bed solutions. The Belter and Chu models were based on following equations

Belter model:

$$\frac{C_t}{C_o} = \frac{1}{2} \left[ 1 + \operatorname{erf} \left( \frac{t - t_{0.5}}{\sqrt{2}\sigma t_{0.5}} \right) \right] \quad (27)$$

Chu model:

$$\frac{C_t}{C_o} = \frac{1}{2} \left[ 1 + \operatorname{erf} \left( \frac{(t - t_{0.5}) (\exp(\pm \sigma(t/t_{0.5})))}{\sqrt{2}\sigma t_{0.5}} \right) \right] \quad (28)$$

where,

$C_t$  = effluent concentration (mg/L)

$C_o$  = influent concentration (mg/L)

$t$  = time (min)

$\sigma$  = standard deviation

$\text{erf}(x)$  = error function of  $x$

By evaluating  $t_{0.5}$  and  $\sigma$  from the experimental column, correlation may be defined, therefore allows the prediction of theoretical breakthrough curves of untested conditions (Brady *et al.*, 1999). Belter model was capable of modeling only symmetric curves employing two parameters,  $\sigma$  and  $t_{0.5}$ , empirically correlated with the process factors. Meanwhile, in Chu model (with + and – sign) are capable of modeling both symmetric and non-symmetric curves with no additional parameters. The advantage of using the equation proposed by Chu is that they can fit breakthrough curves obtained from the solutions, where either mass transfer limitation or flow non-idealities exist (Lodeiro *et al.*, 2006).

The theoretical breakthrough curves generated by both models for single and binary BB3, MB and BY11 were compared with the experimental breakthrough curves (Figures 4.69 – 4.75). From Figure (4.69), Chu (model with negative sign in exponential term) showed a better fit with the experimental breakthrough curve of single BB3 compared to other theoretical breakthrough

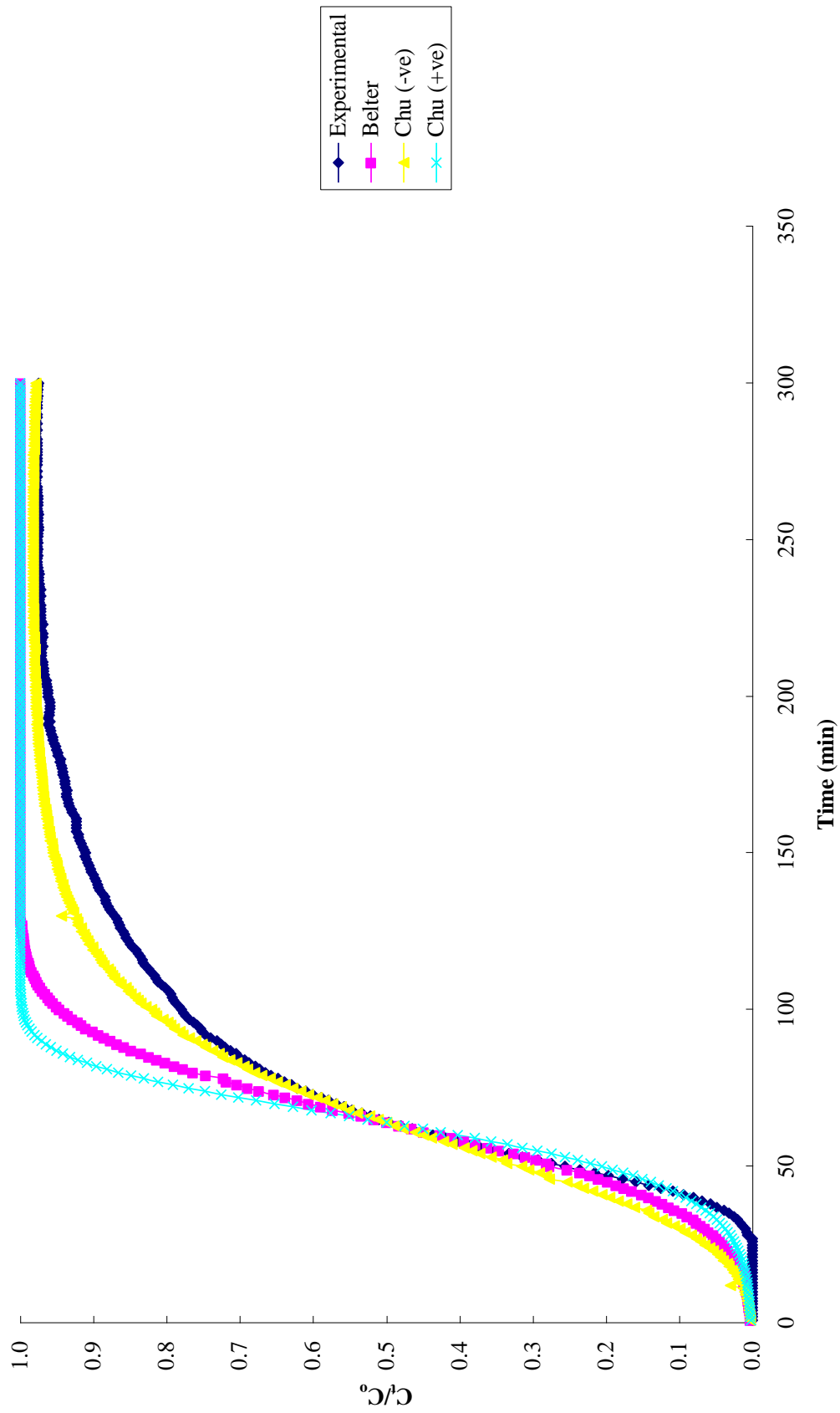


**Figure 4.69: Comparison of the experimental and model fit breakthrough curves for single BB3 by NSB according to: Belter, Chu (-ve) and Chu (+ve)**

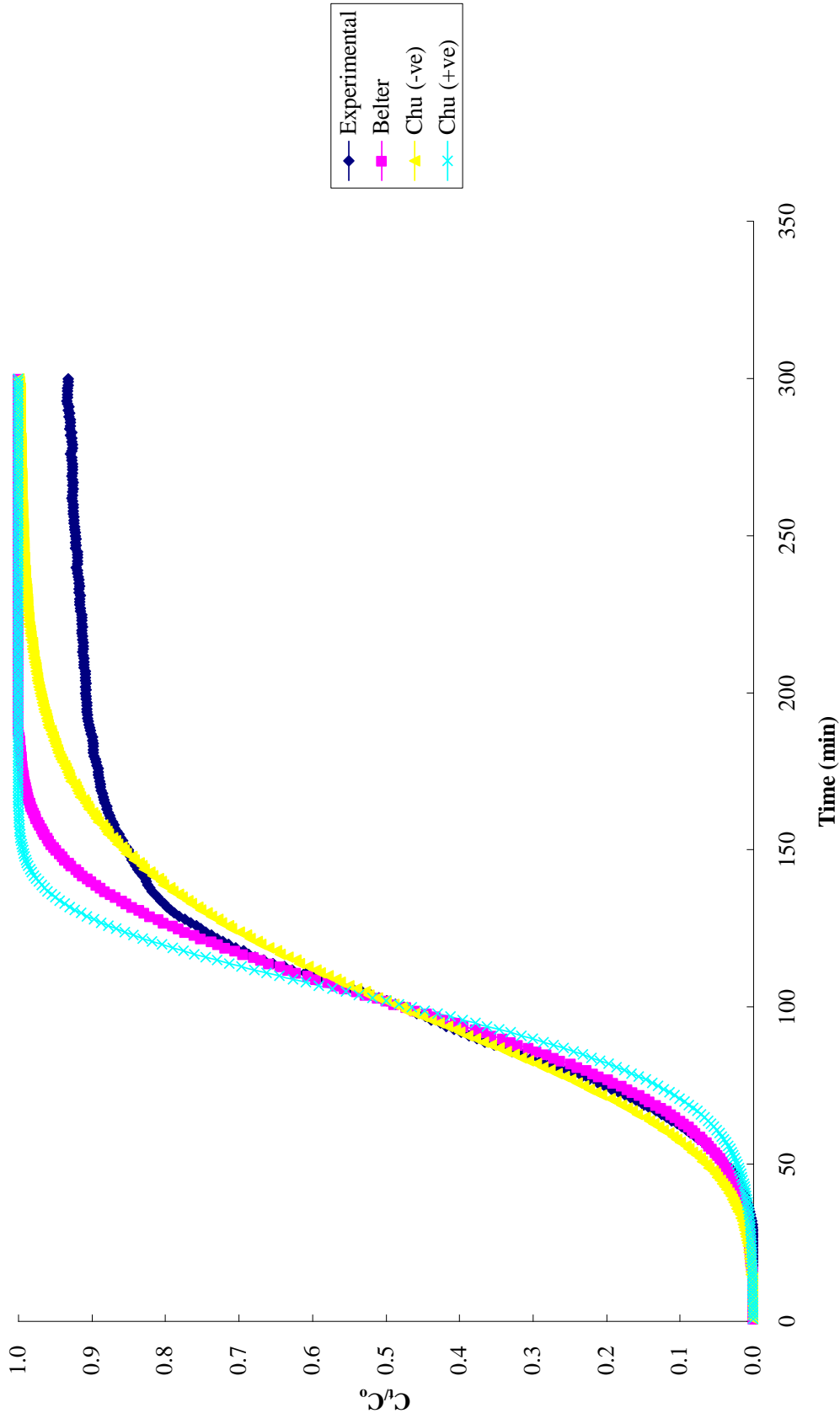


**Figure 4.70: Comparison of the experimental and model fit breakthrough curves for single MB by NSB according to: Belter, Chu (-ve) and Chu (+ve)**

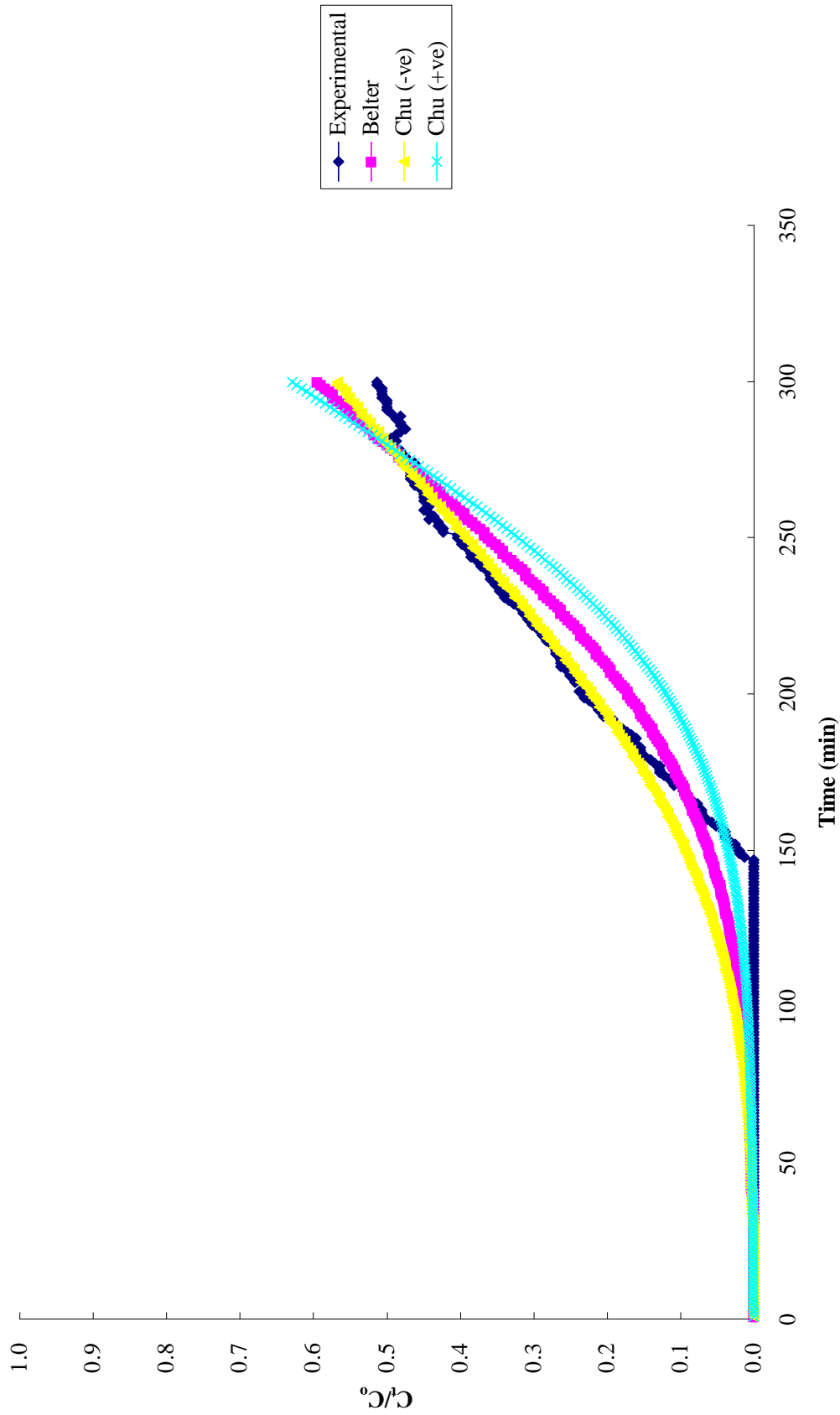


**Figure 4.71: Comparison of the experimental and model fit breakthrough curves for single BY11 by NSB according to: Belter, Chu (-ve) and Chu (+ve)**

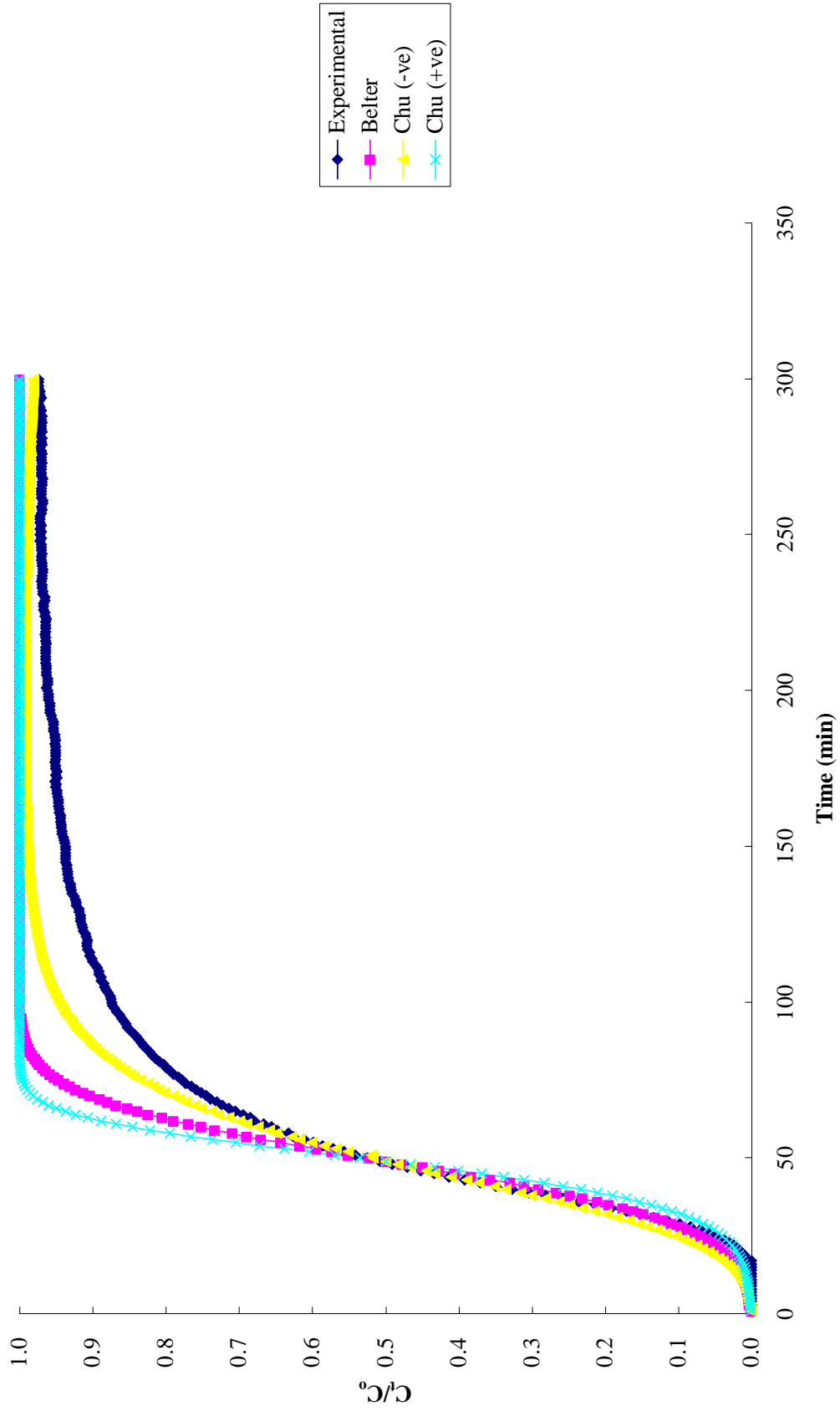


Figure 4.72: Comparison of the experimental and model fit breakthrough curves for binary BB3 of BB3-BY11 by NSB according to: Belter, Chu (-ve) and Chu (+ve)

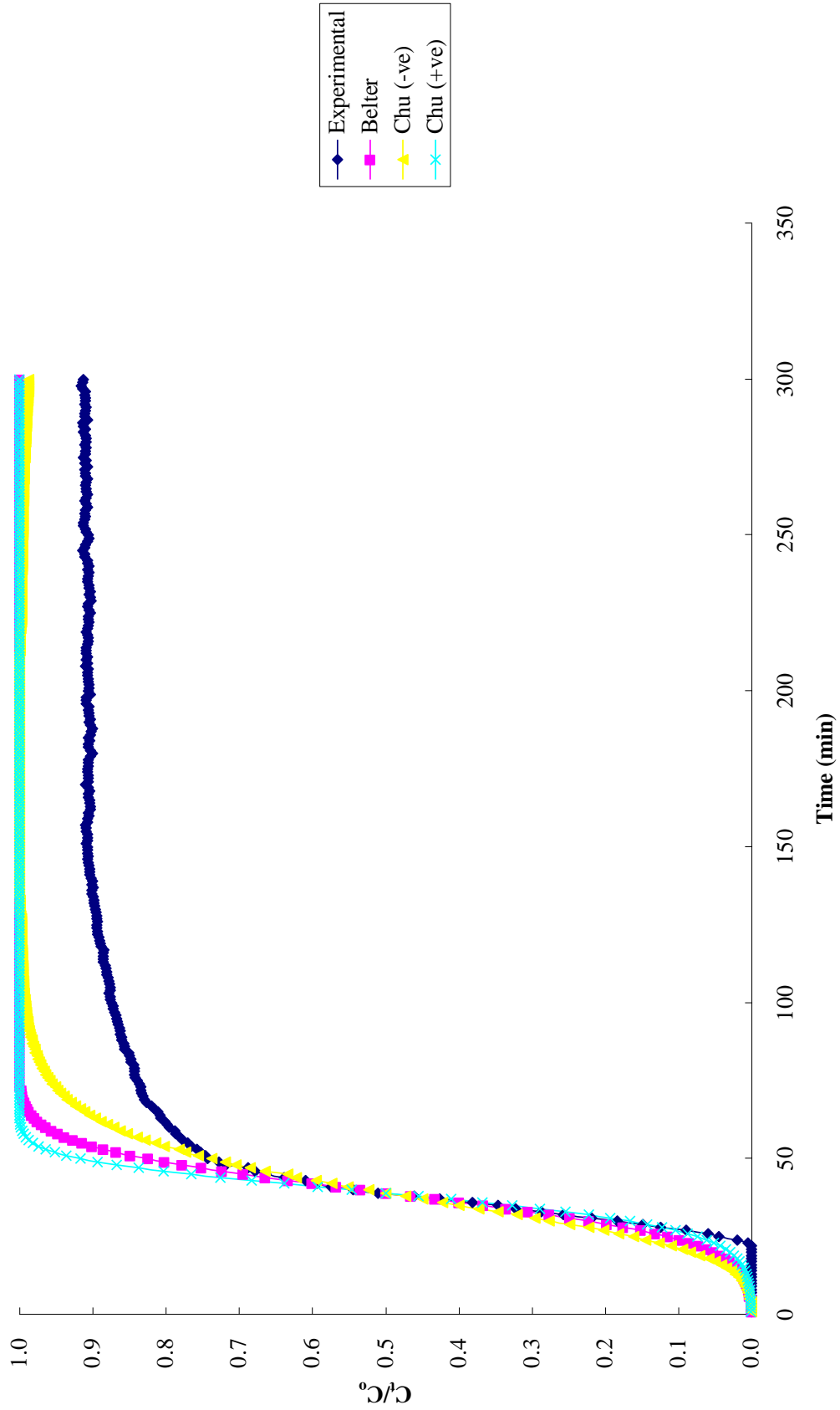
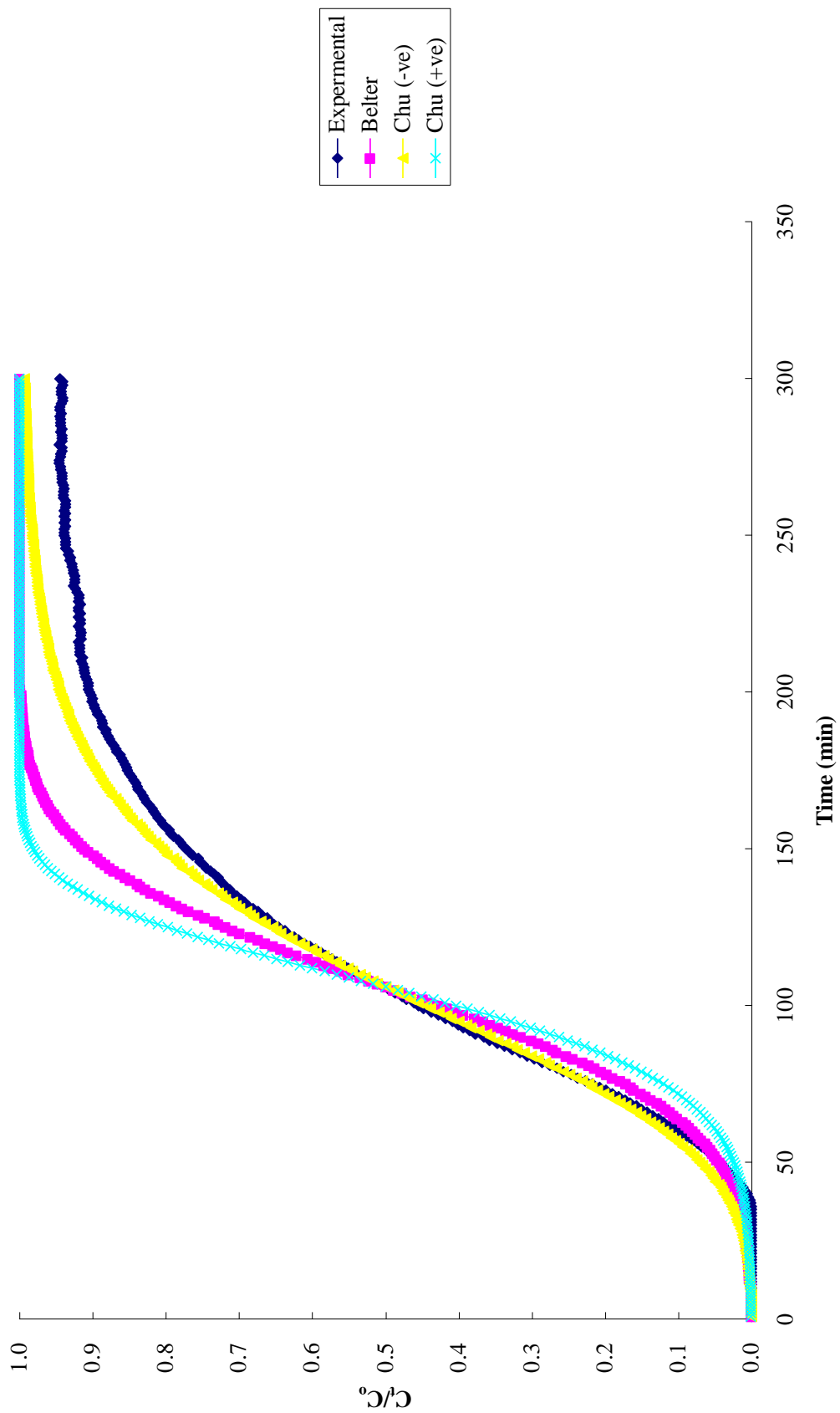
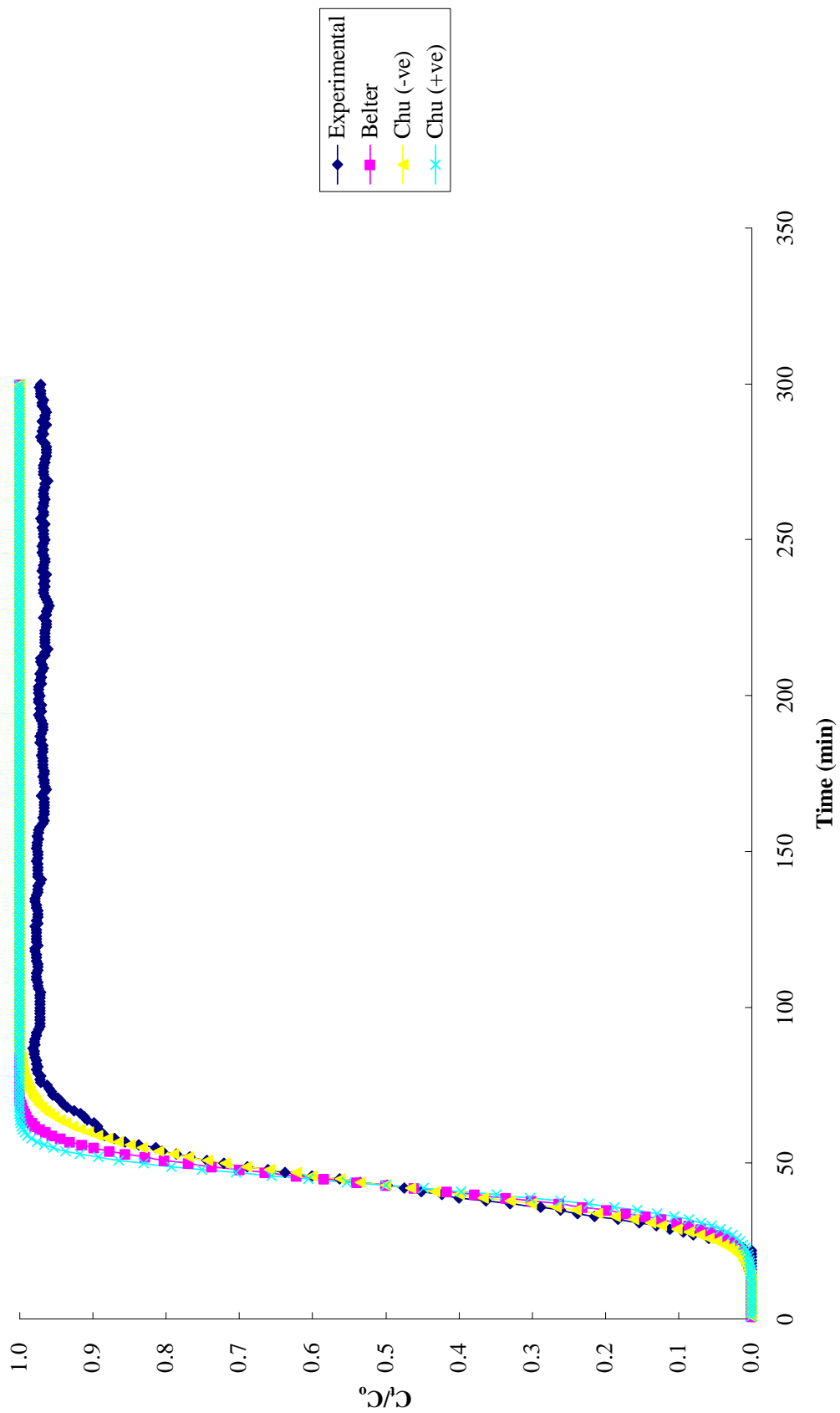


Figure 4.73: Comparison of the experimental and model fit breakthrough curves for binary BY11 of BB3-BY11 by NSB according to: Belter, Chu (-ve) and Chu (+ve)



**Figure 4.74: Comparison of the experimental and model fit breakthrough curves for binary MB of MB-BY11 by NSB according to: Belter, Chu (-ve) and Chu (+ve)**





**Figure 4.75: Comparison of the experimental and model fit breakthrough curves for binary BY11 of MB-BY11 by NSB according to: Belter, Chu (-ve) and Chu (+ve)**

curves. Similar observation was observed in single MB, single BY11 and the both binary dye solutions. Therefore, Chu model can be used as the basis for simplified scale-up design calculation for all the studied dye solutions.

#### 4.8.6 The Bed-Depth/Service Time Analysis (BDST) Model

The BDST model was based on physically measuring the capacity of the bed at different breakthrough values, and it works well and provides useful modeling equation for the changes of system parameters (Ko *et al.*, 2000). The modified form of equation which states that bed height and service time of a column carries a linear relationship (Hutchins, 1973) was shown as:

$$t = \frac{N_o Z}{C_o F} - \frac{1}{K_B C_o} \ln \left( \frac{C_o}{C_t} - 1 \right) \quad (29)$$

where,

$C_t$  = effluent concentration of solute in the liquid phase (mg/L)

$C_o$  = initial concentration of solute in the liquid phase (mg/L)

$F$  = influent linear velocity (cm/min)

$N_o$  = sorption capacity (mg/g)

$K_B$  = rate constant in BDST model (L/mg min)

$t$  = time (min)

$Z$  = bed depth of column (cm)

At 50% breakthrough ( $C_o/C_t = 2$ ), and  $t = t_{0.5}$ , the equation is reduced to:

$$t_{0.5} = \frac{N_o Z}{C_o F} \quad (30)$$

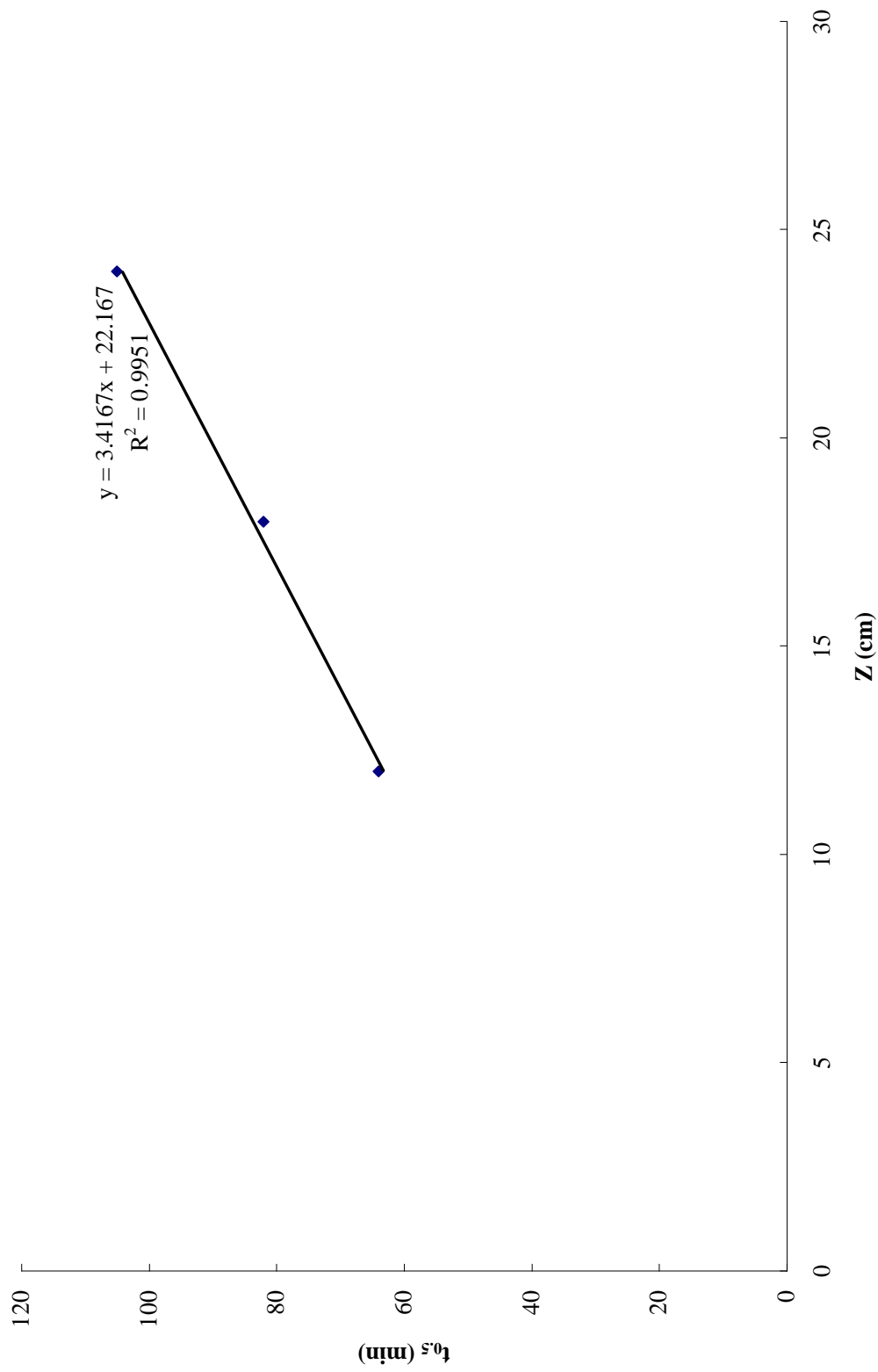
A linear plot of  $t$  against bed depth ( $Z$ ) passing through the origin can be plotted using above equation, provided that the sorption data follow the model.

Figure 4.76 exhibited the plot of  $t$  against  $Z$  at 50% breakthrough for single BB3. The plot gave a straight line however it does not pass through the origin. Similar deviation from the BDST model was reported in the sorption of Basic Blue 3 and Reactive Orange 16 by ethylenediamine modified rice hull (Lee *et al.*, 2008). The nonconformity of the BDST model may due to the presence of more than one-limiting step in the sorption process (Lee *et al.*, 1998). Similar deviation was observed for the other studied solutions (Figures 4.77 – 4.82).

The slope constant for different flow rates can be calculated using the equation below (Goel *et al.*, 2005):

$$t_{0.5} = \frac{N_o Z}{C_o F} \quad (30)$$

where  $a$  and  $F$  are the old slope and influent linear velocity, respectively and  $a'$  and  $F'$  are the new slope and influent linear velocity, respectively.



**Figure 4.76: BDST plots of single BB3 at flow rate of 10 mL/min and influent concentration of 10 mg/L**

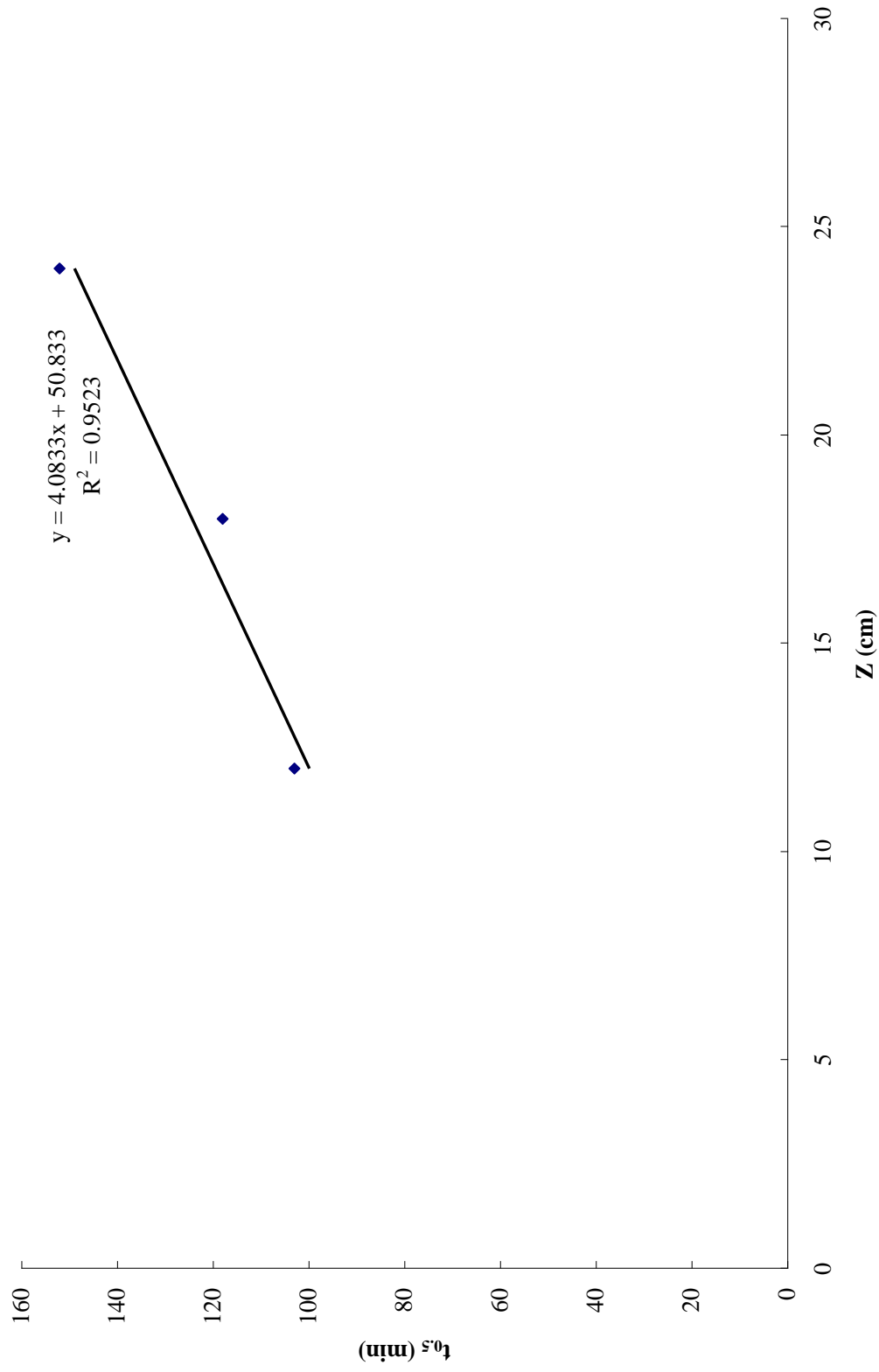


**Figure 4.77: BDST plots of single MB at flow rate of 10 mL/min and influent concentration of 10 mg/L**

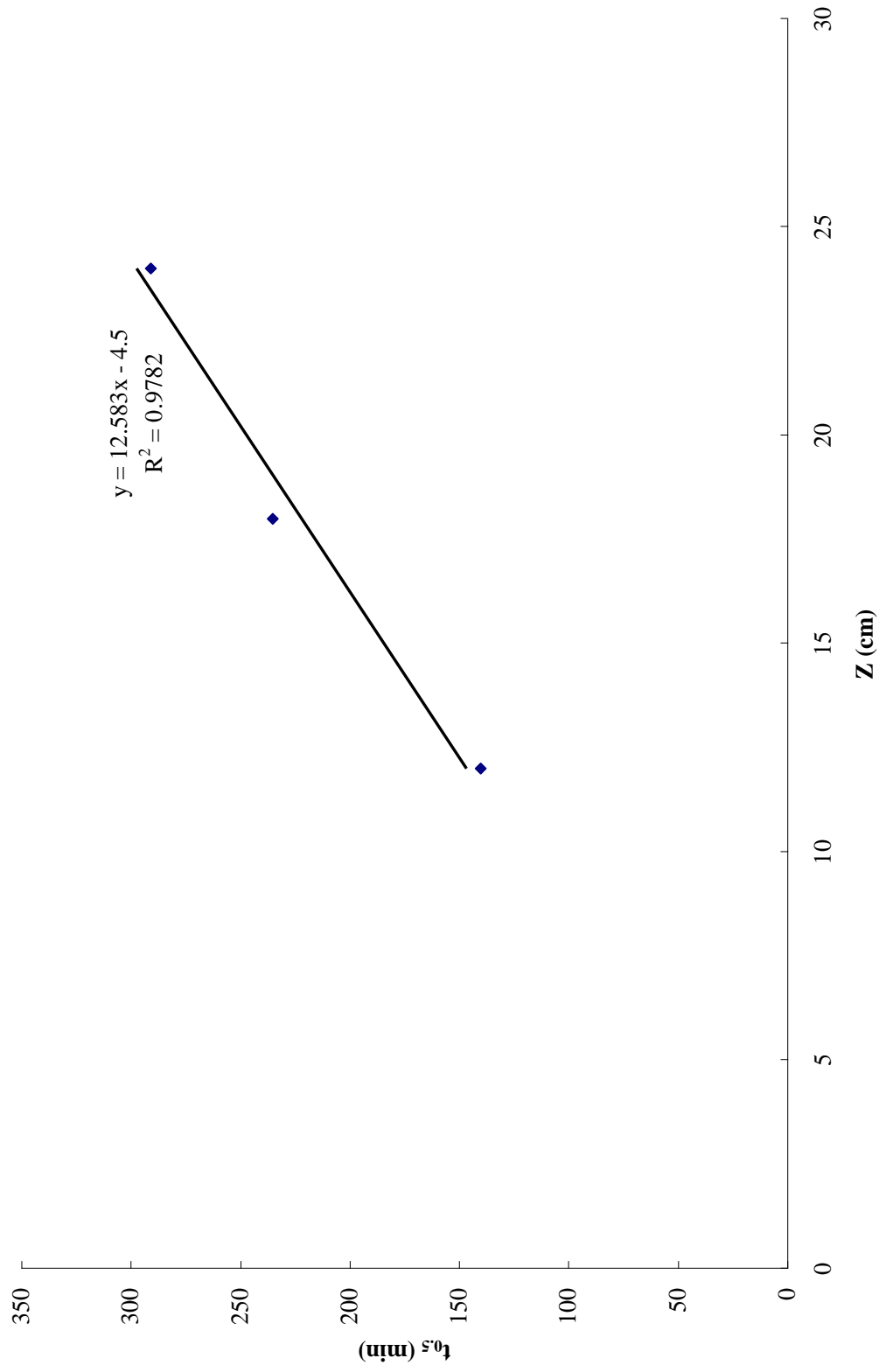


**Figure 4.78: BDST plots of single BY11 at flow rate of 10 mL/min and influent concentration of 10 mg/L**

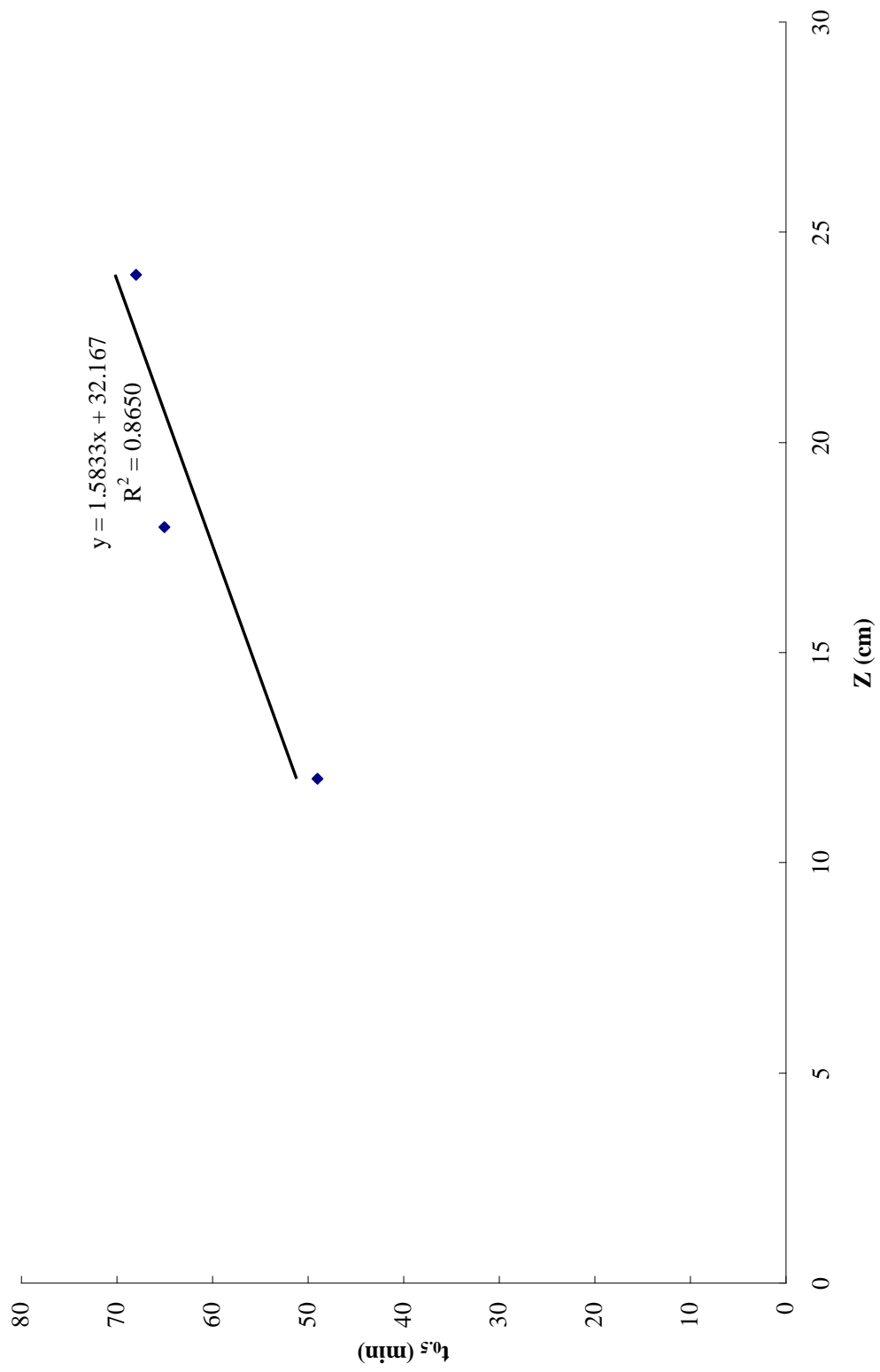


**Figure 4.79: BDST plots of binary BB3 of BB3-BY11 at flow rate of 10 mL/min and influent concentration of 10 mg/L**

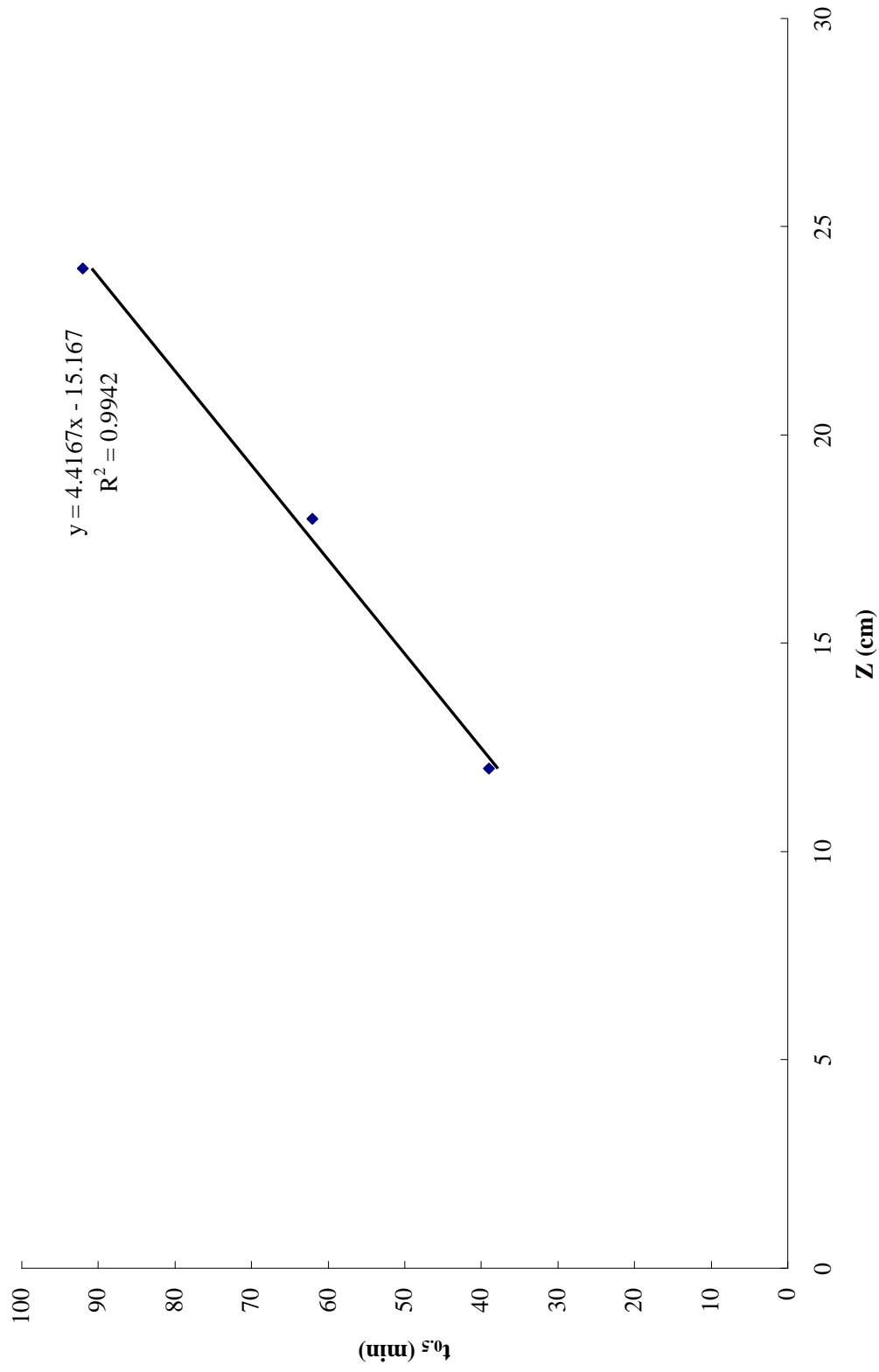


**Figure 4.80: BDST plots of binary BY11 of BB3-BY11 at flow rate of 10 mL/min and influent concentration of 10 mg/L**



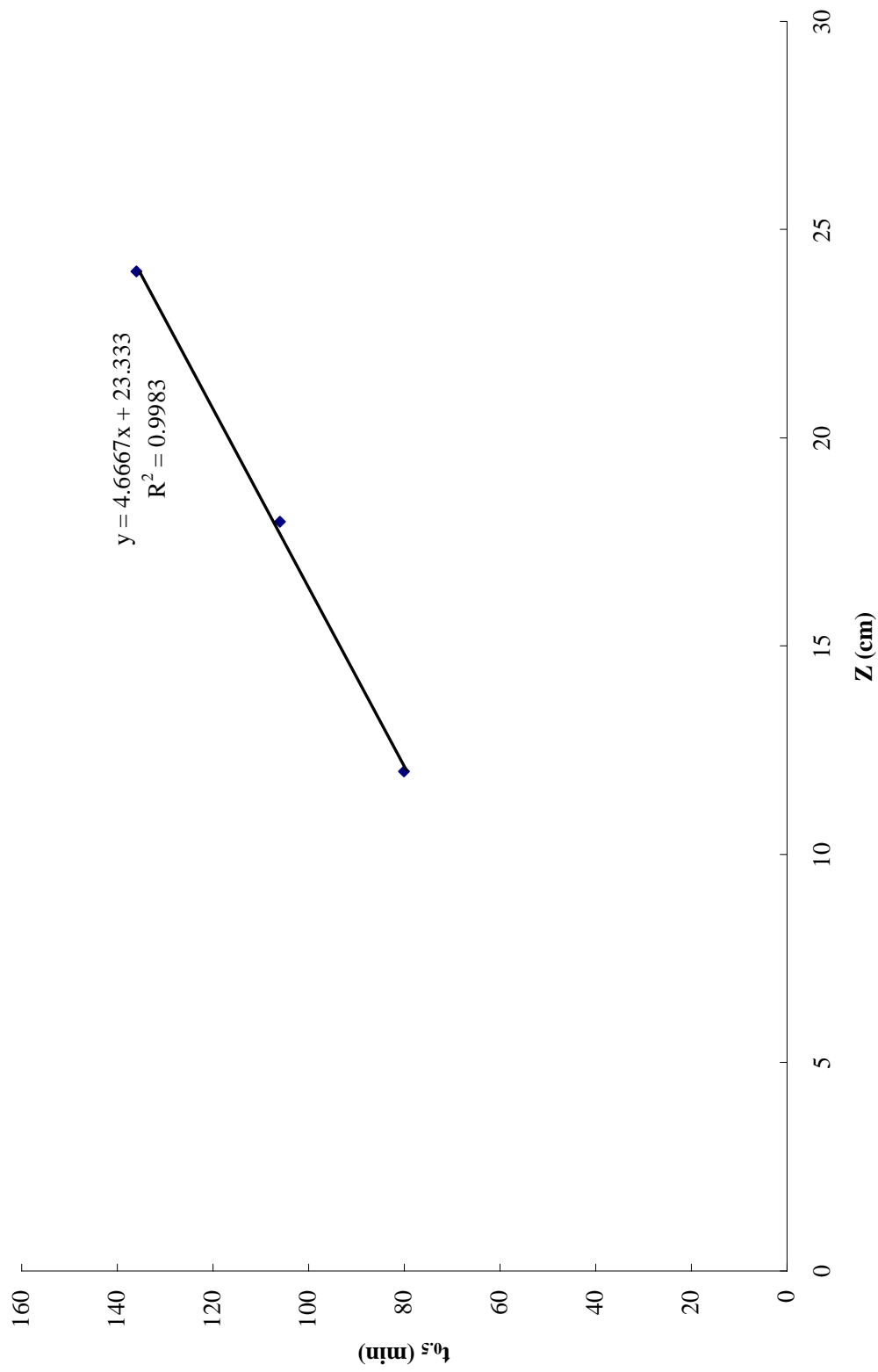


**Figure 4.81: BDST plots of binary MB of MB-BY11 at flow rate of 10 mL/min and influent concentration of 10 mg/L**

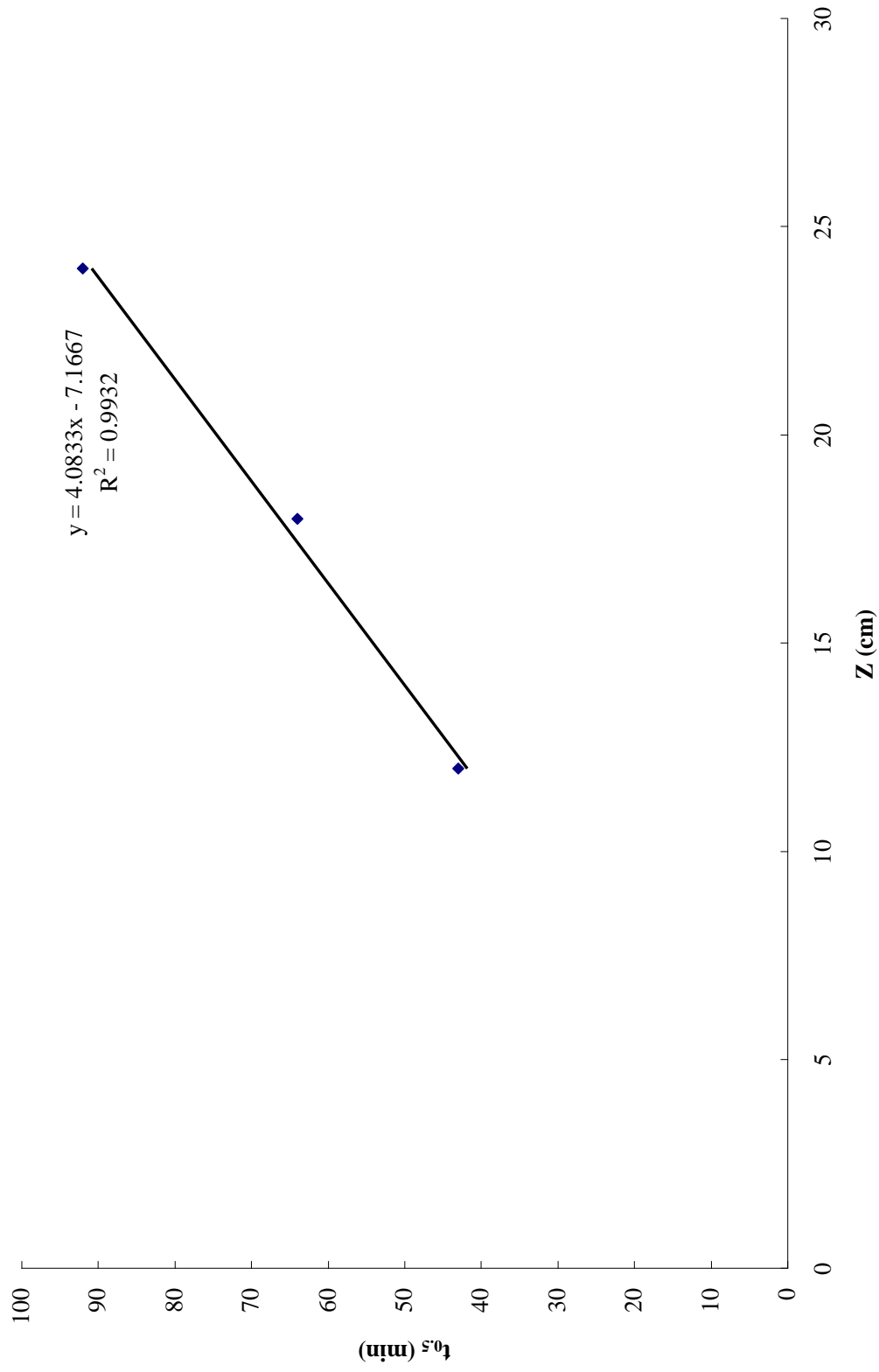


Figure 4.82: BDST plots of binary BY11 of MB-BY11 at flow rate of 10 mL/min and influent concentration of 10 mg/L

Since the column used in this study had the same diameter, therefore the ratio of original (F) and the new influent linear velocity (F') are equal to the ratio of original flow rate (v) and the new flow rate (v')

$$a' = a \left( \frac{F}{F'} \right) = a \left( \frac{v}{v'} \right) \quad (31)$$

For other influent concentrations, the equation is given by a new slope and a new intercept:

$$b' = b \left( \frac{C}{C'} \right) \left( \frac{\ln(C'_o - 1)}{\ln(C_o - 1)} \right) \quad (32)$$

where b' and b are the new and old intercept, respectively and C'<sub>o</sub> and C<sub>o</sub> are the new and old influent concentration, respectively. The prediction of adsorbent performance at lower flow rate of 5 mL/min and influent concentration of 5 mg/L were shown at Table 4.39 and 4.40. The experimental and calculated data showed good agreement for all the studied solutions. Therefore, the model and the constants evaluated can be used to scale up the process at other flow rates and influent concentrations without further experimental run.

Table 4.39: Predicted breakthrough time based on the BDST constants for a new  
flow rate ( $C_o = 10$  mg/L)

Dye solutions	a (min/cm)	b (min)	v	v'	a'	Z (cm)	t <sub>c</sub> (min)	t <sub>e</sub> (min)
Single BB3	3.417	22.167	10	5	6.833	12	104.17	106
Single MB	4.083	50.833	10	5	8.167	12	148.83	151
Single BY11	12.583	-4.500	10	5	25.166	12	297.49	300
Binary BB3	1.583	32.167	10	5	3.167	12	70.17	71
Binary BY11 of BB3-BY11	4.417	-15.167	10	5	8.833	12	90.83	93
Binary MB	4.667	23.333	10	5	9.333	12	135.33	137
Binary BY11 of MB-BY11	4.083	-7.1667	10	5	8.167	12	90.83	89

Table 4.40: Predicted breakthrough time based on the BDST constants for a new  
influent concentration ( $v = 10 \text{ mL/min}$ )

Dye solutions	a (min/cm)	b (min)	$C_o$	$C'_o$	$a'$	$b'$	Z (cm)	$t_c$ (min)	$t_e$ (min)
Single BB3	3.417	22.167	10	5	6.833	27.972	12	109.97	108
Single MB	4.083	50.833	10	5	8.167	64.144	12	162.14	165
Single BY11	12.583	-4.500	10	5	25.166	-5.678	12	296.31	300
Binary BB3	1.583	32.167	10	5	3.167	40.590	12	78.59	81
Binary BY11 of BB3-BY11	4.417	-15.167	10	5	8.833	-19.139	12	86.86	90
Binary MB	4.667	23.333	10	5	9.333	29.443	12	141.44	140
Binary BY11 of MB-BY11	4.083	-7.1667	10	5	8.167	-9.043	12	88.96	90

#### 4.8.7 Column Regeneration Studies

The continuous usage of a sorbent material is a crucial factor in determining its application potential. Regeneration of the sorbent was often carried out by using eluting agent. The eluting agent used must not cause damages on the capacity of the sorbent to ensure that the sorbent can be reused several times. In

addition, it is also needed to ensure that the eluted solution from the regeneration process does not pose any disposal problem (Kalavathy *et al.*, 2010).

Figures 4.83 and 4.84 show the three sorption-desorption cycles for single BB3 dye solution. From the plot, minor decrease in breakthrough time was observed during the regeneration cycles and similar observation was observed for all the studied dye solutions (Figures 4.85 – 4.96). This might be due to the gradual deterioration of NSB because of repeating usage. Table 4.41 exhibits the sorption capacities, which are calculated from the area under the graphs, and the sorption process parameters for all the sorption-desorption cycles. From the table, a decrease in sorption capacity was observed as the cycle proceeds. The loss of sorption performance might be due to the changes of the chemistry and structure of the biosorbent, as well as changes of the flow and mass transport conditions within the column (Volesky *et al.*, 2003).

For all studied dye solutions, the elution curves showed a sharp increase in the initial stage followed by gradual decrease. All the desorption processes were completed by using a small volume of HCl resulting in a highly concentrated dye solution. A high concentration factor is preferable as the eventual recovery of dye will become more feasible (Saeed *et al.*, 2009). The high regeneration efficiency for all studied dye solutions also showed that NSB can be reused repeatedly.

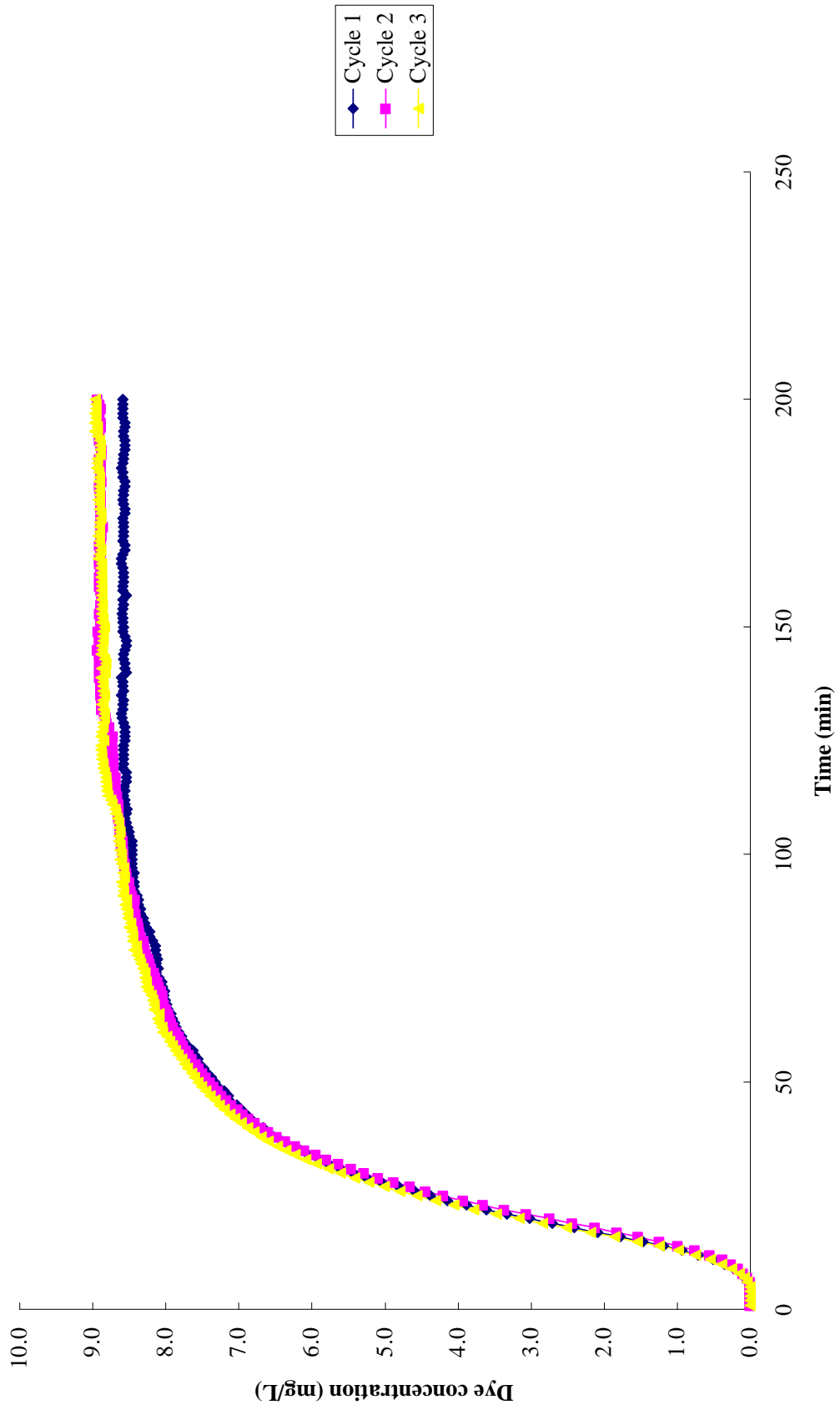


**Figure 4.83: Breakthrough curve for adsorption of single BB3 by NSB during three regeneration cycles**

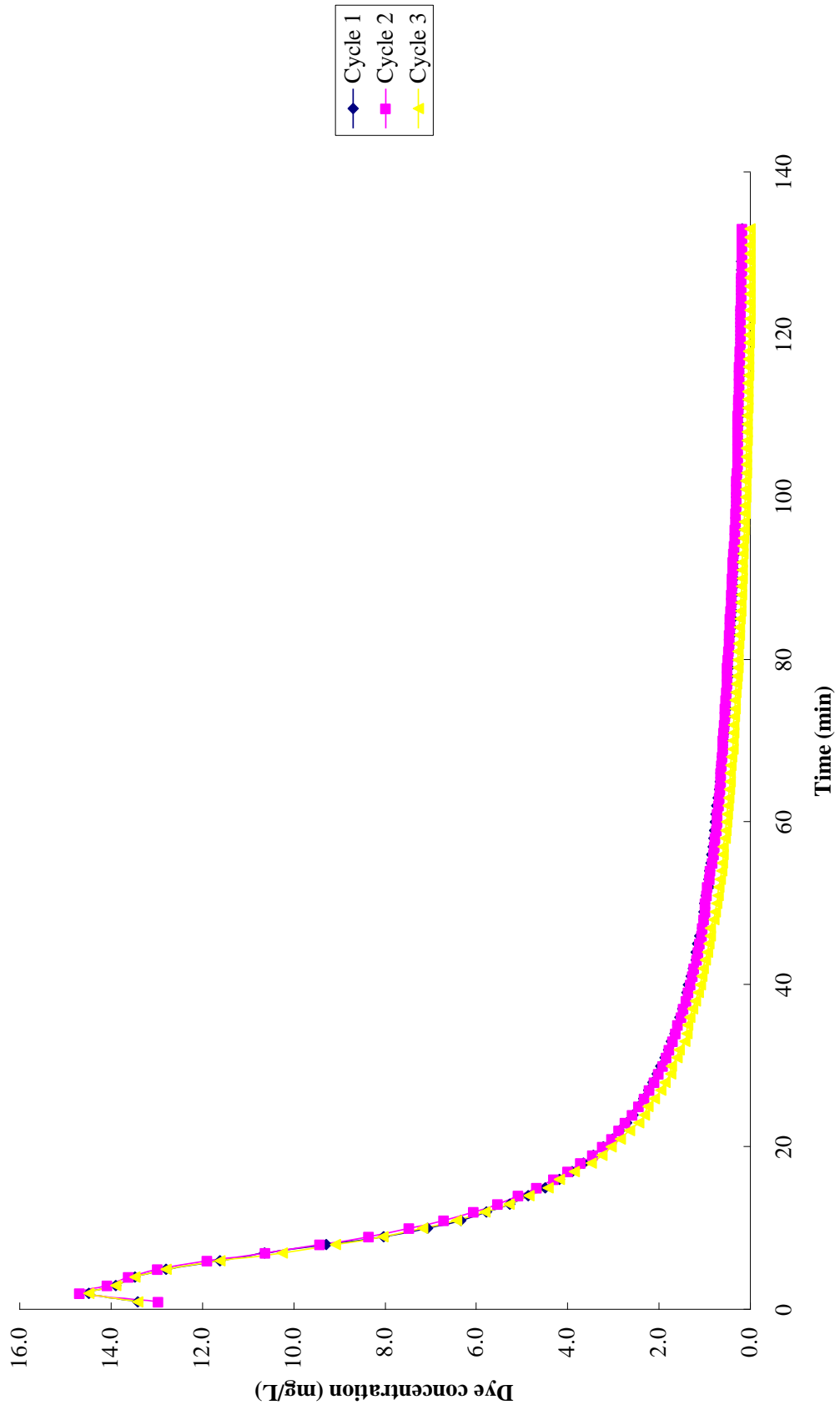


Figure 4.84: Elution curves for single BB3 column using 0.1 M HCl during three regeneration cycles



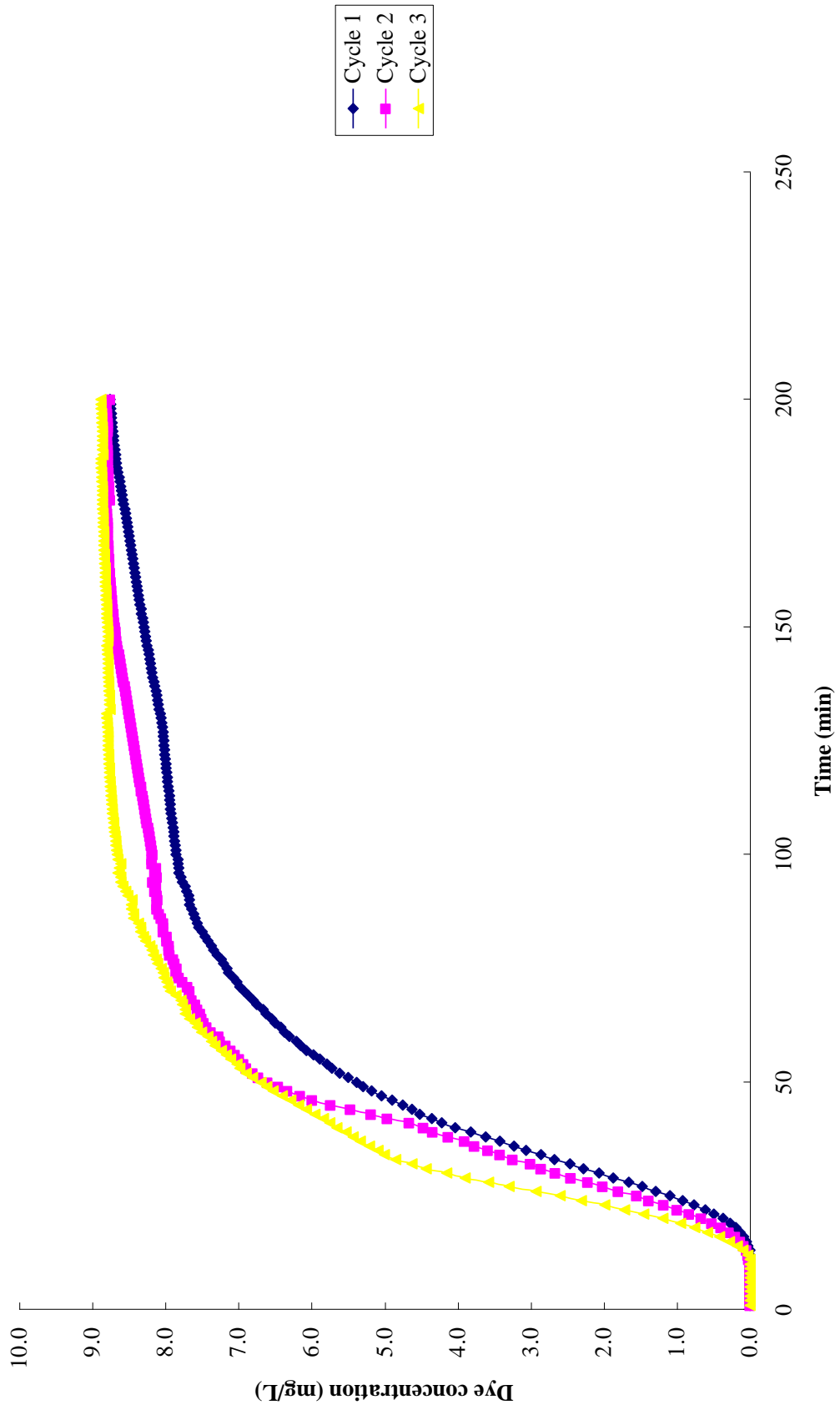
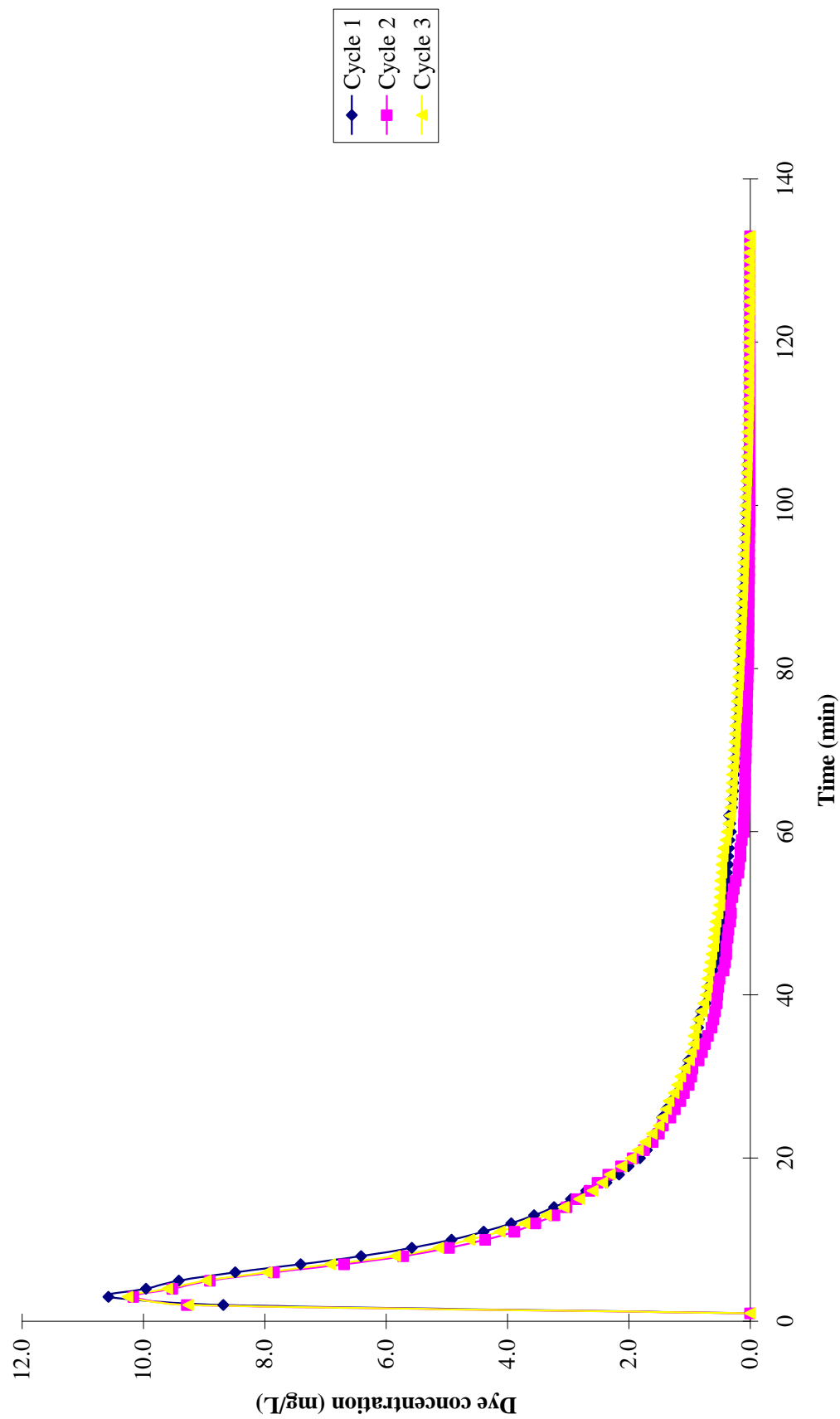
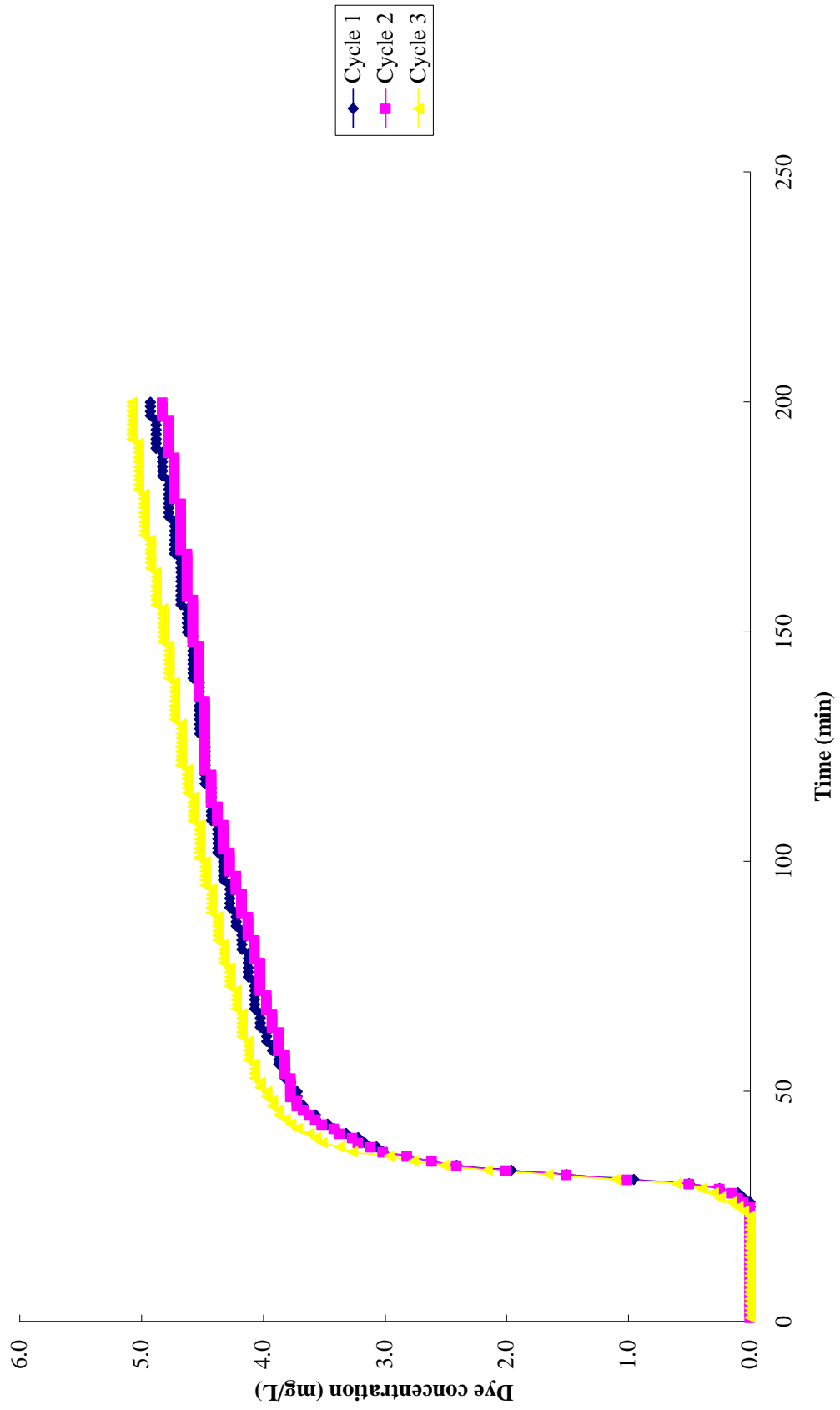


Figure 4.85: Breakthrough curve for adsorption of single MB by NSB during three regeneration cycles



**Figure 4.86: Elution curves for single MB column using 0.1 M HCl during three regeneration cycles**



**Figure 4.87: Breakthrough curve for adsorption of single BY11 by NSB during three regeneration cycles**

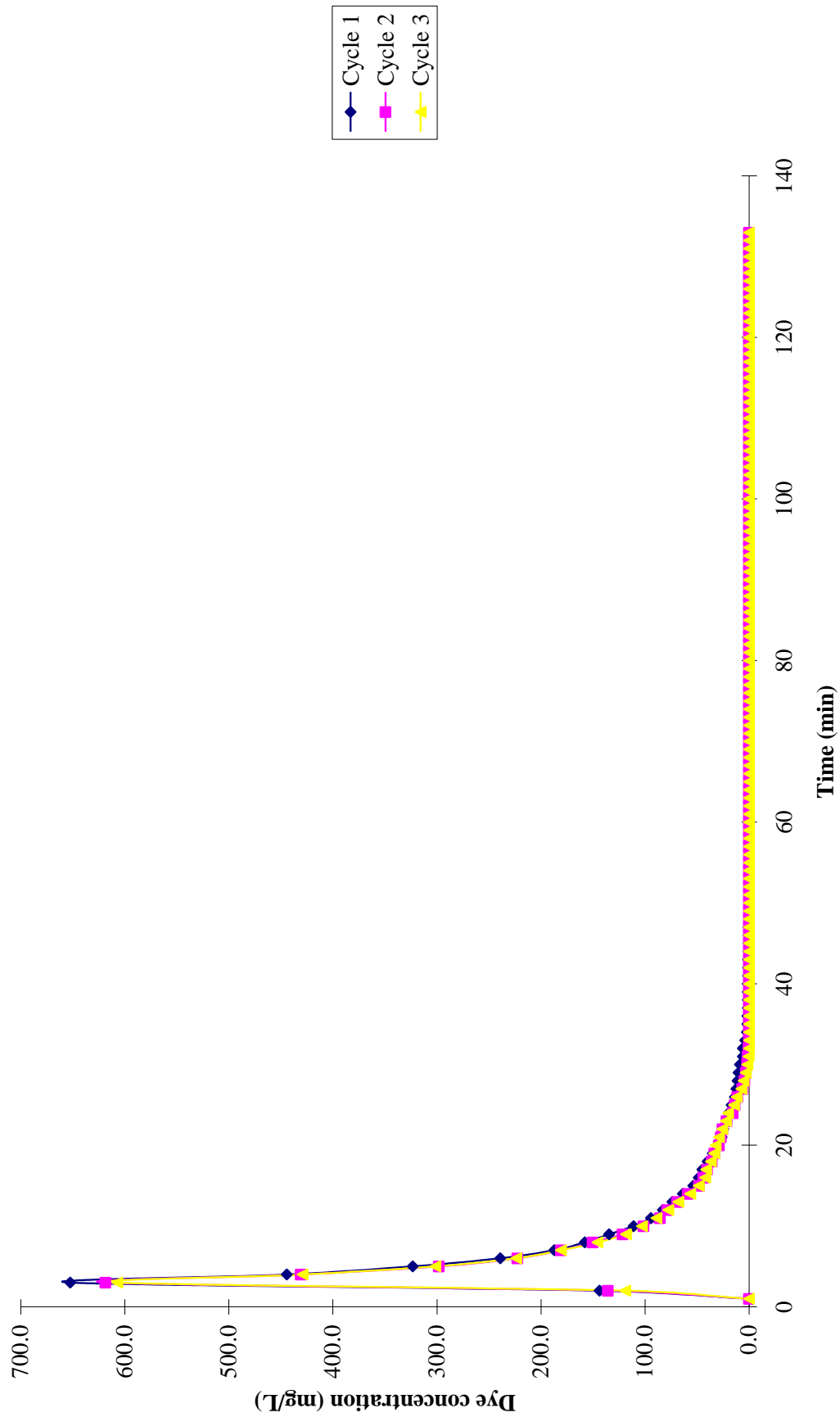
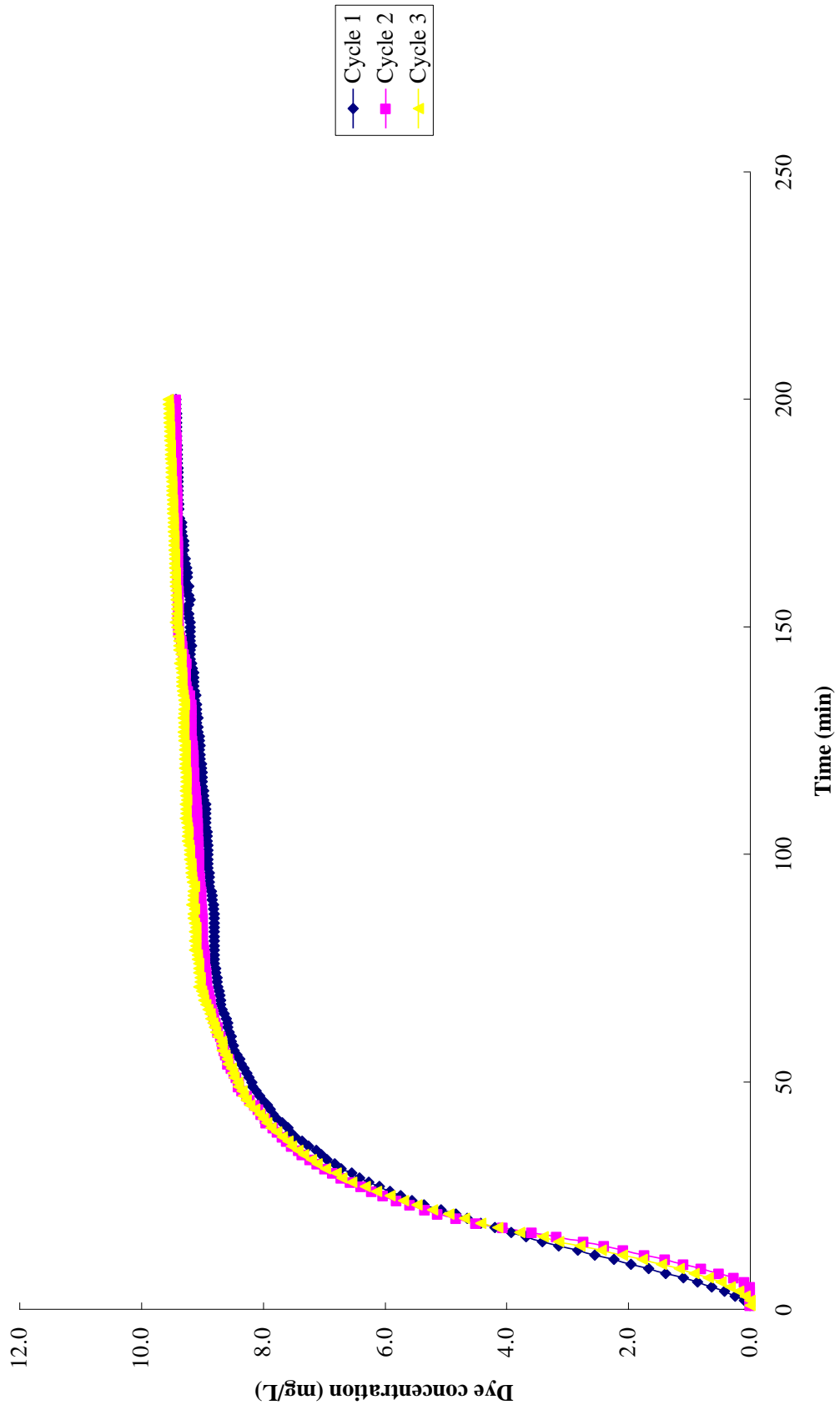


Figure 4.88: Elution curves for single BY11 column using 0.1 M HCl during three regeneration cycles



**Figure 4.89: Breakthrough curve for adsorption of binary BB3 of BB3-BY11 by NSB during three regeneration cycles**

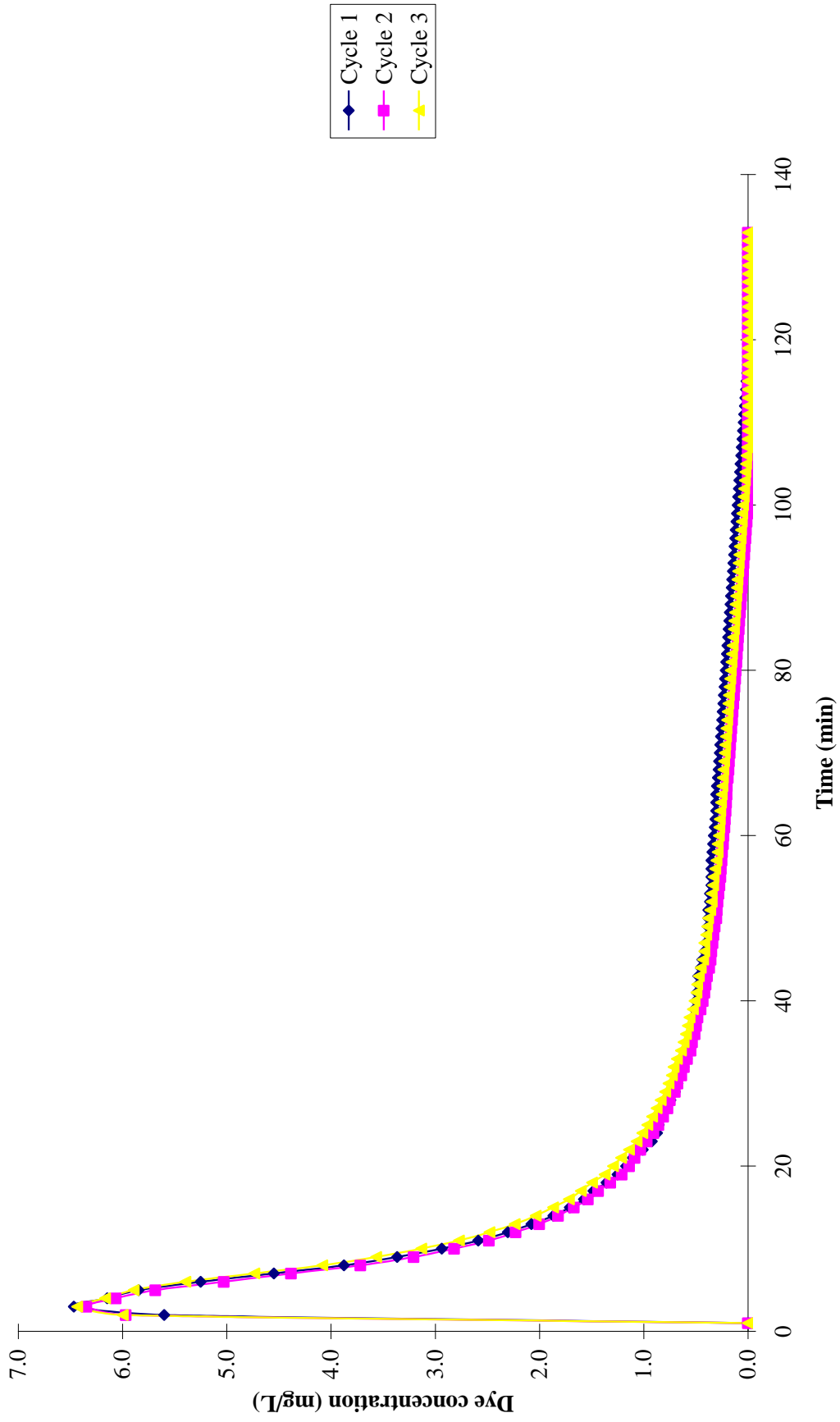


Figure 4.90: Elution curves for binary BB3 of BB3-BY11 column using 0.1 M HCl during three regeneration cycles

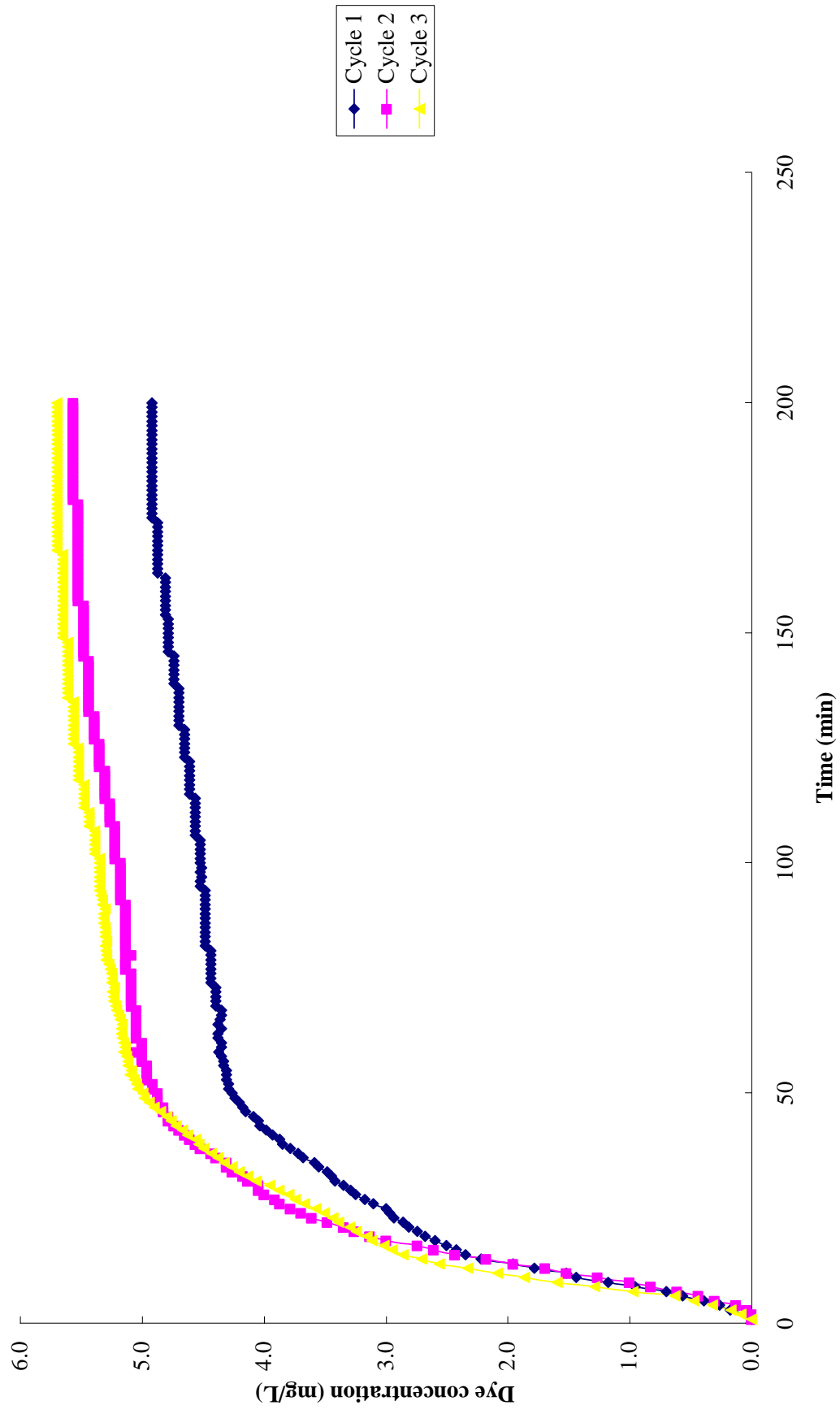


Figure 4.91: Breakthrough curve for adsorption of binary BY11 of BB3-BY11 by NSB during three regeneration cycles

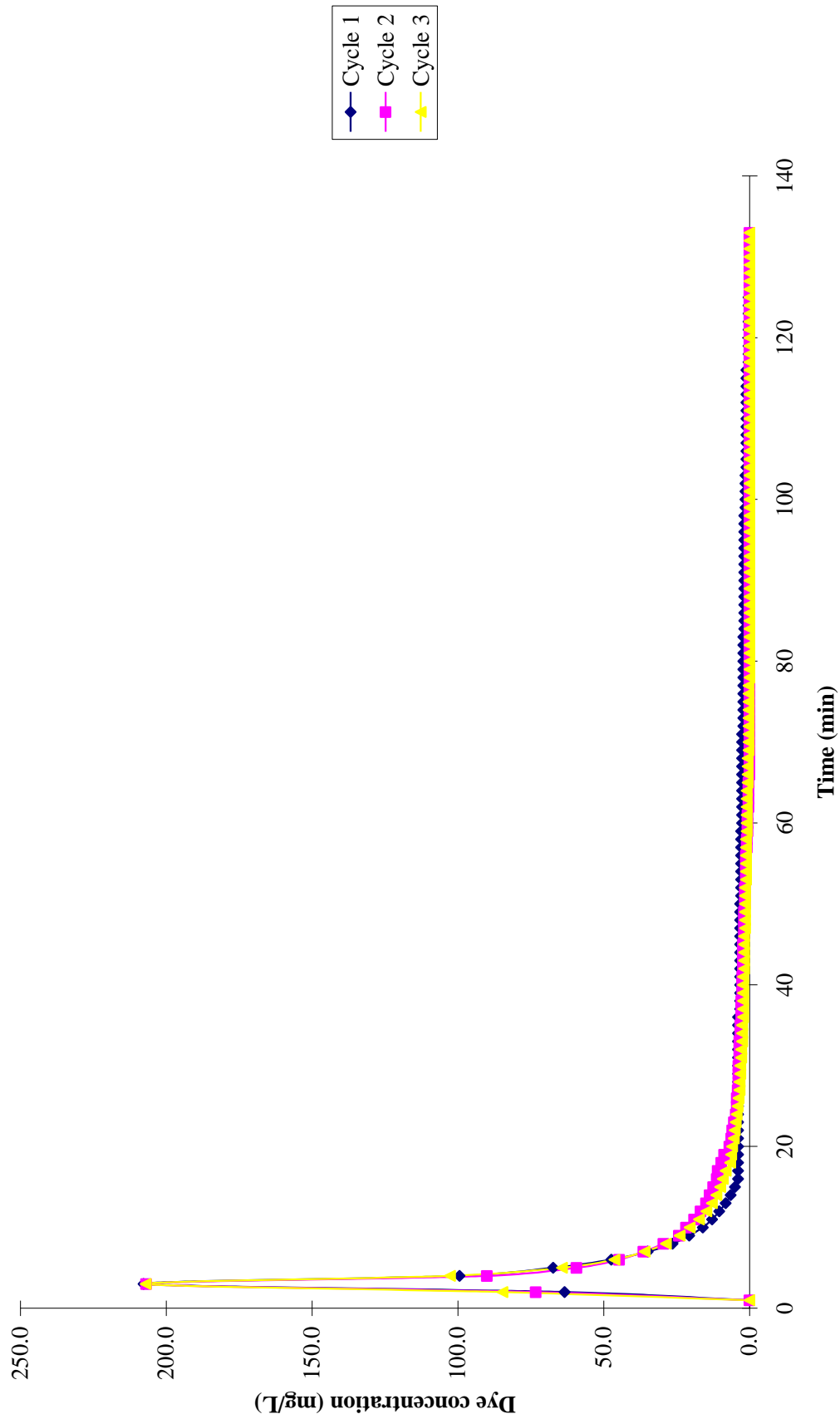
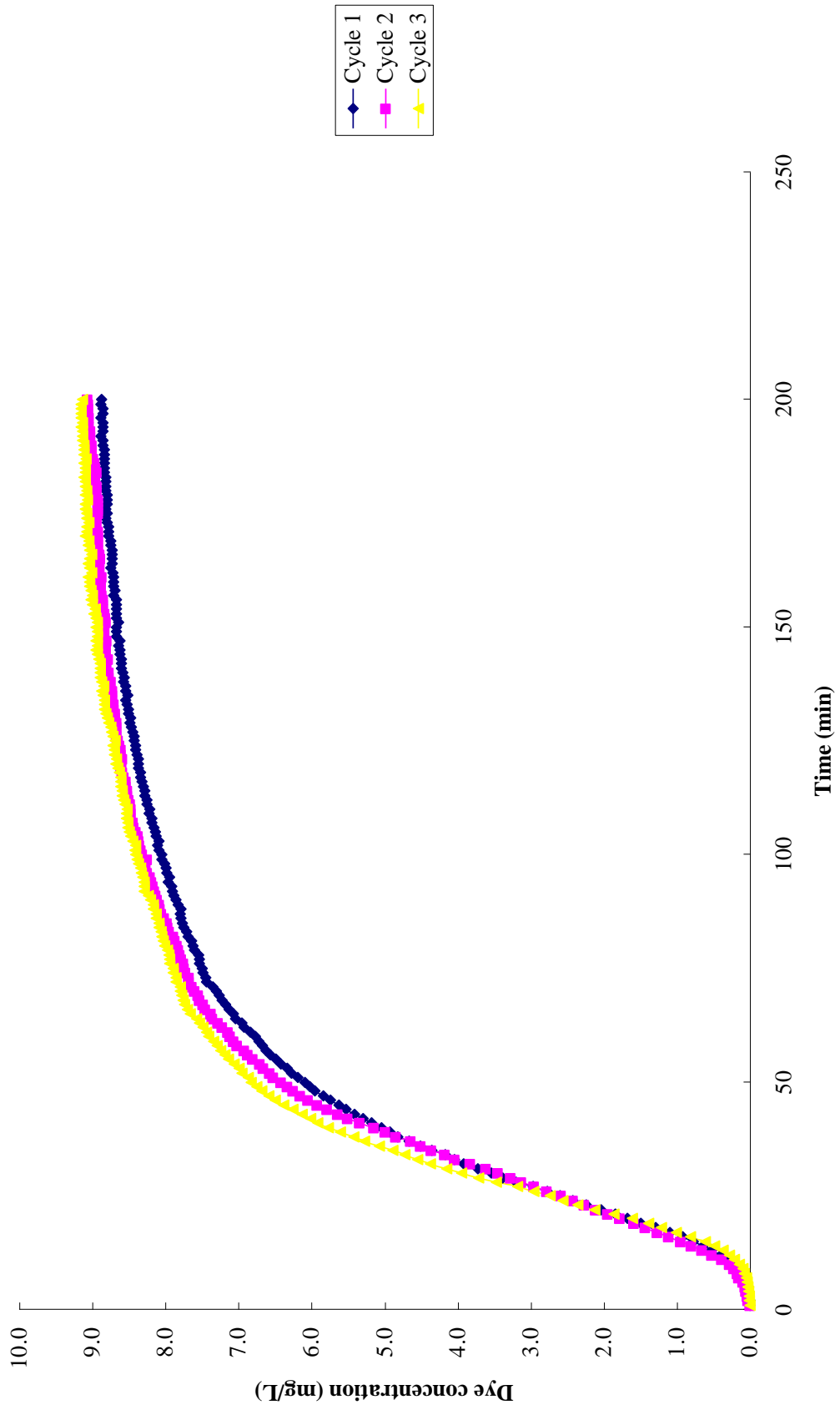


Figure 4-92: Elution curves for binary BY11 of BB3-BY11 column using 0.1 M HCl during three regeneration cycles





**Figure 4.93: Breakthrough curve for adsorption of binary MB of MB-BY11 by NSB during three regeneration cycles**

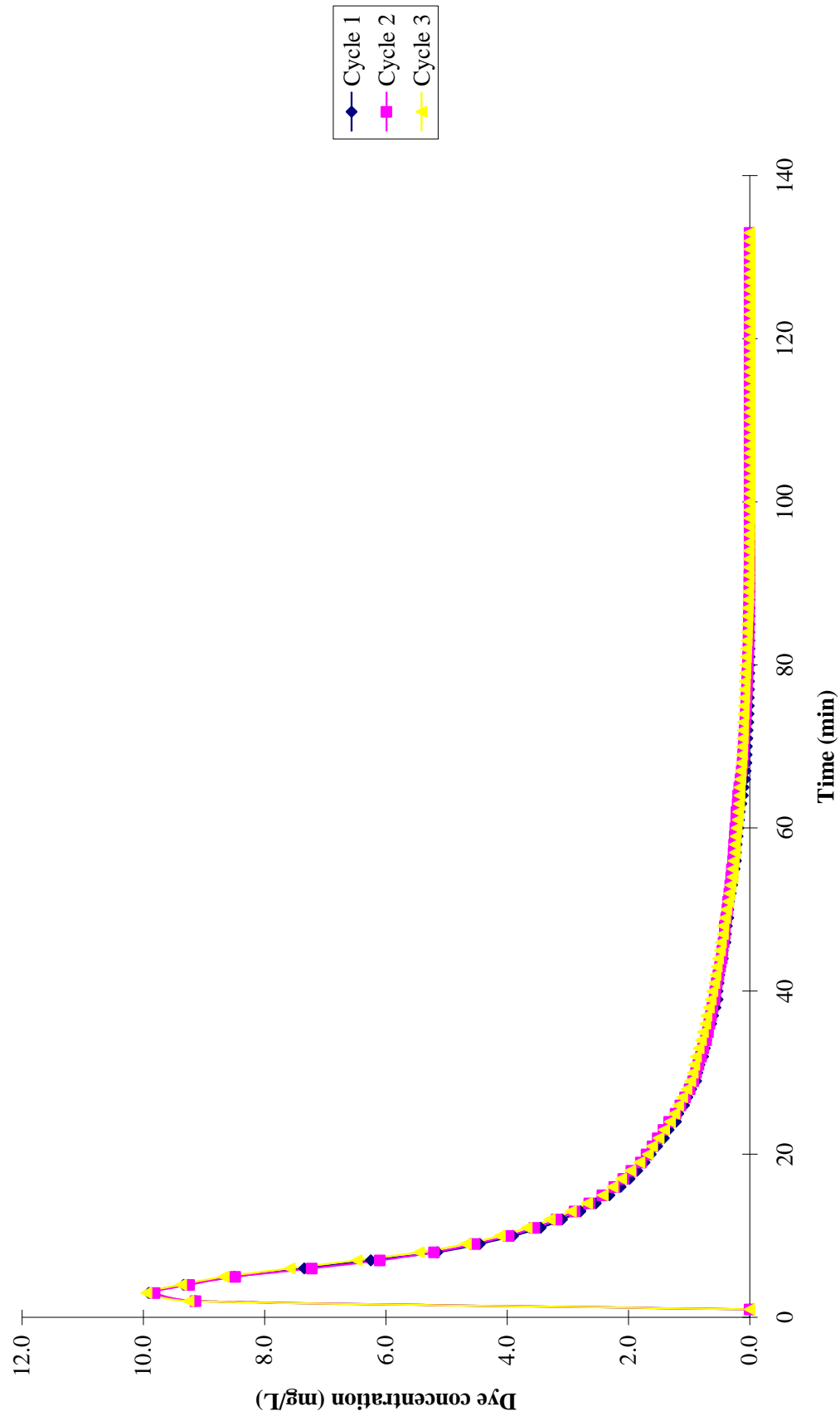
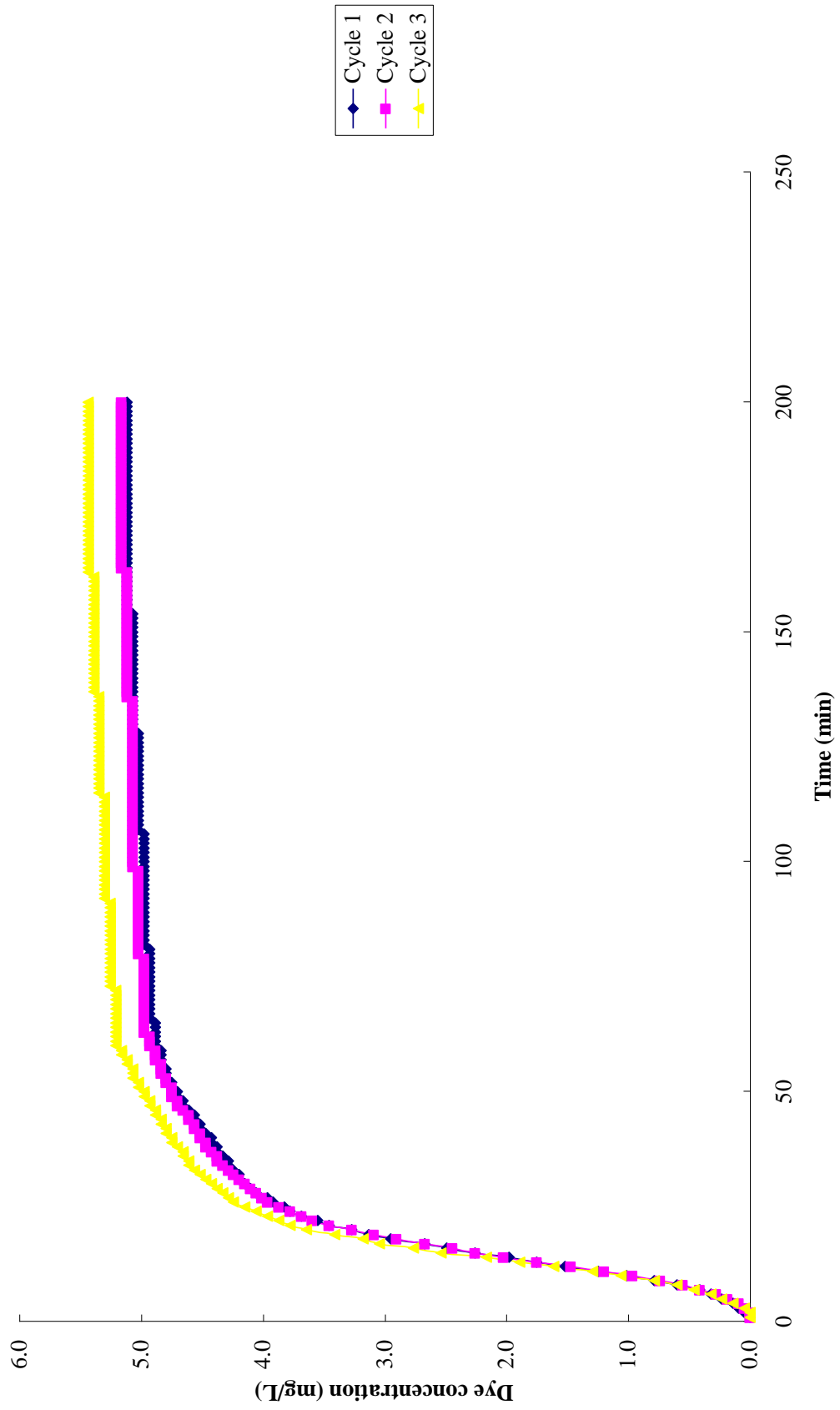


Figure 4.94: Elution curves for binary MB of MB-BY11 column using 0.1 M HCl during three regeneration cycles



**Figure 4.95: Breakthrough curve for adsorption of binary BY11 of MB-BY11 by NSB during three regeneration cycles**

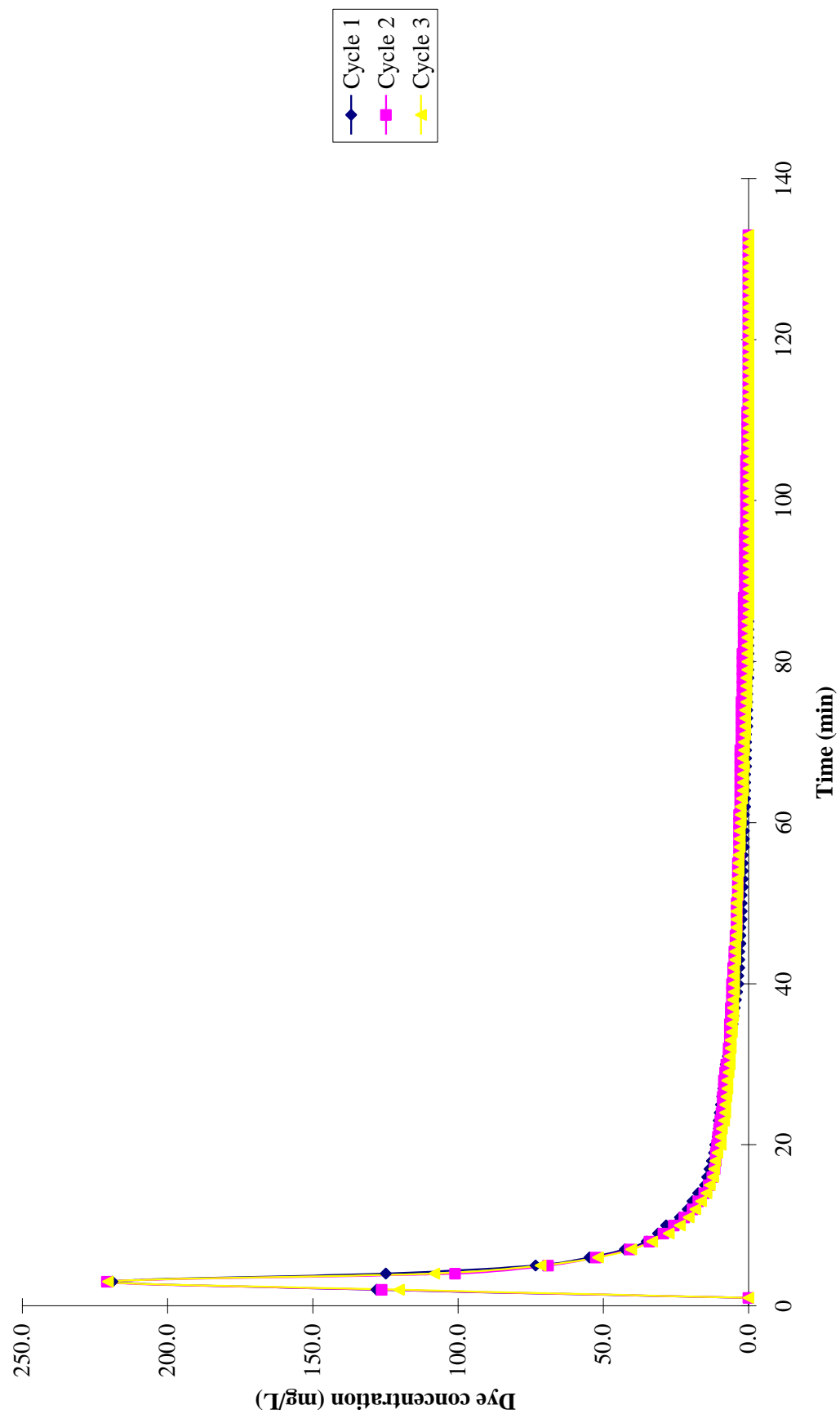


Figure 4.96: Elution curves for binary MB of MB-BY11 column using 0.1 M HCl during three regeneration cycles

Table 4.41: Adsorption process parameters for three adsorption-desorption cycles

Dye solutions	Cycle no.	Sorption capacity (mg/g)	% Removal	Regeneration efficiency (%)
Single BB3	1	5.80	20.77	-
	2	5.68	20.26	97.58
	3	5.39	19.50	93.91
Single MB	1	8.48	30.80	-
	2	7.32	26.41	85.75
	3	6.49	23.13	75.10
Single BY11	1	10.99	39.88	-
	2	10.79	38.93	97.62
	3	10.37	36.98	92.72
Binary BB3	1	5.088	18.21	-
	2	5.01	17.86	98.09
	3	4.68	16.93	92.99
Binary BY11 of BB3-BY11	1	5.90	21.13	-
	2	5.60	19.97	94.51
	3	5.19	18.79	88.92
Binary MB	1	7.01	25.10	-
	2	6.80	24.24	96.54
	3	6.31	22.84	90.97
Binary BY11 of MB-BY11	1	3.94	14.09	-
	2	3.89	13.87	98.47
	3	3.64	13.18	93.54

## CHAPTER 5

### CONCLUSION

In this study, the effectiveness of natural sugarcane bagasses (NSB) as the sorbent for the removal of Basic Blue 3 (BB3), Methylene Blue (MB) and Basic Yellow 11 (BY11) from both single and binary dye solutions was investigated. NSB was found to be capable to remove all studied dye solutions in both batch and column studies. From FT-IR analysis, no significant difference in functional groups occur in the sorbent before and after sorption.

The optimum pH for the removal of the studied dyes was observed in the pH range of 4 – 9 and the sorption reached equilibrium at 60 min. The optimum sorbent dosage was recorded at 0.10 g. The kinetics of dye sorption fitted well in pseudo-second order rate expression and Langmuir isotherm model was applicable for all the dyes under studied. Maximum sorption capacities were 23.64 mg/g, 28.25 mg/g and 67.11 mg/g for BB3, MB and BY11, respectively in single dye solutions. For binary dye solution, the maximum sorption capacities were recorded as 21.834 mg/g, 18.42 mg/g, 26.18 mg/g and 21.14 mg/g for binary BB3 of BB3-BY11, binary BY11 of BB3-BY11, binary MB of MB-BY11 and binary BY11 of MB-BY11, respectively. A decrease in maximum sorption capacities was observed in the binary dye solutions and this might be resulted from the competition of the same binding sites.

For the statistical analysis, Plackett-Burman design has been used to identify the most significant factors for the removal of dyes using NSB. The effect of initial dye concentration and sorbent dosage were identified to be the influential variables for the uptake of single BB3 and MB dye solutions. For binary BB3, the effect of initial dye concentration, pH, contact time and sorbent dosage were the variables responsible for affecting the percentage uptake. Meanwhile, the sorption of MB in binary dye solution was dependent on the effect of initial dye concentration, contact time and sorbent dosage. None of the studied variables were found to be affecting the percentage uptake of BY11 dye solutions.

The interaction between factors and their optimum levels for maximum percentage uptake of BB3 and MB in both single and binary dye solutions were determined using Response Surface Methodology (RSM). All the models were highly significant with correlation coefficients ( $R^2$ ) of 0.9947, 0.9967, 0.9932 and 0.9944 for single BB3, single MB, binary BB3 and binary MB, respectively. For single BB3 dye solution, the percentage uptake of 98.59 were obtained with optimised conditions of 50 mg/L initial dye concentration and sorbent dosage of 0.13 g. Whereas for single MB dye solution, the optimum condition were at 72 mg/L initial dye concentration and 0.18 g of sorbent dosage. Under these conditions, the percentage uptake was found to be 94.19. The experimental values agreed well with the predicted values with percentage error of 2.45, 1.48, 2.20 and 1.54 for single BB3, single MB, binary BB3 and binary MB, respectively.

In column studies, results revealed that breakthrough was influent concentration, flow rate and bed height dependent. The breakthrough occurred faster with increased influent concentration, increased flow rate and decreased bed height. The breakthrough curves exhibited the typical S shape of packed system. The sorption data were modeled using Thomas, Belter and Chu, and bed-depth service time (BDST) equation to determine the characteristic parameters of the column and to predict the breakthrough time under other experimental conditions. The experimental data were in good agreement with the predicted values in BDST modeling. All models used were found to be suitable for describing the sorption process of the dynamic behaviour of the sugarcane bagasse column. The column regeneration studies were carried out and the sorbent was found to be reusable with minimal decrease in its sorption capacities.



## REFERENCES

Abd El-Rahman, et al., 2006. Modeling the sorption kinetics of Cesium and Strontium ions on Zeolite A. *Journal of Nuclear and Radiochemical Sciences*, 7, pp. 21-27.

Ahmad, A.A., Hameed, B.H. and Aziz, N., 2007. Adsorption of direct dye on palm ash: Kinetic and equilibrium modeling. *Journal of Hazardous Materials*, 141, pp. 70-76.

Ahmad, A.A. and Hameed, B.H., 2010. Fixed-bed adsorption of reactive azo dye onto granular activated carbon prepared from waste. *Journal of Hazardous Materials*, 175, pp. 298-303.

Akkaya, G. and Özer, A., 2005. Biosorption of acid red 274 (AR274) on *Dicranella varia*: Determination of equilibrium and kinetic model parameters, *Process Biochemistry*, 40, pp. 3559-3568.

Aksu, Z., Ertuğrul, S. and Dönmez, G., 2009. Single and binary chromium (VI) and Remazol Black B biosorption properties of *Phormidium* sp. *Journal of Hazardous Materials*, 168, pp. 310-318.

Amin, N.K., 2008. Removal of reactive dye from aqueous solutions by adsorption onto activated carbons prepared from sugarcane bagasse. *Desalination*, 223, pp. 152-161.

Annadurai, G., Juang, R.S. and Lee, D.J., 2003. Adsorption of heavy metals from water using banana and orange peels. *Water Sci. Technol.*, 47, pp. 185-190.

Arami, M. et al., 2005. Removal of dyes from colored textile wastewater by orange peel adsorbent: Equilibrium and kinetics studies. *Journal of Colloid and Interface Science*, 288, pp. 371-376.

Ardejani, F.D. et al., 2007. Numerical modeling and laboratory studies on the removal of Direct Red 23 and Direct Red 80 dyes from textile effluents using orange peel, a low cost adsorbent. *Dyes and Pigments*, 73, pp. 178-185.

Azhar, S.S. et al., 2005. Dye removal from aqueous solution by using adsorption on treated sugarcane bagasse. *American Journal of Applied Sciences*, 2, pp. 1499-1503.

Azila, Y.Y., Mashitah, M.D. and Bahtia, S., 2008. Process optimization studies of lead (Pb(II)) biosorption onto immobilized cells of *pycnoporus sanguineus* using response surface methodology. *Bioresource Technology*, 99, pp. 8549-8552.

Banat, F., Al-Asheh, S. and Al-Makhadmeh, L., 2003. Evaluation of the use of raw and activated date pits as potential adsorbents for dye containing waters. *Process Biochemistry*, 39, pp. 182-202.

Barnes. A. C. (1974). *The Sugar Cane*. New York: John Wiley & Sons.

Batzias, F.A. and Sidiras, D.K., 2007. Simulation of dye adsorption by beech sawdust as affected by pH. *Journal of hazardous Materials*, 141, pp. 668-679.

Batzias, F.A. and Sidiras, D.K., 2004. Dye adsorption by calcium chloride treated beech sawdust in batch and fixed-bed systems. *Journal of Hazardous Materials*, B114, pp. 167-174.

Batzias, F.A. and Sidiras, D.K., 2007. Simulation of methylene blue adsorption by salt-treated beech sawdust in batch and fixed-bed systems. *Journal of Hazardous Materials*, 149, pp. 8-17.

Batzias, F.A. and Sidiras, D.K., 2007. Dye adsorption by prehydrolysed beech sawdust in batch and fixed-bed systems. *Bioresource Technology*, 98, pp. 1208-1217.

Belter, P.A., Crussler, E.L. and Hu, W.S., 1988. *Bioseparations, Downstreams Processing for Biotechnology*, John Wiley & Sons, New York.

Benkli, Y.E. et al., 2005. Modification of organo-zeolite surface for the removal of reactive azo dyes in fixed-bed reactors. *Water Research*, 39, pp. 487-493.

Brady, J.M., Tobin, J.M. and Roux, J.C., 1999. Continuous fixed bed biosorption of Cu<sup>2+</sup> ions: application of a simple two parameter mathematical model. *J. Chemical. Technol. and Biotechnol.*, 74, pp. 71-77.

Brit, 2008. *Synthetic Dyes: A look at Environmental & Human Risks* [Online]. Available at: <http://greencotton.wordpress.com/2008/06/18/synthetic-dyes-a-look-at-the-good-the-bad-and-the-ugly> [Accessed: 30 March 2010].

Buckley, C.A., 1992. Membrane technology for the treatment of dyehouse effluents. *Water Sci. Technol.*, 22, pp. 265-274.

Chauhan, K., Trivedi, U. and Patel K.C., 2006. Application of response surface methodology for optimization of lactic acid production using date juice. *J. Microbial Biotechnol.*, Vol 16, pp. 1410-1415.

Crips, C., Bumpus, J.A. and Aust, S.D., 1990. Biodegradation of azo and heterocyclic dyestuffs by *Phanerochaete chrysosporium*. *Appl. Env. Microbiol.*, 56, pp. 114-118.

Essawy, A.A., El-Hag Ali, S. and Abdel-Mottaleb, M.S.A., 2008. Application of novel copolymer-TiO<sub>2</sub> membraned for some textile dyes adsorptive removal from aqueous solution and photocatalytic decolorization. *Journal of Hazardous Materials*, 157, pp. 547-552.

El-Hendawy, A.A., 2006. Variation in FTIR spectra of a biomass under impregnation carbonization and oxidation conditions. *Journal of Analytical and Applied Pyrolysis*, 75, pp. 159-166.

Everett, D.H. and Koopal, L.K., 2002. *Manual of symbols and terminology for physicochemical quantities and unit* [Online]. Available at: [http://old.iupac.org/reports/2001/colloid\\_20001/manual\\_of\\_s\\_and\\_t/node16.html](http://old.iupac.org/reports/2001/colloid_20001/manual_of_s_and_t/node16.html) [Accessed: 11 April 2010].

Fungaro, D.A., Bruno, M. and Grosche, L.C., 2009, Adsorption and kinetic studies of methylene blue on zeolite synthesized from fly ash. *Desal. Water Treatment*, 2, pp. 231-239.

Garg, V.K., Kumar, R. and Gupta, R., 2004. Removal of malachite green dye from aqueous solution by adsorption using agro-industry waste: a case study of *Prosopis cineraria*. *Dyes and Pigments*, 62, pp. 1-10.

Garg, V.K. et al., 2004. Basic dye (methylene blue) removal from simulated wastewater by adsorption using Indian Rosewood sawdust: a timber industry waste. *Dyes Pigments*, 63, pp. 243-250.

Garg, U.K. et al., 2008. Removal of Nickel(II) from aqueous solution by adsorption on agricultural waste biomass using a response surface methodological approach. *Bioresource Technology*, 99, pp. 1325-1331.

Ghorbani, F. et al., 2008. Application of response surface methodology for optimization of cadmium biosorption in an aqueous solution by *Saccharomyces cerevisiae*. *Chemical Engineering Journal*, 145, pp. 267-275.

Goel, J. et al., 2005. Removal of lead(II) by adsorption using treated granular activated carbon: Batch and column studies. *Journal of Hazardous Materials*, 125, pp. 211-220.

Gong, R. et al., 2008. Adsorption behavior of cationic dyes on citric acid esterifying wheat straw: kinetic and thermodynamic profile. *Desalination*, 230, pp. 220-228.

Goshadrou, A. and Mohed, A., 2011. Continuous fixed bed adsorption of C.I. Acid Blue 92 by exfoliated graphite: An experimental and modeling study. *Desalination*, 269, pp. 170-176.

Gregory, A.R., Elliot, S. and Kludge, P., 1991. Ames testing of direct black 3B parallel carcinogenic. *Journal Appl. Toxicology*, 1, pp. 308-313.

Guo, Y., Kaplan, S. and Keranfil, T., 2008. The significance of physical factors on the adsorption of polyaromatic compounds by activated carbons. *Carbon*, 46, pp. 1885-1891.

Gupta, V.K. et al., 2006. Adsorption of hazardous dye, erythrosine, over hen feathers. *Journal of Colloid and Interface Science*, 304, pp. 52-57.



Gurgel, L.V.A., Freitas, R.P. and Gil, L.F., 2008. Adsorption of Cu(II), Cd(II) and Pb(II) from aqueous single metal solutions by sugarcane bagasse and mercerized sugarcane bagasse chemically modified with succinic anhydrous. *Carbohydrate Polymers*, 74, pp. 922-929.

Hamdaoui, Q., 2006. Batch study of liquid-phase adsorption methylene blue using cedar sawdust and crushed brick. *Journal of Hazardous Materials*, B135, pp. 264-273.

Hameed, B.H. and El-Khaiary, M.I., 2008. Removal of basic dye from aqueous medium using a novel agricultural waste material: Pumpkin seed hull. *Journal of Hazardous Materials*, 155, pp. 601-609.

Hameed, B.H., Tan, I.A.W. and Ahmad, A.L., 2008. Optimization of basic dye removal by oil palm fibre-based activated carbon using response surface methodology. *Journal of Hazardous Materials*, 158, pp. 324-332.

Hameed, B.H., 2009. Spent tea leaves: A new non-conventional and low-cost adsorbent for removal of basic dye from aqueous solutions. *Journal of Hazardous Materials*, 161, pp. 753-759.

Hameed, B.H., Krishni, R.R. and Sata, S.A., 2009. A novel agricultural waste adsorbent for the removal of cationic dye from aqueous solutions. *Journal of Hazardous Materials*, 162, pp. 305-311.

Hameed, B.H., 2009. Evaluation of papaya seeds as a novel non-conventional low-cost adsorbent for removal of methylene blue. *Journal of Hazardous Materials*, 162, pp. 939-944.

Han, R.P. et al., 2006. Biosorption of copper(II) and lead(II) from aqueous solution by chaff in a fixed-bed column. *Journal of Hazardous Materials*, B133, pp. 262-268.

Han, R., Wang, Y., Yu, W., Zou, W., Shi, J. and Liu, H. (2007). Biosorption of methylene blue from aqueous solution by rice husk in fixed-bed column. *Journal of Hazardous Materials*, 141, 713-718.

Han, R. et al., 2008. Use of rice husk for the adsorption of congo red from aqueous solution in column mode. *Bioresource Technology*, 99, pp. 2938-2946.

Han, R. et al., 2009. Adsorption of methylene blue by phoenix tree leaf powder in a fixed-bed column: experiments and prediction of breakthrough curves. *Desalination*, 245, pp. 284-297.

Hao, O.J., Kim, H. and Chang, P.C., 2000. Decolorization of wastewater. *Crit. Rev. Env. Sci. Tec.*, 30, pp. 449-505.

Hardin, I.R., 2007. Chemical treatment of textile dye effluent. In Christie, R.M., *Environmental aspects of textile dyeing*. Woodhead Publishing Limited, pp. 191-207.

Hassan, M.M. and Hawkyard, C.J., 2007. Decolorisation of effluent with ozone and re-use of spent dyebath. In: Christie, R., *Environmental aspects of textile dyeing*. Woodhead Publishing Limited, pp.149-190.

Ho, Y.S. and McKay, G., 1999. Pseudo second order model for sorption process. *Proc. Biochem*, 34, pp. 451-465.

Ho, Y.S. and McKay, G., 2000. The kinetics of sorption of divalent metals ions onto sphagnum moss peat. *Wat. Res.*, 34, pp. 735-742.

Ho, Y.S., Chiu, W.T. and Wang, C.C., 2005. Regression analysis for the soption isotherms of basic dyes on sugarcane dust. *Bioresource Technology*, 96, pp. 1285-1291.

Hubbe, M.A. and Rojas, O.J., 2008. Colloidal stability of cellulosics. *Bioresources*, 3(4), pp. 1419-1491.

Hunger K., 2003. Health and safety aspects. In: Hunger, K. and Sewekow, U., *Industrial dyes: chemistry, properties, applications*. Weinheim, Wiley-VCH, pp. 625-641.

Hutchins, R.A., 1973. New method simplifies design of activated carbon system. *Chem. Eng.*, 80, pp. 133-138.

Isa, M.H. et al., 2007. Low cost removal of disperse dyes from aqueous solution palm ash. *Dyes and Pigments*, 74, pp. 446-453.

Jumasiah, A. et al., 2005. Adsorption of basic dye onto palm kernel shell activated carbon: sorption equilibrium and kinetics studies. *Desalination*, 186, pp. 57-64.

Junior, O.K. et al., 2006. Adsorption of heavy metal ion from aqueous single metal solution by chemically modified sugarcane bagasse, *Bioresource Technology*, 98, pp. 1291-1297.

Kadirvelu, K. et al., 2003. Utilization of various agricultural wastes for activated carbon prepared and application for the removal of dyes and metal ions from aqueous solutions. *Bioresource Technology*, 87, pp. 29-132.

Kalavathy, H., Karthik, B. and Miranda, L.R., 2010. Removal and recovery of Ni and Zn from aqueous solution using activated carbon from *Hevea brasiliensis*: Batch and column studies. *Column and Surfaces B: Biointerfaces*, 78, pp. 291-302.

alderis, D. et al., 2008). Adsorption of polluting substances on activated carbons prepared from rice husk and sugarcane bagasse. *Chemical Engineering Journal*, 144, pp. 42-50.

Kandelbauer, A., Cavaco-Paulo, A. and Gübitz, G.M., 2007. Biotechnological treatment of textile dye effluent. In Christie, R.M., *Environmental aspects of textile dyeing*. Woodhead, pp. 212-229.

Khattar, J.I.S. and Shailza, 2009. Optimization of  $\text{Cd}^{2+}$  removal by the cyanobacterium *Synechocystis pevalekii* using the response surface methodology. *Process Biochemistry*, 44, pp. 118-121.

Kim, J.K. et al., 2008. Statistical optimization of enzymatic saccharification and ethanol fermentation using food waste. *Process Biochemistry*, 43, pp. 1308-1312.

Ko, D.C.K., Porter, J.F. and McKay, G., 2000. Optimised correlation for the fixed- bed adsorption of metal ions on bone char. *Chem. Eng. Sci.*, 55, pp. 5819-5829.

Krishnan, K.A. and Anirudhan, T.S., 2008. Kinetic and equilibrium modelling of cobalt(II) adsorption onto bagasse pith based sulphurised activated carbon. *Chemical Engineering Journal*, 137, pp. 257-264.

Lagergren, S., 1898. Zur theorie der sogenannten adsorption geloster stoffe. *Kungliga Svenska Vetenskapsakademiens Handlingar*, 24, pp. 1-39.

Little, A.D., 1990. Executive Summary of Safety and Toxicity Information: Methylene Blue. National Toxicology Program

Lee, C.K., Loh, K.S. and Mah, S.J., 1998. Removal of gold (III) complex by quaternized rice husk. *Advance Environ. Res.*, 2, pp. 351-359.

Lee, C.K., Ong, S.T. and Zainal, Z., 2008. Ethylenediamine modified rice hull as a sorbent for the removal of Basic Blue 3 and Reactive Orange 16. *International Journal of Environment and Pollution*, 34, pp. 1-4.

Levin, L., Papinutti, L. and Forchiassin, F., 2004. Evaluation of Argentinean white rot fungi for their ability to produce lignin-modifying enzymes and decolorize industrial dyes. *Bioresour. Technol.*, 94, pp. 169-176.

Lodeiro, P. Et al., 2006. The use of protonated *Sargassum muticum* as biosorbent for cadmium removal in a fixed-bed column. *Journal of Hazardous Materials*. B137, pp. 244-253.

Malik, P.K., 2003. Use of activated carbons prepared from sawdust and rice-husk for adsorption of acid dyes: A case study of Acid Yellow 36. *Dyes Pigments*, 56, pp. 239-249.

Mckay, G. and Sweeny, A., 1980. Principles of dye removal from textile effluent. *Water, Air, Soil Pollut*, 14, pp. 2-11.

McMullan, G. et al., 2001. Microbial decolourization and degradation of textile dyes, *Appl. Microbial. Biotechnol.*, 56, pp. 81-87.

Montgomery, D. C., 2004. *Design and analysis of experiments*. John Wiley&Sons, USA.

Motola, S. and Agharkar, S.N., 1992. Preformulation Research of Parenteral Medications. In: Avis, K.E., Lieberman, H.A. and Lachman, L., *Pharmaceutical Dosage Forms: Parenteral Medications Volume 1*. Marcel Dekker, Inc., pp. 115-172.



Murat, E., 2002. Response surface methodological approach for inclusion of perfluorocarbon in actinorhodin fermentation medium, *Process Biochem.*, 38, pp. 667-773.

Murugesan, K. et al., 2008. Decolourization of reactive black 5 by laccase: Optimization by response surface methodology. *Dyes and Pigments*, 75, pp. 176-184.

Myers, R.H. and Montgomery, D.C., 2002. Response surface methodology, second ed., John Wiley and Sons Inc.

Namasivayam, C., Radhika, R. and Suba, S., 2001. Uptake of dyes by a promising locally available agricultural solid waste: coir pith. *Waste Manage*, 21, pp. 381-387.

Namboodri, C.G., Perkins, W.S. and Walsh, W.K., 1994a. Decoloring dye with chlorine and ozone: Part I. *Amer. Dyestuff Rep.*, 83(3), pp. 17.

Namboodri, C.G., Perkins, W.S. and Walsh, W.K., 1994b. Decoloring dye with chlorine and ozone: Part II. *Amer. Dyestuff Rep.*, 83(3), pp. 17-25.

Oliveira, L.S. et al., 2008. Evaluation of untreated coffee husks as potential biosorbents for treatment of dye contaminated waters. *Journal of Hazardous Materials*, 155, pp. 507-512.

Ong, S.T., Lee, C.K. and Zainal, Z., 2006. Removal of basic and reactive dyes using ethylenediamine modified rice hull. *Bioresource Technology*, 98, pp. 2792-2799.

Ong, S.T., Lee, C.K. and Zainal, Z., 2005. Removal of basic and reactive dyes using modified rice hull. *J. Phys. Sci.*, 16, pp. 9-19.

Ong, S.T., Lee, C.K. and Zainal, Z., 2008. Ethylenediamine modified rice hull as sorbent for the removal of Basic Blue 3 and Reactive Orange 16. *International Journal of Environment and Pollution*, 34, pp. 1-4.

Ong, S.T. et al., 2009. Nitrilotriacetic acid modified sugarcane bagasse in the removal of Basic Blue 3 from aqueous environment. *International Journal of Environment and Engineering*, (Article in press).

Özdemir, Y., Doğan, M. and Alkan, M., 2006. Adsorption of cationic dyes from aqueous solution by sepiolite. *Microporous and Mesoporous Materials*, 96, pp. 419-427.

Padmesh, T.V.N. et al., 2006. Biosorption of Acid Blue 15 using fresh water macroalga *Azolla filiculoides*: Batch and column studies. *Dyes and Pigments*, 71, pp. 77-82.

Palmieri, G., Cennamo, G. and Sannia, G., 2005. Removal of Brilliant R decolourisation by the fungus *Pleurotus ostreatus* and its oxidative enzymatic system. *Enzyme Microbiol. Technol.*, 36, pp. 17-27.

Parameswaran, B., 2009. Sugarcane Bagasse, In: Nigam, P.S. and Pandey, A., *Biotechnology For Agro-Industries Residues Utilisation: Utilisation of Agro-Residues*. Springer Science + Business Media B.V., pp. 239-252.

Pavan, F.A., Mazzocato, A.C. and Gushilem, Y., 2008. Removal of methylene blue from aqueous solutions by adsorption using yellow passion fruit peel as adsorbent. *Biorsource Technology*, 99, pp. 3162-3165.

Peng, F. et al., 2009. Comparative study of hemicelluloses obtained by graded ethanol precipitation from sugarcane bagasse. *J. Agric. Food Chem.*, 57(14), pp. 6305-6317.

Platzek T., 1997. Gesundheitsgefährdung durch Bekleidungstextilien. *Bundesgesundhbl*, 40, pp. 238–240.

Rajendran, A., Thirugnanam, M. and Thangavelu, V., 2007. Statistical evaluation of medium components by Plackett-Burman experimental design and kinetic modeling of lipase production by *Pseudomonas fluorescens*. *Indian Journal of Biotechnology*, 6, pp. 467-478.

Ravikumar, K., Deebika, B. and Balu, K., 2005. Decolourization of aqueous dye solutions by a novel adsorbent: Application of statistical designs and surface plots for the optimization and regression analysis. *Journal of Hazardous Materials*, B122, pp. 75-83.

Ravikumar, K. et al., 2006. Application of response surface methodology to optimize the process for reactive Red and Acid Brown dye removal using novel adsorbent. *Dyes and Pigments*, 70, pp. 18-26.

Raybin, A., 2009. *Water pollution and the textile industry* [Online]. Available at: <http://blog.airdye.com/goodforbusiness/2009/09/30/water-pollution-and-the-textile-industry> [Accessed: 5 August 2010].

Roger, G.P., 1985. *Design and analysis of experiments*. Marcel Dekker Inc., USA.

Saeed, A., Iqbal., M. and Zafar, S.I., 2009. Immobilization of *Trichoderma viride* for enhanced methylene blue biosorption: Batch and column studies. *Journal of Hazardous Materials*, 168, pp. 406-415.

Sharma, P., Singh, L and Dilbaghi, N., 2009. Response surface methodological approach for the decolorization of simulated dye effluent using *Aspergillus fumigatus fresenius*. *Journal of Hazardous Materials*, 161, pp. 1081-1086.

Shiau, C.Y. and Pan C.C., 2004. Adsorption of basic dyes from aqueous solution by various adsorbents. *Separation Science and Technology*, 39, pp. 1733-1750.

Shigo, A., 2001. *Water and Trees* [Online]. Available at: <http://www.treedictionary.com/DICT2003/shigo/WATER.html> [Accessed: 8 July 2009].

Simončič, B., 2008. Surface properties of cellulose modified by imidazolidinone. *Cellulose*, 15(1), pp. 47-58.

Sivakumar, P. and Palanisamy, P.N., 2009. Packed bed column studies for the removal of Acid blue 92 and Basic red 29 using non-conventional adsorbent. *Indian Journal of Chemical technology*, 16, pp. 301-307.

Spencer, J., 2007. *China Pays Steep Price As Textile Exports Boom, Suppliers to U.S. Stores Accused of Dumping Dyes To Slash Their Costs* [Online]. Available at: <http://online.wsj.com/public/article/SB118580938555882301.html> [Accessed: 30 March 2010].

Sun, Y. and Cheng, J., 2002. Hydrolysis of lignocellulosic materials for ethanol production: a review. *Bioresource. Technol.*, 83, pp 1-11.

Tan, P., 2009. Equilibrium and Kinetics Studies for Basic Yellow 11 Removal by *Sargassum binderi*. *Journal of Applied Sciences* 9, 17, pp. 3005-3012.

Teng, M. and Lin, S., 2006. Removal of basic dye from water onto pristine and HCl-activated montmorillonite in fixed beds. *Desalination*, 194, pp. 156-165.

Turabik, M., 2008. Adsorption of basic dyes from single and binary component system onto bentonite: Simultaneous analysis of Basic Red 46 and Basic Yellow 28 by first order derivative spectrophotometric analysis method. *Journal of Hazardous Materials*, 158, pp. 52-64.

Uddin, M.T., 2009. Adsorption of methylene blue from aqueous solution by jackfruit (*Artocarpus heterophyllus*) leaf powder: A fixed-bed column study. *Journal of Environmental Management*, 90, pp. 3443-3450.

Van Dillewijn, C., 1952. Botany of Sugar Cane, *Chronica Botanica*, Waltham, MA.

Wagner, J., 2001. The four membrane process. In Wagner, J., *Membrane filtration handbook, practical tips and hints*. Osmonics, Inc., pp. 7-8.

Wan Ngah, W.S., Kamari, A. and Koay, Y.J., 2004. Equilibrium and kinetics studies of adsorption of copper (II) on chitosan and chitosan/PVA beads. *International Journal of Hazardous Materials*, B126, pp. 71-77.

Wang, S. et al., 2005. Unburned carbon as a low-cost adsorbent for treatment of methylene blue-containing wastewater. *Journal of Colloid and Interface Science*, 292, pp. 336-343.

Wang, S. and Li, H., 2005). Dye adsorption on unburned carbon; Kinetics and equilibrium. *Journal of Hazardous Materials*, B126, pp. 71-77.

Wang, S. and Li, H., 2007. Kinetic modelling and mechanism of dye adsorption on unburned carbon. *Dyes and Pigments*, 72, pp. 308-314.

Wang, S. and Ariyanto, E., 2007. Competitive adsorption of malachite green and Pb ions on natural zeolite. *Journal of Colloid and Interface Science*, 314, pp. 25-31.

Weng, C.H., Lin, Y.T. and Tzeng, T.W., 2009. Removal of methylene blue from aqueous solution by adsorption onto pineapple leaf powder. *Journal of Hazardous Materials*, 170, pp. 417-424.



Wong, S.Y. et al., 2009. The removal of basic and reactive dyes using quarterised sugar cane bagasse. *Journal of Physical Science*, 20(1), pp. 59-74.

Wu, J. and Wang, T., 2001, Ozonation of aqueous azo dye in a semi-batch reactor. *Water Res.*, 36, pp. 1093-1099.

Yamazaki, I., Mason, S. and Piette, L., 1960. Identification by electro paramagnetic resonance spectroscopy of free radicals generated from substrates by peroxide. *J. Biol. Chem.*, 235, pp. 259-261.